frontiers | Research Topics

Methods in general cardiovascular medicine

Edited by
Silvia Marchiano, Coen van Solingen, Serafino Fazio,
Jin Li and Qingchun Zeng

Published in
Frontiers in Cardiovascular Medicine

ISSN 1664-8714
ISBN 978-2-8325-3461-8
DOI 10.3389/978-2-8325-3461-8

About Frontiers

Frontiers is more than just an open access publisher of scholarly articles: it is a pioneering approach to the world of academia, radically improving the way scholarly research is managed. The grand vision of Frontiers is a world where all people have an equal opportunity to seek, share and generate knowledge. Frontiers provides immediate and permanent online open access to all its publications, but this alone is not enough to realize our grand goals.

Frontiers journal series

The Frontiers journal series is a multi-tier and interdisciplinary set of open-access, online journals, promising a paradigm shift from the current review, selection and dissemination processes in academic publishing. All Frontiers journals are driven by researchers for researchers; therefore, they constitute a service to the scholarly community. At the same time, the *Frontiers journal series* operates on a revolutionary invention, the tiered publishing system, initially addressing specific communities of scholars, and gradually climbing up to broader public understanding, thus serving the interests of the lay society, too.

Dedication to quality

Each Frontiers article is a landmark of the highest quality, thanks to genuinely collaborative interactions between authors and review editors, who include some of the world's best academicians. Research must be certified by peers before entering a stream of knowledge that may eventually reach the public - and shape society; therefore, Frontiers only applies the most rigorous and unbiased reviews. Frontiers revolutionizes research publishing by freely delivering the most outstanding research, evaluated with no bias from both the academic and social point of view. By applying the most advanced information technologies, Frontiers is catapulting scholarly publishing into a new generation.

What are Frontiers Research Topics?

Frontiers Research Topics are very popular trademarks of the *Frontiers journals series*: they are collections of at least ten articles, all centered on a particular subject. With their unique mix of varied contributions from Original Research to Review Articles, Frontiers Research Topics unify the most influential researchers, the latest key findings and historical advances in a hot research area.

Find out more on how to host your own Frontiers Research Topic or contribute to one as an author by contacting the Frontiers editorial office: frontiersin.org/about/contact

Methods in general cardiovascular medicine

Topic editors

Silvia Marchiano — University of Washington, United States
Coen van Solingen — New York University, United States
Serafino Fazio — Federico II University Hospital, Italy
Jin Li — Shanghai University, China
Qingchun Zeng — Southern Medical University, China

Citation

Marchiano, S., van Solingen, C., Fazio, S., Li, J., Zeng, Q., eds. (2023). *Methods in general cardiovascular medicine*. Lausanne: Frontiers Media SA.
doi: 10.3389/978-2-8325-3461-8

Table of contents

05 Editorial: Methods in general cardiovascular medicine
Serafino Fazio, Silvia Marchiano, Coen van Solingen, Jin Li and Qingchun Zeng

07 The Long-Term Results of Three Catheter Ablation Methods in Patients With Paroxysmal Atrial Fibrillation: A 4-Year Follow-Up Study
Ling You, Xiaohong Zhang, Jing Yang, Lianxia Wang, Yan Zhang and Ruiqin Xie

15 The Mechanism of Cardiac Sympathetic Activity Assessment Methods: Current Knowledge
Jiakun Li and Lihui Zheng

23 Reliability and validity of sit-to-stand test protocols in patients with coronary artery disease
Zheng Wang, Jianhua Yan, Shu Meng, Jiajia Li, Yi Yu, Tingting Zhang, Raymond C. C. Tsang, Doa El-Ansary, Jia Han and Alice Y. M. Jones

33 Korotkoff sounds dynamically reflect changes in cardiac function based on deep learning methods
Wenting Lin, Sixiang Jia, Yiwen Chen, Hanning Shi, Jianqiang Zhao, Zhe Li, Yiteng Wu, Hangpan Jiang, Qi Zhang, Wei Wang, Yayu Chen, Chao Feng and Shudong Xia

45 A prospective, multicenter, single-arm clinical trial cohort to evaluate the safety and effectiveness of a novel stent graft system (WeFlow-JAAA) for the treatment of juxtarenal abdominal aortic aneurysm: A study protocol
Jiang-Ping Gao, Hong-Peng Zhang, Xin Jia, Jiang Xiong, Xiao-Hui Ma, Li-Jun Wang, Min-Hong Zhang, Yong-Le Xu and Wei Guo

54 Digital preventive measures for arterial hypertension (DiPaH) – a mixed-methods study protocol for health services research
Dunja Bruch, Felix Muehlensiepen, Susann May, Eileen Wengemuth, Olen Johannsen, Katrin Christiane Reber, Eva-Lotta Blankenstein, Gerrit Fleige, Martin Middeke, Johannes Albes, Martin Heinze, Marc Lehnen and Sebastian Spethmann

62 Randomized, crossover, controlled trial on the modulation of cardiac coronary sinus hemodynamics to develop a new treatment for microvascular disease: Protocol of the MACCUS trial
Helen Ullrich, Maximilian Olschewski, Thomas Münzel and Tommaso Gori

68 Early vascular healing after neXt-generation drug-eluting stent implantation in Patients with non-ST Elevation acute Coronary syndrome based on optical coherence Tomography guidance and evaluation (EXPECT): study protocol for a randomized controlled trial
Yong-Xiang Zhu, Li Liang, Ramya Parasa, Zheng Li, Qian Li, Shang Chang, Wen-Rui Ma, Si-Li Feng, Yang Wang, Bo Xu, Christos V. Bourantas and Yao-Jun Zhang

76 The ReInforcement of adherence via self-monitoring app orchestrating biosignals and medication of RivaroXaban in patients with atrial fibrillation and co-morbidities: a study protocol for a randomized controlled trial (RIVOX-AF)
Minjae Yoon, Jin Joo Park, Taeho Hur, Cam-Hao Hua, Chi Young Shim, Byung-Su Yoo, Hyun-Jai Cho, Seonhwa Lee, Hyue Mee Kim, Ji-Hyun Kim, Sungyoung Lee and Dong-Ju Choi for the RIVOX-AF investigators

84 Threshold values of brachial cuff-measured arterial stiffness indices determined by comparisons with the brachial–ankle pulse wave velocity: a cross-sectional study in the Chinese population
Xujie Zhang, Yumin Jiang, Fuyou Liang and Jianping Lu

96 State-of-the-art methodologies used in preclinical studies to assess left ventricular diastolic and systolic function in mice, pitfalls and troubleshooting
Gianluigi Pironti

frontiers | Frontiers in Cardiovascular Medicine

TYPE Editorial
PUBLISHED 29 August 2023
DOI 10.3389/fcvm.2023.1277373

OPEN ACCESS

EDITED AND REVIEWED BY
Pietro Enea Lazzerini,
University of Siena, Italy

*CORRESPONDENCE
Serafino Fazio
fazio0502@gmail.com

RECEIVED 14 August 2023
ACCEPTED 18 August 2023
PUBLISHED 29 August 2023

CITATION
Fazio S, Marchiano S, van Solingen C, Li J and Zeng Q (2023) Editorial: Methods in general cardiovascular medicine.
Front. Cardiovasc. Med. 10:1277373.
doi: 10.3389/fcvm.2023.1277373

Editorial: Methods in general cardiovascular medicine

Serafino Fazio[1]*, Silvia Marchiano[2], Coen van Solingen[3], Jin Li[4] and Qingchun Zeng[5]

[1]Federico II University Hospital, Naples, Italy, [2]University of Washington, Seattle, WA, United States, [3]New York University, New York City, NY, United States, [4]Shanghai University, Shanghai, China, [5]Southern Medical University, Guangzhou, China

KEYWORDS

methods, protocols, cardiac function, atrial fibrillation, arterial stiffness

Editorial on the Research Topic
Methods in general cardiovascular medicine

Cardiovascular diseases are the leading cause of death worldwide. The advancement of scientific knowledge and clinical practice in general cardiovascular medicine relies on innovative and groundbreaking approaches. The Research Topic *Methods in General Cardiovascular Medicine* has collected 11 valid manuscripts that will help researchers and clinicians to design, conduct, evaluate and apply the best evidence-based interventions to prevent, diagnose and treat cardiovascular diseases.

This editorial highlights the important aspects discussed in the published manuscripts of the Topic.

Pironti, in his review paper, carries out an in-depth analysis of the methods used to perform an effective evaluation of the systolic and diastolic cardiac function in mice, including pitfalls and alternative solutions.

The study by Li and Zheng reviewed the methods currently available for the evaluation of the sympathetic heart tone in clinic and research, explaining the principles underlying these methods. The authors conclude that all methods for assessing cardiac sympathetic activity are based on the anatomy and physiology of the heart, and, particularly, on the innervation and sympathetic regulation of the heart. For this reason, technological advances, the overlapping of disciplines and an improved understanding of the sympathetic innervation and regulation of the heart will certainly promote the development of new, more accurate methods of assessing cardiac sympathetic activity.

In another study published in this Research Topic, Lin et al. used Korotkoff sounds to measure blood pressure, with the application of Deep Learning (DL); they suggested that the application of DL to Korotkoff tones might be used for the early diagnosis of heart failure (HF). Considering the high mortality and morbidity of HF, and the importance of an early diagnosis, this novel application of Korotkoff sounds could be very useful, particularly in some rural areas, or in areas where advanced medical instruments are not easily accessible.

The following three studies of this Research Topic are Original Research studies. The study by You et al. retrospectively compares the results obtained with three catheter ablation methods in patients with episodes of paroxysmal atrial fibrillation (PAF). Their results showed no statistically significant differences in PAF recurrence among the three methods used, (radiofrequency, cryoablation and a combination of the two), suggesting that the type of ablative procedure is not a determinant in AF recurrence. They also

found that only left atrial appendage emptying velocity resulted to be an independent predictor of PAF recurrence.

Zhang et al. in their study describe a method to establish the threshold values of Arterial Velocity-pulse index (AVI) and Arterial Pressure-Volume index (API), measured by a brachial cuff, indicative of arterial stiffness. The study demonstrated that AVI and API can be used to perform a preliminary screening of increased arterial stiffness. Because of the direct correlation between increased arterial stiffness and the risk of cardiovascular events, this simple method allows the early identification of subjects in the general population more at risk of cardiovascular events, enabling a prompt preventive treatment.

The study by Wang et al. aimed to evaluate the reliability, convergent and known-groups validity of protocols that used sit-to-stand tests (STS) to estimate the level of risk for cardiovascular events in patients with coronary artery disease (CAD). The conclusions of the study were that all three STS tests (Five times STS test, 30-s STS test, 1-min STS test) had good test-retest reliability, convergent and known-groups validity, and that these tests can distinguish low-risk CAD patients from high-risk ones of cardiovascular events.

The other five manuscripts of this Research Topic describe the protocols used in their respective studies to obtain reproducible results.

In their manuscript, Yoon et al. describe a study protocol for a randomized controlled trial aimed to verify if, applying smartphone applications and mobile health platforms, was possible to improve the adherence to treatment with Rivaroxaban, a non-vitamin k antagonist oral anticoagulant (NOACs).

Bruch et al. in their manuscript, describe the protocol of a study to determine which factors (including comorbidities and social-economic status) influence the implementation of digital prevention of arterial hypertension, particularly in the most remote and sparsely populated areas, and thus improve cardiovascular outcomes.

In *Early vascular healing after neXt-generation drug-eluting stent implantation in Patients with non-ST Elevation acute Coronary syndrome based on optical coherence Tomography guidance and evaluation (EXPECT): study protocol for a randomized controlled trial* by Zhu et al. the authors assess early vascular healing after next-generation drug-eluting stents (DES) implantation in patients with non-ST elevation acute coronary syndrome (NST-ACS) guided and evaluated by optical coherence tomography (OCT). The study includes 60 patients randomized at 1:1:1 ratio to OCT guide percutaneous coronary intervention (PCI). The primary endpoint of the study is to verify the rate of vascular healing at the stent level in the three study groups. The data from the study are expected to provide new insights into vessel wall healing in an NST-ACS population following next-generation DES implantation, underscore the value of OCT in speeding vessel healing, and evaluate the possibility of early discontinuation of dual antiplatelet therapy in this population.

Gao et al. in their manuscript, describe a study protocol for an innovative off-the-shelf aortic endograft system for the treatment of juxta renal abdominal aortic aneurisms. The primary efficacy endpoints will be the frequency of immediate technical success of the implant and the number of reoperations within 12 months of the procedure. There will also be a primary safety endpoint: the frequency of major adverse events within 30 days of implant. The authors also describe the strengths and limitations of the study protocol. In particular, the major limitation of this study is the lack of a control group.

Finally, the manuscript of Ullrich et al. describes the protocol to verify whether an improvement in vascular resistance of coronary artery can be achieved by increasing retrograde pressure in the coronary sinus (CS). The changes of coronary vascular resistance could improve the symptoms of microvascular angina, making the pathophysiology of the disease better understood, and indicating new therapeutic perspectives. The study design will be randomized and crossover, with patients in whom coronary hemodynamics will be analyzed during partial balloon occlusion in the CS, and patients in whom coronary hemodynamics will be measured with a completely deflated balloon. The primary endpoint of the study will be the change in the hemodynamically obtained coronary resistance index following acute changes in CS pressure.

Author contributions

SF: Writing – original draft. SM: Writing – review and editing. CS: Writing – review and editing. JL: Writing – review and editing. QZ: Writing – review and editing.

Funding

The author(s) declare that no financial support was received for the research, authorship, and/or publication of this article.

Conflict of interest

The authors declare that the research was conducted in the absence of any commercial or financial relationships that could be construed as a potential conflict of interest.

The author(s) declared that they were an editorial board member of Frontiers, at the time of submission. This had no impact on the peer review process and the final decision.

Publisher's note

frontiers in Cardiovascular Medicine

ORIGINAL RESEARCH
published: 14 October 2021
doi: 10.3389/fcvm.2021.719452

The Long-Term Results of Three Catheter Ablation Methods in Patients With Paroxysmal Atrial Fibrillation: A 4-Year Follow-Up Study

*Ling You, Xiaohong Zhang, Jing Yang, Lianxia Wang, Yan Zhang and Ruiqin Xie**

Second Hospital of Hebei Medical University, Shijiazhuang, China

Aims: Catheter ablation of paroxysmal atrial fibrillation (PAF) has been shown to be effective and safe. However, recurrence of PAF varies between 10 and 30% for radiofrequency ablation. There have been no reports comparing long-term recurrence rates following radiofrequency ablation, cryoablation, and three-dimensional guided cryoablation plus radiofrequency ablation. The aim of this study was to observe the long-term recurrence rate of PAF when treated by these three catheter ablation methods, and to explore clinical factors that can potentially predict PAF recurrence following catheter ablation.

Methods: There were 238 patients involved in this study, including 106 radiofrequency (RF) ablation cases (RF group), 66 cryoablation cases (Freeze group), and 66 cases treated by three-dimensional guided cryoablation combined with radiofrequency ablation (Freeze-plus-RF group). All patients underwent standardized follow-up. The recurrence rate of atrial fibrillation (AF) in the three groups was calculated. Predictive factors for the recurrence of AF were also investigated.

Results: At 48 months (the median follow-up period), the sinus rhythm maintenance rate was 77.4% in the RF group, 72.7% in the Freeze group, and 81.8% in the Freeze-plus-RF group. The maintenance rate of sinus rhythm was highest in the Freeze-plus-RF group, but differences among the three groups were not statistically significant. Further analysis found that the preoperative left atrial appendage emptying velocity (LAAEV) (recurrence vs. no recurrence, 56.58 ± 18.37 vs. 65.59 ± 18.83, respectively, $p = 0.003$), left atrial (LA) anteroposterior dimension (recurrence vs. no recurrence, 36.56 ± 4.65 vs. 35.00 ± 4.37, respectively; $p = 0.028$), and LA vertical dimension (recurrence vs. no recurrence, 56.31 ± 6.96 vs. 53.72 ± 6.52, respectively; $p = 0.035$) were related to postoperative recurrence. Multiple Cox regression analysis showed that only LAAEV was predictive of postoperative recurrence of PAF (hazard ratio: 0.979; 95% confidence interval: 0.961–0.997).

Conclusion: Our study found that there was no statistically significant difference in long-term recurrence rates among the RF, Freeze, and Freeze-plus-RF groups. Preoperative LAAEV is an independent predictor of postoperative recurrence of PAF.

Keywords: catheter ablation, paroxysmal atrial fibrillation, recurrence, cryoablation, cryoablation plus radiofrequency ablation, radiofrequency ablation

OPEN ACCESS

Edited by:
Robert Sheldon, University of Calgary, Canada

Reviewed by:
Osmar Antonio Centurion, National University of Asunción, Paraguay
Kumar Narayanan, Medicover Hospitals, India

****Correspondence:***
Ruiqin Xie
xieruiqin88@163.com

Specialty section:
This article was submitted to Cardiac Rhythmology, a section of the journal Frontiers in Cardiovascular Medicine

Received: *02 June 2021*
Accepted: *30 August 2021*
Published: *14 October 2021*

Citation:
You L, Zhang X, Yang J, Wang L, Zhang Y and Xie R (2021) The Long-Term Results of Three Catheter Ablation Methods in Patients With Paroxysmal Atrial Fibrillation: A 4-Year Follow-Up Study. Front. Cardiovasc. Med. 8:719452. doi: 10.3389/fcvm.2021.719452

INTRODUCTION

Atrial fibrillation (AF) occurs in 0.71% of the Chinese population aged 35 years or older, and the incidence increases sharply with age (1). In patients who have AF even after medical treatment, catheter ablation is an alternative approach that can reduce complications and improve quality of life (2, 3).

Previous studies have confirmed the effectiveness and safety of catheter ablation in the treatment of paroxysmal atrial fibrillation (PAF) (4–6). Electrical isolation of the pulmonary vein (PV) is essential for catheter ablation of AF, which traditionally is achieved by radiofrequency catheter ablation (RCA) (7). However, in recent years a second method, cryoablation, has become a popular surgical approach for catheter ablation of atrial fibrillation (8). The PV must be treated for a shorter time with cryoablation than with RCA, and there are fewer postoperative complications (9, 10). Cryoablation produces a clear boundary, less thrombosis, and a lower incidence of cardiac perforation (11, 12).

However, due to the size and shape of the cryoablation equipment and the anatomical structure of the pulmonary vein, complete pulmonary vein isolation is in some cases difficult to achieve during cryoablation (13). We combined radiofrequency (RF) and cryoablation, called three-dimensional mapping guided cryoablation plus RF (Freeze plus RF), to achieve more perfect pulmonary vein isolation (14).

Recent studies have reported on the rate of recurrence of PAF 1–2 years following cryoablation and three-dimensional mapping-guided cryoablation (14), but the rate over longer periods has not been reported. This study aims to observe the long-term recurrence rate of these three approaches to catheter ablation in patients with PAF and explore potential clinical factors that can predict PAF recurrence after catheter ablation.

MATERIALS AND METHODS

Study Population

This study involved 275 patients whose first catheter ablation of PAF was conducted in our center from March 2015 to March 2017. Among them, 238 patients were monitored for 4 years, and this cohort was divided into one of the three treatment groups: RCA, 106 patients; Freeze, 66; and Freeze plus RF, 66.

PAF is defined as spontaneous cessation of atrial fibrillation within 7 days of onset. Patient inclusion criteria included the following: (1) the ablation was the first for the patient, (2) there was no evidence of valvular heart disease, (3) there were more than two episodes of atrial fibrillation within the previous 6 months for which antiarrhythmic medication had been ineffective, and (4) the patient was followed up after the operation. Patients with atrial thrombus visible in transesophageal echocardiography were excluded.

All patients signed an informed consent form before their operation, and this study was approved by the ethics committee of the second hospital of Hebei Medical University.

Catheter Ablation Procedure

Radiofrequency Ablation

Each patient underwent circumferential pulmonary vein isolation, with no additional ablation at extrapulmonary sites unless the patient was diagnosed with atrial flutter before the operation. In 3D electro-anatomical mapping (Carto 3, Biosense Webster), a mapping catheter is used to record pulmonary vein potentials before, during, and after circumferential pulmonary vein ablation (Lasso® NAV eco, Biosense Webster). All patients in the radiofrequency group were treated using a 3.5-mm irrigated tip ablation catheter (SmartTouch, Biosense Webster). The operation was carried out for 20–30 min after blocking entrance and exit of pulmonary vein potentials. Pulmonary vein potential conduction was then monitored, and if there was recovery, ablation was continued. Tricuspid isthmus ablation was carried out for patients with a preoperative diagnosis of atrial flutter. All patients had CT scans of the pulmonary vein-left atrium before the operation to visualize the structure of the left atrium and pulmonary veins. Patients who experienced recurrence of atrial fibrillation during the first 3 months of postoperative follow-up were not considered for repeat radiofrequency ablation.

Cryoablation

Cryoablation was carried out with a single cryoballoon (Arctic Front Advance™ Cardiac CryoAblation Catheter, Medtronic, Minneapolis, MN) under fluoroscopy. The diameter of the cryoballoon was 28 mm or 23 mm according to the results of the pulmonary vein CT scan. The circular mapping catheter (Achieve, Medtronic) was first passed through the balloon catheter into the lumen of the pulmonary vein. The longest application of the first generation cryoballoon was 240 s and the lowest temperature was −60°C, while the longest application of the second generation cryoballoon was 180 s and the lowest temperature was −55°C. If two applications of the cryoablation were unsuccessful, additional cryoablation treatments could be carried out until complete electrical isolation of the pulmonary veins and bidirectional block of electrical conduction between the pulmonary veins and left atrium were achieved. No patients had any residual PV connection after acute application of the cryoballoon. If the patient had atrial flutter during freezing, additional radiofrequency ablation was applied.

Among the 66 patients in the Freeze group, 24 (36.4%) used the first generation cryoballoon. Before carrying out right pulmonary vein ablation, a secondary catheter was placed into the superior vena cava. During cryoablation, a cycle time of 999 ms was used to make the right phrenic nerve pulsate. If diaphragm movement was reduced or became undetectable, cryoablation was immediately terminated.

Cryoablation Combined With Radiofrequency Ablation

Cryoballoon ablation combined with RF ablation was used under the guidance of the EnSite NavX 3D mapping system. A circular mapping catheter (Achieve, Medtronic) was used to construct the configuration and build the structures of the pulmonary vein. The cryoballoon was positioned during

cryoablation according to the results of the 3D mapping. At least 2 cryoablations were conducted for each pulmonary vein. If there was still electrical conduction in the pulmonary veins after two cryoablations, radiofrequency ablation could be used at additional locations, and complete electrical isolation of the pulmonary veins and bidirectional block of electrical conduction between the pulmonary veins and left atrium could finally be achieved. Among the 66 patients in the Freeze-plus-RF group, 7 (10.6%) used the first generation cryoballoon. An additional RF ablation was required to achieve pulmonary vein isolation in 9 patients. If the patient had atrial flutter during freezing, additional RF ablation was applied.

Patient Follow-Up

In this study, patients were followed up weekly in the first month and then visited at 2, 3, 6, 9, and 12 months after discharge. The patients were then followed up once a year. ECGs, 24-h Holter records, and echocardiography images were examined at all visits. Patients with any palpitation discomfort during this period could come to the hospital at any time. In this study, recurrence of atrial fibrillation was defined by an ECG or 24-h ECG record of atrial fibrillation, atrial flutter, or atrial tachycardia lasting more than 30 s.

Echocardiographic Examination

Examinations of real-time 3D ultrasound, 2D ultrasound, and transesophageal and Doppler echocardiography were carried out to measure left atrial size and function in all patients using a cardiac ultrasound device (iE33 machine equipped with X3-1 and X7-2t, Philips Medical Systems, Eindhoven, the Netherlands). Ultrasound parameters were measured under sinus rhythm in all patients. Left atrial (LA) dimensions were measured in the parasternal long axis view using 2D methods. LAMax refers to left atrial volume at the end of systole before opening of the mitral valve, while LAMin refers to the end of diastole before closing of the mitral valve. All patients underwent preoperative transesophageal echocardiography to obtain left atrial appendage emptying velocity (LAAEV). Left atrial appendage images were obtained from the base of the heart with the probe rotated by 0°, 45°, 90°, and 180°. LAAEV was measured using 1 representative value when rhythm was stable, or by averaging the value of 5 consecutive sinus waves when rhythm was variable due to respiration.

Statistical Analysis

- Continuous variables are presented as mean ± standard deviation, and categorical variables as percentage with counts. Differences in continuous data between groups were compared using ANOVA. Chi-square tests or Fisher's exact tests were used for categorical variables. Receiver operating characteristic analysis was performed to determine the optimal cut-off value for the LAAEV in predicting AF recurrence after a single procedure. Survival curves were generated by Kaplan-Meier analysis.
- To evaluate predictors for recurrence of AF, Cox regression analysis was performed. All the predictors were evaluated by univariate Cox regression. Factors that were statistically significant in the univariate model were further investigated using the multiple Cox regression model.
- $P < 0.05$ was considered statistically significant. SPSS software (version 26.0, Chicago, IL) was used.

TABLE 1 | Patient characteristics at baseline before ablation.

	RF (106 cases)	Freeze (66 cases)	Freeze plus RF (66 cases)	*P*-value
Age, years	58.05 ± 10.04	59.20 ± 11.89	61.68 ± 11.57	0.110
Male sex, n (%)	64 (60.4)	35 (53.0)	41 (62.1)	0.518
Diabetes, n (%)	13 (12.3)	10 (15.2)	14 (21.2)	0.288
Hypertension, n (%)	48 (45.3)	40 (57.6)	38 (57.6)	0.001
SBP, mmHg	133.98 ± 19.73	130.45 ± 15.72	135.21 ± 18.58	0.297
DBP, mmHg	83.10 ± 14.29	81.56 ± 11.97	82.17 ± 11.29	0.738
Heart rate, beats per minute	73.47 ± 15.27	75.77 ± 16.83	72.94 ± 16.22	0.443
Heart failure, n (%)	5 (4.7)	4 (6.1)	6 (9.1)	0.515
History of CAD, n (%)	1 (0.9)	1 (1.5)	2 (3.0)	0.581
Smoking, n (%)	15 (14.2)	9 (13.6)	14 (21.2)	0.390
Alcohol, n (%)	12 (11.3)	6 (9.1)	13 (19.7)	0.152
Phrenic nerve injury, n (%)	0	1 (1.5)	1 (1.5)	0.509
Vascular injuries (%)	2 (1.8)	1 (1.5)	1 (1.5)	0.216
Gastrointestinal bleeding, n (%)	1 (0.9)	0	0	0.458
Pericardial tamponade, n (%)	1 (0.9)	0	0	0.458

RESULTS

Patients

There were 238 patients enrolled in this study, including 106 patients in the RF group (mean age 58.05 ± 10.04 years), 66 patients in the Freeze group (mean age 59.2 ± 11.89 years), and 66 patients in the Freeze-plus-RF group (mean age 61.68 ± 11.57 years). Baseline demographics of the patients are shown in **Table 1**. Except for the low proportion of hypertensive patients in the RF group, there were no statistically significant differences between the three groups. The operation achieved complete pulmonary vein isolation for all patients. One patient developed pericardial effusion 2 h after the operation and recovered after pericardiocentesis. During follow-up, one patient developed gastrointestinal bleeding 3 months after surgery. There were no operation-related deaths, although two patients died of gastric cancer, and one died in an accident.

Clinical Outcomes After a Single Procedure

Survival curves for the three groups are shown in **Figure 1**. The median follow-up was 48 months for all three groups. The recurrence rates at 1, 2, 3, and 4 years for the RF group were 15.1,

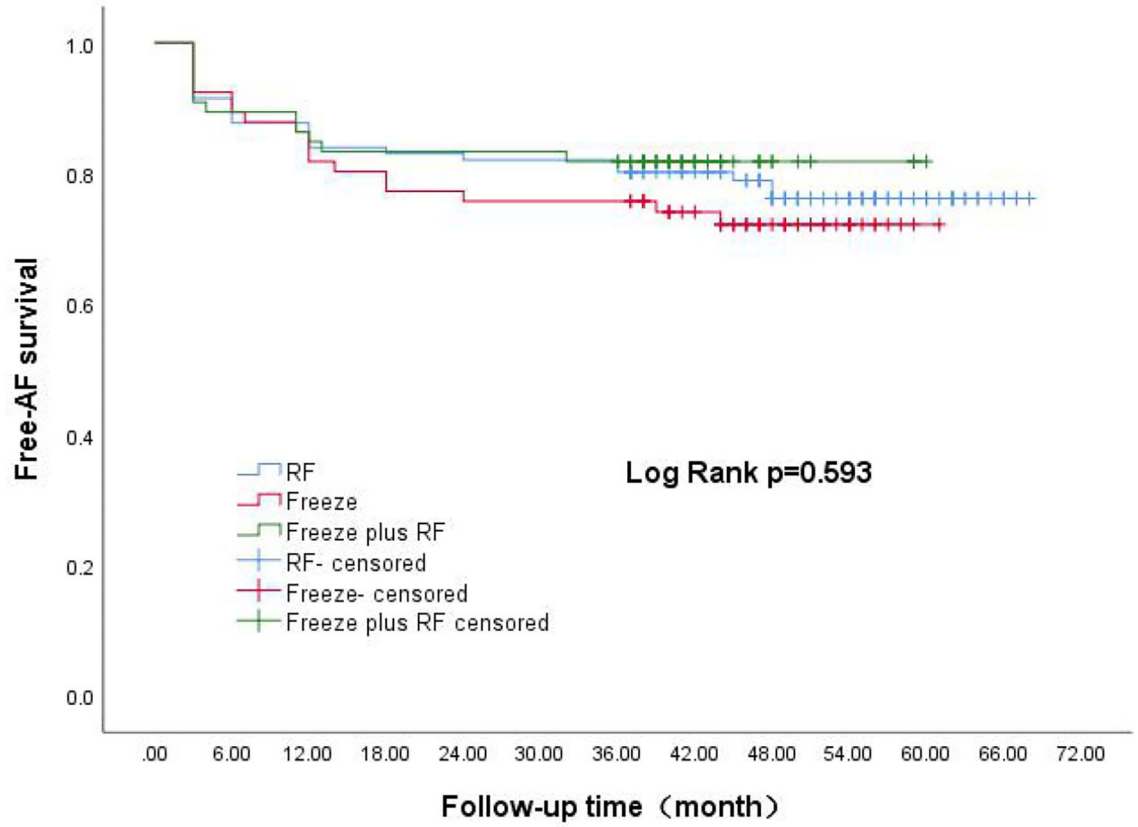

FIGURE 1 | Kaplan-Meier analysis of AF-free rate after three different surgical procedures. AF, atrial fibrillation.

TABLE 2 | Sinus rhythm after different periods of follow-up in the 3 groups.

	3 months	6 months	12 months	24 months	36 months	48 months
RF	97 (91.5%)	93 (87.7%)	90 (84.9%)	87 (82.1%)	85 (80.2%)	82 (77.4%)
Freeze	61 (92.4%)	59 (89.4%)	54 (81.8%)	51 (77.3%)	50 (75.8%)	48 (72.7%)
Freeze 3D	60 (90.9%)	59 (89.4%)	55 (83.3%)	55 (83.3%)	54 (81.8%)	54 (81.8%)
p	0.951	0.923	0.866	0.634	0.666	0.460

17.9, 19.8, and 22.6%, respectively. The corresponding recurrence rates were 18.2, 22.7, 24.2, and 27.3% for the Freeze group and 16.8, 16.8, 18.2, and 18.2% for the Freeze-plus-RF group. Our study found that most recurrence of AF occurred in the first year after AF surgery, which accounted for 70.7% (RF), 66.7% (Freeze), and 81.8% (Freeze plus RF) of all recurrences ($P = 0.234$, **Table 2**). At 4 years, the maintenance rate of sinus rhythm was highest in the Freeze-plus-RF group (81.8%), but this was not significantly different from the RF (77.4%) and Freeze (72.7%) groups ($P = 0.593$). This may be due to the combination of the two ablation techniques used to achieve more complete pulmonary vein isolation. Of the recurrent patients, there was one case of atrial flutter in the Freeze group, and one case each of atrial flutter and atrial tachycardia in the Freeze-plus-RF group. All other atrial arrhythmias were atrial fibrillation.

Factors Associated With Recurrence of Atrial Fibrillation After Catheter Ablation

LAAEV was significantly lower in recurrent than in non-recurrent patients (56.58 ± 18.37 vs. 65.59 ± 18.83, respectively; $p = 0.003$). As shown in **Table 3**, the LA anteroposterior and vertical dimensions in recurrent patients (36.56 ± 4.65 and 56.31 ± 6.96, respectively) were both larger than in non-recurrent patients (35.00 ± 4.37 and 53.72 ± 6.52, respectively) ($p = 0.028$ and $p = 0.035$, respectively, for the two LA dimensions). All factors were further analyzed by the Cox regression model. Patients with higher LAAEV had a lower risk of recurrence of PAF (hazard ratio: 0.979; 95% confidence interval: 0.961–0.997) according to multivariate Cox regression (**Table 4**). Receiver operating characteristic curve analysis showed that the optimal cut-off value for LAAEV was 59.5 cm/s for predicting late recurrence of AF after a single procedure with a sensitivity of 62%

TABLE 3 | Characteristics of recurrence and no-recurrence patients.

	All patients	Recurrence	No recurrence	*P*-value (recurrence vs. no recurrence)
Age, years	59.37 ± 11.06	57.30 ± 10.32	59.98 ± 11.22	0.117
Male, n (%)	130 (54.6)	26 (48.1)	114 (62.0)	0.070
Diabetes, n (%)	37 (15.6)	11 (20.4)	26 (14.1)	0.266
Hypertension n (%)	126 (52.9)	29 (53.7)	97 (52.7)	0.898
SBP (mm Hg)	133.34 ± 18.39	131.39 ± 22.11	133.91 ± 17.17	0.376
DBP (mm Hg)	82.41 ± 12.84	82.54 ± 15.66	82.37 ± 11.94	0.934
Heart rate, beats per minute	73.96 ± 15.96	74.04 ± 15.61	73.94 ± 16.10	0.969
Smoking, n (%)	44 (18.5)	9 (16.7)	35 (19.0)	0.695
Alcohol, n (%)	31 (13.0)	6 (11.1)	25 (13.6)	0.635
History of CAD, n (%)	4 (1.6)	1 (1.8)	3 (1.6)	0.911
Heart failure, n (%)	14 (5.9)	6 (11.1)	8 (4.4)	0.065
LVEF (%)	55.91 ± 16.52	57.59 ± 16.41	55.35 ± 16.57	0.421
LA anteroposterior dimension (mm)	35.37 ± 4.48	36.56 ± 4.65	35.00 ± 4.37	0.028
LA transverse dimension (mm)	38.35 ± 6.95	38.76 ± 4.59	38.21 ± 7.58	0.688
LA vertical dimension (mm)	54.34 ± 6.69	56.31 ± 6.96	53.72 ± 6.52	0.035
LAAEV (cm/s)	63.56 ± 19.07	56.58 ± 18.37	65.59 ± 18.83	0.003
LAVmax (mL/m^2)	55.67 ± 17.19	59.72 ± 15.40	54.37 ± 17.60	0.145
LAVmin (mL/m^2)	27.66 ± 12.40	30.97 ± 11.65	26.60 ± 12.51	0.099

SBP, systolic blood pressure; DBP, diastolic blood pressure; LVEF, left ventricular ejection fraction; LAAEV, left atrial appendage emptying velocity; LAVmax, left atrial maximum volume index; LAVmin, left atrial minimum volume index.

and specificity of 61%. The area under the curve was 0.631 ($P = 0.005$; **Figure 2**).

DISCUSSION

This is the first study to compare long-term recurrence of PAF among patients treated by radiofrequency ablation, cryoablation, or cryoablation plus RF. More than half the recurrences in each of the three groups occurred in the first year after surgery. The study also found that LAAEV was a predictor of late recurrence after ablation.

Our study found that there were no differences in long-term recurrence among the RF ablation, cryoablation, and cryoablation-plus-RF groups. Previous studies have reported no difference in recurrence rate between radiofrequency ablation and cryoablation (10, 12, 15–17), which is consistent with our results. A meta-analysis reported by Maltoni et al. (10) showed no significant difference in efficacy between radiofrequency ablation and cryoablation in avoiding recurrence of atrial arrhythmia in patients with paroxysmal atrial fibrillation. Some studies have used radiofrequency ablation for supplementary treatment when complete pulmonary vein isolation was not achieved during cryoablation (15, 18), however, there was no comparison of recurrence between RF, cryoablation, and cryoablation supplemented by RF ablation. Kettering et al. (13) used both cryoballoon and radiofrequency ablation during secondary surgery on patients with recurrence following cryoballoon ablation. In their study, radiofrequency ablation was safer and more effective for patients with recurrence after cryoballoon ablation.

Several risk factors have been reported to be associated with recurrence of AF after ablation, such as hypertension and LA size and volume, among others (19–21). Two studies have found that a decrease in LAAEV is a predictor of recurrence of atrial fibrillation 1 year after radiofrequency ablation (22, 23). A decrease in LAAEV can also be used as a predictor of cardioversion in patients with nonvalvular AF (24–26). Our study found that high LAAEV was associated with a lower rate of AF recurrence. LAAEV is an important indicator of left atrial function (27). During development of atrial fibrillation, structural remodeling, atrial fibrosis and abnormal formation of atrial matrix will occur, resulting in decline of the left atrial function. These mechanisms are also the basis of AF recurrence after both drug and surgical cardioversion (28).

Wang et al. (6) reported that more than two-thirds of AF recurrence were in the first year after single or multiple procedures. Other studies have also shown that the rate of early recurrence of AF (ERAF, defined as AF recurrence within a 3-month blanking period) ranged from approximately 38.2–58.6% after a single ablation, and that ERAF significantly predicted late recurrence of AF (29–33). The mechanism of ERAF is unclear but is generally considered to involve acute thermal injury and an inflammatory response caused by radiofrequency energy and a transient reversible process (34, 35). In our study, we found that more than half of all recurrences were in the first year after a single operation. In addition to the above factors, others such as acute thermal injury and inflammatory response caused by catheter ablation may contribute to recurrence of AF. In addition, recovery of electrical connectivity between the pulmonary vein and left atrium, as well as trigger foci outside the pulmonary vein, may be more likely to occur 1 year after AF surgery.

Patients in this study came from a single center, which limited data variability. Both first and second generation cryoballoons were used with the Freeze and the Freeze-plus-RF groups, and there may have been differences in surgical outcomes using the two types of balloons. No patients had implanted devices that allowed continuous rhythm monitoring, and so some recurrences may have gone undetected. The main limitation of this article is that it was a non-randomized observational study, introducing potential bias which may have confounded the results.

CONCLUSION

Our study found that long-term recurrence rates were not significantly different between the three surgical methods. The first year after the operation had the highest rate of recurrence following catheter ablation. Left atrial appendage emptying

TABLE 4 | Univariate and multivariate Cox regression analysis to recognize predictors of AF recurrence after a single procedure.

	Univariate			Multivariate		
Variables	**HR**	**CI**	***p***	**OR**	**CI**	***p***
Age, years	0.984	0.962–1.006	0.144			
Male, n (%)	0.619	0.363–1.056	0.079			
SBP (mm Hg)	0.994	0.979–1.009	0.420			
DBP (mm Hg)	1.000	0.979–1.021	0.988			
Heart rate, beats per minute	1.000	0.983–1.017	0.998			
Smoking, n (%)	0.881	0.431–1.802	0.728			
Alcohol, n (%)	0.846	0.362–1.978	0.700			
Hypertension, n (%)	1.056	0.618–1.804	0.841			
Diabetes, n (%)	1.510	0.779–2.930	0.222			
History of CAD, n (%)	1.153	0.159–8.350	0.888			
Heart failure, n (%)	2.148	0.919–5.020	0.078			
LVEF (%)	1.008	0.990–1.026	0.378			
LAAEV (cm/s)	0.976	0.961–0.992	0.003	0.979	0.961–0.997	0.023
LA anteroposterior dimension (mm)	1.066	1.004–1.132	0.037	1.049	0.963–1.143	0.276
LA vertical dimension (mm)	1.053	1.003–1.105	0.038	1.029	0.971–1.090	0.335
LA transverse dimension (mm)	1.008	0.964–1.054	0.740			
LAVmax (ml/m^2)	1.014	0.995–1.034	0.154			
LAVmin (ml/m^2)	1.023	0.996–1.050	0.094			

SBP, systolic blood pressure; DBP, diastolic blood pressure; LVEF, left ventricular ejection fraction; LAAEV, left atrial appendage emptying velocity; LAVmax, left atrial maximum volume index; LAVmin, left atrial minimum volume index.

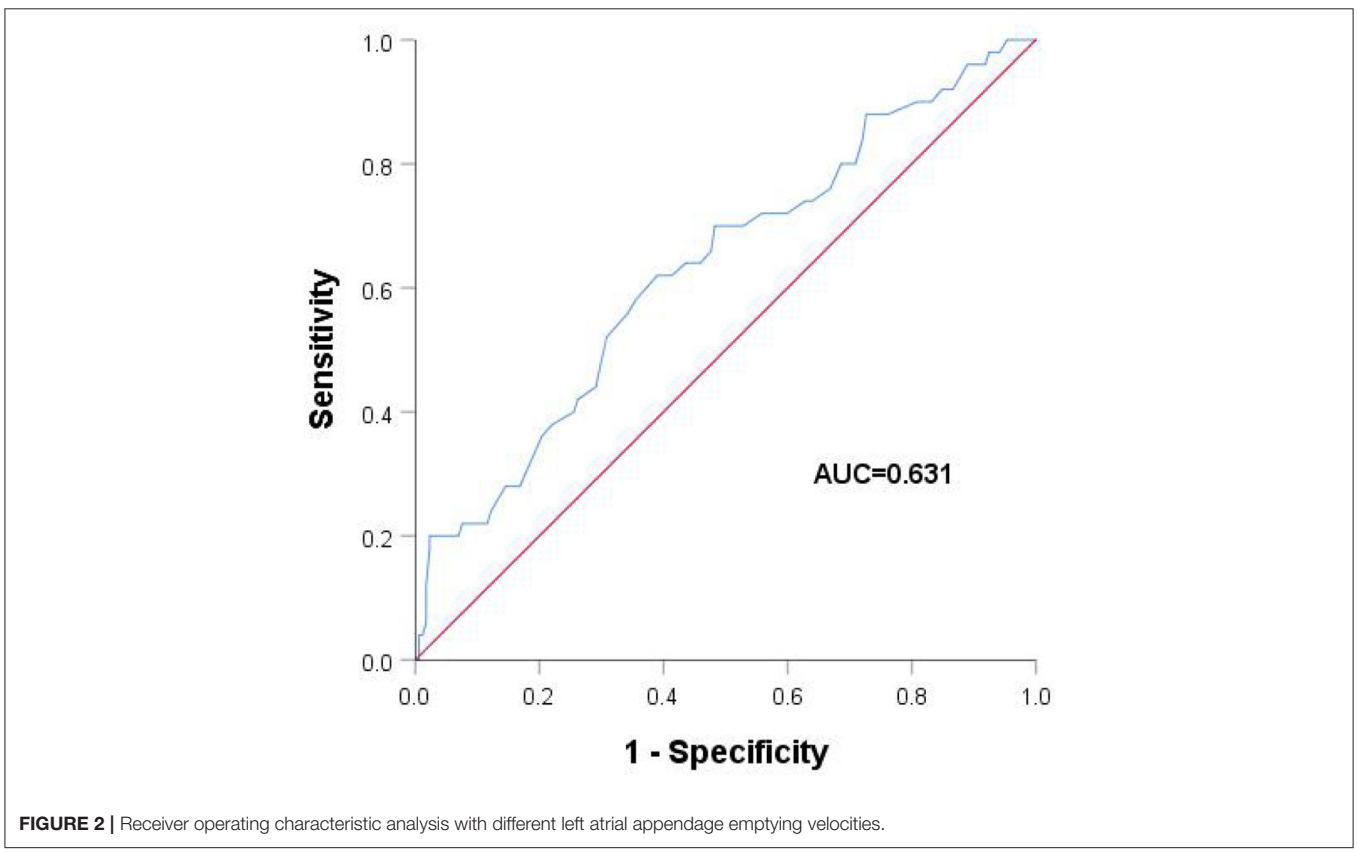

FIGURE 2 | Receiver operating characteristic analysis with different left atrial appendage emptying velocities.

velocity is a predictor of long-term recurrence of paroxysmal atrial fibrillation after a single operation.

DATA AVAILABILITY STATEMENT

The original contributions presented in the study are included in the article/supplementary material, further inquiries can be directed to the corresponding author.

ETHICS STATEMENT

The studies involving human participants were reviewed and approved by the Second Hospital of Hebei Medical University. The patients/participants provided their written informed consent to participate in this study. Written informed consent was obtained from the individual(s) for the publication of any potentially identifiable images or data included in this article.

AUTHOR CONTRIBUTIONS

LY is the first author responsible for thesis writing and data statistics. XZ, JY, LW, and YZ were responsible for data collection and follow-up. RX is responsible for the design of research ideas. All authors contributed to the article and approved the submitted version.

REFERENCES

1. Wang Z, Chen Z, Wang X, Zhang L, Li S, Tian Y, et al. The disease burden of atrial fibrillation in china from a national cross-sectional survey. *Am J Cardiol.* (2018) 122:793–8. doi: 10.1016/j.amjcard.2018.05.015
2. Ichijo S, Miyazaki S, Kusa S, Nakamura H, Hachiya H, Kajiyama T, et al. Impact of catheter ablation of atrial fibrillation on long-term clinical outcomes in patients with heart failure. *J Cardiol.* (2018) 72:240–6. doi: 10.1016/j.jjcc.2018.02.012
3. Blomström-Lundqvist C, Gizurarson S, Schwieler J, Jensen SM, Bergfeldt L, Kennebäck G, et al. Effect of catheter ablation vs antiarrhythmic medication on quality of life in patients with atrial fibrillation: the CAPTAF randomized clinical trial. *JAMA.* (2019) 321:1059–68. doi: 10.1001/jama.2019.0335
4. Jongnarangsin K, Suwanagool A, Chugh A, Crawford T, Good E, Pelosi F, et al. Effect of catheter ablation on progression of paroxysmal atrial fibrillation. *J Cardiovasc Electrophysiol.* (2012) 23:9–14. doi: 10.1111/j.1540-8167.2011.02137.x
5. Hakalahti A, Biancari F, Nielsen JC, Raatikainen MJ. Radiofrequency ablation vs. antiarrhythmic drug therapy as first line treatment of symptomatic atrial fibrillation: systematic review and meta-analysis. *Europace.* (2015) 17:370–8. doi: 10.1093/europace/euu376
6. Wang Y, Xu Y, Ling Z, Chen W, Su L, Du H, et al. Radiofrequency catheter ablation for paroxysmal atrial fibrillation: outcomes during a 3-year follow-up period. *J Int Med Res.* (2019) 47:1636–48. doi: 10.1177/0300060519828522
7. Calkins H, Hindricks G, Cappato R, Cappato R, Kim Y-H, Saad EB, et al. 2017 HRS/EHRA/ECAS/APHRS/SOLAECE expert consensus statement on catheter and surgical ablation of atrial fibrillation. *Europace.* (2018) 20:e1–e160. doi: 10.1016/j.hrthm.2017.05.012
8. Chen S, Schmidt B, Bordignon S, Bologna F, Perrotta L, Nagase T, et al. Atrial fibrillation ablation using cryoballoon technology: recent advances and practical techniques. *J Cardiovasc Electrophysiol.* (2018) 29:932–43. doi: 10.1111/jce.13607
9. Boveda S. Cryoballoon ablation in atrial fibrillation: advantages and drawbacks. *Rev Port Cardiol.* (2017) 36(Suppl. 1):19–24. doi: 10.1016/j.repc.2017.09.008
10. Maltoni S, Negro A, Camerlingo MD, Pecoraro V, Sassone B, Biffi et al. Comparison of cryoballoon and radiofrequency ablation techniques for atrial fibrillation: a meta-analysis. *J Cardiovasc Med (Hagerstown).* (2018) 19:725–38. doi: 10.2459/JCM.0000000000000725
11. Mukai M, Miyazaki S, Hasegawa K, Ishikawa E, Aoyama D, Nodera M, et al. Cryothermal atrial linear ablation in patients with atrial fibrillation: an insight from the comparison with radiofrequency atrial linear ablation. *J Cardiovasc Electrophysiol.* (2020) 31:1075–82. doi: 10.1111/jce.14420
12. Wasserlauf J, Pelchovitz DJ, Rhyner J, Verma N, Bohn M, Li Z, et al. Cryoballoon versus radiofrequency catheter ablation for paroxysmal atrial fibrillation. *Pacing Clin Electrophysiol.* (2015) 38:483–9. doi: 10.1111/pace.12582
13. Kettering K, Gramley F. Catheter ablation of atrial fibrillation: radiofrequency catheter ablation for redo procedures after cryoablation. *World J Cardiol.* (2013) 5:280–7. doi: 10.4330/wjc.v5.i8.280
14. You L, Yao L, Zhou B, Jin L, Yin H, Wu J, et al. Effects of different ablation strategies on long-term left atrial function in patients with paroxysmal atrial fibrillation: a single-blind randomized controlled trial. *Sci Rep.* (2019) 9:7695. doi: 10.1038/s41598-019-44168-5
15. Kühne M, Suter Y, Altmann D, Ammann P, Schaer B, Osswald S, et al. Cryoballoon versus radiofrequency catheter ablation of paroxysmal atrial fibrillation: biomarkers of myocardial injury, recurrence rates, and pulmonary vein reconnection patterns. *Heart Rhythm.* (2010) 7:1770–6. doi: 10.1016/j.hrthm.2010.08.028
16. Linhart M, Bellmann B, Mittmann-Braun E, Schrickel JW, Bitzen A, Andrié R, et al. Comparison of cryoballoon and radiofrequency ablation of pulmonary veins in 40 patients with paroxysmal atrial fibrillation: a case-control study. *J Cardiovasc Electrophysiol.* (2009) 20:1343–8. doi: 10.1111/j.1540-8167.2009.01560.x
17. Yokokawa M, Chugh A, Latchamsetty R, Ghanbari H, Crawford T, Jongnarangsin K, et al. Ablation of paroxysmal atrial fibrillation using a second-generation cryoballoon catheter or contact-force sensing radiofrequency ablation catheter: a comparison of costs and long-term clinical outcomes. *J Cardiovasc Electrophysiol.* (2018) 29:284–90. doi: 10.1111/jce.13378
18. Kubala M, Hermida JS, Nadji G, Quenum S, Traulle S, Jarry G. Normal pulmonary veins anatomy is associated with better AF-free survival after cryoablation as compared to atypical anatomy with common left pulmonary vein. *Pacing Clin Electrophysiol.* (2011) 34:837–43. doi: 10.1111/j.1540-8159.2011.03070.x
19. den Uijl DW, Tops LF, Delgado V, Schuijf JD, Kroft LJ, de Roos A, et al. Effect of pulmonary vein anatomy and left atrial dimensions on outcome of circumferential radiofrequency catheter ablation for atrial fibrillation. *Am J Cardiol.* (2011) 107:243–9. doi: 10.1016/j.amjcard.2010.08.069
20. Cai L, Yin Y, Ling Z, Su L, Liu Z, Wu J, et al. Predictors of late recurrence of atrial fibrillation after catheter ablation. *Int J Cardiol.* (2013) 164:82–7. doi: 10.1016/j.ijcard.2011.06.094
21. Kato S, Foppa M, Roujol S, Basha T, Berg S, Kissinger KV, et al. Left ventricular native T1 time and the risk of atrial fibrillation recurrence after pulmonary vein isolation in patients with paroxysmal atrial fibrillation. *Int J Cardiol.* (2016) 203:848–54. doi: 10.1016/j.ijcard.2015.11.073
22. Ma XX, Zhang YL, Hu B, Jiang WJ, Wang M, Zheng DY, et al. Association between left atrial appendage emptying velocity, N-terminal plasma brain natriuretic peptide levels, and recurrence of atrial fibrillation after catheter ablation. *J Interv Card Electrophysiol.* (2017) 48:343–50. doi: 10.1007/s10840-016-0216-4
23. He Y, Zhang B, Zhu F, Hu Z, Zhong J, Zhu W. Transesophageal echocardiography measures left atrial appendage volume and function and predicts recurrence of paroxysmal atrial fibrillation

after radiofrequency catheter ablation. *Echocardiography*. (2018) 35:985–90. doi: 10.1111/echo.13856
24. Pálinkás A, Antonielli E, Picano E,Pizzuti A, Varga A, Nyúzó B, et al. Clinical value of left atrial appendage flow velocity for predicting of cardioversion success in patients with non-valvular atrial fibrillation. *Eur Heart J.* (2001) 22:2201–8. doi: 10.1053/euhj.2001.2891
25. Antonielli E, Pizzuti A, Pálinkás A, Tanga M, Gruber N, Michelassi C, et al. Clinical value of left atrial appendage flow for prediction of long-term sinus rhythm maintenance in patients with nonvalvular atrial fibrillation. *J Am Coll Cardiol.* (2002) 39:1443–9. doi: 10.1016/S0735-1097(02)01800-4
26. Akdeniz B, Badak O, Bariş N, Aslan O, Kirimli O, Göldeli O, et al. Left atrial appendage-flow velocity predicts cardioversion success in atrial fibrillation. *Tohoku J Exp Med.* (2006) 208:243–50. doi: 10.1620/tjem.208.243
27. Hwang SH, Oh YW, Kim MN, Park SM, Shim WJ, Shim J, et al. Relationship between left atrial appendage emptying and left atrial function using cardiac magnetic resonance in patients with atrial fibrillation: comparison with transesophageal echocardiography. *Int J Cardiovasc Imaging.* (2016) 32(Suppl. 1):163–71. doi: 10.1007/s10554-016-0893-1
28. Pandozi C, Santini M. Update on atrial remodelling owing to rate; does atrial fibrillation always 'beget' atrial fibrillation? *Eur Heart J.* (2001) 22:541–53. doi: 10.1053/euhj.2000.2441
29. Liang JJ, Elafros MA, Chik WW, Santangeli P, Zado ES, Frankel DS, et al. Early recurrence of atrial arrhythmias following pulmonary vein antral isolation: timing and frequency of early recurrences predicts long-term ablation success. *Heart Rhythm.* (2015) 12:2461–8. doi: 10.1016/j.hrthm.2015.07.015
30. Miyazaki S, Taniguchi H, Nakamura H, Takagi T, Iwasawa J, Hachiya H, et al. Clinical significance of early recurrence after pulmonary vein antrum isolation in paroxysmal atrial fibrillation – insight into the mechanism. *Circ J.* (2015) 79:2353–9. doi: 10.1253/circj.CJ-15-0475
31. Pokushalov E, Romanov A, Corbucci G, Artyomenko S, Turov A, Shirokova N, et al. Use of an implantable monitor to detect arrhythmia recurrences and select patients for early repeat catheter ablation for atrial fibrillation: a pilot study. *Circ Arrhythm Electrophysiol.* (2011) 4:823–31. doi: 10.1161/CIRCEP.111.964809
32. Willems S, Khairy P, Andrade JG, Hoffmann BA, Levesque S, Verma A, et al. Redefining the blanking period after catheter ablation for paroxysmal atrial fibrillation: insights from the ADVICE (Adenosine Following Pulmonary Vein Isolation to Target Dormant Conduction Elimination) Trial. *Circ Arrhythm Electrophysiol.* (2016) 9:e003909. doi: 10.1161/CIRCEP.115.003909
33. Yanagisawa S, Inden Y, Kato H, Fujii A, Mizutani Y, Ito T, et al. Effect and significance of early Reablation for the treatment of early recurrence of atrial fibrillation after catheter ablation. *Am J Cardiol.* (2016) 118:833–41. doi: 10.1016/j.amjcard.2016.06.045
34. Koyama T, Tada H, Sekiguchi Y, Arimoto T, Hamasaki H, Kuroki K, et al. Prevention of atrial fibrillation recurrence with corticosteroids after radiofrequency catheter ablation: a randomized controlled trial. *J Am Coll Cardiol.* (2010) 56:1463–72. doi: 10.1016/j.jacc.2010.04.057
35. Lim HS, Schultz C, Dang J, Alasady M, Lau DH, Brooks AG, et al. Time course of inflammation, myocardial injury, and prothrombotic response after radiofrequency catheter ablation for atrial fibrillation. *Circ Arrhythm Electrophysiol.* (2014) 7:83–9. doi: 10.1161/CIRCEP.113.000876

Conflict of Interest: The authors declare that the research was conducted in the absence of any commercial or financial relationships that could be construed as a potential conflict of interest.

Publisher's Note: All claims expressed in this article are solely those of the authors and do not necessarily represent those of their affiliated organizations, or those of the publisher, the editors and the reviewers. Any product that may be evaluated in this article, or claim that may be made by its manufacturer, is not guaranteed or endorsed by the publisher.

frontiers | Frontiers in Cardiovascular Medicine

REVIEW
published: 23 June 2022
doi: 10.3389/fcvm.2022.931219

The Mechanism of Cardiac Sympathetic Activity Assessment Methods: Current Knowledge

*Jiakun Li and Lihui Zheng**

National Center for Cardiovascular Diseases, Fuwai Hospital, Chinese Academy of Medical Sciences and Peking Union Medical College, Beijing, China

This review has summarized the methods currently available for cardiac sympathetic assessment in clinical or under research, with emphasis on the principles behind these methodologies. Heart rate variability (HRV) and other methods based on heart rate pattern analysis can reflect the dominance of sympathetic nerve to sinoatrial node function and indirectly show the average activity level of cardiac sympathetic nerve in a period of time. Sympathetic neurotransmitters play a key role of signal transduction after sympathetic nerve discharges. Plasma or local sympathetic neurotransmitter detection can mediately display sympathetic nerve activity. Given cardiac sympathetic nerve innervation, i.e., the distribution of stellate ganglion and its nerve fibers, stellate ganglion activity can be recorded either directly or subcutaneously, or through the surface of the skin using a neurophysiological approach. Stellate ganglion nerve activity (SGNA), subcutaneous nerve activity (SCNA), and skin sympathetic nerve activity (SKNA) can reflect immediate stellate ganglion discharge activity, i.e., cardiac sympathetic nerve activity. These cardiac sympathetic activity assessment methods are all based on the anatomy and physiology of the heart, especially the sympathetic innervation and the sympathetic regulation of the heart. Technological advances, discipline overlapping, and more understanding of the sympathetic innervation and sympathetic regulation of the heart will promote the development of cardiac sympathetic activity assessment methods.

Keywords: cardiac sympathetic activity assessment, sympathetic innervation, sympathetic regulation, mechanism, stellate ganglion

OPEN ACCESS

Edited by:
Bert Vandenberk,
University of Calgary, Canada

Reviewed by:
Swati Dey,
Vanderbilt University Medical Center, United States
Minglong Chen,
The First Affiliated Hospital of Nanjing Medical University, China

***Correspondence:**
Lihui Zheng
zhenglihui@263.net

Specialty section:
This article was submitted to Cardiac Rhythmology, a section of the journal Frontiers in Cardiovascular Medicine

Received: *28 April 2022*
Accepted: *20 May 2022*
Published: *23 June 2022*

Citation:
Li J and Zheng L (2022) The Mechanism of Cardiac Sympathetic Activity Assessment Methods: Current Knowledge. Front. Cardiovasc. Med. 9:931219. doi: 10.3389/fcvm.2022.931219

INTRODUCTION

The cardiac autonomic nervous system (ANS) is one of the most significant structures of the neurohumoral system that regulates cardiac function. ANS can be divided into the sympathetic nerves and the parasympathetic nerves depending on the composition of the nerves (1, 2). A vast number of research studies have proved that sympathetic nerve dysfunction engages in the pathophysiological process of coronary heart disease, hypertension, heart failure, arrhythmia, etc. (3, 4). Consequently, the evaluation of autonomic nervous activity is in favor to understand the regulation of cardiovascular activity and the pathogenesis of cardiovascular disease (CVD). Meanwhile, the clinicians can assess treatment response, progression, and risk of recurrence in patients with CVD depending on the evaluation of autonomic nervous activity (5–7). In this review,

we discussed the methods of cardiac sympathetic activity assessment applied in the clinical or under research with emphasis on the mechanism beneath these approaches, aiming at a thorough understanding of current sympathetic activity assessment and further exploration.

NEUROANATOMY AND NEUROPHYSIOLOGY OF THE HEART

Sympathetic Innervation of the Heart

The ANS is divided into the sympathetic and parasympathetic subsystems, controlled by regulatory centers in the midbrain, hypothalamus, pons, and medulla. The cardiac sympathetic nerve center is located on the medial lateral column of the first to fifth thoracic segment of the spinal cord. The cardiac sympathetic innervation consists of extrinsic and intrinsic components according to anatomical position (8, 9). The extrinsic sympathetic nerve comes from the superior cervical ganglia and the cervicothoracic (stellate) ganglia, which, respectively, connect with the cervical nerves C1–C3 and with the cervical nerves C7–C8 to the thoracic nerves T1–T2 (10). In addition, the thoracic ganglia (as low as at least the fourth thoracic ganglion) also contribute to the sympathetic innervation of the heart (11). These ganglia hold the cell bodies of most postganglionic sympathetic neurons whose axons form the superior, middle, and inferior cardiac nerves and terminate on the surface of the heart (3). These descending sympathetic neurons' postganglionic fibers reach the surface of the heart, communicate with each other, and form nerve fibers network and ganglion plexuses, which constitute the intrinsic sympathetic nerve of the heart (12). In addition, sympathetic postganglionic fibers, which originate from the superior cervical and stellate ganglion, are widely distributed in the skin of the upper limb and chest (13).

Sympathetic Regulation of the Heart

Cardiac sympathetic nerves play a vital role in regulating sinoatrial node, atrioventricular node, and activity of the segmental myocardium, which depend on neurotransmitters [norepinephrine (NE), dopamine, etc.] released by synapses at sympathetic nerve terminals and NE receptors on the cell membrane (14–16).

Norepinephrine is mainly synthesized by tyrosine hydroxylase at the sympathetic nerve terminals and stored in the vesicles (15). Once the sympathetic nerves are triggered, NE will be emitted and bound to the receptors on the cell membrane of sinoatrial node, atrioventricular node, and myocardium, which, respectively, increases heart rate, enhances atrioventricular node conduction, accelerates the repolarization of myocytes, and strengthen contractile ability of myocardium (14, 16, 17). Jung et al. uncovered that an increase in stellate ganglia sympathetic activity is followed by an increase in heart rate, and the circadian rhythms of heart rate are highly consistent with circadian rhythms of cardiac sympathetic nerve activity (18). After signal transduction, much of the NE will be reabsorbed by sympathetic nerve terminals, while only a little NE will get into circulation and be inactivated in the liver and kidney (19).

CARDIAC SYMPATHETIC ACTIVITY ASSESSMENT

Nowadays, the methods of cardiac sympathetic activity assessment applied in the clinical practice or under research are based on the anatomy and physiology of the heart, especially the sympathetic innervation and the sympathetic regulation of the heart.

Heart Rate Variability Analysis

Heart rate variability originates from the study on the heart rate patterns and cardiac rhythms, which could date back to 1965. In the 30 years since more and more clinicians had recognized the physiological and pathological significance of HRV. Until 1996, the European Society of Cardiology and the North American Society of Pacing and Electrophysiology published the standard of measurement, physiological interpretation, and clinical use of HRV (20, 21).

Heart rate variability relies on the analysis of every heartbeat, which is directly controlled by sympathetic and parasympathetic activities. Consequently, analyzing the patterns of heart rate, more precisely, analyzing beat-to-beat changes in the R-wave to R-wave intervals can indirectly reflect and evaluate the overall balance state of the cardiac autonomic nerve (21, 22). HRV analysis includes time-domain analysis, frequency-domain analysis, and non-linear analysis (**Table 1**). Time-domain analysis quantifies the amount of HRV observed during monitoring periods that may range from 5 min to 24 h. Frequency-domain values calculate the absolute or relative amount of signal energy within component bands. Non-linear measurements quantify the unpredictability and complexity of a series of interbeat intervals (23, 24).

Time domain analysis is used to measure and analyze the variability of the R-R interval of sinus rhythm by statistical and geometric methods (**Table 1**). Among the commonly used indexes, mean standard deviation (SDANN, estimate of long-term components of HRV), mean standard deviation index (SDNNI), and HRV triangular index (estimate of overall HRV) can reflect the sympathetic nerve tension. The smaller the value is, the greater the sympathetic nerve tension is. The overall SD (SDNN, estimate of overall HRV) reflects the balance between the sympathetic nerve and parasympathetic nerve (20, 22). In clinical practice, low HRV, which implicates increased sympathetic activity, is associated with a poor prognosis of CVDs, such as myocardial infarction (MI) and heart failure. In a randomized, double-blind control study of 3,717 patients with postmyocardial infarction and depressed left ventricular function, Camm found that low HRV (HRV triangular index $\leq$ 20 baseline width unit) independently identified a subpopulation at high risk of mortality (25, 26).

Frequency-domain analysis is to analyze the spectrum curve formed by the R-R interval time series signal of sinus rhythm (**Table 1**). The spectrum curve obtained by power spectral density (PSD) analysis provides the basic information on how power (i.e., variance) distributes as a function of frequency (20, 21). Usually, spectral analysis, calculated by taking a 5-min

TABLE 1 | Overview of heart rate variability (HRV) analysis for sympathetic nerve activities.

Variable	Units	Description	Correlation with autonomic activities
Time domain analysis			
SDANN	ms	Standard deviation of the averages of NN intervals in all 5 min segments of the entire recording	negative correlation with sympathetic nerve
SDNNI	ms	Mean of the standard deviations of all NN intervals for all 5 min segments of the entire recording	negative correlation with sympathetic nerve
SDNN	ms	Standard deviation of all NN intervals	the balance between the sympathetic nerve and parasympathetic nerve
HRV triangular index		Total number of all NN intervals divided by the height of the histogram of all NN intervals measured on a discrete scale with bins of 7.8125 ms (1/128 s)	negative correlation with sympathetic nerve
Frequency domain analysis			
Very low frequency	ms^2	Power in the very low frequency range	efferent sympathetic nerve activities
Low frequency	ms^2	Power in the low frequency range	sympathetic nerve (< 0.1 Hz) and parasympathetic nerve activities
LF norm	n.u.	LF power in normalized units	
High frequency	ms^2	Power in the high frequency range	parasympathetic nerve activities
HF norm	n.u.	HF power in normalized units	
LF/HF		Ratio LF (ms^2)/HF (ms^2)	the ratio between sympathetic nerve and parasympathetic nerve activities
Non-linear measurements			
S	ms	area of the ellipse	total HRV
SD1	ms	Poincaré plot standard deviation perpendicular the line of identity	SD1 predicts diastolic BP, HR Max – HR Min, RMSSD, pNN50, SDNN, and power in the LF and HF bands, and total power during 5 min recordings
SD2	ms	Poincaré plot standard deviation along the line of identity	SD2 measures short- and long-term HRV in ms and correlates with LF power
Approximate entropy		brief time series in which some noise may be present	measurement of the regularity and complexity of a time series
DFA		the correlations between successive RR intervals over different time scales	description of short- or long-term fluctuations

electrocardiograph (ECG) recording, includes three main spectral components: very low frequency (VLF, $\leq$ 0.04 Hz), low frequency (LF, 0.04–0.15 Hz), and high frequency (HF, 0.15–0.4 Hz) components. LF is mainly related to sympathetic activity and the low-frequency and high-frequency power ratio (LF/HF) is correlated to the ratio between sympathetic nerve and parasympathetic nerve activities. The central frequencies of LF and HF are not fixed but vary with the modulation of ANS to the cardiac rhythm. Therefore, the normalized LF [LF power in normalized units, LF/(Total Power − VLF) × 100] and HF [HF power in normalized units, HF/(Total Power − VLF) × 100] could be more valuable (20–22). Frequency-domain measures of heart period variability can also be evaluation indicators of CVDs, such as MI, hypertension, and heart failure (27, 28).

Time- and frequency-domain analyses of HRV are fairly simple and stable methods for sympathetic nerve activity assessment. However, these methods could not extract key information from complex interactions of hemodynamic, electrophysiological, and humoral variables, as well as by autonomic and central nervous regulations, called non-linear phenomena (20, 21). Hence, analysis of HRV based on the methods of non-linear dynamics (i.e., non-linear measurements) might elicit valuable information for the physiological interpretation of HRV (**Table 1**). Non-linear measurements are achieved by plotting every R-R interval against the prior interval, creating a scatter plot called Poincaré plot (return map). S (area of the ellipse which represents total HRV), SD1 (Poincaré plot SD perpendicular to the line of identity), SD2 (Poincaré plot SD along the line of identity) are commonly used indices. Detrended fluctuation analysis (DFA), extracting the correlations between successive R-R intervals over different time scales, could analyze a time series that spans hours of data. Approximate or sample entropy could give a judgment to the predictability of fluctuations in successive R-R intervals (20, 29). Gronwald found that DFA performs well in the analysis of complex autonomic activity at rest or during intense exercise. Moreover, Boos et al. found that non-linear HRV is more sensitive to the effects of high altitude than time- and frequency-domain indices. These proofs indicate that non-liner has more potential application prospect in complex or untraditional situations (30–32).

The application of HRV analysis is not only limited to CVDs, but also can be applied to obesity, tumor, and other diseases with autonomic nervous disorders (33, 34). While HRV is influenced by a number of physiological and pathological factors. Awareness of these mediators or confounders is of great importance in the analysis and assessment of HRV both in scientific studies and in clinical practice (**Table 2**). In the clinical use of HRV, age,

gender, and ethnic origin should take into consideration firstly. In addition, diseases (sepsis, lung diseases, metabolic diseases, and psychiatric diseases) and internal and external factors (smoking or increased body weight, sporting activity, alcohol abuse, noise, medications, night shift work, or harmful substances) may also exert influence on HRV (6, 35).

Besides HRV, blood pressure variability, resting heart rate, and so on are also closely related to the state of ANS, which, therefore, are available to evaluate cardiac sympathetic activity (36, 37).

Sympathetic Neurotransmitters Detection

Sympathetic neurotransmitters, released by synapses at sympathetic nerve terminals, are the transmitter between the sympathetic and the heart, which could be the target of cardiac sympathetic activity detection (38, 39).

Most of the sympathetic neurotransmitters, such as NE, dopamine, and epinephrine, will be reabsorbed by sympathetic nerve terminals after signal transduction, but there will also be a little NE getting into circulation and can be detected by a peripheral blood test (40, 41). Plasma catecholamine levels are normally positively correlated to sympathetic activities (**Table 2**). Moreover, William et al. (41) found that exercise could cause an increase in plasma catecholamine level, with a precipitous drop in the levels at 5 min of recovery. In addition, the more intense the exercise, the higher the plasma catecholamine level. However, it is worth noting that plasma catecholamine level reflects the sympathetic activities of the whole body, not specifically referring to cardiac sympathetic activities (42). Measurement of the coronary sinus and arterial blood catecholamine concentrations can be a possible solution to estimate transcardiac NE despite its possible surgical risks. Kaye et al. found that arterial and transcardiac NE are significantly higher in heart failure with preserved ejection fraction patients than controls (43). However, the risks of interventional surgery make it difficult to implement for general patients.

The measurement of local catecholamine levels seems quite challenging, while radio imaging combined with cardiovascular physiology makes it possible to precisely detect cardiac local sympathetic neurotransmitters at a micromolar level (44). Applying iodine-123 meta-iodobenzylguanidine (^{123}I-mIBG) or other radiolabeled neurotransmitter analogs, cardiac neurotransmission imaging with single photon emission computed tomography (SPECT) and positron emission tomography (PET) allows *in vivo* assessment of presynaptic reuptake and neurotransmitter storage and of regional distribution and activity of postsynaptic receptors (**Table 2**) (5, 44). Heart-to-mediastinum ratio (HMR) and mIBG wash-out (WO) rate are the most commonly used scientific parameters. HMR is the indicator of mIBG uptake, and retention of NE by sympathetic neurons can be semiquantified by WO rate, specifically, comparing early and delayed activities (45). Yasushi et al. found that lower HMR was the independent predictor of the transit from idiopathic paroxysmal atrial fibrillation (AF) to permanent AF, manifesting the fact that cardiac sympathetic nerve activity abnormal plays a key role in the development of atrial fibrillation (46).

Poor imaging quality and difficulty in distinguishing different cardiac structures were the main problems that limited the application of this technique for a long time in the past. However, the recent development of solid-state gamma camera technology with significantly improved sensitivity, spatial resolution, and energy resolution has enabled high-quality SPECT imaging with a spatial resolution of $\leq$ 5 mm (44, 47). In addition, the injection of radiolabeled neurotransmitter analogs and their possible radiation damage may cause concern among patients and block their clinical use (44).

Sympathetic Nerve Activity Recording

A stellate ganglion can directly regulate the activity of the cardiac sympathetic nerve and then regulate cardiac activity. Enhanced discharge activity of stellate ganglion can accelerate heart rate and raise blood pressure (48). Sympathetic nerve activity record of the heart is on the basis of sympathetic nerve innervation using neuroelectrophysiological methods, which went through three stages of exploration——stellate ganglion nerve activity (SGNA), subcutaneous nerve activity (SCNA), and skin sympathetic nerve activity (SKNA) (18, 49–51).

Stellate Ganglion Nerve Activity

Lavian et al. (52) directly placed recording electrodes on the surface of canine stellate ganglion nerve fibers to record the discharge of stellate ganglion after thoracotomy and can record the nerve activity in living dogs within 1 min. Jung et al. (18) further improved the method, so that SGNA recording can complete recording lasting more than 40 days for 24 h. It is found that after SGNA recording showed the discharge signal of the stellate ganglion, the heart rate and blood pressure of dogs were increased secondary. At the same time, the discharge of stellate ganglion shows circadian rhythm, which is consistent with the circadian rhythm of heart rate (18). Subsequently, Tan et al. (53) found that the occurrence of arrhythmia diseases, such as atrial tachycardia, ventricular tachycardia, and atrial fibrillation, is related to the abnormal discharge of stellate ganglion through the SGNA recording of dog model, and the discharge patterns of stellate ganglion are also different for different arrhythmia diseases. In the SGNA recording of complex CVDs, such as MI, heart failure, and sudden death, Zhou et al. (54) found that the increase of discharge activity of stellate ganglion is an important reason for the progression of ventricular arrhythmia and other CVDs (55, 56). These findings provide scientific evidence for understanding the changes in cardiac sympathetic nerve activity in the occurrence and development of CVDs and finding appropriate treatment methods (57, 58).

Stellate ganglion nerve activity recording can be recorded continuously for more than 40 days for 24 h in living animals. It can record the immediate discharge activity of stellate ganglion without affecting the survival and daily activities of animals. It is an important tool to study the cardiac sympathetic nerve activity (57, 58). However, SGNA recording is carried out by thoracotomy, which has great trauma and is difficult to be

TABLE 2 | Comparison of cardiac sympathetic nerve activities assessment methods.

Methods	Theoretical cornerstone	Measurement	Indices	Clinical interpretation	Periods of time	Advantages	Disadvantages
HRV	sympathetic nerve activities regulation of Sinus node	ECG recording	See **Table 1**	sympathetic activities, balance between sympathetic and parasympathetic nerve activities	several minutes to 24 h	simple, non-invasive, stable	influenced by many factors
plasma catecholamine detection	release of neurotransmitters after sympathetic excitation	peripheral or coronary sinus blood	plasma catecholamine concentration	global sympathetic activities	a few minutes	simple, easy to interpret	inaccuracy in cardiac sympathetic activities assessment
cardiac neurotransmission imaging	release of neurotransmitters after sympathetic excitation	radiolabeled neurotransmitter analogues, SPECT and PET	Heart-to-mediastinum ratio (HMR) and mIBG wash-out (WO) rate	uptake and retention of norepinephrine	a few minutes	Location information of abnormal cardiac sympathetic activities	invasive, expensive
SKNA	detection of stellate ganglion discharge from the skin surface	ADInstruments PowerLab or ME6000 portable biomonitor with increased bandwidth and sampling rate	average SKNA and SKNA burst	average sympathetic nerves activity, number of sympathetic nerves burst discharges after excitation during selected period	instant, several minutes to 24 h	simple, non-invasive, continuous evaluation	lack of a complete evaluation system and reliable reference value

routinely applied in the clinic. In order to reduce the trauma caused by recording, a new recording method, SCNA recording, has been published (49).

Subcutaneous Nerve Activity

In addition to innervating the heart, some postganglionic fibers of the stellate ganglion are widely distributed in the skin and subcutaneous tissue of the neck and chest, and there is extensive cross-linking in the whole neural network (49, 59). Robinson et al. (49) speculated that when the stellate ganglion discharges, the stellate nerve postganglionic fiber terminals of the skin and subcutaneous tissue of the neck and chest appear synchronous discharge.

Robinson et al. (49) implanted the recording electrode into the subcutaneous tissue of the dog's chest to record the SCNA and performed SGNA recording by thoracotomy. The results showed that before the dog's heart rate accelerated, SGNA and SCNA recording showed synchronized neural discharge activities, and the 24 h recording results showed that SGNA recording and SCNA recording had consistent circadian rhythm changes. Through the statistical analysis, it is found that SGNA recording has strong correlation with SCNA recording, and the correlation coefficient is 0.7, indicating that SCNA recording can replace SGNA recording to reflect the neural activities of stellate ganglion and the activity of cardiac sympathetic nerve (49).

Subsequently, Chan et al. (60) conducted 56 days of SGNA recording (direct measurement of stellate ganglion activity), SCNA recording, and HRV analysis on the canine model of MI. The absolute values of the correlation coefficients between integrated SGNA and SCNA were significantly larger than those between SGNA and HRV analysis based on time domain, frequency domain, and non-linear analyses, respectively, at baseline and after MI. The results showed that SCNA recording is better than HRV analysis in assessing cardiac sympathetic tone in dogs after MI. The feasibility of using SCNA recording to reflect cardiac sympathetic nerve activity is further verified (60). In addition, Doytchinova et al. (61) found that SCNA recording has a certain predictive value for the onset of ventricular tachycardia and ventricular fibrillation in dogs after MI and sudden cardiac death in rats with chronic renal failure (61).

Subcutaneous nerve activity recording avoids the huge trauma caused by SGNA recording that requires thoracotomy. By embedding the recording electrode in the subcutaneous tissue of the chest, SCNA recording can also complete the recording of nerve activity for more than 40 days for 24 h, reflecting the immediate SGNA and even cardiac sympathetic nerve activity (49, 61). However, it still has certain surgical trauma, which limits its clinical application. Jiang et al. (50) further explored the non-invasive recording of SKNA on the basis of SCNA recording.

Skin Sympathetic Nerve Activity

The histological evidence of human skin biopsy shows that there are abundant sympathetic nerves in the arteriovenous anastomosis, arrector pili muscle, and arterioles. Given the feasibility of SCNA record, Jiang et al. (50) further speculated that it is also feasible to directly record sympathetic nerve activities through the skin (**Table 2**).

Jiang et al. (50) directly attached the traditional ECG recording electrode to the dog's chest skin for original signal recording, obtaining the signal of single lead ECG and SKNA by setting appropriate recording parameters and filtering parameters, and recorded SGNA as the gold standard (50, 51). The study found

that in the resting state or stress state, SGNA and SKNA maintain a strong correlation, and the correlation coefficient is between 0.75 and 0.88, indicating that SKNA recording was consistent with SGNA recording (50). Doytchinova et al. (62) further verified the feasibility of SKNA recording on the recruited healthy volunteers and clinical patients. In total, nine healthy volunteers received cold-water stress test and Valsalva action successively. After the cold-water stress test began, the recorded SKNA signal increased significantly, and the subjects' heart rate accelerated secondarily. After the Valsalva action, the SKNA signal of the subjects decreased rapidly, followed by a decrease in heart rate (62). In nine patients who underwent bilateral stellate ganglion block, the researchers found that SKNA signal was decreased by 63% from baseline after lidocaine injection into bilateral stellate ganglion (51). These studies further verified the feasibility of the SKNA recording to reflect the neural activity of stellate ganglion and even the activity of cardiac sympathetic nerve. Kumar et al. (63) further applied SKNA recording in patients with various CVDs, such as vasovagal syncope, heart failure with decreased ejection fraction, paroxysmal atrial fibrillation, and long QT interval syndrome to explore the role of cardiac sympathetic nerve activity in the pathogenesis and development of these diseases (64–69).

Skin sympathetic nerve activity can record cardiac sympathetic nerve non-invasively and continuously for 24 h. There are also several limitations to its usage, patients' daily activities and even body movements have a great impact on the quality of recorded signals (50). Of note, Xing et al. (70) recently found a system-level modification by combining a commercial analog front end chip with a low-noise first-stage amplifier and an adaptive power-line-interference (PLI) filter and outliers clipping may reduce the system noise floor and reject the PLI and motion artifacts in the signal. The performance and effectiveness of this system have been verified in the laboratory experiment and clinical experiment (70). This may contribute to the popularization of SKNA. In addition, the parameters for SKNA are also limited to average SKNA (aSKNA, average sympathetic nerves activity during selected period, several min to h) and SKNA burst (number of sympathetic nerves burst discharges after excitation during the selected period). Due to the lack of large sample clinical studies, a well-established standard is warranted (50, 51).

CONCLUSION

Sympathetic nerve dysfunction engages in the pathophysiological process of coronary heart disease, hypertension, heart failure, arrhythmia, and other CVDs. It is necessary to evaluate cardiac sympathetic activity. Generally speaking, these cardiac sympathetic activity assessment methods can be divided into three levels. Firstly, to evaluate the global sympathetic activities by plasma catecholamine levels, blood pressure variability, and so on. The evaluation results obtained by these methods may not be consistent with the true cardiac sympathetic activity state, which needs to be combined with other clinical evidence. Secondly, using HRV, cardiac neurotransmission imaging with SPECT and PET or SKNA evaluates the average state of sympathetic activity during a selected period of time. Thirdly, to monitor immediate sympathetic nerve activity by SKNA, which is impossible for other assessment methods.

What is noteworthy is that these cardiac sympathetic activity assessment methods are all based on the anatomy and physiology of the heart, especially the sympathetic innervation and the sympathetic regulation of the heart. Therefore, the depth of our understanding of the sympathetic innervation and sympathetic regulation of the heart determines the approaches we can take to evaluate cardiac sympathetic activity. Moreover, the development of cardiac neurotransmission imaging with SPECT, PET, and SKNA gives us a hint that technological advances and discipline overlapping are the important driving forces for improving cardiac sympathetic activity assessment methods.

AUTHOR CONTRIBUTIONS

JL wrote the manuscript. LZ modified and polished the manuscript. Both authors contributed to the article and approved the submitted version.

FUNDING

This work was supported by the Capital Municipal Science and Technology Commission (Z191100006619019).

REFERENCES

1. Herring N, Kalla M, Paterson DJ. The autonomic nervous system and cardiac arrhythmias: current concepts and emerging therapies. *Nat Rev Cardiol.* (2019) 16:707–26. doi: 10.1038/s41569-019-0221-2
2. Goldberger JJ, Arora R, Buckley U, Shivkumar K. Autonomic nervous system dysfunction: JACC focus seminar. *J Am Coll Cardiol.* (2019) 73:1189–206. doi: 10.1016/j.jacc.2018.12.064
3. Shen MJ, Zipes DP. Role of the autonomic nervous system in modulating cardiac arrhythmias. *Circ Res.* (2014) 114:1004–21. doi: 10.1161/CIRCRESAHA.113.302549
4. Florea VG, Cohn JN. The autonomic nervous system and heart failure. *Circ Res.* (2014) 114:1815–26. doi: 10.1161/CIRCRESAHA.114.302589
5. Orimo S, Yogo M, Nakamura T, Suzuki M, Watanabe H. (123)I-meta-iodobenzylguanidine (MIBG) cardiac scintigraphy in α-synucleinopathies. *Ageing Res Rev.* (2016) 30:122–33. doi: 10.1016/j.arr.2016.01.001
6. Sammito S, Böckelmann I. Reference values for time- and frequency-domain heart rate variability measures. *Heart Rhythm.* (2016) 13:1309–16. doi: 10.1016/j.hrthm.2016.02.006
7. Zheng L, Sun W, Liu S, Liang E, Du Z, Guo J, et al. The diagnostic value of cardiac deceleration capacity in vasovagal syncope. *Circ Arrhythm Electrophysiol.* (2020) 13:e008659. doi: 10.1161/CIRCEP.120.008659
8. Ardell JL, Armour JA. Neurocardiology: structure-based function. *Compr Physiol.* (2016) 6:1635–53. doi: 10.1002/cphy.c150046
9. Beaumont E, Salavatian S, Southerland EM, Vinet A, Jacquemet V, Armour JA, et al. Network interactions within the canine intrinsic cardiac nervous system: implications for reflex control of regional cardiac function. *J Physiol.* (2013) 591:4515–33. doi: 10.1113/jphysiol.2013.259382

10. Hou Y, Scherlag BJ, Lin J, Zhang Y, Lu Z, Truong K, et al. Ganglionated plexi modulate extrinsic cardiac autonomic nerve input: effects on sinus rate, atrioventricular conduction, refractoriness, and inducibility of atrial fibrillation. *J Am Coll Cardiol.* (2007) 50:61–8. doi: 10.1016/j.jacc.2007.02.066
11. Armour JA. Functional anatomy of intrathoracic neurons innervating the atria and ventricles. *Heart Rhythm.* (2010) 7:994–6. doi: 10.1016/j.hrthm.2010.02.014
12. Armour JA. Physiology of the intrinsic cardiac nervous system. *Heart Rhythm.* (2011) 8:739. doi: 10.1016/j.hrthm.2011.01.033
13. Taniguchi T, Morimoto M, Taniguchi Y, Takasaka M, Totoki T. Cutaneous distribution of sympathetic postganglionic fibers from stellate ganglion: a retrograde axonal tracing study using wheat germ agglutinin conjugated with horseradish peroxidase. *J Anesth.* (1994) 8:441–9. doi: 10.1007/BF02514624
14. Yeh YH, Ehrlich JR, Qi X, Hébert TE, Chartier D, Nattel S. Adrenergic control of a constitutively active acetylcholine-regulated potassium current in canine atrial cardiomyocytes. *Cardiovasc Res.* (2007) 74:406–15. doi: 10.1016/j.cardiores.2007.01.020
15. Kimura K, Ieda M, Fukuda K. Development, maturation, and transdifferentiation of cardiac sympathetic nerves. *Circ Res.* (2012) 110:325–36. doi: 10.1161/CIRCRESAHA.111.257253
16. Wilson RF, Johnson TH, Haidet GC, Kubo SH, Mianuelli M. Sympathetic reinnervation of the sinus node and exercise hemodynamics after cardiac transplantation. *Circulation.* (2000) 101:2727–33. doi: 10.1161/01.cir.101.23.2727
17. Wallick DW, Stuesse SL, Masuda Y. Sympathetic and periodic vagal influences on antegrade and retrograde conduction through the canine atrioventricular node. *Circulation.* (1986) 73:830–6. doi: 10.1161/01.cir.73.4.830
18. Jung BC, Dave AS, Tan AY, Gholmieh G, Zhou S, Wang DC, et al. Circadian variations of stellate ganglion nerve activity in ambulatory dogs. *Heart Rhythm.* (2006) 3:78–85. doi: 10.1016/j.hrthm.2005.09.016
19. Liang CS. Cardiac sympathetic nerve terminal function in congestive heart failure. *Acta Pharmacol Sin.* (2007) 28:921–7. doi: 10.1111/j.1745-7254.2007.00585.x
20. Camm AJ, Bigger JT Jr, Breithardt G, Cerutti S, Cohen RJ, Coumel P, et al. Heart rate variability. Standards of measurement, physiological interpretation, and clinical use. Task Force of the European Society of Cardiology and the North American Society of Pacing and Electrophysiology. *Eur Heart J.* (1996) 17:354–81.
21. Berntson GG, Bigger JT Jr., Eckberg DL, Grossman P, Kaufmann PG, Malik M, et al. Heart rate variability: origins, methods, and interpretive caveats. *Psychophysiology.* (1997) 34:623–48. doi: 10.1111/j.1469-8986.1997.tb02140.x
22. Monfredi O, Lyashkov AE, Johnsen AB, Inada S, Schneider H, Wang R, et al. Biophysical characterization of the underappreciated and important relationship between heart rate variability and heart rate. *Hypertension.* (2014) 64:1334–43. doi: 10.1161/HYPERTENSIONAHA.114.03782
23. van Ravenswaaij-Arts CM, Kollée LA, Hopman JC, Stoelinga GB, van Geijn HP. Heart rate variability. *Ann Intern Med.* (1993) 118:436–47. doi: 10.7326/0003-4819-118-6-199303150-00008
24. Hamilton JL, Alloy LB. Atypical reactivity of heart rate variability to stress and depression across development: systematic review of the literature and directions for future research. *Clin Psychol Rev.* (2016) 50:67–79. doi: 10.1016/j.cpr.2016.09.003
25. Camm AJ, Pratt CM, Schwartz PJ, Al-Khalidi HR, Spyt MJ, Holroyde MJ, et al. AzimiLide post infarct surVival evaluation (ALIVE) investigators. Mortality in patients after a recent myocardial infarction: a randomized, placebo-controlled trial of azimilide using heart rate variability for risk stratification. *Circulation.* (2004) 109:990–6. doi: 10.1161/01.CIR.0000117090.01718.2A
26. Chattipakorn N, Incharoen T, Kanlop N, Chattipakorn S. Heart rate variability in myocardial infarction and heart failure. *Int J Cardiol.* (2007) 120:289–96. doi: 10.1016/j.ijcard.2006.11.221
27. Bigger JT Jr., Fleiss JL, Steinman RC, Rolnitzky LM, Kleiger RE, Rottman JN. Frequency domain measures of heart period variability and mortality after myocardial infarction. *Circulation.* (1992) 85:164–71. doi: 10.1161/01.cir.85.1.164
28. Cha SA, Park YM, Yun JS, Lee SH, Ahn YB, Kim SR, et al. Time- and frequency-domain measures of heart rate variability predict cardiovascular outcome in patients with type 2 diabetes. *Diabetes Res Clin Pract.* (2018) 143:159–69. doi: 10.1016/j.diabres.2018.07.001
29. Shaffer F, Ginsberg JP. An Overview of Heart Rate Variability Metrics and Norms. *Front Public Health.* (2017) 5:258. doi: 10.3389/fpubh.2017.00258
30. Stein PK, Reddy A. Non-linear heart rate variability and risk stratification in cardiovascular disease. *Indian Pacing Electrophysiol J.* (2005) 5:210–20.
31. Boos CJ, Bye K, Sevier L, Bakker-Dyos J, Woods DR, Sullivan M, et al. High altitude affects nocturnal non-linear heart rate variability: PATCH-HA study. *Front Physiol.* (2018) 9:390. doi: 10.3389/fphys.2018.00390
32. Gronwald T, Hoos O, Ludyga S, Hottenrott K. Non-linear dynamics of heart rate variability during incremental cycling exercise. *Res Sports Med.* (2019) 27:88–98. doi: 10.1080/15438627.2018.1502182
33. Strüven A, Holzapfel C, Stremmel C, Brunner S. Obesity, nutrition and heart rate variability. *Int J Mol Sci.* (2021) 22:4215. doi: 10.3390/ijms22084215
34. Wu S, Chen M, Wang J, Shi B, Zhou Y. Association of short-term heart rate variability with breast tumor stage. *Front Physiol.* (2021) 12:678428. doi: 10.3389/fphys.2021.678428
35. Sammito S, Böckelmann I. Factors influencing heart rate variability. *Int Cardiovasc Forum J.* (2016) 6:18–22. doi: 10.17987/icfj.v6i0.242
36. Zhang J, Kesteloot H. Anthropometric, lifestyle and metabolic determinants of resting heart rate. A population study. *Eur Heart J.* (1999) 20:103–10. doi: 10.1053/euhj.1999.1230
37. Stevens SL, Wood S, Koshiaris C, Law K, Glasziou P, Stevens RJ, et al. Blood pressure variability and cardiovascular disease: systematic review and meta-analysis. *BMJ.* (2016) 354:i4098. doi: 10.1136/bmj.i4098
38. Goldstein DS, Brush JE Jr., Eisenhofer G, Stull R, Esler M. In vivo measurement of neuronal uptake of norepinephrine in the human heart. *Circulation.* (1988) 78:41–8. doi: 10.1161/01.cir.78.1.41
39. Simmons WW, Freeman MR, Grima EA, Hsia TW, Armstrong PW. Abnormalities of cardiac sympathetic function in pacing-induced heart failure as assessed by [123I]metaiodobenzylguanidine scintigraphy. *Circulation.* (1994) 89:2843–51. doi: 10.1161/01.cir.89.6.2843
40. Anderson EJ, Efird JT, Kiser AC, Crane PB, O'Neal WT, Ferguson TB, et al. Plasma catecholamine levels on the morning of surgery predict post-operative atrial fibrillation. *JACC Clin Electrophysiol.* (2017) 3:1456–65. doi: 10.1016/j.jacep.2017.01.014
41. Kraemer WJ, Noble B, Culver B, Lewis RV. Changes in plasma proenkephalin peptide F and catecholamine levels during graded exercise in men. *Proc Natl Acad Sci USA.* (1985) 82:6349–51. doi: 10.1073/pnas.82.18.6349
42. Grouzmann E, Lamine F. Determination of catecholamines in plasma and urine. *Best Pract Res Clin Endocrinol Metab.* (2013) 27:713–23. doi: 10.1016/j.beem.2013.06.004
43. Kaye DM, Nanayakkara S, Wang B, Shihata W, Marques FZ, Esler M, et al. Characterization of cardiac sympathetic nervous system and inflammatory activation in HFpEF patients. *JACC Basic Transl Sci.* (2022) 7:116–27. doi: 10.1016/j.jacbts.2021.11.007
44. Carrió I. Cardiac neurotransmission imaging. *J Nucl Med.* (2001) 42:1062–76.
45. Raffel DM, Wieland DM. Development of mIBG as a cardiac innervation imaging agent. *JACC Cardiovasc Imaging.* (2010) 3:111–6. doi: 10.1016/j.jcmg.2009.09.015
46. Akutsu Y, Kaneko K, Kodama Y, Li HL, Suyama J, Shinozuka A, et al. Iodine-123 mIBG imaging for predicting the development of atrial fibrillation. *JACC Cardiovasc Imaging.* (2011) 4:78–86. doi: 10.1016/j.jcmg.2010.10.005
47. Stirrup J, Gregg S, Baavour R, Roth N, Breault C, Agostini D, et al. Hybrid solid-state SPECT/CT left atrial innervation imaging for identification of left atrial ganglionated plexi: technique and validation in patients with atrial fibrillation. *J Nucl Cardiol.* (2020) 27:1939–50. doi: 10.1007/s12350-018-01535-5
48. Wu G, DeSimone CV, Suddendorf SH, Asirvatham RS, Asirvatham SJ, Huang C, et al. Effects of stepwise denervation of the stellate ganglion: novel insights from an acute canine study. *Heart Rhythm.* (2016) 13:1395–401. doi: 10.1016/j.hrthm.2016.03.010
49. Robinson EA, Rhee KS, Doytchinova A, Kumar M, Shelton R, Jiang Z, et al. Estimating sympathetic tone by recording subcutaneous nerve activity in ambulatory dogs. *J Cardiovasc Electrophysiol.* (2015) 26:70–8. doi: 10.1111/jce.12508
50. Jiang Z, Zhao Y, Doytchinova A, Kamp NJ, Tsai WC, Yuan Y, et al. Using skin sympathetic nerve activity to estimate stellate ganglion nerve activity in dogs. *Heart Rhythm.* (2015) 12:1324–32. doi: 10.1016/j.hrthm.2015.02.012

51. Kusayama T, Wong J, Liu X, He W, Doytchinova A, Robinson EA, et al. Simultaneous noninvasive recording of electrocardiogram and skin sympathetic nerve activity (neuECG). *Nat Protoc.* (2020) 15:1853–77. doi: 10.1038/s41596-020-0316-6
52. Lavian G, Kopelman D, Shenhav A, Konyukhov E, Gardi U, Zaretzky A, et al. In vivo extracellular recording of sympathetic ganglion activity in a chronic animal model. *Clin Auton Res.* (2003) 13(Suppl. 1):I83–8. doi: 10.1007/s10286-003-1121-3
53. Tan AY, Zhou S, Ogawa M, Song J, Chu M, Li H, et al. Neural mechanisms of paroxysmal atrial fibrillation and paroxysmal atrial tachycardia in ambulatory canines. *Circulation.* (2008) 118:916–25. doi: 10.1161/CIRCULATIONAHA.108.776203
54. Zhou S, Jung BC, Tan AY, Trang VQ, Gholmieh G, Han SW, et al. Spontaneous stellate ganglion nerve activity and ventricular arrhythmia in a canine model of sudden death. *Heart Rhythm.* (2008) 5:131–9. doi: 10.1016/j.hrthm.2007.09.007
55. Ogawa M, Tan AY, Song J, Kobayashi K, Fishbein MC, Lin SF, et al. Cryoablation of stellate ganglia and atrial arrhythmia in ambulatory dogs with pacing-induced heart failure. *Heart Rhythm.* (2009) 6:1772–9. doi: 10.1016/j.hrthm.2009.08.011
56. Piccirillo G, Ogawa M, Song J, Chong VJ, Joung B, Han S, et al. Power spectral analysis of heart rate variability and autonomic nervous system activity measured directly in healthy dogs and dogs with tachycardia-induced heart failure. *Heart Rhythm.* (2009) 6:546–52. doi: 10.1016/j.hrthm.2009.01.006
57. Shen MJ, Shinohara T, Park HW, Frick K, Ice DS, Choi EK, et al. Continuous low-level vagus nerve stimulation reduces stellate ganglion nerve activity and paroxysmal atrial tachyarrhythmias in ambulatory canines. *Circulation.* (2011) 123:2204–12. doi: 10.1161/CIRCULATIONAHA.111.018028
58. Han S, Kobayashi K, Joung B, Piccirillo G, Maruyama M, Vinters HV, et al. Electroanatomic remodeling of the left stellate ganglion after myocardial infarction. *J Am Coll Cardiol.* (2012) 59:954–61. doi: 10.1016/j.jacc.2011.11.030
59. Meijborg VMF, Boukens BJD, Janse MJ, Salavatian S, Dacey MJ, Yoshie K, et al. Stellate ganglion stimulation causes spatiotemporal changes in ventricular repolarization in pig. *Heart Rhythm.* (2020) 17(5 Pt A):795–803. doi: 10.1016/j.hrthm.2019.12.022
60. Chan YH, Tsai WC, Shen C, Han S, Chen LS, Lin SF, et al. Subcutaneous nerve activity is more accurate than heart rate variability in estimating cardiac sympathetic tone in ambulatory dogs with myocardial infarction. *Heart Rhythm.* (2015) 12:1619–27. doi: 10.1016/j.hrthm.2015.03.025
61. Doytchinova A, Patel J, Zhou S, Chen LS, Lin H, Shen C, et al. Subcutaneous nerve activity and spontaneous ventricular arrhythmias in ambulatory dogs. *Heart Rhythm.* (2015) 12:612–20. doi: 10.1016/j.hrthm.2014.11.007
62. Doytchinova A, Hassel JL, Yuan Y, Lin H, Yin D, Adams D, et al. Simultaneous noninvasive recording of skin sympathetic nerve activity and electrocardiogram. *Heart Rhythm.* (2017) 14:25–33. doi: 10.1016/j.hrthm.2016.09.019
63. Kumar A, Wright K, Uceda DE, Vasallo PA III, Rabin PL, Adams D, et al. Skin sympathetic nerve activity as a biomarker for syncopal episodes during a tilt table test. *Heart Rhythm.* (2020) 17(5 Pt A):804–12. doi: 10.1016/j.hrthm.2019.10.008
64. He W, Tang Y, Meng G, Wang D, Wong J, Mitscher GA, et al. Skin sympathetic nerve activity in patients with obstructive sleep apnea. *Heart Rhythm.* (2020) 17:1936–43. doi: 10.1016/j.hrthm.2020.06.018
65. Han J, Ackerman MJ, Moir C, Cai C, Xiao PL, Zhang P, et al. Left cardiac sympathetic denervation reduces skin sympathetic nerve activity in patients with long QT syndrome. *Heart Rhythm.* (2020) 17:1639–45. doi: 10.1016/j.hrthm.2020.03.023
66. Zhang P, Liang JJ, Cai C, Tian Y, Dai MY, Wong J, et al. Characterization of skin sympathetic nerve activity in patients with cardiomyopathy and ventricular arrhythmia. *Heart Rhythm.* (2019) 16:1669–75. doi: 10.1016/j.hrthm.2019.06.008
67. Uradu A, Wan J, Doytchinova A, Wright KC, Lin AYT, Chen LS, et al. Skin sympathetic nerve activity precedes the onset and termination of paroxysmal atrial tachycardia and fibrillation. *Heart Rhythm.* (2017) 14:964–71. doi: 10.1016/j.hrthm.2017.03.030
68. Yuan Y, Hassel JL, Doytchinova A, Adams D, Wright KC, Meshberger C, et al. Left cervical vagal nerve stimulation reduces skin sympathetic nerve activity in patients with drug resistant epilepsy. *Heart Rhythm.* (2017) 14:1771–8. doi: 10.1016/j.hrthm.2017.07.035
69. Kusayama T, Wan J, Doytchinova A, Wong J, Kabir RA, Mitscher G, et al. Skin sympathetic nerve activity and the temporal clustering of cardiac arrhythmias. *JCI Insight.* (2019) 4:e125853. doi: 10.1172/jci.insight.125853
70. Xing Y, Zhang Y, Yang C, Li J, Li Y, Cui C, et al. Design and evaluation of an autonomic nerve monitoring system based on skin sympathetic nerve activity. *Biomed Signal Process Control.* (2022) 76:103681. doi: 10.1016/j.bspc.2022.103681

Conflict of Interest: The authors declare that the research was conducted in the absence of any commercial or financial relationships that could be construed as a potential conflict of interest.

frontiers | Frontiers in Cardiovascular Medicine

TYPE Original Research
PUBLISHED 25 August 2022
DOI 10.3389/fcvm.2022.841453

OPEN ACCESS

EDITED BY
Paolo Calabrò,
University of Campania Luigi Vanvitelli, Italy

REVIEWED BY
Milo Alan Puhan,
University of Zurich, Switzerland
Ilaria Cavallari,
Policlinico Universitario Campus Bio-Medico, Italy

*CORRESPONDENCE
Jia Han
jia.han@canberra.edu.au
Alice Y. M. Jones
a.jones15@uq.edu.au

†These authors have contributed equally to this work and share first authorship

SPECIALTY SECTION
This article was submitted to Coronary Artery Disease, a section of the journal Frontiers in Cardiovascular Medicine

RECEIVED 22 December 2021
ACCEPTED 04 August 2022
PUBLISHED 25 August 2022

CITATION
Wang Z, Yan J, Meng S, Li J, Yu Y, Zhang T, Tsang RCC, El-Ansary D, Han J and Jones AYM (2022) Reliability and validity of sit-to-stand test protocols in patients with coronary artery disease.
Front. Cardiovasc. Med. 9:841453.
doi: 10.3389/fcvm.2022.841453

Reliability and validity of sit-to-stand test protocols in patients with coronary artery disease

Zheng Wang[1†], Jianhua Yan[2†], Shu Meng[2†], Jiajia Li[1], Yi Yu[2], Tingting Zhang[2], Raymond C. C. Tsang[3], Doa El-Ansary[1,4,5], Jia Han[6*] and Alice Y. M. Jones[7*]

[1]Department of Sport Rehabilitation, School of Kinesiology, Shanghai University of Sport, Shanghai, China, [2]Department of Cardiology, Xinhua Hospital Affiliated to Shanghai Jiao Tong University School of Medicine, Shanghai, China, [3]Department of Physiotherapy, MacLehose Medical Rehabilitation Center, Hospital Authority, Hong Kong, China, [4]Department Nursing and Allied Health, Swinburne University of Technology, Melbourne, VIC, Australia, [5]Department of Surgery, Melbourne Medical School, University of Melbourne, Melbourne, VIC, Australia, [6]Department of Physiotherapy, College of Rehabilitation Sciences, Shanghai University of Medicine and Health Sciences, Shanghai, China, [7]Department of Physiotherapy, School of Health and Rehabilitation Sciences, The University of Queensland, Brisbane, QLD, Australia

Background: Sit-To-Stand (STS) tests are reported as feasible alternatives for the assessment of functional fitness but the reliability of these tests in people with coronary artery disease (CAD) has not been reported. This study explored the test-retest reliability, convergent and known-groups validity of the five times, 30-sec and 1-min sit-to-stand test (FTSTS test, 30-s STS test and 1-min STS test respectively) in patients with CAD. The feasibility of applying these tests to distinguish the level of risk for cardiovascular events in CAD patients was also investigated.

Methods: Patients with stable CAD performed a 6MWT and 3 STS tests in random order on the same day. Receiver operating characteristic (ROC) curve analyses were conducted using STS test data to differentiate patients with low or high risk of cardiovascular events based on the risk level determined by distance covered in the 6MWT as $>$ or $\leq$419 m. Thirty patients repeated the 3 STS tests on the following day.

Results: 112 subjects with diagnoses of atherosclerosis or post-percutaneous coronary intervention, or post-acute myocardial infarction (post-AMI) participated in the validity analysis. All 3 STS tests demonstrated moderate and significant correlation with the 6MWT (coefficient values *r* for the FTSTS, 30-s STS and 1-min STS tests were−0.53, 0.57 and 0.55 respectively). Correlations between left ventricular ejection fraction (LVEF) and all STS tests and between 6MWT and LVEF were only weak (*r values* ranged from 0.27 to 0.31). Subgroup analysis showed participants in the post-AMI group performed worse in all tests compared to non-myocardial infarction (non-MI) group. The area under the curve (AUC) was 0.80 for FTSTS (sensitivity: 75.0%, specificity: 73.8%, optimal cut-off: $>$11.7 sec), and the AUC, sensitivity, specificity and optimal cut-off for 30-s STS and 1-min STS test were 0.83, 75.0%, 76.2%, $\leq$12 repetitions and 0.80, 71.4%, 73.8%, $\leq$23 repetitions respectively. The intraclass correlation coefficients (ICC) for repeated measurements of the FTSTS,

30-s STS and 1-min STS tests were 0.96, 0.95 and 0.96 respectively, with the minimal detectable change (MDC_{95}) computed to be 1.1 sec 1.8 repetitions and 3.9 repetitions respectively.

Conclusions: All STS tests demonstrated good test-retest reliability, convergent and known-groups validity. STS tests may discriminate low from high levels of risk for a cardiovascular event in patients with CAD.

KEYWORDS

coronary artery disease, sit-to-stand, reliability, validity, discriminative ability, 6-minute walk test

Introduction

Coronary artery disease (CAD) is the leading cause of death worldwide and accounts for a significant disease burden in developing countries (1, 2). Cardiac rehabilitation (CR) is supported by evidence as key to CAD management and functional capacity is often a clinical outcome used to reflect the success of a CR programme (3). The 6-min walk test (6MWT) has been used as a prognostic tool to predict the risk of myocardial infarct, heart failure and death in CAD patients (4). The 6MWT demands no expensive or complicated equipment, however it does require a corridor which is at least 30 meters in length, and the full assessment procedure takes at least 20 min. Further, patient performance can be confounded by the motivation and unintentional encouragement provided by the operators (5). In contrast, the sit-to-stand (STS) test requires a chair and minimal space. It was first introduced in 1985 for the evaluation of lower limb muscle strength (6). Recently, an incremental STS test protocol was reported to be highly correlated with peak oxygen consumption during an exercise test in healthy individuals (7). STS tests are now considered feasible alternative tests for the assessment of functional fitness in older adults and in various patient populations (8–10).

Tests or measures in clinical medicine are normally used for three purposes: discriminate between patient characteristics, predict an outcome or inform the prognosis of a condition, and evaluate change over time or change after certain intervention (11). The STS tests have been used to discriminate levels of functional capacity in people with chronic respiratory illness (12, 13) and have also been used to evaluate the effect of pulmonary rehabilitation in people with chronic obstructive pulmonary disease (COPD) (14). The 1-min STS test was shown to be a strong predictor of 2-year mortality in people with COPD (15).

While the reliability and discriminative properties of various STS test protocols, including the five times sit-to-stand (FTSTS) test, 30-sec STS (30-s STS) test and 1-min STS (1-min STS) test, have been reported in different populations (16–18), a gold standard for testing the criterion validity of STS tests in discriminating levels of functional capacity in people with CAD is not yet available. There is therefore a need to establish the construct (convergent and known-groups) validity of STS tests in this population. Further, while STS test performance in patients with heart failure (19) and in patients enrolled in CR (20) have been reported, comparison of the reliability of various STS test protocols in patients with CAD has not been reported.

The focus of this current study is to examine the discriminative properties of the FTSTS, 30-s STS and 1-min STS tests. The primary objective of this current study is to examine the test-retest reliability, convergent and known-groups validity of the 3 STS tests. Convergent validity was examined through investigation of the correlation between STS test scores and the distance covered by the 6MWT, a valid test for measurement of functional capacity. Known-groups validity was examined through the evaluation of statistical and clinically important differences in STS tests of known groups, that is, participants with post-AMI and those without myocardial infarction (non-MI).

Following the assumption that STS tests are feasible alternative measurement tool for functional capacity, the secondary objective of the study was to explore the feasibility of using STS test protocols to discriminate the level of risk of cardiovascular events in people with CAD. Categorization of risk of cardiovascular events was adopted from a previous report, that patients who covered $\leq$ 419 m during a 6MWT were classified at high risk of cardiovascular events (4).

Abbreviations: CAD, coronary artery disease; CR, cardiac rehabilitation; 6MWT, 6-min walk test; STS, sit-to-stand; FTSTS test, five times sit-to-stand test; 30-s STS test, 30-sec sit-to-stand test; 1-min STS test, 1-min sit-to-stand test; LVEF, left ventricular ejection fraction; post-PCI, post percutaneous coronary intervention; non-MI, non-myocardial infarction; post-AMI, post-acute myocardial infarction; BP, blood pressure; HR, heart rate; SD, standard deviation; ICC, intraclass correlation coefficient; LoA, limits of agreement; SEM, standard error of measurement; MDC_{95}, minimal detectable change with 95% confidence interval; ANOVA, one-way analysis of variance; ROC, receiver operating characteristic; AUC, area under the curve; COPD, chronic obstructive pulmonary disease; 6MWD, the distance of 6MWT; MCID, minimal clinically important difference; MD, mean difference.

Materials and methods

Study design and participants

A cross-sectional study (Chinese Clinical Trial Registry Number: 2000037435) was conducted from July 2020 to February 2021. Approval to conduct the study was granted by the Ethics Committee of Xinhua Hospital Affiliated to Shanghai Jiaotong University School of Medicine (Approval Number: XHEC-C-2020-078-1). Participants were considered eligible for enrolment if they were older than 18 years with CAD with a diagnosis of atherosclerosis (as confirmed by angiography), post percutaneous coronary intervention, or at least 6 months post-acute myocardial infarction (post-AMI). The exclusion criteria included: a) raised cardiac troponin I level, b) acute infectious disease, respiratory disease, uncontrolled metabolic disease or hypertension; c) with neuromusculoskeletal, cognitive disorders, visual or auditory dysfunction that would affect performance of STS tests; d) heart failure at Class III or IV of the New York Heart Association (NYHA) classification; e) having previously participated in a CR program.

Procedures

Patients attending follow up at the Xinhua Hospital were screened for eligibility for this study. Eligible patients were invited to participate, with the nature of the study explained and written informed consent obtained from each patient prior to commencement of the study. The socio-demographic characteristics of each participant were then recorded.

Participants were asked to complete a 6MWT, FTSTS, 30-s STS and 1-min STS tests at random order on the same day. All tests were performed once only without any trial runs. This was deemed appropriate as test-retest reliability of FTSTS test was shown to be reliable with a single evaluation session (17). The order of testing was written in a card placed in a sealed envelope and the participants were asked to draw an envelope with the concealed order enclosed. A rest period of 30 min was set between the 6MWT and any of the STS tests, and all participants were given a 5-min rest period between each STS test protocol (21). Blood pressure (BP), heart rate (HR) and level of fatigue (using a CR-10 Borg scale) were recorded before and immediately after each test. Any adverse events were documented. All tests were conducted by the same physiotherapist.

All participants were also invited to draw from another sealed envelope which determined whether they were invited to return on the follow day to repeat the 3 STS tests.

Sit-to-stand test protocols

A chair without arms, with rubber tips on the legs, a hard seat of fixed height 46 cm was positioned against a wall. All 3 STS test protocols required the participant to commence in a seated position with the feet resting flat and ankle joints in the neutral position. All participants were given the instruction to perform the sit-to-stand task as quickly as possible with their arms crossed over the chest and hands on the shoulders (8). A standard STS movement was viewed as the legs being fully straightened when the stand phase concluded and the hip landing firmly on the chair when seated. A test would be terminated if the participant required assistance or was unable to complete the movement. No encouragement was provided during any STS test protocol.

The time for the participant to complete the STS movement five times was recorded for the FTSTS test (12). For 30-s and 1-min STS tests, subjects were required to perform as many STS movements as possible within 30 sec (22) or 1 min, respectively. The number of STS movements completed within the time required was recorded, as appropriate.

6MWT

The 6MWT was conducted following the American Thoracic Society guidelines for the 6MWT (23). All participants completed the 6MWT on a 30-meter flat corridor.

Statistical analysis

Data analyses were performed using the IBM SPSS Statistics 25.0 for Windows (IBM Corp., Armonk, NY) and the MedCalc 18.2.1 (Ostend, Belgium). Continuous variables were reported as mean and standard deviation (SD), and categorical data were shown as a number and percentage. The Kolmogorov-Smirnov test was used to check the normality of data distribution. Test-retest reliability, defined as consistency of the STS test scores recorded in the two separate days, was determined by the intraclass correlation coefficient (ICC) calculated by a two-way mixed model with absolute agreement method (24). The ICC was considered as poor, fair, good and excellent with values of <0.5, 0.5 to 0.75, 0.75 to 0.9, >0.9 respectively (25). Bland-Altman plots were constructed to display the distribution difference of repeated measurements and calculate the limits of agreement (LoA) *via* mean difference $\pm$ 1.96 SD of difference (26). Standard error of measurement (SEM) and a minimal detectable change with 95% confidence intervals (MDC_{95}) were calculated with the formulae $SD\sqrt{1-ICC}$ and $SEM \times \sqrt{2} \times 1.96$ respectively, to estimate the measurement variability (27). Pearson's or Spearman's correlation coefficients were used to measure the magnitude of correlation between STS tests, 6MWT and LVEF, depending on the data distribution. The correlation was considered "negligible to weak," "moderate,"

and "well-accepted" with values <0.3, 0.3 to 0.6, and >0.6 respectively (28, 29). One way to support the convergent validity of the STS tests was a satisfactory correlation value between the STS scores and outcomes recorded with another tool valid for measurement of functional capacity, thus it was hypothesized that the correlation value (r) generated between STS tests and recorded 6MWD should be at least 0.5. Independent Samples *t* test or Mann-Whitney test was used to explore the known-groups validity through analysis of the differences in all tests between groups of patients with non-MI and post-AMI. Based on previous reported values of minimal clinically important differences (MCID) in STS tests in subjects with COPD, the between-group mean difference (MD) in STS tests was hypothesized to be ≥1.3s for the FTSTS test (12), ≥2 repetitions for 30-s STS test (14) and ≥3 repetitions for the 1-min STS test (30). Chi-square test was used to compare distributions of gender, coronary artery lesions, cardiovascular risk factors and type of medications between subgroups.

Lastly, if STS tests are deemed feasible alternatives to 6MWT in assessment of functional capacity in people with CAD, we wish to explore whether STS tests were able to discriminate participants with high and low risk of cardiovascular events, thus, receiver operating characteristic (ROC) curve analyses (31) were performed. The area under the curve (AUC) of the ROC curve would indicate the discriminative ability of the STS tests to differentiate the risk of cardiovascular events. The selection of the optimal cut-off scores for the STS tests was based on principle of minimizing the misclassification with minimum absolute difference between sensitivity and specificity (32). Based on a previous report by Beatty and colleagues, the "cut-off" value adopted in this study to differentiate participants with low or high risk of cardiovascular events was 419 m from the 6MWT (4). The AUC of all STS tests were compared. All statistical tests were two-tailed with the level of significance set at 0.05.

Sample size estimation

With two observations per subject, to achieve 80% power to detect an estimated ICC of 0.8 under the alternative hypothesis, and with the ICC estimated as 0.5 under the null hypothesis, with a significance level of 0.05, the minimum sample size for the STS test-retest reliability was computed as 22. For the known-groups validity testing, the sample size estimation was based on a hypothesized effect size index of 0.6 in testing the mean STS test difference between groups of non-MI and post-AMI patients, using a two-tailed independent *t*-test with a level of significance of 0.05 and statistical power of 0.8. A minimum of 90 patients was required. In the ROC curve analyses of STS tests for differentiating patients with low or high risk of cardiovascular events, a minimum sample of 82 patients was required to achieve 80% power to detect a difference of 0.15 between the AUC of the ROC curve analysis under the null hypothesis of 0.70 and an AUC under the alternative hypothesis of 0.85 using a two-sided z-test at a significance level of 0.05. All the sample size estimations were performed using the PASS 15.0.5 (NCSS, Kaysville, Utah, USA).

Results

Subjects characteristics

A total of 112 patients (mean age 63.9 ± 8.8 years, male 69%) were included in the study and the mean age of the 30 patients participated in the reliability tests was 64.3 ± 7.3 years, (males 53%). The number of post-AMI and non-MI participants was 48 and 64 respectively. Demographic characteristics of all patients are summarized in Table 1. Table 2 displays the HR, BP and level of fatigue at pre and immediately post STS tests and 6MWT. There was no adverse event during all tests. In the post-AMI group, 1 patient required a permanent pacemaker, 2 patients received coronary arterial bypass grafting operations.

Relative and absolute reliability

The relative reliability for FTSTS, 30-s STS, 1-min STS tests were excellent with ICC values all above 0.95 between the two testing days in all STS tests. The minimum detectable change values with 95% confidence interval (MDC_{95}) were 1.11 s, 1.79 repetitions and 3.86 repetitions, respectively (Table 3).

Convergent validity

Correlation between performance of 6MWT and the 3 STS tests were moderate (FTSTS test, $r = -0.53$, $p < 0.001$; 30-s STS test, $r = 0.57$, $p < 0.001$; 1-min STS test, $r = 0.55$, $p < 0.001$). Correlations between recorded LVEF and STS performance or with 6MWT were both weak (Table 4, Figure 1).

Known-groups validity

Table 5 displays results of known-groups validity analyses between patients in the post-AMI and non-MI groups. Patients with post-AMI required significantly longer time in completion of the FTSTS test, means difference (MD) and 95%CI being 1.4 s, 0.3 to 2.6, ($p = 0.009$), less repetitions in both the 30-s STS, MD−2.0, 95% CI: −3.1 to −0.7, ($p = 0.002$) and 1-min STS test MD−3.4, 95%CI: −5.9 to −1.0 ($p = 0.006$); the distance covered in the 6MWT (431.5 ± 64.6 vs. 480.3 ± 57.3, MD −48.8, 95% CI: −71.7 to −25.9, $p < 0.001$) was also less in this group (Table 5, Figure 2). These mean differences were similar or larger than the

TABLE 1 Demographics characteristics of the participants.

Characteristic	Validity study ($n = 112$)	Reliability study ($n = 30$)
Age (years)	63.9 ± 8.8	64.3 ± 7.3
Gender		
Male	77 (69%)	16 (53%)
Female	35 (31%)	14 (47%)
BMI (kg/m^2)	24.6 ± 3.5	24.8 ± 3.5
Diagnosis		
Atherosclerosis	34	10
post-PCI	30	10
post AMI	48	10
Coronary artery lesions		
Single-vessel	41 (37%)	14 (47%)
Double-vessel	24 (21%)	7 (23%)
Triple-vessel	47 (42%)	9 (30%)
Cardiovascular risk factors		
Hypertension	69 (62%)	17 (57%)
Diabetes	43 (38%)	13 (43%)
Hyperlipidaemia	64 (57%)	15 (50%)
Smoking	71 (63%)	20 (67%)
Blood tests		
FBG (mg/dl)	107.91 ± 26.20	110.13 ± 33.43
TC (mg/dl)	144.46 ± 39.04	140.99 ± 25.84
TG (mg/dl)	164.64 ± 144.30	190.14 ± 139.95
HDL (mg/dl)	39.78 ± 10.89	37.51 ± 10.50
LDL (mg/dl)	79.39 ± 31.51	77.03 ± 21.50
NT-proBNP (pg/ml)	283.90 ± 597.48	322.90 ± 811.73
Current medications		
Antiplatelet agents	102 (91%)	27 (90%)
ACEI/ARB	48 (43%)	11 (37%)
β-Blocker	108 (96%)	28 (93%)
Lipid-lowing agents	107 (96%)	29 (97%)
Hypoglycemic agents	36 (32%)	10 (33%)

PCI, percutaneous coronary intervention; post-AMI, post-acute myocardial infarction; BMI; body mass index; FBG, fasting blood glucose; TC, total cholesterol; TG, triglycerides; HDL, high density lipoprotein; LDL, low density lipoprotein; NT-proBNP, N-terminal pro b-type Natriuretic Peptide; ACEI, angiotensin-converting enzyme inhibition; ARB, angiotensin receptor blocker.

pre-specified differences with reference to the MCID values of the STS tests of patients with COPD.

ROC curve analysis

A total of 84 patients achieved more than 419 m in their 6MWT and were thus classified as low- risk cardiovascular event group (4), 28 patients who covered ≤ 419 m were in the high-risk group. ROC curve analysis illustrated that the AUC of FTSTS, 30-s STS,and 1-min STS tests were 0.80 (sensitivity: 75.0%, specificity: 73.8%, optimal cut-off: 11.7 s), 0.83 (sensitivity: 75.0%, specificity: 76.2%, optimal cut-off: 12 repetitions), and 0.80 (sensitivity: 71.4%, specificity: 73.8%, optimal cut-off: 23 repetitions) respectively (Table 6). There were no statistically significant differences in the AUC of the ROC curve analyses among the three STS tests.

Discussion

The use of FTSTS test has been shown to be an instrument of high reliability in healthy adults (33) as well as in people with spinal cord injury (34), hip arthroplasty (17) and in people with chronic obstructive pulmonary disease (12). The 1-min STS test and 30-s STS test were also shown to be reliable measures in people with pulmonary hypertension (22), total knee arthroplasty (35), with COPD (13) and cystic fibrosis (36). This current study is the first that compared all three STS tests in the same population of people with CAD. Findings of our study demonstrated excellent test-retest reliability for all 3 STS tests in this subject-cohort. Further, we found that compared to FTSTS and 30-s STS tests, the 1-min STS test induced the greatest changes in heart rate and SBP, and associated with the highest post-test fatigue score (Table 2). Amongst the 3 STS tests, changes induced by the 1-min STS test were closest to the physiological changes induced by the 6MWT. This suggests that the 1-min STS test is superior than 30-s STS and FTSTS tests if considered as an assessment tool for functional capacity in people with CAD. Our findings were in accord with a previous report which recommended the 1-min STS test to be a superior STS protocol for evaluation of functional capacity in subjects with COPD (8). Further, oxygen consumption was shown to be highest during a 1-min STS test compared to FTSTS in a cohort of patients with COPD (30). Although we have not measured oxygen consumption during the STS tests in our participants with CAD, we postulate that the pattern of oxygen uptake during STS tests would be similar in our subject cohort compared to those with COPD; further analysis is necessary to confirm this assumption.

As anticipated, findings of the current study illustrated moderate correlation between the 3 STS tests and the 6MWT, the correlation coefficient data of our study are similar to those previously reported in community-dwelling older adults (10) and in a cohort of patients with COPD (37). The correlation between LVEF and 6MWT and between LVEF and any STS tests was however only weak. This is not surprising. A lack of correlation between distanced covered in a 6MWT and ejection fraction was also reported in patients with heart failure (38). Exercise capacity was shown to be inversely associated with diastolic dysfunction but not associated with variation of left ventricular systolic function in people with LVEF within

TABLE 2 Hemodynamic data and fatigue score at pre- and immediately post-tests ($n = 112$).

		6MWT	FTSTS	30-s STS	1-min STS	p-value$^{\Delta}$ across groups
HR	pre	72.9 ± 8.3	71.1 ± 6.8 73.8	72.7 ± 8.6	72.3 ± 8.2 87.5	$p = 0.35$
(beats/min)	post	85.9 ± 8.4	± 7.8	79.6 ± 9.2	± 8.9	
	% change	+17.8%	+3.8%	+9.5%	+21.0%	$p < 0.001$
p-value*		$p < 0.001$	$p < 0.001$	$p < 0.001$	$p < 0.001$	
SBP (mmHg)	pre	125.0 ± 12.5	124.9 ± 13.3	125.3 ± 13.5	128.2 ± 12.6	$p = 0.18$
	post	146.8 ± 14.1	130.4 ± 12.4	139.4 ± 16.3	149.3 ± 14.8	
	% change	+17.4%	+4.4%	+11.3%	+16.5%	$p < 0.001$
p-value*		$p < 0.001$	$p < 0.001$	$p < 0.001$	$p < 0.001$	
DBP (mmHg)	pre	73.0 ± 9.7	73.3 ± 8.8 73.4	74.3 ± 8.4	75.3 ± 7.5 84.5	$p = 0.20$
	post	81.5 ± 8.6	± 9.3	83.0 ± 8.7	± 8.8	
	% change	+11.6%	0.1%	+11.7%	+12.2%	$p < 0.001$
p-value*		$p < 0.001$	$p = 0.90$	$p < 0.001$	$p < 0.001$	
Fatigue score	pre	0.2 ± 0.4	0.2 ± 0.5	0.2 ± 0.6	0.2 ± 0.5	$p = 0.93$
	post	4.0 ± 0.9	0.3 ± 0.6	2.4 ± 1.1	4.2 ± 1.7	$p < 0.001$
p-value*		$p < 0.001$	$p = 0.05$	$p < 0.001$	$p < 0.001$	

HR, heart rate, SBP, systolic blood pressure, DBP, diastolic blood pressure, 6MWT, six-minute walk test, FTSTS, five times sit-to-stand, 30-s STS, 30-second sit-to-stand, 1-min STS, 1-minute sit-to-stand. Mean diff, mean difference between pre and post values.
*p-value determined by paired t-test or Wilcoxon signed rank test; $^{\Delta}$p-value determined by repeated measures ANOVA or Kruskal-Wallis H test.

TABLE 3 Relative and absolute reliability results of the three STS tests ($n = 30$).

	ICC (95% CI)	1st measure	2nd measure	SEM	MDC_{95}	95% LoA
FTSTS (sec)	0.96 (0.92–0.98)	12.01 ± 2.04	11.85 ± 2.14	0.40	1.11	−0.96–1.26
30–s STS (repetitions)	0.95 (0.91–0.98)	13.07 ± 3.06	12.97 ± 3.02	0.65	1.79	−1.71–1.91
1–min STS (repetitions)	0.96 (0.91–0.98)	24.67 ± 6.69	25.10 ± 6.69	1.39	3.86	−4.31–3.44

ICC, intraclass correlation coefficient; 95% CI, 95% confidence interval; SEM, standard error of measurement; MDC_{95}, minimum detectable change with 95% CI; LoA, 95% limits of agreement; FTSTS, five times sit–to–stand; 30–s STS, 30–sec sit–to–stand; 1–min STS, 1–min sit–to–stand.

TABLE 4 Correlation analysis between STS tests with 6MWT and LVEF.

		FTSTS	30–s STS	1–min STS	6MWT
6MWT	r	$r_s = -0.53$	$r_s = 0.57$	$r_p = 0.55$	–
	p	< 0.001	< 0.001	< 0.001	–
LVEF	r	$r_s = -0.27$	$r_s = 0.31$	$r_s = 0.27$	$r_s = 0.29$
	p	0.003	0.001	0.004	0.002

FTSTS, five times sit–to–stand; 30–s STS, 30–sec sit–to–stand; 1–min STS, 1–min sit–to–stand; 6MWT, six–min walk test; LVEF, left ventricular ejection fraction.
r = Rho; r_p = Pearson correlation coefficient; r_s = Spearman correlation coefficient; p = p–value.

normal range (39). The LVEF of our patient cohort was all above 56%, it is therefore not surprising that there existed only a weak correlation between LVEF and exercise capacity (reflected by 6MWT or STS tests). While cardiac dysfunction partly contributes to poor exercise capacity, skeletal muscle fatigability plays an important mechanism in exercise tolerance (40); further, in patients with a normal ejection fraction, exercise capacity is associated with left ventricular dimensions (41), however, assessment of skeletal muscle fatigability and appraisal of left ventricular dimension was outside of the scope of this study.

The 6MWT has been suggested to be a prognostic tool for cardiovascular events in patients with stable CAD (4). Beatty and colleagues reported that patients in the lowest quartile of 6MWD of 87-419 m had 4 times the risk of cardiovascular events compared to those in the highest 6MWD quartile of 544-837 m. Based on Beatty and colleagues' work, we used 6MWD of 419 m to demarcate high or low-risk cardiovascular

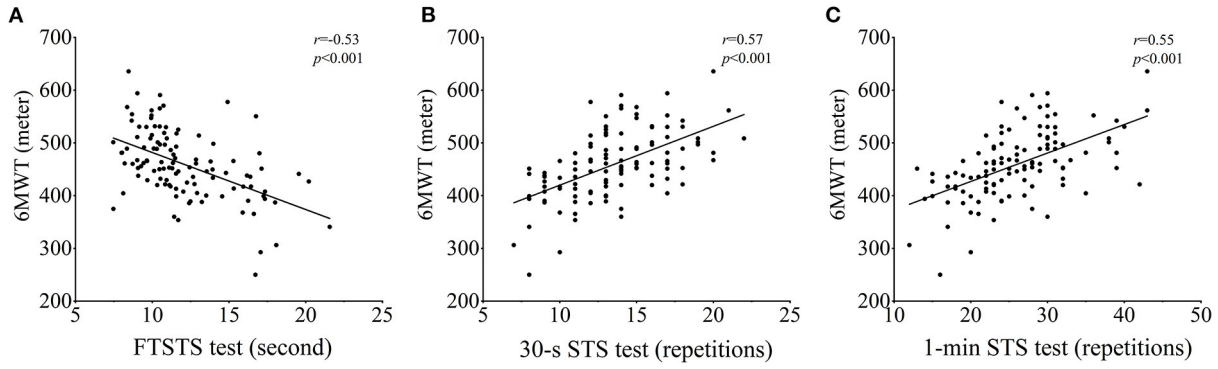

FIGURE 1
Correlations between 6MWT and the 3 STS tests. FTSTS test: five times sit-to-stand test, 30-s STS test: 30-sec sit-to-stand test, 1-min STS test: 1-min sit-to-stand test, 6MWT: six-min walk test.

TABLE 5 Comparison of STS tests and 6MWT performance between post–AMI and non–MI groups.

	post–AMI	non–MI	Mean Difference	95% CI	*p*–value
FTSTS test (sec)	12.9 ± 3.3	11.5 ± 2.8	1.4	0.3 ∼ 2.6	$P = 0.009^{**}$
30–s STS test (repetitions)	12.4 ± 2.9	14.4 ± 3.3	−2.0	−3.1 ∼ −0.7	$p = 0.002^{**}$
1–min STS test (repetitions)	24.1 ± 5.9	27.5 ± 6.8	−3.4	- 5.9 ∼ −1.0	$p = 0.006^{**}$
6MWT (meter)	431.5 ± 64.6	480.3 ± 57.3	−48.8	−71.7 ∼ −25.9	$p < 0.001^{**}$

post–AMI, post–acute myocardial infarction; 95% CI, 95% confidence interval; FTSTS test, five times sit–to–stand test; 30–s STS test, 30–sec sit–to–stand test; 1–min STS test, 1–min sit–to–stand test; 6MWT, six–min walk test.
** $p < 0.01$.

event groups. With ROC curve analysis of our data, we showed that the 3 STS tests demonstrated good discriminative ability to differentiate patients between high and low risk cardiovascular events. Results of this analysis suggest that for patients with CAD, those who required more than 11.7 sec to complete a FTSTS test, or those who completed < 12 repetitions of STS sequence in 30 sec or < 23 STS-repetitions in 1 min were subjected to higher risk of cardiovascular events.

The MDC_{95} data generated from this study illustrated the measurement errors on repeated measurements of the STS tests. The MDC_{95} value for FTSTS test was previously reported in patients with COPD to be 3.1s (12). Our study showed that the MDC_{95} value for FTSTS test in people with CAD was 1.1s. This suggests that the measurement error of FTSTS test was less in our cohort of participants with CAD compared to people with COPD. Similarly, MDC_{95} value for the 30-s STS test reported in subjects with COPD (42) was also higher than that generated in this study. The MDC_{95} of 1-min STS test reported by Crook and colleagues (30) was however smaller than our results (2.2 repetitions compared to 3.86 repetitions in our CAD cohort). Direct comparison between our study and previous reports however may not be appropriate. As the MDC_{95} in other reports were generated from tests conducted in patients with COPD, whose exercise capacity was limited by impairment of the ventilatory system, and our data were obtained from patients with CAD, whose functional capacity is often restricted by cardiac performance.

Smoking, hyperlipaemia, hyperglycaemia, and hypertension are known risks factors of cardiovascular disease (43). Table 1 shows that the rate of smoking is high amongst our participants. Unfortunately, China is the largest consumer of tobacco in the world (WHO-Tobacco in China) (44) and smoking prevalence is about 26.6% (45); there are more than 300 million smokers in China, this suggests that greater effort is required to foster public health strategies of smoking cessation.

In summary, this study showed that all 3 STS tests have excellent test-retest reliability. The MDC_{95} values reported in this study provide a useful guide for the versatile use of STS protocols. The relationship of the STS tests with 6MWT demonstrated that these tests have good convergent validity in assessment of functional capacity in patients with CAD. Known-groups validity of these STS test was illustrated through distinct performance level by non-MI and post-AMI groups. STS tests are easy to perform and can be used as an assessment as well as an exercise training tool. Lastly this study inferred that STS test can also be considered as a discriminative tool to predict high or low risk of cardiovascular events in patients with CAD.

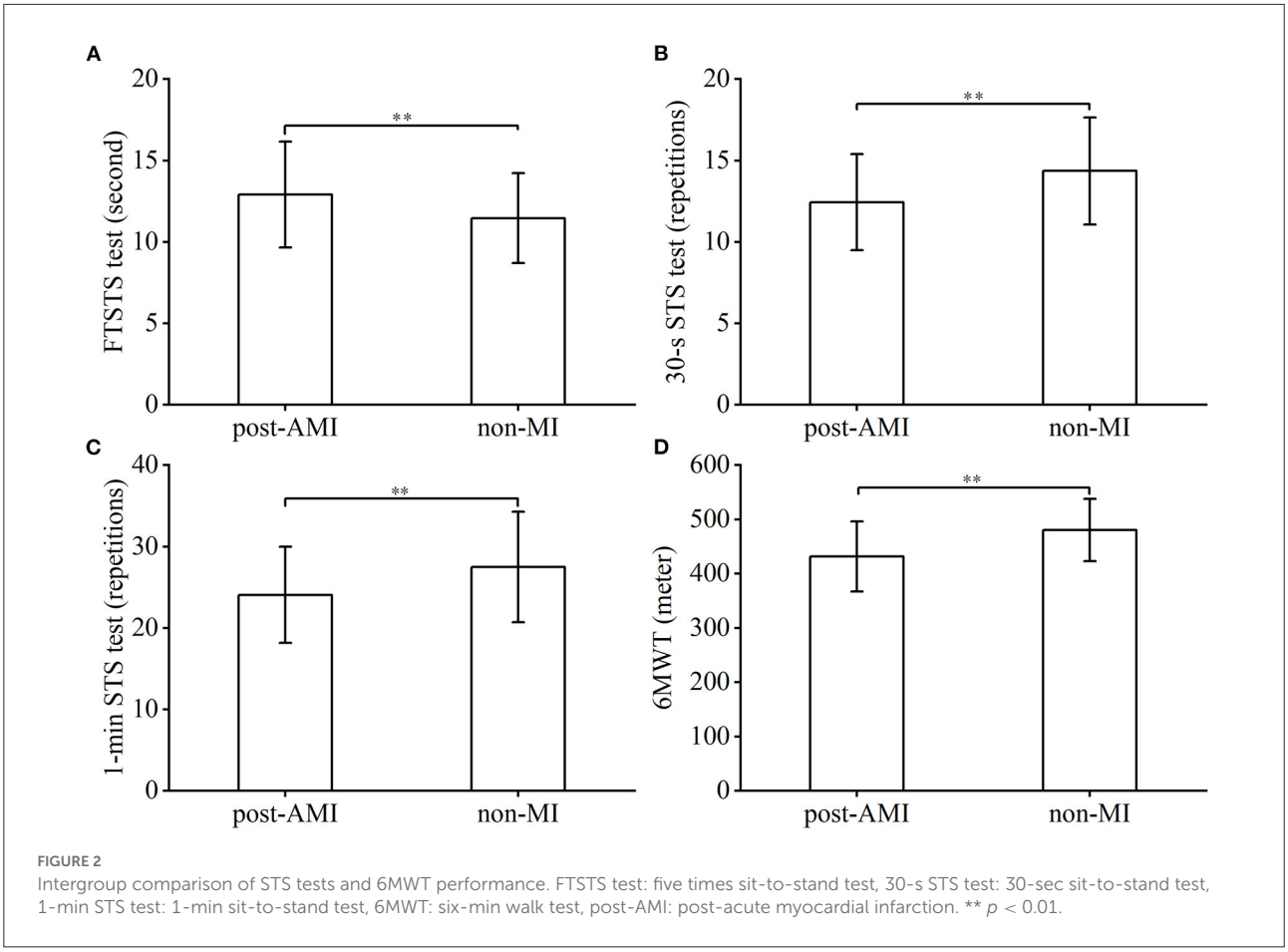

FIGURE 2
Intergroup comparison of STS tests and 6MWT performance. FTSTS test: five times sit-to-stand test, 30-s STS test: 30-sec sit-to-stand test, 1-min STS test: 1-min sit-to-stand test, 6MWT: six-min walk test, post-AMI: post-acute myocardial infarction. ** $p < 0.01$.

TABLE 6 ROC analysis of discriminatory capability of STS tests on 6MWD over 419 m.

Tests	AUC (95% CI)	optimal cut-off	Sensitivity	Specificity	*p*-values
FTSTS (second)	0.80 (0.71–0.87)	>11.7	75.0%	73.8%	$p<0.001$**
30-s STS (repetitions)	0.83 (0.75–0.89)	≤12	75.0%	76.2%	$p<0.001$**
1-min STS (repetitions)	0.80 (0.71–0.87)	≤23	71.4%	73.8%	$p<0.001$**

ROC, receiver operating characteristic; 6MWD, distance of six-min walk; AUC, area under the curve; FTSTS, five times sit-to-stand; 30-s STS, 30-sec sit-to-stand; 1-min STS, 1-min sit-to-stand.
** p <0.01.

Limitations of the study

This study demonstrated a satisfactory correlation between 6MWD and the STS tests and proposed that STS tests can be considered as a useful tool to assess function capacity. While we have demonstrated similar haemodynamic responses between 6MWT and the STS test, we did not have appropriate equipment to measure oxygen consumption during the STS tests. Information on oxygen uptake during the STS test would provide a more detailed picture of physiological demands of STS tests.

High and low risk cardiovascular events was categorized using 6MWD of 419 m as the demarcation level. While the predictive validity of this assumption was proven (4), inclusion of cumulative biometric risk factors may provide a stronger profile of risks of cardiovascular events. Validity of an index which combines the 6MWD and biometric risk factors requires further investigation.

The focus of this study was to establish discriminative properties of the three STS tests; establishment of the evaluative and prognostic properties of these tests in people with CAD was outside the scope of this study. Further research in

examining the evaluative and prognostic value of STS tests is warranted.

Conclusion

This is the first study that compared FTSTS test, 30-s STS test, and 1-min STS test in patients with CAD. This study showed that all 3 STS tests had good test-retest reliability, convergent and known-groups validity in assessing functional capacity in CAD patients. All 3 STS tests demonstrated good discriminative property in distinguishing patients with high and low risk of cardiovascular events and as such may inform the individualized clinical management, targeted exercise programmes and rehabilitation in this patient population.

Data availability statement

The original contributions presented in the study are included in the article/supplementary material, further inquiries can be directed to the corresponding authors.

Ethics statement

The studies involving human participants were reviewed and approved by the Ethics Committee of Xinhua Hospital Affiliated to Shanghai Jiaotong University School of Medicine (Approval Number: XHEC-C-2020-078-1). The patients/participants provided their written informed consent to participate in this study.

Author contributions

Study conceptualization: ZW, JY, SM, JL, JH, and AJ. Data curation: ZW, JY, SM, JL, YY, and TZ. Statistical analysis: RT and DE-A. Manuscript preparation and writing the first draft: ZW, JY, and SM. Writing the section of the manuscript: JL, YY, TZ, DE-A, RT, JH, and AJ. All authors contributed to manuscript revision and have read and approved the final version of the manuscript.

Funding

This work was supported by the National Natural Science Foundation of China (No. 31870936).

Conflict of interest

The authors declare that the research was conducted in the absence of any commercial or financial relationships that could be construed as a potential conflict of interest.

Publisher's note

All claims expressed in this article are solely those of the authors and do not necessarily represent those of their affiliated organizations, or those of the publisher, the editors and the reviewers. Any product that may be evaluated in this article, or claim that may be made by its manufacturer, is not guaranteed or endorsed by the publisher.

References

1. World Health Organisation. *The Top 10 Causes of Death*. (2021). Available online at: https://www.who.int/news- room/fact-sheets/detail/the-top-10-causes-of-death (accessed May 22, 2022).

2. Roser M, Ritchie H., Burden of disease. Institute for health metrics and evaluation. (2018). Available online at: : https://ourworldindata.org/burden-of-disease (accessed May 22, 2022).

3. Prabhu NV, Maiya AG, Prabhu NS. Impact of cardiac rehabilitation on functional capacity and physical activity after coronary revascularization: a scientific review. *Cardiol Res Pract.* (2020) 2020:1–9. doi: 10.1155/2020/1236968

4. Beatty AL, Schiller NB, Whooley MA. Six-Minute walk test as a prognostic tool in stable coronary heart disease. *Arch Int Med.* (2012) 172:2198. doi: 10.1001/archinternmed.2012.2198

5. Singh SJ, Puhan MA, Andrianopoulos V, Hernandes NA, Mitchell KE, Hill CJ, et al. An official systematic review of the European Respiratory Society/American Thoracic Society: measurement properties of field walking tests in chronic respiratory disease. *Eur Res J.* (2014) 44:1447–78. doi: 10.1183/09031936.00150414

6. Csuka M, McCarty DJ. Simple method for measurement of lower extremity muscle strength. *Am J Med.* (1985) 78:77–81. doi: 10.1016/0002-9343(85)90465-6

7. Nagasawa Y, Nakamura K, Yokokawa Y, Ohira M. Validity and reproducibility of an incremental sit-to-stand exercise test in healthy middle-aged individuals. *J Physical Therapy Sci.* (2019) 31:414–7. doi: 10.1589/jpts.31.414

8. Morita AA, Bisca GW, Machado FVC, Hernandes NA, Pitta F, Probst VS, et al. Best protocol for the sit-to-stand test in subjects with COPD. *Respir Care.* (2018) 63:1040–9. doi: 10.4187/respcare.05100

9. Silva PF, Quintino LF, Franco J, Faria CD. Measurement properties and feasibility of clinical tests to assess sit-to-stand/stand-to-sit tasks in subjects with neurological disease: a systematic review. *Brazilian J Phys Therapy.* (2014) 18:99–110. doi: 10.1590/S1413-35552012005000155

10. Yee XS, Ng YS, Allen JC, Latib A, Tay EL, Abu Bakar HM, et al. Performance on sit-to-stand tests in relation to measures of functional fitness and sarcopenia diagnosis in community-dwelling older adults. *Eur Rev Aging Phys Activity.* (2021) 18:1. doi: 10.1186/s11556-020-00255-5

11. Kirshner B, Guyatt G. A methodological framework for assessing health indices. *J Chronic Dis.* (1985) 38:27–36. doi: 10.1016/0021-9681(85)90005-0

12. Jones SE, Kon SSC, Canavan JL, Patel MS, Clark AL, Nolan CM, et al. The five-repetition sit-to-stand test as a functional outcome measure in COPD. *Thorax.* (2013) 68:1015–20. doi: 10.1136/thoraxjnl-2013-203576

13. Reychler G, Boucard E, Peran L, Pichon R, Le Ber-Moy C, Ouksel H, et al. One minute sit-to-stand test is an alternative to 6MWT to measure functional exercise performance in COPD patients. *Clin Respir J.* (2018) 12:1247–56. doi: 10.1111/crj.12658

14. Zanini A, Crisafulli E, D'Andria M, Gregorini C, Cherubino F, Zampogna E, et al. Minimum clinically important difference in 30-s sit-to-stand test after

pulmonary rehabilitation in subjects with COPD. *Respir Care.* (2019) 64:1261–9. doi: 10.4187/respcare.06694

15. Puhan MA, Siebeling L, Zoller M, Muggensturm P, Riet GT. Simple functional performance tests and mortality in COPD. *Eur Resp J.* (2013) 42:956–63. doi: 10.1183/09031936.00131612

16. Jones CJ, Rikli RE, Beam WC. A 30-s chair-stand test as a measure of lower body strength in community-residing older adults. *Res Quarter Ex Sport.* (1999) 70:113–9. doi: 10.1080/02701367.1999.10608028

17. Özden F, Coşkun G, Bakirhan, S. The test-retest reliability and concurrent validity of the five times sit to stand test and step test in older adults with total hip arthroplasty. *Experimental Gerontol.* (2020) 142:111143. doi: 10.1016/j.exger.2020.111143

18. Reychler G, Pincin L, Audag N, Poncin W, Caty G. One-minute sit-to-stand test as an alternative tool to assess the quadriceps muscle strength in children. *Res Med Res.* (2020) 78:100777. doi: 10.1016/j.resmer.2020.100777

19. Yang C, Xu G, Lan Y. The measurement of 5-minutes-sit-to-stand test performance in patients with chronic heart failure. *Chin J Rehabili Med.* (2015) 30:661–6. doi: 10.3969/j.issn.1001-1242.2015.07.006

20. Puthoff ML, Saskowski D. Reliability and responsiveness of gait speed, five times sit to stand, and hand grip strength for patients in cardiac rehabilitation. *Cardiopulm Phys Ther J.* (2013) 24:31–7. doi: 10.1097/01823246-201324010-00005

21. Gurses HN, Zeren M, Denizoglu Kulli H, Durgut E. The relationship of sit-to-stand tests with 6-minute walk test in healthy young adults. *Medicine.* (2018) 97:e9489. doi: 10.1097/MD.0000000000009489

22. Kahraman BO, Ozsoy I, Akdeniz B, Ozpelit E, Sevinc C, Acar S, et al. Test-retest reliability and validity of the timed up and go test and 30-second sit to stand test in patients with pulmonary hypertension. *Int J Cardiol.* (2020) 304:159–63. doi: 10.1016/j.ijcard.2020.01.028

23. Statement ATS. American Journal of Respiratory and Critical Care. *Medicine.* (2002) 166:111–17. doi: 10.1164/ajrccm.166.1.at1102

24. Qin S, Nelson L, McLeod L, Eremenco S, Coons SJ. Assessing test-retest reliability of patient-reported outcome measures using intraclass correlation coefficients: recommendations for selecting and documenting the analytical formula. *Quality Life Res.* (2019) 28:1029–33. doi: 10.1007/s11136-018-2076-0

25. Koo TK, Li MY. A guideline of selecting and reporting intraclass correlation coefficients for reliability research. *J Chiropr Med.* (2016) 15:155–63. doi: 10.1016/j.jcm.2016.02.012

26. Giavarina D. Understanding bland altman analysis. *Biochemia medica.* (2015) 25:141–51. doi: 10.11613/BM.2015.015

27. Furlan L, Sterr A. The applicability of standard error of measurement and minimal detectable change to motor learning research—a behavioral study. *Front Human Neurosci.* (2018) 12:95 doi: 10.3389/fnhum.2018.00095

28. Andresen EM.. Criteria for assessing the tools of disability outcomes research. *Arch Physical Med Rehabili.* (2000) 81(12 Suppl. 2):S15–20. doi: 10.1053/apmr.2000.20619

29. Post MW. What to do with "Moderate" reliability and validity coefficients? *Arch Physical Med Rehabili.* (2016) 97:1051–2. doi: 10.1016/j.apmr.2016.04.001

30. Crook S, Büsching G, Schultz K, Lehbert N, Jelusic D, Keusch S, et al. A multicentre validation of the 1-min sit-to-stand test in patients with COPD. *Euro Resp J.* (2017) 49:1601871. doi: 10.1183/13993003.01871-2016

31. Streiner DL, Cairney J. What's under the ROC? an introduction to receiver operating characteristics curves. *Can J Psychiatry.* (2007) 52:121–8. doi: 10.1177/070674370705200210

32. Unal I. Defining an optimal cut-point value in roc analysis: an alternative approach. *Comput Math Methods Med.* (2017) 2017:1–14. doi: 10.1155/2017/3762651

33. Northgraves MJ, Hayes SC, Marshall P, Madden LA, Vince RV. The test-retest reliability of four functional mobility tests in apparently healthy adults. *Isokinet Exerc Sci.* (2016) 24:171–9. doi: 10.3233/IES-160614

34. Khuna L, Thaweewannakij T, Wattanapan P, Amatachaya P, Amatachaya S. Five times sit-to-stand test for ambulatory individuals with spinal cord injury: a psychometric study on the effects of arm placements. *Spinal Cord.* (2020) 58:356–64. doi: 10.1038/s41393-019-0372-3

35. Unver B, Kalkan S, Yuksel E, Kahraman T, Karatosun V. Reliability of the 50-foot walk test and 30-sec chair stand test in total knee arthroplasty. *Acta Ortopedica Brasileira.* (2015) 23:184–7. doi: 10.1590/1413-78522015230401018

36. Radtke T, Puhan MA, Hebestreit H, Kriemler S. The 1-min sit-to-stand test A simple functional capacity test in cystic fibrosis? *J Cystic Fibrosis.* (2016) 15:223–6. doi: 10.1016/j.jcf.2015.08.006

37. Zhang Q, Li Y, Li X, Yin Y, Li R, Qiao X, et al. A comparative study of the five-repetition sit-to-stand test and the 30-second sit-to-stand test to assess exercise tolerance in COPD patients. *Int J Chron Obstruct Pulmon Dis.* (2018) 13:2833–9. doi: 10.2147/COPD.S173509

38. Muoneme AS, Isiguzo GC, Iroezindu MO, Okeahialam BN. Relationship between Six-Minute Walk Test and Left Ventricular Systolic Function in Nigerian Patients with Heart Failure. *West Afr J Med.* (2015) 34:133–8.

39. Grewal J, McCully RB, Kane GC, Lam C, Pellikka PA. Left ventricular function and exercise capacity. *JAMA.* (2009) 301:286–94. doi: 10.1001/jama.2008.1022

40. Keller-Ross ML, Larson M, Johnson BD. Skeletal muscle fatigability in heart failure. *Front Physiol.* (2019) 10:129. doi: 10.3389/fphys.2019.00129

41. Meyer M, McEntee RK, Nyotowidjojo I, Chu G, Lewinter MM. Relationship of exercise capacity and left ventricular dimensions in patients with a normal ejection fraction. *An Exploratory Study Plos ONE.* (2015) 10:e0119432. doi: 10.1371/journal.pone.0119432

42. Hansen H, Beyer N, Frlich A, Godtfredsen N, Bieler T. Intra- and inter-rater reproducibility of the 6-minute walk test and the 30-second sit-to-stand test in patients with severe and very severe COPD. *Int J Chron Obstruct Pulmon Dis.* (2018) 13:3447–57. doi: 10.2147/COPD.S174248

43. Fioranelli M, Bottaccioli AG, Bottaccioli F, Bianchi M, Rovesti M, Roccia MG. Stress and Inflammation in Coronary Artery Disease: A Review Psychoneuroendocrineimmunology-Based. *Front Immunol.* (2018) 9:031 doi: 10.3389/fimmu.2018.02031

44. World Health Organisation. *Tobacco in China*. Available online at: https://www.who.int/China/health-topics/tobacco (accessed May 20, 2022).

45. Chinese Center for Disease, Control, and Prevention. Chinese Adults Tobacco Survey Report (2018).

frontiers | Frontiers in Cardiovascular Medicine

TYPE Review
PUBLISHED 26 August 2022
DOI 10.3389/fcvm.2022.940615

OPEN ACCESS

EDITED BY
Chayakrit Krittanawong,
New York University, United States

REVIEWED BY
Joseph Hadaya,
University of California, Los Angeles, United States
Alessandro Maloberti,
University of Milano Bicocca, Italy

*CORRESPONDENCE
Shudong Xia
shystone@zju.edu.cn

†These authors have contributed equally to this work

SPECIALTY SECTION
This article was submitted to Cardiovascular Epidemiology and Prevention, a section of the journal Frontiers in Cardiovascular Medicine

RECEIVED 10 May 2022
ACCEPTED 18 July 2022
PUBLISHED 26 August 2022

CITATION
Lin W, Jia S, Chen Y, Shi H, Zhao J, Li Z, Wu Y, Jiang H, Zhang Q, Wang W, Chen Y, Feng C and Xia S (2022) Korotkoff sounds dynamically reflect changes in cardiac function based on deep learning methods
Front. Cardiovasc. Med. 9:940615.
doi: 10.3389/fcvm.2022.940615

Korotkoff sounds dynamically reflect changes in cardiac function based on deep learning methods

Wenting Lin[1†], Sixiang Jia[1†], Yiwen Chen[1†], Hanning Shi[2], Jianqiang Zhao[1], Zhe Li[1], Yiteng Wu[1], Hangpan Jiang[1], Qi Zhang[1], Wei Wang[1], Yayu Chen[1], Chao Feng[1] and Shudong Xia[1*]

[1]Department of Cardiology, The Fourth Affiliated Hospital, Zhejiang University School of Medicine, Yiwu, China, [2]Department of Anime and Comics, Hangzhou Normal University, Hangzhou, China

Korotkoff sounds (K-sounds) have been around for over 100 years and are considered the gold standard for blood pressure (BP) measurement. K-sounds are also unique for the diagnosis and treatment of cardiovascular diseases; however, their efficacy is limited. The incidences of heart failure (HF) are increasing, which necessitate the development of a rapid and convenient pre-hospital screening method. In this review, we propose a deep learning (DL) method and the possibility of using K-methods to predict cardiac function changes for the detection of cardiac dysfunctions.

KEYWORDS

Korotkoff sounds, cardiac function, heart failure, deep learning, prediction

Introduction

Blood pressure (BP) measurement using Korotkoff sounds (K-sounds), which are considered the gold standard for BP measurement, has been performed for over 100 years (1). When done by a trained clinical practitioner, the K-sounds approach may yield more accurate results than the automated oscillometric method (2). Accurate BP measurement facilitates daily monitoring of an individual's vital signs, while inaccurate results can cause unnecessary panic, as a 5-mmHg error can halve or double the number of hypertensive patients (2, 3).

Accurate BP monitoring is clinically important. Prolonged inappropriate elevations of BP can lead to a series of adverse cardiovascular events that eventually result in cardiovascular end-stage heart failure (HF) (4, 5). HF is a slow myocardial remodeling process, and as a complex group of clinical symptoms, clinical guidelines emphasize its prevention (6–11). Thus, various prediction models for HF have emerged, and they have substantially improved in the last decade. These predictive models are generally based on patients' laboratory findings, with some accessible clinical features that enrich model heterogeneity and quantify the risk score, but they are more cumbersome and complex in their operationalization (12). Moreover, they do not reflect dynamic changes in cardiac functions.

Heart failure involves the deterioration of cardiac functions. The onset of acute HF is attributed to various triggers (11, 13, 14). It is difficult to predict at which point HF will occur; however, it is still feasible to stabilize cardiac functions, thereby preventing the onset of HF through reasonable monitoring. However, currently, the assessment of cardiac functions is challenging.

The K-sounds are not limited to BP measurements, and some clinical treatments have long been noted. In 1972, Cotoi et al. evaluated the possibility of using K-sounds to assess ventricular performance (15). As a result of the limitations of relevant equipment in that era, the theory was not well accepted. Due to widespread awareness of BP measurements and the high prevalence of hypertension and HF, Cotoi's vision using K-sounds can still be used to monitor cardiac functions. The five temporal phases of K-sounds are complex, and currently, the intrinsic mechanisms have not been fully established (16).

Technological advances have introduced the use of artificial intelligence (AI) algorithms in various fields. The medical field is also benefiting from the advances in AI algorithms, which have increased collaborations in medical–industrial crossover projects (17–19). Deep learning (DL) algorithms have been developed (20, 21). These algorithms can mine informative data features from massive data, and they only need to give good data annotations to obtain satisfactory training results. Based on the characteristics of DL, it may be challenging to establish signal differences between K-sounds in patients suffering from HF and patients with normal cardiac functions. It is reasonable to perform data labeling of actual clinical outcomes, which will enable the use of DL-based approaches to dynamically monitor cardiac functions with K-sounds and to predict the onset and progression of HF.

We hypothesized that HF occurrence involves alterations of K-sounds signals, and the use of the K-sounds approach to assessing cardiac functions will aid clinical decisions. Based on this idea, we propose a feasible means of early screening with respect to the cardiac function. We present a review of the rational use of K-sounds to evaluate changes in cardiac functions in real-time for rapid detection of patients with cardiac dysfunction roughly. Currently, the diagnosis of HF with preserved ejection fraction (HFpEF) is clinically demanding and inaccurate, necessitating the need for suitable alternatives in a follow-up study.

Origin and mechanisms of Korotkoff-sounds

During the Russo-Japanese War, the Russian surgeon (Nikolai Korotkoff) aimed at using reliable clinical signs to predict the feasibility of plasmatic flow after vascularization of traumatic aneurysms. He found that when fully compressing the distal end of a patient with a brachial aneurysm and gradually relaxing the cuff pressure, a series of sounds could be heard with a stethoscope under the compressed distal artery. This was found to be applicable in the normal population (22–24). He made detailed notes and analysis of the audio (**Table 1**) (1, 16, 25, 26).

In simple terms, K-sounds are based on the opening and closing of the brachial artery wall due to changes in external pressure. Many hypotheses and theoretical mechanisms have been proposed for the occurrence of K-sounds (22, 23, 27–34).

I) **The water hammer mechanism:** Water hammer usually occurs in a pressurized line. When some inappropriate external forces are applied, they result in changes in the water flow. However, due to inertia, the water flow creates a shock wave, resulting in the water strike phenomenon.

The brachial artery acts as a "pressure conduit," the pressure exerted by the cuff can be seen as an external factor that alters the blood flow and its velocity in the brachial artery, resulting in K-sounds.

II) **The pistol shot mechanism:** It is like a process where a bullet is loaded and then fired. Rapid motions of arterial walls result in disturbances in downstream flow. These transient changes in the flow are thought to produce the K-sounds.

III) **"Jet" theory:** Partially constricted vessels result in the formation of downstream fluid jets, even with constant inlet and outlet pressures. The K-sounds are thought to be produced by the impact of jet force on the blood vessels.

Recently, Babbs et al. replicated the three mechanisms mentioned above and combined them with the numerical model. They proposed that the spring–mass–damper model faithfully reproduces the time-domain waveforms of actual K-sounds in humans (16). Although opinions vary, the core idea was that arterial walls' oscillation produces sound based on the turbulence theory of the blood flow. The K-sounds triggered by dynamic changes in the blood flow provide good evidence for subsequent prediction of cardiac functions; after

TABLE 1 The phases of Korotkoff sounds (K-sounds) and related properties.

The phase of Korotkoff sound	Qualitative
I	Appearance: The first loud tapping sound heard, systolic pressure
II	Softening: Weakened clapping sound and soft wind-like murmur
III	Sharpening: Blowing wind-like murmur disappears
IV	Muffling: The tone is suddenly dull
V	Disappearance: Loss of sound, diastolic pressure

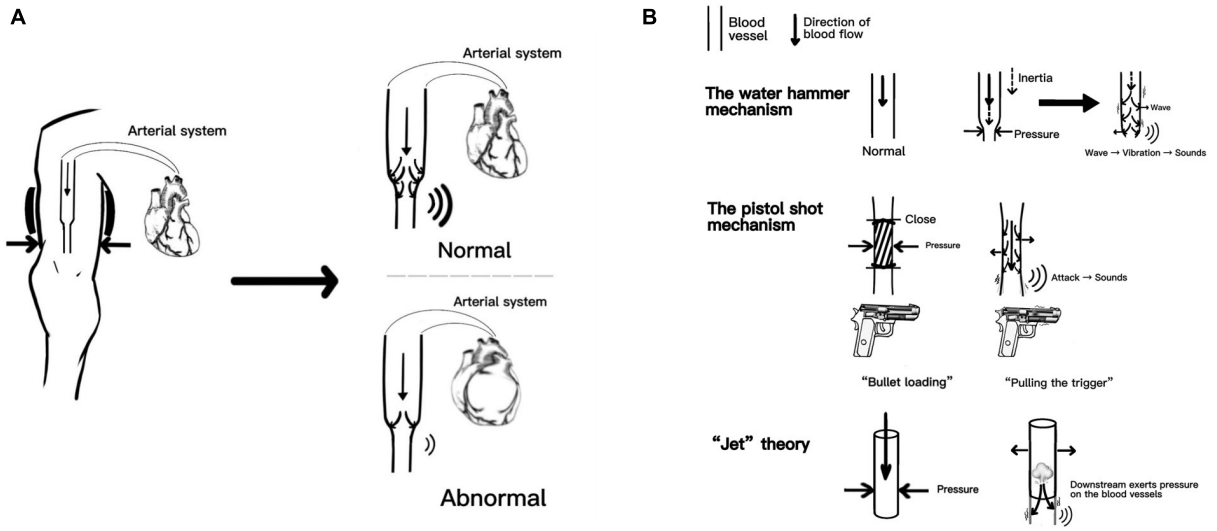

FIGURE 1
Part **A** reproduces the "core" theory of the Korotkoff sounds (K-sounds) mechanism and compares the changes in K-sounds produced by normal and abnormal cardiac function. Part **B** reasonably reproduces the three hypothese.

all, the fundamental power for blood flow originates from the cardiac system. We specifically mapped the production of K-sounds related mechanisms, as shown in **Figure 1**. **Figure 1A** reproduces the "core" theory of the K-sounds mechanism and compares the changes in K-sounds produced by normal and abnormal cardiac function. **Figure 1B** reasonably reproduces the three hypotheses.

Past and current states of Korotkoff-sounds in clinical applications

Blood pressure measurement using the auscultation method of K-sounds has become an essential clinical skill.

Usually, the patient's upper arm is positioned at the level of the heart. The examiner first palpates the brachial artery pulsation at the elbow fossa and then places the stethoscope at the strongest pulsation point of the brachial artery. Then, the cuff is inflated and auscultation is performed at the same time. When brachial pulsation disappears, the mercury column is raised by 20–30 mmHg and then deflation is started at a rate of 2–3 mmHg/s. The moment at which the K-sounds appear and disappear is used to determine the patient's systolic and diastolic BP levels (25, 35).

However, in rapid pre-hospital consultations, this cumbersome K-sounds measurement of BP has too many limitations. First, although it is a simple process, it is also slow. Moreover, it may exhibit errors that arise from interferences in cuff pressure, surrounding environment, the position of the stethoscope, clinical experience or hearing or concentration of the observer during measurement, and the patient's muscle tension, age, and respiratory rate among other factors (36–41). The efficacy of the use of the K-sounds method for BP measurements in children and pregnant women has not been conclusively determined, especially with regard to the use of IV or V phases of K-sounds for diastolic BP. In the adolescent population, the II and III phases of K-sounds are differentially altered (42, 43). The use of K-sounds methods for BP measurement in patients with persistent atrial fibrillation is further limited because their pulse rate is less than their heart rate (35, 44, 45).

The above-mentioned limitations should not hinder the clinical applications of K-sounds. Currently, efforts have been made to enhance the accuracy of BP measurements using the principle of K-sounds. This promotes the clinical applications of K-sounds and informs on clinical treatment. Moreover, it provides the basis for subsequent dynamic monitoring of cardiac function changes using K-sounds.

Advances in artificial intelligence (AI) have benefited the use of K-sounds for BP measurements. AI is essential for reducing errors and has the potential for achieving accuracy with greater precision. The convolutional neural network (CNN) based on the DL module has been applied for accurate BP measurements *via* K-sounds (2, 46, 47). There is a need for good labeling and correct training of data, and the K-sounds can be accurately mined.

The CNN was initially proposed for processing images, speech, and time series (2). Guided by the CNN, BP measurements using K-sounds have better accuracy, compared to the automatic oscillometric method. Pan et al. used a

DL method to assess variations in K-sounds (46). Chang et al. improved on the former and added the ResNet module for automatic identification of the association between pulse oscillation waves and K-sounds (2). The filtered signal stack can also be used as a picture input. This is important for enhancing the robustness of K-sounds and achieving accurate recognition.

In summary, differences in K-sound signals, which are attributed to the experience of the healthcare provider, the environment, or the individual state of the patient, should not be a matter of significant concern. Moreover, pulse signals in time phases II and III can be adequately read. Currently, it is challenging to determine frequency changes in phases II and III among cardiac insufficiency patients. However, a follow-up study using the idea of DL on the basis of K-sounds should be performed to establish differences in the acoustic spectrum on the brachial artery in healthy individuals and patients with abnormal cardiac functions.

In addition, on the basis of K-sounds, other novel BP measurement techniques have been evaluated. For instance, the light volume method for measuring systolic blood pressure has been proposed by Shalom E (48). Given hearing differences among examiners, Celler et al. developed visualized a non-invasive BP measurement approach (49) while Zhang et al. developed a smart application for accurate BP measurements (50). However, these approaches only enhance the accuracy of systolic and diastolic measurements and do not promote information mining as DL does.

A unique advantage of CNN is that the signal can be accurately obtained. The traditional manual K-sounds method for BP measurement has been largely eliminated in modern diagnostic medicine. In its place, non-invasive blood pressure (NIBP) monitoring methods have been introduced. Celler et al. recorded optimal K-sounds in their experiments using the multiparameter clinical monitoring unit (CMU) from Telemedcare Pty Ltd.[1] and a National Instruments 16-bit A/D converter (cRIO-9215) (49). Considering the characterization of weaker cardiac output in HF, we are full of concerns about the extraction of feature signals of K-sounds in these populations. However, the instrument of Celler BG's team seems to have allayed our concerns.

Biological signals that originate from the cardiac are adequately recorded at the brachial artery and entirely analyzed using DL methods relatively. However, in terms of data acquisition for follow-up study, there is a need to improve on BP devices, including cuff and data logging to obtain massive amounts of data in a more convenient way to cater to the needs of DL.

1 http://www.telemedcare.com

Korotkoff sounds-associated clinical applications

Korotkoff-sounds are not limited to BP measurements in clinical practice. In 1967, Libanoff and Rodbard found that K-sounds can reflect the ability of cardiac electrical activity, left bundle branch block (51). In 1979, Bercu et al. elucidated the QKd (the interval between the onset of QRS of the electrocardiogram and the arrival of the pulse wave at the brachial artery, as detected by the appearance of Korotkoff sounds at diastolic pressure) theory (52). By that time, these authors had prospectively proposed that the QKd-based theory is appropriate for assessing cardiovascular disease, thyroid functions, and catecholamine levels. In 2001, Abassade et al. fully investigated the QKd theory, suggesting that QKd is not only an index for arterial dilation but also to some extent it reflects related functions of the left ventricle (53). This was in tandem with Cotoi's proposal in 1972, which suggested the use of K-sounds to reflect the left ventricular systolic functions. However, the theory that QKd reflects cardiac functions was shelved. Therefore, the application of K-sounds to dynamically predict changes in cardiac functions is not far-fetched. Its feasibility has not been scientifically established due to various limitations, including inadequate technical equipment.

Korotkoff-sound measurements are mediated by the brachial artery, and these sounds highly reflect the atherosclerotic capacity. The correlation between brachial artery wall and frequency of K-sounds was proposed as early as 1970 by Brookman et al. (54). The ability of K-sounds to reflect atherosclerosis was suggested by Sánchez Torres et al. in 1974 (55). In 1994, Gosse et al. evaluated the effects of QKd arterial distensibility on blood pressure measurements (56). In 2013, by performing the K-sounds BP measurements, they proved that atherosclerotic events are independently predictive in hypertensive patients (57). In 2015, El Tahlawi et al. showed that K-sounds can be used to predict the lesions associated with cardiac coronary arteries (58). In 2016, Ramakrishnan et al. used K-sounds methods to assess vascular compliance in different age groups (59).

The early stages of hypertension and coronary artery disease do not manifest any subjective clinical symptoms. However, at this time, normal body structures are altered, leading to spasms and contraction of small arteries, which is attributed to early hypertension, ischemia, and remodeling of the myocardium as a result of coronary artery sclerosis (4, 60). When the normal structure is "occupied" by some fatty or fibrous tissues, some fatal chest pain or headache symptoms are manifested, and damage to ventricles or blood vessels is often irreversible. Early detection, early diagnosis, and early treatment enhance recovery from various diseases. The K-sounds approach can be used for the early screening of cardiovascular diseases by monitoring dynamic cardiac functions.

The K-sounds are excellent for the evaluation of cardiovascular status and endocrinology. Keller et al. evaluated the use of K-sounds for simple screening tests of hyperthyroidism (61). This mechanism is a derivation of the QKd theory. In 1983, Osburne et al. noted that T3 levels can be roughly reflected using K-sounds (62). Climie et al. used the brachial-to-radial systolic pressure theory to assess hemodynamics in patients with diabetes (63).

The above-mentioned endocrine system disorders are inextricably linked to cardiovascular diseases. Clinically, the most common arrhythmia of the hyperthyroid heart is atrial fibrillation (64, 65). The efficacy of K-sounds for the assessment of BP in patients with atrial fibrillation has not been conclusively established. Due to the characteristics of atrial fibrillation and inconsistency between pulse rate and heart rate, K-sounds often result in significant measurement errors, which contradict the suggestion for the use of K-sounds to treat cardiovascular diseases, while proving the generalization ability of K-sounds for diagnosis. Based on the precise mapping of CNN, K-sounds are capable of overcoming the above-mentioned limitations while maximizing their advantages. Diabetes is also an independent risk factor for cardiovascular disease—blood vessels are immersed in "sugar water" for a long time, and the brachial artery is no exception (66, 67). Therefore, it is not surprising that K-sounds can assess vascular functions.

The advantages of K-sounds treatment have already been established; however, dynamic prediction of changes in cardiac functions using the K-sounds method is yet to be fully elucidated. The suggestion for the use of K-sounds for clinical diagnosis and treatment may be inextricably linked to cardiac functions. The end-stage for all cardiovascular diseases is heart failure, and insufficient coronary blood supply to the myocardium and diminished arterial compliance among others are early warning signs for deterioration of cardiac functions. This supports our use of K-sounds to determine cardiac functions.

The epidemiology of heart failure and clinical limitations for its diagnosis

Heart failure refers to abnormal changes in the structure or function of the heart, resulting in impaired ventricular systolic or diastolic functions, which leads to various complex pathophysiological changes in the body, including fluid retention, difficulties in breathing, limited physical activities, and severe cognitive impairment among others (11, 13, 68, 69). Weakening of cardiac functions affects peripheral blood supply. The blood flow in the brachial artery is also affected by cardiac output. This implies that K-sound dynamics can be used to predict changes in cardiac functions.

TABLE 2 Current diagnostic criteria for heart failure (HF).

Type of HF	Diagnostic criteria		
HFrEF	Signs and/or symptoms of HF	LVEF < 40%	
HFmrEF		LVEF 40–49%	Elevated natriuretic peptide and meet at least one of the following: Left ventricular hypertrophy and/or left ventricular enlargement; Abnormal diastolic function of the cardiac.
HFpEF		LVEF ≥ 50%	

Currently, the diagnosis of HF relies on clinical symptoms combined with relevant ancillary tests. The left ventricle ejection fraction (LVEF), which is dependent on cardiac ultrasound, remains the "gold standard" for assessing cardiac functions. Based on LVEF, the HF population is divided into three (**Table 2**) (11, 68, 69).

As guidelines are updated and HF therapies are optimized, prognostic outcomes for patients with HF are improving. However, the prevalence of HF is increasing. HF is silently affecting 1–3% of the global population, and in developed countries, the prevalence is ≥2% (70, 71). Thus, to reduce the prevalence of HF, various predictive and prognostic models of HF have been developed. However, these models are not available for some clinical practical implications (12). The reasons for their inability include:

i) The construction of these clinical models is guided by combining mathematics and science. Therefore, they are susceptible to influences of sample sizes and population characteristics.
ii) Determination of some serological markers [including BNP, NT-proBNP, mid-regional pro-adrenomedullin (MR-proADM), cardiac troponins, soluble ST2 (sST2), and growth differentiation factors (GDF)-15, galectin-3] is easily influenced by the laboratory criteria (9).

Clinically, based on the urgency of its occurrence, HF can be divided into acute heart failure (AHF) and chronic heart failure (CHF). Most acute patients progress to the chronic phase as their HF symptoms (such as chest tightness, shortness of breath, and edema) are able to be relieved due to timely treatment. They may remain in CHF after prompt treatment due to their primary cardiovascular disease. With some inappropriate HF triggers, CHF patients require hospitalization due to symptomatic deterioration (11, 72–74). The phase of AHF and CHF states may be so cyclical.

Regrettably, patients with cardiovascular disease are unaware of changes in their functional status, and they may even have quietly progressed from the compensated phase to the decompensated phase of cardiac functions. Often, the

compensatory phase allows the "ventricular remodeling" phase to proceed long enough, and the fibrotic myocardial structure often makes "HF" a ticking time bomb. Therefore, there is a need to develop effective approaches for the timely prediction of cardiac functions to reduce HF incidences. The K-sounds can be used for these predictions because:

1) Heart failure is the endpoint for all cardiovascular diseases, of which hypertension and coronary artery disease are high-risk factors. To reduce the prevalence of HF, it is important to monitor disease progression from an early stage. This can be achieved by frequently monitoring various indicators, including the use of electrocardiogram (ECG) monitors, which are not advisable for out-of-hospital applications. Patients who are at risk of cardiac dysfunction are not very diligent about going to the hospital to complete some serologic tests; therefore, serologically relevant HF prediction models are like "a clever woman cannot cook without rice." The late presentation of HF-associated symptoms is not ideal for its diagnosis.
2) Korotkoff-sounds hold great potential for monitoring changes in atherosclerosis and cardiac functions. While taking antihypertensive medications, hypertensive patients require regular monitoring of their BP so that adjustment of their medications can be done in a timely manner. We are confident that prevention can be achieved if the K-sounds theory is utilized and the measurement method is appropriately modified.

Applications of the K-sounds approach to monitoring cardiac functions are associated with convenience and low costs. In the future, patients with impaired cardiac functions may need to have their BP taken once a day to assess their health status. Aggressive screening slows down cardiovascular disease progression and improves the patients' quality of life.

Heart failure diagnosis and treatment using deep learning

In the era of big data and relative maturity of Intelligent Medical, DL has long been introduced in the diagnosis and treatment of cardiovascular diseases, and a majority of advanced techniques are based on related auxiliary examinations (75). These techniques include:

Electrocardiogram

Kwon et al. developed and validated a deep learning algorithm for ECG-based HF identification (76). Jahmunah et al. developed a system to assist in the diagnosis of congestive HF using ECG signals, and they subsequently improved the technique by adding the automatic assessment of coronary artery disease and myocardial infarction to the single ECG shape (77, 78). Akbilgic et al. used CNNs to identify ECG signals and verified that ECG-AI-based models rely solely on information extracted from ECG to independently predict HF (79). Cho et al. used a short-time Fourier transform (STFT) and CNN to sequentially detect left ventricular systolic dysfunction from ECG results (80). Sun et al. demonstrated that a well-trained CNN algorithm may be used as a low-cost and non-invasive method to identify patients with left ventricular dysfunction (81). Khurshid et al. used the arithmetic power of AI to complete the mass assessment of the left ventricle by ECG (82).

Heart sound

Yang et al. proposed a deep convolutional generative adversarial network (DCGAN) model-based data augmentation (DA) method to expand the heart sound (HS) database of left ventricular diastolic dysfunction for model training (83). Gao et al. used the gated recurrent unit (GRU) network to refine heart sound analysis for HF screening (84).

Chest X-ray

Matsumoto et al. showed that diagnosing HF from chest X-ray images using DL achieved satisfactory results (85).

Cardiac ultrasound

Pandey A explored a deep neural network (DNN) model that interprets multidimensional echocardiographic data to identify distinct patient subgroups with heart failure and preserved ejection fractions (HFpEF) (86). Kwon et al. derived and validated an echocardiography-based mortality prediction model for HD *via* deep learning (DL) (87).

Various novel algorithms and treatment approaches have been developed, and DL has become more attractive than the traditional algorithms, with the receiver operating characteristic (ROC) curves for DL exhibiting superior outcomes in various studies. However, whether ECG or HS, their results require professional apparatus integrated with specialized interpretation to obtain a reasonable explanation. In addition, diverse ancillary tests have their corresponding limitations. For instance, the connection of the lead ECG may be easily affected by the state of the patient's skin, and if too dry, it is easy to result in drifts in the baseline of ECG, which affects result interpretation. The whole procedure is tedious, and patients admitted with acute HF are not able to cooperate well with the examination process. Moreover, HS is easily influenced by the patient's physical

condition. If a person has a BMI of over 28 and a thicker layer of skin fat, then HS will be weaker. At this point, the heart sound signal should be distinguished from obesity. Chest X-ray for HF is less common. If ambient noise is complex, the robustness of the results will be seriously affected. But no so with K-sounds, where a intelligent audio-acquired cuff is wrapped around the arm and an appropriate DL algorithm is use, cardiac function could be easily monitored.

In some remote areas, economic conditions and knowledge base are far less than those in developed areas; therefore, patients with cardiovascular disease in these areas do not routinely present themselves for screening and physical examination of related diseases. Over time, under long-term neurohumoral regulation mechanisms, HF occurrence and development will be natural. The convenience of the BP monitor is much easier than ECG, chest X-ray, and other routine screening approaches; thus, the K-sounds method combined with the DL theory can be used to predict cardiac functions, so as to reduce the prevalence of HF.

Combining Korotkoff-sounds with deep learning to predict changes in cardiac functions

Korotkoff-sounds exhibited various advantages in the assessment of cardiac functions (15). In a previous study, we found that brachial artery blood flow and cardiac output essentially maintained a constant value of 1.23% in the resting state (88). In this study, which had a small sample size, the value of 1.23% was not found to be significant in patients with abnormal cardiac functions due to insufficiency of HF patients. Moreover, this value only represents the level of a population and cannot be applied for individualization, but it does provide a theoretical basis for the use of K-sounds to assess cardiac functions. By combining the mechanism of K-sounds generation and peripheral blood volume characteristics of HF, it is not difficult to deduce that the frequency and signals of K-sounds in patients with HF differ from those of the normal population. However, capture and analysis of these signals cannot be conventionally achieved.

Clinically, DL plays a distinct role in accurate BP measurements and screening of HF patients. Accurate BP measurements using CNN based on K-sounds have been able to exclude external interference, and map the corresponding systolic and diastolic BP in the time phases I and V. Therefore, we do not have to worry about the environment of the ward or the interference of external noise affecting the quality of K-sounds. Moreover, the PVDF membrane pressure sensors can be used while collecting K-sounds, which can reduce the loss of available signals (89). Celler et al. optimized the collection of K-sounds (49). In patients with HF, the frequency and nature of K-sounds may change as blood flow impinges on the brachial artery due to changes in the vascular endothelium or reduction in cardiac output per beat. Therefore, when training the network, data from patients with HF should be well labeled, which makes it possible for the CNN to identify K-sound frequencies that are specific to patients with HF.

However, CNNs alone are not efficient at identifying patients with HF. Patients with HF are often prone to a fast heart rate, which is attributed to a diminished pumping capacity of the heart and associated compensatory mechanisms. Therefore, to complete the K-sounds measurement, it is difficult to establish how many cardiac cycles are included, but errors from CNNs alone exponentially grow with time, which may lead to the failure of identifying characteristic signals of HF.

The K-sounds that have a great similarity to HS have been reported. They can be seen as a "migration" of HS signals and can be realized in the brachial artery as biological signals. The unique gating mechanisms of long short-term memory (LSTM) prevent the signal from disappearing; therefore, we propose the use of a multimodal composite network for the HF recognition function of K-sounds (90, 91).

The acoustic spectrogram is directly obtained for K-sound variations using the CNN, and image features are extracted using a convolutional structure. This reduces the number of parameters and computation, but also makes the network deeper and enhances the non-linearity as well as the fitting ability of the network and dropout structure to avoid the overfitting phenomenon of the network. The recurrent neural network (RNN) uses a cyclic cell structure, where each cell accepts as input the current time step and the processed state of the previous time step. The LSTM has a gating unit to adjust the delivery process of information flow, solving the challenge associated with gradient disappearance and gradient explosion that is inherent in RNN, ensuring that information can be shared at multiple time steps. Such a network has fast convergence and greater generalization abilities. CNN performs feature analysis on the frequency domain of K-sounds, while RNN performs analysis on the time domain of K-sounds, and finally, the vector features obtained from these two networks are spliced together into "the little black box" to complete signal interpretation of K-sounds. A schematic presentation of this process is shown in **Figure 2**.

This network is only an HS-based reference and needs constant debugging to be put into practice. The output of the network may be a dichotomous variable about cardiac functions—normal or abnormal. But it can also reflect changes in cardiac functions to some extent. Audio processing involves many techniques, including short-time Fourier transform, using hidden Markov modeling, etc (91). The formation of multilayer networks requires various DL-specific output

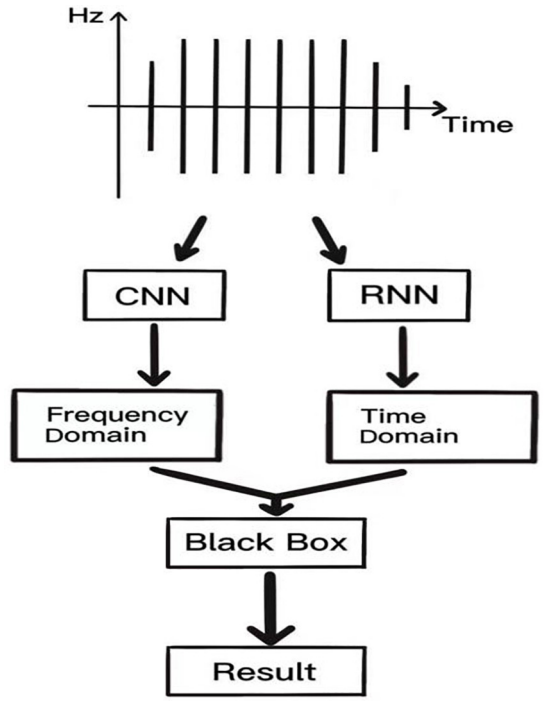

FIGURE 2
Schematic diagram of a proposed neural network.

structures, which are not described in this review. It is desirable to use DL to monitor cardiac functions by the K-sounds.

Discussion, limitations, and future perspectives

Heart failure is the end-stage outcome for patients with cardiovascular disease (11, 68, 69). Although treatments and diagnostic guidelines for HF are constantly being updated, there is a continuous increase in HF cases. Therefore, there is a need to develop appropriate methods for reducing the incidences of preclinical HF. The brachial artery-mediated K-sounds BP measurement is one of the most intimately used methods for obtaining preclinical vital signs for patients; however, it has a single use and only a limited number of clinically available parameters. There is a possibility of combining these two variables using DL, so as to determine cardiac function status using simple BP measurements. LVEF covariates can be used as the criterion for assessing cardiac functions. Further, the prediction of cardiac outputs by measuring BP has the potential for becoming the "heart failure meter" prototype.

The advantages of DL in determining patients with HF have been reported. Hypertension, a common cause of HF, is a severe cardiovascular disease that is associated with high mortality rates (5). The process from the onset of symptoms to clinically confirmed hypertension is long. Hypertensive patients may not present any clinical symptoms, and clinical characteristics for BP vary, such as the "spoon" and "reverse spoon" mechanisms, the circadian rhythms of which can quietly affect the clinical status of patients. Patients do not notice abnormalities during the occasional BP measurements. In this case, hypertension is detected *via* some routine medical examinations, such as taking 24 h ambulatory BP to find the time points of elevated BP or by finding abnormal urine microprotein levels, which indicates kidney damage due to hypertension. When the myocardium is slowly compensating for its pumping function, and myocardial cells and related vascular endothelial functions are changing, these outcomes lay a "solid foundation" for HF. This is also the reason for the high prevalence of HF. Therefore, K-sounds make sense as an early screening tool for cardiovascular diseases.

Korotkoff-sounds can also be used for the diagnosis and treatment of atherosclerosis, coronary blood flow, and arrhythmia. These are the invisible "poisonous hands" that lead to HF. Therefore, the success of the heart failure meter will go far beyond measuring BP.

This review has various limitations:

1. The use of K-sounds for early screening of cardiac dysfunction in a sick population is a variant of a widely known risk prediction model. The primary goal of risk prediction models is to accurately quantify risks in the general population using readily available clinical variables. Our use of K-sounds alone as a covariate to predict changes in cardiac functions is one-sided, and it may need to be combined with additional clinical data covariates to produce more convincing outcomes. Our idea is novel, but since there is no clinical data to support it, to make the initial practice more desirable, we just want to make a crude determination of the presence of cardiac dysfunction in patients with cardiovascular disease based purely on a dichotomous approach (with LVEF $< 50\%$ as the cutoff). Based on the theory proposed by Cotoi, using the property that K-sounds can assess changes in cardiac function and do not take into account the heterogeneity of the population with HFpEF, our work is still full of challenges.
2. Although DL has achieved promising results in the recognition of subtle signals, its accuracy is supported by algorithms and large amounts of data. The algorithms for DL in this review are based on published literature and are only combined at the theoretical level; subsequent practice will require improvement of the algorithms to meet real-world needs.

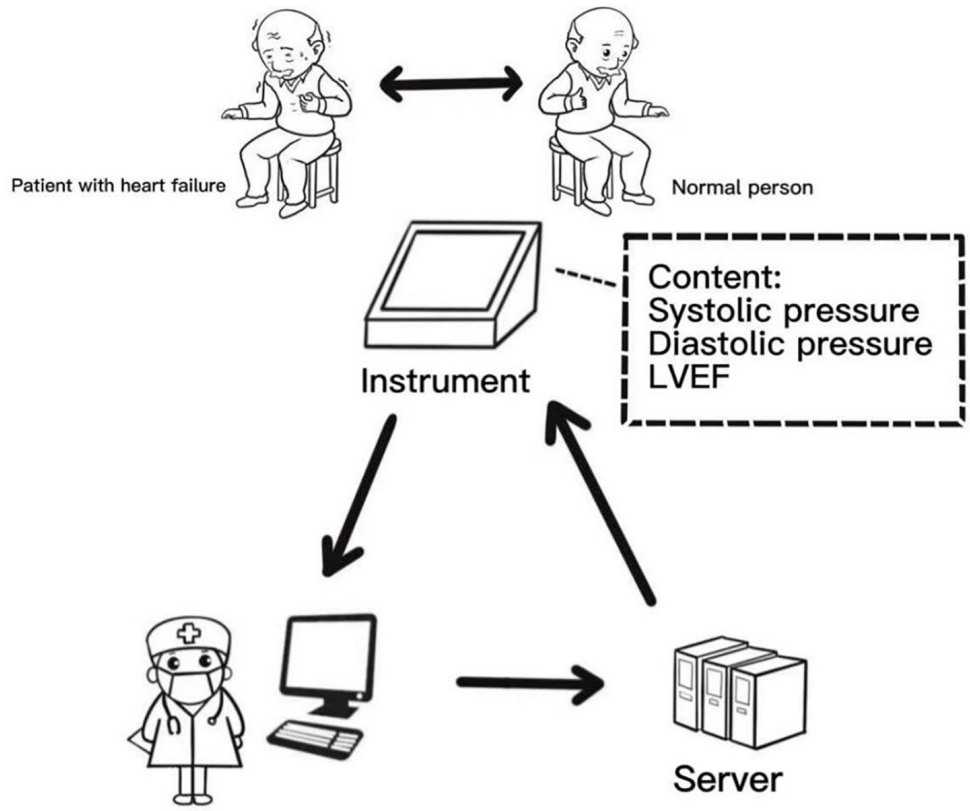

FIGURE 3
Schematic diagram of operation mode of future intelligent sphygmomanometer.

3. In terms of data collection, (i) given that the popular preclinical BP measurement method is still the electronic oscillometric cuff method, which did not affect our audio acquisition, Celler et al. had promising results in the collection and analysis of K-sounds. Our initial intention was not to reproduce the original K-sounds during blood pressure measurements, but only to acquire K-sound audio data from HF. The PVDF membrane technique by Xiong et al. can minimize the loss of audio signals during the acquisition process (89). We modified the cuff of the electronic oscilloscope by adding PVDF membranes, but the actual effect is yet to be further tested. In addition, the definition of a patient with HF requires a cardiologist. (ii) The article has also previously mentioned: HF is silently affecting 1–3% of the global population (70, 71). In clinical practice, however, there do not seem to be that many typical patients with HF, and the preliminary data collection is necessarily time-consuming and laborious. The lack of typical characteristic data can make the screening ability of our model substantially weaker. The reduction of positive data can cause a substantial increase in false-negative results in subsequent models.

Here, we offer a small vision of the future for this purpose:

Our early screening model is more suitable for some rural areas (some places where advanced medical equipment is inaccessible) or some countries with less-developed medical care. The use of a "heart failure meter" can also be promoted in primary hospitals or daily life. If successful, patients will not have to go through the tedious process of cardiac ultrasound and blood tests for the assessment of cardiac function (however, there may be false-negative or false-positive results), so that they can actively treat the primary disease or intervene in time, which will make the evolution to end-stage for patients with cardiovascular disease significantly longer as far as possible, thus improving their survival outcomes.

Figure 3 shows our proposed pre-desired and more ideal way of data model acquisition. The heart failure meter will detect instantaneous changes in cardiac functions and transmit the results to the cloud for correction by an experienced internist. We hope to use this way to improve the specificity ability of the model. Furthermore, our idea will be more clinically useful when we develop an automated K-sounds collection and judgment system suitable for this review.

Author contributions

All authors participated in the creation of this manuscript, contributed to the article, and approved the submitted version.

Funding

This article was supported by the National Natural Science Foundation of China (No. 81971688) and the Fundamental Research Funds for the Central Universities (226-2022-00095).

Acknowledgments

Thanks to all the authors of this article for their joint efforts and hard work.

Conflict of interest

The authors declare that the research was conducted in the absence of any commercial or financial relationships that could be construed as a potential conflict of interest.

Publisher's note

References

1. Beevers G, Lip GY, O'Brien E. ABC of hypertension: Blood pressure measurement. Part II-conventional sphygmomanometry: Technique of auscultatory blood pressure measurement. *BMJ.* (2001) 322:1043–7. doi: 10.1136/bmj.322.7293.1043

2. Chang JH, Doh I. Deep learning-based robust automatic non-invasive measurement of blood pressure using Korotkoff sounds. *Sci Rep.* (2021) 11:23365. doi: 10.1038/s41598-021-02513-7

3. Turner MJ, Speechly C, Bignell N. Sphygmomanometer calibration–why, how and how often? *Aust Fam Physician.* (2007) 36:834–8.

4. Slivnick J, Lampert BC. Hypertension and heart failure. *Heart Fail Clin.* (2019) 15:531–41. doi: 10.1016/j.hfc.2019.06.007

5. Di Palo KE, Barone NJ. Hypertension and heart failure: Prevention, targets, and treatment. *Heart Fail Clin.* (2020) 16:99–106.

6. Mouton AJ, Rivera OJ, Lindsey ML. Myocardial infarction remodeling that progresses to heart failure: A signaling misunderstanding. *Am J Physiol Heart Circ Physiol.* (2018) 315:H71–9. doi: 10.1152/ajpheart.00131.2018

7. Kim GH, Uriel N, Burkhoff D. Reverse remodelling and myocardial recovery in heart failure. *Nat Rev Cardiol.* (2018) 15:83–96. doi: 10.1038/nrcardio.2017.139

8. Bacmeister L, Schwarzl M, Warnke S, Stoffers B, Blankenberg S, Westermann D, et al. Inflammation and fibrosis in murine models of heart failure. *Basic Res Cardiol.* (2019) 114:19. doi: 10.1007/s00395-019-0722-5

9. Kemp CD, Conte JV. The pathophysiology of heart failure. *Cardiovasc Pathol.* (2012) 21:365–71. doi: 10.1016/j.carpath.2011.11.007

10. Dhalla NS, Rangi S, Babick AP, Zieroth S, Elimban V. Cardiac remodeling and subcellular defects in heart failure due to myocardial infarction and aging. *Heart Fail Rev.* (2012) 17:671–81.

11. van der Meer P, Gaggin HK, Dec GW. ACC/AHA versus ESC guidelines on heart failure: JACC guideline comparison. *J Am Coll Cardiol.* (2019) 73:2756–68. doi: 10.1016/j.jacc.2019.03.478

12. Sahle BW, Owen AJ, Chin KL, Reid CM. Risk prediction models for incident heart failure: A systematic review of methodology and model performance. *J Card Fail.* (2017) 23:680–7. doi: 10.1016/j.cardfail.2017.03.005

13. Rogers C, Bush N. Heart failure: Pathophysiology, diagnosis, medical treatment guidelines, and nursing management. *Nurs Clin North Am.* (2015) 50:787–99.

14. Berliner D, Hänselmann A, Bauersachs J. The treatment of heart failure with reduced ejection fraction. *Dtsch Arztebl Int.* (2020) 117:376–86.

15. Cotoi S, Constantinescu L, Cazacu A. Korotkoff sounds in the evaluation of ventricular performance. *Rev Roum Med Intern.* (1972) 9:551–8.

16. Babbs CF. The origin of Korotkoff sounds and the accuracy of auscultatory blood pressure measurements. *J Am Soc Hypertens.* (2015) 9:935–50.e3. doi: 10.1016/j.jash.2015.09.011

17. Hamet P, Tremblay J. Artificial intelligence in medicine. *Metabolism.* (2017) 69S:S36–40.

18. Mintz Y, Brodie R. Introduction to artificial intelligence in medicine. *Minim Invasive Ther Allied Technol.* (2019) 28:73–81.

19. Ranka S, Reddy M, Noheria A. Artificial intelligence in cardiovascular medicine. *Curr Opin Cardiol.* (2021) 36:26–35.

20. van Velzen SGM, Lessmann N, Velthuis BK, Bank IEM, van den Bongard DHJG, Leiner T, et al. Deep learning for automatic calcium scoring in CT: Validation using multiple cardiac CT and chest CT protocols. *Radiology.* (2020) 295:66–79. doi: 10.1148/radiol.2020191621

21. Kwon JM, Lee Y, Lee Y, Lee S, Park J. An algorithm based on deep learning for predicting in-hospital cardiac arrest. *J Am Heart Assoc.* (2018) 7:e008678.

22. Dock W. Occasional notes. Korotkoff's sounds. *N Engl J Med.* (1980) 302:1264–7. doi: 10.1056/NEJM198005293022220

23. Ur A, Gordon M. Origin of Korotkoff sounds. *Am J Physiol.* (1970) 218:524–9.

24. Paskalev D, Kircheva A, Krivoshiev S. A centenary of auscultatory blood pressure measurement: A tribute to Nikolai Korotkoff. *Kidney Blood Press Res.* (2005) 28:259–63. doi: 10.1159/000090084

25. O'Brien E, Asmar R, Beilin L, Imai Y, Mallion JM, Mancia G, et al. European Society of Hypertension recommendations for conventional, ambulatory and home blood pressure measurement. *J Hypertens.* (2003) 21:821–48.

26. Geddes LA, Hoff HE, Badger AS. Introduction of the auscultatory method of measuring blood pressure–including a translation of Korotkoff's original paper. *Cardiovasc Res Cent Bull.* (1966) 5:57–74.

27. Drzewiecki GM, Melbin J, Noordergraaf A. The Korotkoff sound. *Ann Biomed Eng.* (1989) 17:325–59.

28. Geddes LA, Moore AG. The efficient detection of Korotkoff sounds. *Med Biol Eng.* (1968) 6:603–9.

29. Lange RL, Carlisle RP, Hecht HH. Observations on vascular sounds: The pistol-shot sound and the Korotkoff sound. *Circulation.* (1956) 13:873–83. doi: 10.1161/01.cir.13.6.873

30. Venet R, Miric D, Pavie A, Lacheheb D. Korotkoff sound: The cavitation hypothesis. *Med Hypotheses.* (2000) 55:141–6. doi: 10.1054/mehy.1999.1036

31. Chungcharoen D. Genesis of Korotkoff sounds. *Am J Physiol.* (1964) 207:190–4.

32. Geddes LA, Spencer WA, Hoff HE. Graphic recording of the Korotkoff sounds. *Am Heart J.* (1959) 57:361–70.

33. Kakuda H. [Clinical studies on the korotkoff sound. 3. Production mechanismus of the Korotkoff sound]. *Jpn Circ J.* (1964) 28:967–9. Japanese. doi: 10.1253/jcj.28.967

34. Conrad WA, McQueen DM, Yellin EL. Steady pressure flow relations in compressed arteries: Possible origin of Korotkoff sounds. *Med Biol Eng Comput.* (1980) 18:419–26. doi: 10.1007/BF02443311

35. James GD, Gerber LM. Measuring arterial blood pressure in humans: Auscultatory and automatic measurement techniques for human biological field studies. *Am J Hum Biol.* (2018) 30:e23063. doi: 10.1002/ajhb.23063

36. Pereira E, Prys-Roberts C, Dagnino J, Anger C, Cooper GM, Hutton P. Auscultatory measurement of arterial pressure during anaesthesia: A reassessment of Korotkoff sounds. *Eur J Anaesthesiol.* (1985) 2:11–20.

37. Song S, Lee J, Chee Y, Jang DP, Kim IY. Does the accuracy of blood pressure measurement correlate with hearing loss of the observer? *Blood Press Monit.* (2014) 19:14–8. doi: 10.1097/MBP.0000000000000016

38. Zheng D, Di Marco LY, Murray A. Effect of respiration on Korotkoff sounds and oscillometric cuff pressure pulses during blood pressure measurement. *Med Biol Eng Comput.* (2014) 52:467–73.

39. Pan F, Chen F, Liu C, Yang Z, Liu Z, Zheng D. Quantitative comparison of Korotkoff sound waveform characteristics: Effects of static cuff pressures and stethoscope positions. *Ann Biomed Eng.* (2018) 46:1736–44. doi: 10.1007/s10439-018-2080-0

40. Veerman DP, van Montfrans GA, Wieling W. Effects of cuff inflation on self-recorded blood pressure. *Lancet.* (1990) 335:451–3. doi: 10.1016/0140-6736(90)90676-v

41. Brinton TJ, Walls ED, Yajnik AK, Chio SS. Age-based differences between mercury sphygmomanometer and pulse dynamic blood pressure measurements. *Blood Press Monit.* (1998) 3:125–9.

42. Walker SP, Higgins JR, Brennecke SP. The diastolic debate: Is it time to discard Korotkoff phase IV in favour of phase V for blood pressure measurements in pregnancy? *Med J Aust.* (1998) 169:203–5. doi: 10.5694/j.1326-5377.1998.tb140223.x

43. O'Sullivan J, Allen J, Murray A. The forgotten Korotkoff phases: How often are phases II and III Present, and how do they relate to the other Korotkoff phases? *Am J Hypertens.* (2002) 15:264–8. doi: 10.1016/s0895-7061(01)02276-2

44. Sykes D, Dewar R, Mohanaruban K, Donovan K, Nicklason F, Thomas DM, et al. Measuring blood pressure in the elderly: Does atrial fibrillation increase observer variability? *BMJ.* (1990) 300:162–3.

45. Zimetbaum P. Atrial fibrillation. *Ann Intern Med.* (2017) 166:ITC33–48. Erratum in: Ann Intern Med. 2017;166(12):920. doi: 10.7326/AITC201703070

46. Pan F, He P, Liu C, Li T, Murray A, Zheng D. Variation of the Korotkoff stethoscope sounds during blood pressure measurement: Analysis using a convolutional neural network. *IEEE J Biomed Health Inform.* (2017) 21:1593–8. doi: 10.1109/JBHI.2017.2703115

47. Pan F, He P, Chen F, Zhang J, Wang H, Zheng D. A novel deep learning based automatic auscultatory method to measure blood pressure. *Int J Med Inform.* (2019) 128:71–8. doi: 10.1016/j.ijmedinf.2019.04.023

48. Shalom E, Hirshtal E, Slotki I, Shavit L, Yitzhaky Y, Engelberg S, et al. Systolic blood pressure measurement by detecting the photoplethysmographic pulses and electronic Korotkoff-sounds during cuff deflation. *Physiol Meas.* (2020) 41:034001. doi: 10.1088/1361-6579/ab7b41

49. Celler BG, Le P, Basilakis J, Ambikairajah E. Improving the quality and accuracy of non-invasive blood pressure measurement by visual inspection and automated signal processing of the Korotkoff sounds. *Physiol Meas.* (2017) 38:1006–22. doi: 10.1088/1361-6579/aa6b7e

50. Zhang Z, Xi W, Wang B, Chu G, Wang F. A convenient method to verify the accuracy of oscillometric blood pressure monitors by the auscultatory method: A smartphone-based app. *J Clin Hypertens (Greenwich).* (2019) 21:173–80. doi: 10.1111/jch.13460

51. Libanoff AJ, Rodbard S. The delay in the Korotkoff sounds in left bundle-branch block. *JAMA.* (1967) 201:666–70.

52. Bercu BB, Haupt R, Johnsonbaugh R, Rodbard D. The pulse wave arrival time (QKd interval) in normal children. *J Pediatr.* (1979) 95(Pt 1):716–21. doi: 10.1016/s0022-3476(79)80717-9

53. Abassade P, Baudouy PY, Gobet L, Lhosmot JP. Etude du couple aorte-ventricule gauche par échocardiographie Doppler et mesure ambulatoire de la pression artérielle [Aorta-left ventricular relationship evaluated by Doppler echocardiography and ambulatory arterial prsesure monitoring]. *Arch Mal Coeur Vaiss.* (2001) 94:767–70. French.

54. Brookman BJ Jr., Dalton C, Geddes LA. The relationship between vessel-wall elasticity and Korotkoff-sound frequency. *Med Biol Eng.* (1970) 8:149–58. doi: 10.1007/BF02509324

55. Sánchez Torres G. Auscultación de los ruidos de Korotkoff en las arterias periféricas. Um método nuevo de exploración arterial [Auscultation of Korotkoff's sounds in the peripheral arteries. A new method of arterial examination]. *Arch Inst Cardiol Mex.* (1974) 44:223–36. Spanish.

56. Gosse P, Guillo P, Ascher G, Clementy J. Assessment of arterial distensibility by monitoring the timing of Korotkoff sounds. *Am J Hypertens.* (1994) 7:228–33.

57. Gosse P, Cremer A, Papaioannou G, Yeim S. Arterial stiffness from monitoring of timing of korotkoff sounds predicts the occurrence of cardiovascular events independently of left ventricular mass in hypertensive patients. *Hypertension.* (2013) 62:161–7. doi: 10.1161/HYPERTENSIONAHA.113.01039

58. El Tahlawi M, Abdelbaset M, Gouda M, Hussein I. Can we predict the presence of coronary lesions from blood pressure measurement? A new clinical method. *Hypertens Res.* (2015) 38:260–3.

59. Ramakrishnan D. Using Korotkoff sounds to detect the degree of vascular compliance in different age groups. *J Clin Diagn Res.* (2016) 10:CC04–7. doi: 10.7860/JCDR/2016/16225.7198

60. Malakar AK, Choudhury D, Halder B, Paul P, Uddin A, Chakraborty S. A review on coronary artery disease, its risk factors, and therapeutics. *J Cell Physiol.* (2019) 234:16812–23. doi: 10.1002/jcp.28350

61. Keller MF. Korotkoff-Töne: Einfacher screening-test zum Erfassen von Hyperthyreosen [Korotkoff sounds: Simple screening test for the diagnosis of hyperthyroidism]. *Schweiz Med Wochenschr.* (1970) 100:630–3. German.

62. Osburne RC, Myers EA, Rodbard D, Burman KD, Georges LP, O'Brian JT. Adaptation to hypocaloric feeding: Physiologic significance of the fall in serum T3 as measured by the pulse wave arrival time (QKd). *Metabolism.* (1983) 32:9–13. doi: 10.1016/0026-0495(83)90148-8

63. Climie RE, Picone DS, Keske MA, Sharman JE. Brachial-to-radial systolic blood pressure amplification in patients with type 2 diabetes mellitus. *J Hum Hypertens.* (2016) 30:404–9. doi: 10.1038/jhh.2015.101

64. Vargas-Uricoechea H, Bonelo-Perdomo A, Sierra-Torres CH. Effects of thyroid hormones on the heart. *Clin Investig Arterioscler.* (2014) 26:296–309. doi: 10.1016/j.arteri.2014.07.003

65. Reddy V, Taha W, Kundumadam S, Khan M. Atrial fibrillation and hyperthyroidism: A literature review. *Indian Heart J.* (2017) 69:545–50. doi: 10.1016/j.ihj.2017.07.004

66. Wilkinson-Berka JL. Diabetes and retinal vascular disorders: Role of the renin-angiotensin system. *Expert Rev Mol Med.* (2004) 6:1–18.

67. Romero-Aroca P, Baget-Bernaldiz M, Pareja-Rios A, Lopez-Galvez M, Navarro-Gil R, Verges R. Diabetic macular edema pathophysiology: Vasogenic versus inflammatory. *J Diabetes Res.* (2016) 2016:2156273. doi: 10.1155/2016/2156273

68. King M, Kingery J, Casey B. Diagnosis and evaluation of heart failure. *Am Fam Physician.* (2012) 85:1161–8.

69. Chaudhry SP, Stewart GC. Advanced heart failure: Prevalence, natural history, and prognosis. *Heart Fail Clin.* (2016) 12:323–33.

70. Ziaeian B, Fonarow GC. Epidemiology and aetiology of heart failure. *Nat Rev Cardiol.* (2016) 13:368–78.

71. Mosterd A, Hoes AW. Clinical epidemiology of heart failure. *Heart.* (2007) 93:1137–46.

72. Arrigo M, Jessup M, Mullens W, Reza N, Shah AM, Sliwa K, et al. Acute heart failure. *Nat Rev Dis Primers.* (2020) 6:16.

73. Kurmani S, Squire I. Acute heart failure: Definition, classification and epidemiology. *Curr Heart Fail Rep.* (2017) 14:385–92.

74. Sinnenberg L, Givertz MM. Acute heart failure. *Trends Cardiovasc Med.* (2020) 30:104–12.

75. Krittanawong C, Johnson KW, Rosenson RS, Wang Z, Aydar M, Baber U, et al. Deep learning for cardiovascular medicine: A practical primer. *Eur Heart J.* (2019) 40:2058–73.

76. Kwon JM, Kim KH, Jeon KH, Kim HM, Kim MJ, Lim SM, et al. Development and validation of deep-learning algorithm for electrocardiography-based heart failure identification. *Korean Circ J.* (2019) 49:629–39. doi: 10.4070/kcj.2018.0446

77. Jahmunah V, Oh SL, Wei JKE, Ciaccio EJ, Chua K, San TR, et al. Computer-aided diagnosis of congestive heart failure using ECG signals - A review. *Phys Med.* (2019) 62:95–104. doi: 10.1016/j.ejmp.2019.05.004

78. Jahmunah V, Ng EYK, San TR, Acharya UR. Automated detection of coronary artery disease, myocardial infarction and congestive heart failure using GaborCNN model with ECG signals. *Comput Biol Med.* (2021) 134:104457. doi: 10.1016/j.compbiomed.2021.104457

79. Akbilgic O, Butler L, Karabayir I, Chang PP, Kitzman DW, Alonso A, et al. ECG-AI: Electrocardiographic artificial intelligence model for prediction of heart failure. *Eur Heart J Digit Health.* (2021) 2:626–34. doi: 10.1093/ehjdh/ztab080

80. Cho J, Lee B, Kwon JM, Lee Y, Park H, Oh BH, et al. Artificial intelligence algorithm for screening heart failure with reduced ejection fraction using electrocardiography. *ASAIO J.* (2021) 67:314–21.

81. Sun JY, Qiu Y, Guo HC, Hua Y, Shao B, Qiao YC, et al. A method to screen left ventricular dysfunction through ECG based on convolutional neural network. *J Cardiovasc Electrophysiol.* (2021) 32:1095–102. doi: 10.1111/jce.14936

82. Khurshid S, Friedman S, Pirruccello JP, Di Achille P, Diamant N, Anderson CD, et al. Deep learning to predict cardiac magnetic resonance-derived left ventricular mass and hypertrophy from 12-Lead ECGs. *Circ Cardiovasc Imaging.* (2021) 14:e012281. doi: 10.1161/CIRCIMAGING.120.012281

83. Yang Y, Guo XM, Wang H, Zheng YN. Deep learning-based heart sound analysis for left ventricular diastolic dysfunction diagnosis. *Diagnostics (Basel).* (2021) 11:2349. doi: 10.3390/diagnostics11122349

84. Gao S, Zheng Y, Guo X. Gated recurrent unit-based heart sound analysis for heart failure screening. *Biomed Eng Online.* (2020) 19:3. doi: 10.1186/s12938-020-0747-x

85. Matsumoto T, Kodera S, Shinohara H, Ieki H, Yamaguchi T, Higashikuni Y, et al. Diagnosing heart failure from chest X-Ray images using deep learning. *Int Heart J.* (2020) 61:781–6.

86. Pandey A, Kagiyama N, Yanamala N, Segar MW, Cho JS, Tokodi M, et al. Deep-learning models for the echocardiographic assessment of diastolic dysfunction. *JACC Cardiovasc Imaging.* (2021) 14:1887–900.

87. Kwon JM, Kim KH, Jeon KH, Park J. Deep learning for predicting in-hospital mortality among heart disease patients based on echocardiography. *Echocardiography.* (2019) 36:213–8.

88. Jia S, Wu Y, Wang W, Lin W, Chen Y, Zhang H, et al. An exploratory study on the relationship between brachial arterial blood flow and cardiac output. *J Healthc Eng.* (2021) 2021:1251199. doi: 10.1155/2021/1251199

89. Li X, Panicker GV, Im JJ. A study for the development of K-sound based automatic blood pressure device using PVDF film. *Annu Int Conf IEEE Eng Med Biol Soc.* (2016) 2016:255–8. doi: 10.1109/EMBC.2016.7590688

90. Deng M, Meng T, Cao J, Wang S, Zhang J, Fan H. Heart sound classification based on improved MFCC features and convolutional recurrent neural networks. *Neural Netw.* (2020) 130:22–32. doi: 10.1016/j.neunet.2020.06.015

91. Li W, Yang XD, Chen K. Heart sound classification based on CNN and RNN. *Comput Eng Design.* (2020) 41:46–51. doi: 10.1016/j.cmpb.2021.105940

frontiers | Frontiers in Cardiovascular Medicine

TYPE Study Protocol
PUBLISHED 28 September 2022
DOI 10.3389/fcvm.2022.1013834

OPEN ACCESS

EDITED BY
Konstantinos Spanos,
University of Thessaly, Greece

REVIEWED BY
Karin Pfister,
University Medical Center Regensburg, Germany
Edoardo Pasqui,
University of Siena, Italy

*CORRESPONDENCE
Wei Guo
guoweiplagh@sina.com

†These authors have contributed equally to this work and share first authorship

SPECIALTY SECTION
This article was submitted to Structural Interventional Cardiology, a section of the journal Frontiers in Cardiovascular Medicine

RECEIVED 07 August 2022
ACCEPTED 13 September 2022
PUBLISHED 28 September 2022

CITATION
Gao J-P, Zhang H-P, Jia X, Xiong J, Ma X-H, Wang L-J, Zhang M-H, Xu Y-L and Guo W (2022) A prospective, multicenter, single-arm clinical trial cohort to evaluate the safety and effectiveness of a novel stent graft system (WeFlow-JAAA) for the treatment of juxtarenal abdominal aortic aneurysm: A study protocol.
Front. Cardiovasc. Med. 9:1013834.
doi: 10.3389/fcvm.2022.1013834

A prospective, multicenter, single-arm clinical trial cohort to evaluate the safety and effectiveness of a novel stent graft system (WeFlow-JAAA) for the treatment of juxtarenal abdominal aortic aneurysm: A study protocol

Jiang-Ping Gao[1,2†], Hong-Peng Zhang[1†], Xin Jia[1], Jiang Xiong[1], Xiao-Hui Ma[1], Li-Jun Wang[1], Min-Hong Zhang[1], Yong-Le Xu[1] and Wei Guo[1*]

[1]Department of Vascular Surgery, Chinese PLA General Hospital, Beijing, China, [2]Medical School of Chinese PLA, Beijing, China

Introduction: Juxtarenal abdominal aortic aneurysms (JRAAAs) are challenging to cure by traditional endovascular aortic repair (EVAR). Due to the inherent disadvantages of the customized fenestrated and/or branched aortic endografts (such as delayed cycles with a risk of aneurysm rupture, unavailable in emergency or confine operations), several off-the-shelf devices have been developed for the treatment of JRAAA. However, these devices being used in clinical trials have been proven to have a non-negligible risk of reintervention and inadequate anatomic applicability. We have developed a new off-the-shelf aortic endograft system (WeFlow-JAAA) with a mixed design of inner branches and modified fenestrations. The purpose of this cohort study is to assess the safety and effectiveness of the innovative aortic endograft system.

Methods and analysis: This is a prospective, multicenter, single-armed clinical trial cohort study. The enrolment will take place in 29 centers in China, and 106 adult patients with JRAAA will be enrolled in total. Clinical information and CT angiography (CTA) images will be collected and recorded. Patients will be followed up for 5 years. The primary safety endpoint is the rate of no major adverse event within 30 days after index EVAR. The primary efficacy endpoint is the rate of immediate technical success and no JRAAA-related reintervention within 12 months after the procedure.

KEYWORDS

abdominal aortic aneurysm, juxtarenal, endovascular aortic repair, endovascular repair, WeFlow-JAAA

Strengths and limitations of this study

- This is a prospective, multicentre, single-armed clinical trial cohort to evaluate the safety and efficacy of WeFlow-JAAA, a newly developed aortic endograft system, for the treatment of juxtarenal abdominal aortic aneurysms that are challenging for traditional endovascular aortic repair.
- A major strength of this study is that it evaluates a novel abdominal aortic endograft system based on a mixed design of inner branches and "mini-inner-cuff" reinforced fenestrations.
- The main limitations of this study are the regional limitation (China) and lack of control arms.

Introduction

Juxtarenal abdominal aortic aneurysm (JRAAA) poses significant challenges in endovascular aortic repair (EVAR). In the European Society for Vascular Surgery (ESVS) 2019 clinical practice guidelines on the management of AAA, JRAAA is defined as an aneurysm extending up to but not involving the renal arteries, i.e., a short neck (<10 mm) (1). During the past 20 years, custom-made fenestrated and/or branched aortic endografts (i.e., Cook Zenith Fenestration) have largely replaced open surgery for the treatment of anatomically suitable JRAAA (2, 3), which is also recommended by the ESVS2019 clinical practice guidelines on the management of AAA (1).

Due to the inherent disadvantages of the customized device (delayed cycles with a risk of rupture, unavailable in emergency or confine operation) (4, 5), several "off-the-shelf" devices have been developed for the treatment of JRAAA, such as Cook p-Branch and Endologix Ventana (6, 7). According to a recent systematic review, clinical outcomes for the off-the-shelf devices in the treatment of complex AAA are promising, with no 30-day mortality, a 1.7% rate of paraplegia, a 97.6% 30-day target vessel patency rate, and a 3.3% rate of type I endoleak (8). However, high rates of late postoperative reintervention and narrow anatomic indications hampered the development of devices for JRAAA. Sveinsson et al. (7) found a 48% rate of reintervention during the 5 years follow-up of p-Branch. The device study of Endologix Ventana was also placed on hold for a high reintervention rate of renal arteries (9). Additionally, these off-the-shelf fenestrated devices are only anatomically suitable for 30–40% of all patients (10, 11). Thus, a safer and more effective off-the-shelf device with less reintervention and wider anatomic indications for the treatment of JRAAA is needed.

In collaboration with Endonom Medtech (Hangzhou, China), we have developed a novel off-the-shelf modular endograft system (WeFlow-JAAA, **Figure 1A**) which consists of four components, a proximal body graft (**Figures 1B,C**), a distal bifurcated body graft (**Figure 1D**), iliac leg grafts (**Figure 1E**) and self-expanding branch grafts (**Figure 1F**). The proximal body graft (**Figure 1C**), with two standard inner branches (1.5 cm in length) of renal arteries (RA), one 3 mm "mini-inner-cuff" reinforced fenestrations with a sealing ring for superior mesenteric artery (SMA), and one scallop with a sealing ring for celiac axis (CA), has three important advantages. The first was inner branch design of bilateral renal arteries could significantly reduce branch instability or type III endoleak with matched branch stent grafts. The second advantage was that the modified fenestration reinforced with a 3 mm "mini-inner-cuff" and a sealing ring allows better seal at the attachment site, potentially reducing the risk of endoleak, without adding to the bulk of the device. The above two points lead to wider anatomic indications of this device, which was the third advantage. The anatomic indications of an aortic stent graft system depend on three aspects, including aortic related (especially the aortic diameter of the neck and branch level), branch vessel related, and approach related. The inner branch design could combine the benefits of external branch and fenestration and improve the anatomical fitness of aorta diameter. While the "mini-inner-cuff" reinforced fenestration could increase the sealing without compromising the approach-related anatomical fitness, which was precisely what the three preset guidewires (RAs, SMA) rather than preset catheters designed for.

The first-in-human (FIM) study (NCT04745546) of WeFlow-JAAA was initiated in October 2019 and is being conducted in a single center (data unpublished). This FIM study involved a total of 15 patients with 14 JRAAA and 1 suprarenal AAA, and all patients have currently completed at least 6 months of follow-up imaging. The main objective of this study was to evaluate the safety and effectiveness of this abdominal aortic stent graft system (WeFlow-JAAA) in preparation for its dissemination to maximumly benefit patients with JRAAA.

Methods and analysis

This study was designed following the Standard Protocol Items "Recommendations for Interventional Trials statement" and is registered with the US National Institute of Health (**Table 1**). The protocol ID is WEIQIANG202101. The actual study start date was 23 February 2022, and the estimated study completion date is 31 December 2028.

Study design

This is a prospective, multicenter, single-arm, cohort study evaluating the safety and efficacy of a novel fenestrated and branched stent graft system for endovascular repair of JRAAA. This study is being initiated by the Chinese PLA General Hospital and will involve patients from an additional 28 high-volume tertiary referral hospitals across all geographic

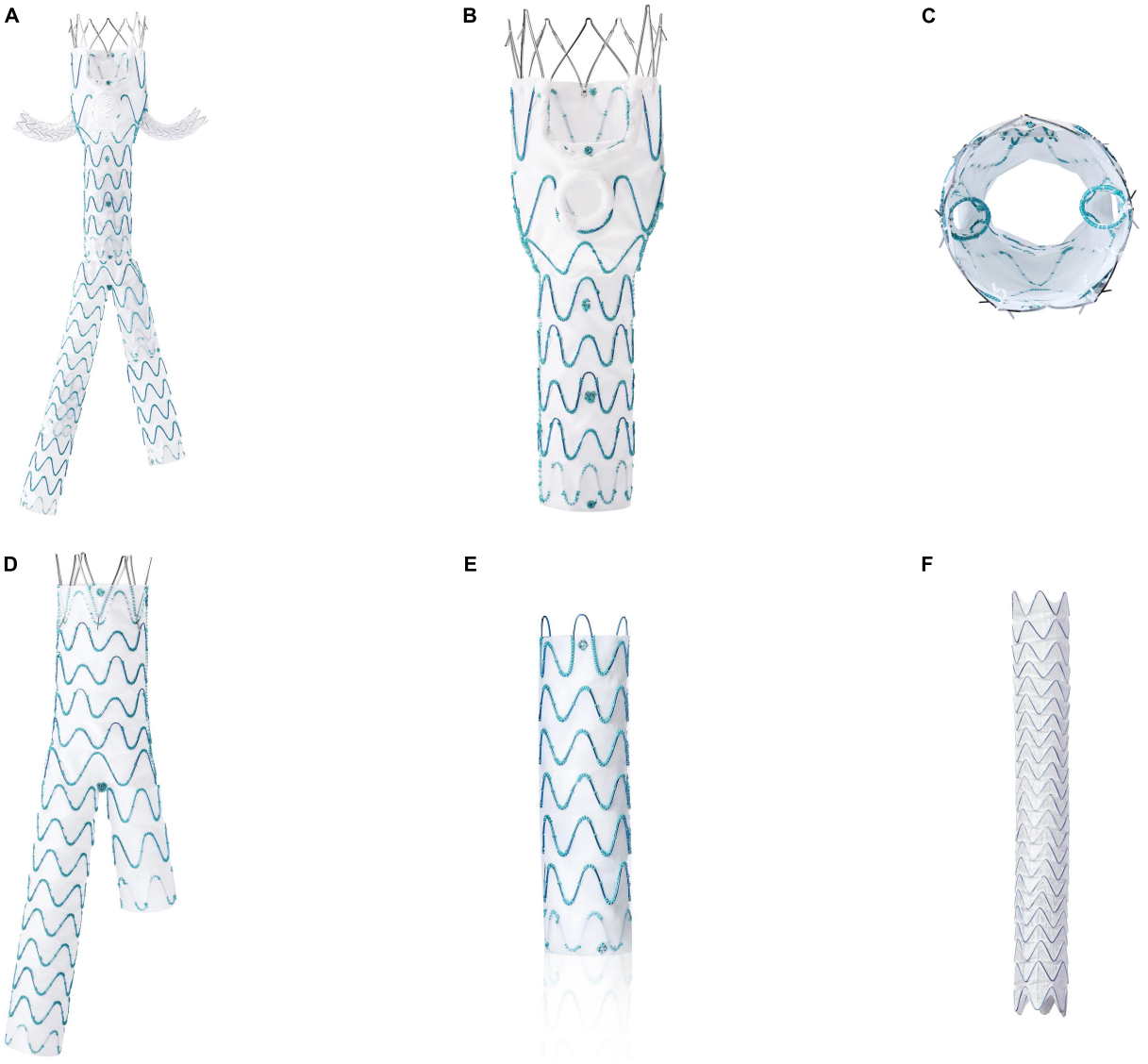

FIGURE 1
The WeFlow-JAAA system: a new, off-the-shelf, abdominal aortic stent graft system **(A)** for JRAAA, comprising a proximal body graft **(B,C)**, a distal bifurcated body graft **(D)**, iliac leg grafts **(E)** and self-expanding branch grafts **(F)**. The most major characteristic of this device was the design of proximal body graft with two standard inner branches of renal arteries, one 3 mm "mini-inner-cuff" reinforced fenestration for superior mesenteric artery, and one scallop for celiac axis.

areas of China (Table 2). All participating hospitals have performed endovascular treatment in more than 50 patients with anatomically complex abdominal aortic aneurysms in the last 5 years.

Study endpoints

Primary safety endpoint

The primary safety endpoint is the rate of survival without major adverse events (MAEs) within 30 days after the index endovascular procedure. The MAEs include all-cause death, myocardial infarction, intestinal ischemia, renal failure needing continuous dialysis, respiratory failure, stroke, and permanent paraplegia.

Primary efficacy endpoint

The primary efficacy endpoint is the rate of clinical success within 12 months after the operation. Clinical success included immediate technical success (which is defined as correct system deployment without any unintentional occlusion of the aortic visceral branches or both hypogastric arteries, no type I or III endoleak, or conversion to open surgery), and no aneurysm or device-related death, no type I or III endoleak,

TABLE 1 Trial registration data.

Date category	Information
Primary registry and trial identifying number	ClinicalTrials.gov NCT05179967
Date of registration in primary registry	6 January, 2022
Secondary identifying numbers	WEIQIANG202101
Source(s) of monetary or material support	Hangzhou Endonom Medtech Co., Ltd.
Primary sponsor	Hangzhou Endonom Medtech Co., Ltd.
Secondary sponsor(s)	None
Contact for public queries	Wei Guo, Professor, email: pla301dml@vip.sina.com
Contact for scientific queries	Wei Guo, Professor
Brief title	Safety and Efficacy Study of WeFlow-JAAA Stent Graft System for Complex Abdominal Aortic Aneurysm (GREAT Study)
Official title	Guo's visceRal artEries Reconstruction: The Prospective, Multiple Center, Objective Performance Criteria Clinical Trial About the sAfTy and Efficacy of WeFlow-JAAATM Stent Graft System (GREAT Study)
Countries of recruitment	China
Problem(s) studied	Endovascular treatment for Juxtarenal Abdominal Aortic Aneurysm (JAAA)
Intervention(s)	Fenestrated/branched abdominal stent graft system
Key inclusion criteria	Age 18–80 years at the time of informed consent signature Maximum diameter of JRAAA > 50 mm, or rapid growth of sac > 5 mm in diameter in the most recent 6 months, or rapid growth > 10 mm in diameter with 1 year The distance between the upper edge of the aneurysm and the lower edge of the opening of SMA ≥ 4 mm The angle between the proximal aneurysm neck and the aortic long axis near the opening of SMA ≤ 60° The aortic diameter at the opening of SMA ranges from 18 to 34 mm The diameter range of the starting part of SMA is 5–12 mm The diameter range of the initial part of bilateral RAs is 4.5–10 mm Length of non-bifurcated segment of SMA and RA ≥ 10 mm The diameter at the bifurcation of abdominal aorta ≥ 16 mm The length of distal anchoring area of iliac artery ≥ 15 mm The diameter range of distal anchoring area of iliac artery is 8–24 mm Feasible iliofemoral artery and upper patent upper extremity access
Key exclusion criteria	Ruptured aortic aneurysm in unstable hemodynamic instability Aneurysmal aortic dissection Infected or mycotic aortic aneurysm Local or systemic infection that may result in endoprosthesis infection Takayasu arteritis, Marfan syndrome (or other connective tissue diseases) Severe stenosis, calcification, and mural thrombosis in the proximal anchoring area of the stent Diagnosis of acute myocardial infarction within the last 3 months Transient ischemic attacks or strokes within the past 3 months A history of abdominal aortic surgery or endovascular repair Hepatic insufficiency comorbidity (ALT OR AST ≥ 5 times the upper limit of normal value, or total serum bilirubin ≥ 2 times the upper limit of normal value), serum creatinine ≥ 150 μmol/L, left ventricular ejection fraction < 50% Severe pulmonary insufficiency inability to tolerate general anesthesia Severe coagulation dysfunction An allergic history for anticoagulants, antiplatelet drugs, stent graft, or materials of the delivery system Contraindicated for antiplatelet agents or anticoagulants Serious vital organ dysfunction or other serious diseases Patients participating in other clinical trials or not completed or withdrawn from other clinical trials within 3 months at the time of the screening period Planning pregnancy, pregnancy, or breastfeeding Life expectancy < 1 year Patients not appropriate for endovascular repair based on the investigators' clinical judgment
Study type	Interventional
Date of first enrolment	February 2022
Target sample size	106
Recruitment status	Recruiting
Primary outcome(s)	Safety outcome: rate of no major adverse event (time frame: 30 days after index endovascular procedure) Efficacy outcome: rate of immediate technical success and no JRAAA-related reintervention (time frame: within 12 months after index endovascular procedure)
Key secondary outcomes	Outcome: device-related complications (time frame: intraoperative and within 30 days after index procedure) Outcomes: Rate of all-cause mortality, aneurysm-related mortality (time frame: 30 days, 6, 12 months, and 2–5 years after index procedure)

JRAAA, Juxtarenal Abdominal Aortic Aneurysm; SMA, superior mesenteric artery; RA, renal artery; ALT, alanine transaminase; AST aspartate aminotransferase.

TABLE 2 Trial centers.

Center	Geographic region
Chinese PLA General Hospital	North China
Beijing Anzhen Hospital, Capital Medical University	North China
Zhongshan Hospital, Fudan University	East China
The Second Xiangya Hospital of Central South University	Central China
People's Hospital of Xinjiang Uygur Autonomous Region	Northwest China
The First Hospital of China Medical University	Northeast China
Peking University People's Hospital	North China
West China Hospital of Sichuan University	West China
The First Affiliated Hospital, Sun Yat-sen University	South China
Nanjing Drum Tower Hospital	East China
The First Affiliated Hospital, Zhejiang University	East China
The Second Affiliated Hospital of Harbin Medical University	Northeast China
Fuwai Central China Cardiovascular Hospital	Central China
The First Affiliated Hospital of Fujian Medical University	South China
Jiangsu Province Hospital	East China
The First Affiliated Hospital of Zhengzhou University	Central China
The First Affiliated Hospital of Chongqing Medical University	Southwest China
Shandong Provincial Hospital	North China
The First People's Hospital of Yunnan Province	Southwest China
Peking Union Medical College Hospital	North China
Shanghai Ninth People's Hospital	East China
Tianjin Medical University General Hospital	North China
Xijing Hospital	Northwest China
The Second Affiliated Hospital of Nanchang University	East China
Qilu Hospital of Shandong University	North China
First Affiliated Hospital of Kunming Medical University	Southwest China
Yan'an Hospital of Kunming City	Southwest China
The First Affiliated Hospital of Harbin Medical University	Northeast China
The First Hospital of Lanzhou University	Northwest China

no graft infection or thrombosis, no aneurysm expansion > 5 mm or rupture, no conversion to open surgery, no graft migration, or a failure of device integrity within 12 months after the procedure.

Secondary safety endpoints

The following secondary safety endpoints will be evaluated: all-cause mortality, aortic-related mortality, the incidence of device-related adverse events, and the incidence of serious adverse events (resulting in death or serious deterioration of health) before discharge and at 30 days, 6 months, 12 months, and 2–5 years postoperatively.

Secondary efficacy endpoints

The following secondary efficacy endpoints will be evaluated: the patency rate of postoperative branches, the incidence of type I/III endoleak, graft migration, open surgery conversion, and JRAAA-related reintervention at 6 months, 12 months, and 2–5 years postoperatively.

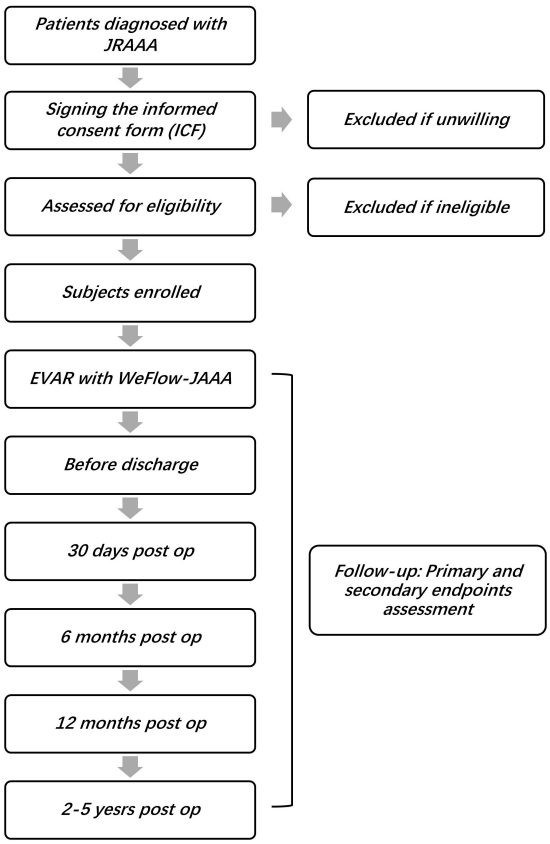

FIGURE 2
The study flow chart. (JRAAA, juxtarenal abdominal aortic aneurysm; EVAR, endovascular aortic repair; op, operation).

Patient recruitments

We are intent to recruit 106 patients between 18 and 80 years who are diagnosed with JRAAA. As the JRAAA is relatively common in clinical practice, the patient recruitment is non-competitive, and the enrollment number of each center shall be evenly distributed as far as possible to ensure the representativeness of the region. Of course, appropriate adjustments will be made according to the actual situation such as the enrollment process of each center. Figure 2 shows the time schedule of the study.

Table 1 gives a detailed overview of the inclusion and exclusion criteria. Vascular surgeons will judge the patients' eligibility according to the criteria. Engineers from Hangzhou Endonom Medtech will provide on-site guidance regarding device manipulations for the early cases treated in participating hospitals.

Device description

The design concept of WeFlow-JAAA is to revascularize the renovisceral arteries using a fenestration-and-branch mixed stent graft with two standard inner branches for the renal arteries, one 3 mm "mini-inner-cuff" reinforced fenestration for SMA, and one scallop for celiac axis (CA). The advantages of this mixed design have been proposed in the introduction.

The proximal body graft, constructed of woven polyester fabric sewn to self-expanding nitinol stents, consists of a bare stent part, an upper part (two fenestrations for SMA and CA, two inner branches for RAs), and a lower part that has a smaller diameter than the upper part (**Figures 1B,C**). A radiopaque "o" marker fixed at the 12 o'clock of the proximal end and two "I" markers are, respectively, fixed at the 4 and 8 o'clock positions of the proximal end (two sides of the scallop), coupled with one "o" marker between the scallop of CA and the fenestration of SMA to allow accurate positioning. The outlets and inlets of the inner branch and the fenestration of SMA are outlined by circular markers to facilitate cannulation. Two radiopaque "o" markers are positioned in the proximal end and distal end of the lower portion to identify the distal landing position and overlapping length with a distal bifurcated body graft.

The bare stent at the proximal end of the proximal body graft contains barbs for additional fixation of the device. The bare stent portion has lengths of 13 and 15 mm. The upper part of the proximal body graft has a diameter of 20–38 mm (2 mm increments) and lengths of 26 and 31 mm. The two inner branches sewn to the internal face of the upper part and the outlets are designed at the same level. The inner branches have three diameters available, 6, 7, and 8 mm, with a fixed length of 15 mm. The fenestration of SMA is positioned at 6 o'clock, with two diameters available, 8 and 10 mm. The lower part of the stent graft is 50–100 in length and 16–30 mm in diameter (2 mm increments). A total of 10 series with 41 types of WeFlow-JAAA endografts are available, all of which require a 22F inner diameter femoral sheath introducer, regardless of the stent graft size. To facilitate visceral artery cannulation, the delivery system of the system has three preloaded guidewires for the two inner branches and fenestration of SMA.

The self-expanding bridging branch stent graft (for the reno-visceral arteries) is constructed using a unique interwoven nitinol wire sandwiched by two thin layers of expanded polytetrafluorethylene (ePTFE), which can provide favorable flexibility, fracture resistance, and low-profile features. The branch graft diameter is 6–12 mm at the proximal end and 5–10 mm at the distal end, and the stent graft length is 20–150 mm. An inner 8–9F introducer sheath is required, depending on the stent graft diameter (8F: 6–9 mm; 9F: 10–12 mm).

The distal bifurcated body graft and iliac legs are constructed of woven polyester fabric sewn to self-expanding nitinol stents. The bifurcated body graft also has barbs in the proximal portion to prevent graft migration. A variety of sizes for distal bifurcated body graft and iliac legs are available to accommodate the different diameters of the proximal body graft and individual arterial anatomical variations.

The detailed product size series is shown in **Supplementary Appendix 2**.

Endovascular technique

The index endovascular procedures are performed in a hybrid operating room under fluoroscopic control with the patient under general anesthesia. After surgical exposure of the left brachial artery, intravenous heparin loading is started with a bolus of 100IU/kg body weight to achieve an activated clotting time of at least 250 s. The activated clotting time would be measured at 30 min intervals throughout the procedure. A subsequent dose of heparin will be administered if required. The left brachial artery is directly punctured to establish the access through which the thoracic descending aorta is catheterized. An 8F long sheath is introduced into the descending thoracic aorta. The bilateral common femoral artery is percutaneously punctured and a 5/6Fsheath inserted. Two Perclose ProGlide devices were exchanged to provide "preclose" sutures on the main body side, while one on the contralateral side.

Detailed visualization of the operative procedure is shown in **Supplementary Appendix 1**. After the endovascular repair is finished, selective angiography is used to identify endoleaks, stent graft migration, stenosis, or occlusion. Relining bare metal stents are not routinely used unless a significant stent graft compression is noted.

Medications

Single antiplatelet therapy (aspirin or clopidogrel) is recommended as a long-term treatment. Other medical treatments (such as anticoagulation, antihypertensive, antibiotic therapy, et al.) will be administered depending on the individual's comorbidities.

CT angiography

CT angiography (CTA) scans in the arterial and venous phases from the supra-aortic arch to the common femoral arteries will be performed preoperatively, before discharge, at 6 and 12 months postoperatively. CTAs are mandatory within 90 days and then at 1 and 5 years after the operation, or in case of unexpected events during the follow-up. For patients with substantially impaired renal function, postoperative CTA will be replaced by plain CT and Doppler ultrasonography.

TABLE 3 Evaluation schedule of the study.

	Entry	Operation	Discharge	30 days (± 7 days)	6 months (± 30 days)	12 months (± 30 days)	24 months (± 60 days)	36 months (± 60 days)	48 months (± 60 days)	60 months (± 60 days)
Informed consent	X									
Eligibility screen	X									
Demographic data	X									
Medical/clinical history	X									
Vital signs	X	X	X							
Blood routine	X		X							
Urine routine	X		X							
Liver/renal function	X		X	X	X	X				
Coagulation function	X		X							
Enzymology test	X		X							
Pregnancy test	X									
Heart function	X		X							
Lung function	X									
CTA	X		X	X	X	X	*	*	*	X
DSA		X								
Operative recording		X								
Medications	X	X	X	X	X	X				
Adverse events	X	X	X	X	X	X	X	X	X	X

CTA, CT angiography; DSA, Digital Subtraction Angiography. *Duplex Ultrasound Scan (CTAs are mandatory within 90 days and then at 1 and 5 years after the operation, or in case of unexpected events during the follow-up).

10.3389/fcvm.2022.1013834

Patient timeline

Each patient will attend a total of 10 visits, including one preoperative visit and nine postoperative visits for eligibility screening, baseline data extraction, and safety/efficacy evaluation of the stent graft system (**Table 3**). Unless an unexpected event occurred, Doppler ultrasonography rather than CTA is planned for 2, 3, and 4 years postoperatively. Adverse events and defects of the devices will be strictly monitored throughout follow-up.

Data extraction, entry, and monitoring

The clinical database contains the data of participants' electronic medical records (EMR), CTA images, and follow-up conditions. Preoperative data will be extracted from the EMR and entered into the database before the operation, while postoperative in-hospital data will be collected within 2 weeks after discharge. The headline of each patient's DICOM format image at each timepoint will be modified before data extraction, with the identifying information (patient ID, name, date of birth) replaced by a random 6-digit number. Preoperative CTA image data will be extracted before the operation, while postoperative CTA image data will be extracted within 2 weeks after the image data is acquired. Postoperative CTA images obtained at each follow-up timepoint will be independently analyzed by two experienced vascular surgeons who are blinded to the CTA findings at the preoperative or other postoperative timepoints, patients' EMR, and follow-up information. After the completion of data extraction, the discrete data from CTA scans will be integrated into one database according to the predesigned 6-digit number. All CTA images will be measured and assessed by the 3Mensio workstation (V.8.1; 3Mensio Medical Imaging). At least 10% of the total CTA scans (including preoperative and postoperative scans) will be randomly selected and re-analyzed by the two vascular surgeons to assess interobserver and interobserver agreement.

Data will be registered *via* an electronic data capture system (EDC) and centrally stored in a secure password-protected server. Double data entry, range checks, and logical consistency checking methods will be used to ensure the quality of data. Clinical research associates who are independent of the investigators will review the study documentation and records held at each site to ensure that the study is conducted in compliance with the regulatory requirements.

Sample size calculation

Currently, no guiding principle exists regarding objective performance criteria (OPC) for a fenestrated/branched stent graft system in China. As the endpoints of this study differ from that of the p-Branch (off-the-shelf) and Zenith Fenestrations (customized) studies, the expected endpoint incidences were obtained based on data extracted from previous studies (7, 12). We hypothesized that the performance of the WeFlow-JAAA stent graft system will not be inferior to that of the p-Branch and be similar to that of Zenith fenestrations.

In this setting, combined with the current experience of clinical experts, it is estimated that the objective performance of clinical success rate at 12 months (the primary efficacy endpoint) is set to 70% and the target of WeFlow-JAAA is set to 85%. According to statistical requirements, we used 0.025 as α and 0.10 as β for a single-sided test. A sample size of 82 cases was thus obtained. Besides, the objective performance of the rate of survival without MAEs in 30 days (the primary safety endpoint) is set to 71% and the target of WeFlow-JAAA is set to 86%. As $\alpha = 0.025$ and $\beta = 0.10$ for a single-sided test, a sample size of 80 patients is required. Both endpoints need to be achieved. Considering the shedding, the sample size increased by 20%. At least 103 subjects are required for this study eventually. Considering the facilitation of the study center allocation, it is expected to enroll 106 patients. The sample size is calculated as follows:

$$n = \frac{\left[Z_{1-\alpha/2}\sqrt{P_0(1-P_0)} + Z_{1-\beta}\sqrt{P_T(1-P_T}\right]^2}{(P_T - P_0)^2}$$

(P_T presents the expected rate of the test instrument and P_0 presents the target value).

Statistical analysis

The analysis will be done on all participants of the study as a primary analysis population. Patient demographic data, safety endpoints, and efficacy endpoints will be analyzed descriptively, with continuous data expressed as means with SD or medians (IQR), and categorical data will be expressed as numbers and percentages.

The primary safety and efficacy endpoints will be summarized as numbers and percentages with their two-sided 95% exact CI, using the Clopper-Pearson method. In addition, the Kaplan-Meier method will be used to estimate the cumulative rate of each endpoint. Statistics calculations will be performed using SAS software V.9.4 (SAS Institute).

Patient and public involvement

Patients or the public will not be involved in the design, conduct, reporting, or dissemination plans of our study.

Ethics statement

The studies involving human participants were reviewed and approved by the Ethics Committee of Chinese PLA

General Hospital. The patients/participants provided their written informed consent to participate in this study.

Author contributions

J-PG and H-PZ drafted the manuscript. WG initiated the design of the study, while H-PZ, XJ, JX, X-HM, L-JW, M-HZ, and Y-LX helped with the implementation. All authors read and approved the final version of the manuscript.

Funding

This study was funded by Hangzhou Endonom Medtech Corporation (Hangzhou, China) (Grant No. WEIQIANG202101).

Acknowledgments

We would like to thank all investigators and participants of the study.

Conflict of interest

The authors declare that the research was conducted in the absence of any commercial or financial relationships that could be construed as a potential conflict of interest.

Publisher's note

Supplementary material

The Supplementary Material for this article can be found online at: https://www.frontiersin.org/articles/10.3389/fcvm.2022.1013834/full#supplementary-material

References

1. Wanhainen A, Verzini F, Van Herzeele I, Allaire E, Bown M, Cohnert T, et al. Editor's choice – European society for vascular surgery (ESVS) 2019 clinical practice guidelines on the management of abdominal aorto-iliac artery aneurysms. *Eur J Vasc Endovasc Surg.* (2019) 57:8–93. doi: 10.1016/j.ejvs.2018.09.020

2. Belczak SQ, Lanziotti L, Botelho Y, Aun R, Silva ES, Puech-Leão P, et al. Open and endovascular repair of juxtarenal abdominal aortic aneurysms: a systematic review. *Clinics.* (2014) 69:641–6. doi: 10.6061/clinics/2014(09)11

3. Jones AD, Waduud MA, Walker P, Stocken D, Bailey MA, Scott DJA. Meta-analysis of fenestrated endovascular aneurysm repair versus open surgical repair of juxtarenal abdominal aortic aneurysms over the last 10 years. *BJS Open.* (2019) 3:572–84. doi: 10.1002/bjs5.50178

4. Gallitto E, Faggioli G, Spath P, Pini R, Mascoli C, Ancetti S, et al. The risk of aneurysm rupture and target visceral vessel occlusion during the lead period of custom-made fenestrated/branched endograft. *J Vasc Surg.* (2020) 72:16–24. doi: 10.1016/j.jvs.2019.08.273

5. Katsargyris A, Uthayakumar V, Marques de Marino P, Botos B, Verhoeven EL. Aneurysm rupture and mortality during the waiting time for a customised fenestrated/branched stent graft in complex endovascular aortic repair. *Eur J Vasc Endovasc Surg.* (2020) 60:44–8. doi: 10.1016/j.ejvs.2020.03.003

6. Quiñones-Baldrich WJ, Holden A, Mertens R, Thompson MM, Sawchuk AP, Becquemin JP, et al. Prospective, multicenter experience with the ventana fenestrated system for juxtarenal and pararenal aortic aneurysm endovascular repair. *J Vasc Surg.* (2013) 58:1–9. doi: 10.1016/j.jvs.2012.12.065

7. Sveinsson M, Sonesson B, Dias N, Björses K, Kristmundsson T, Resch T. Five year results of off the shelf fenestrated endografts for elective and emergency repair of juxtarenal abdominal aortic aneurysm. *Eur J Vasc Endovasc Surg.* (2021) 61:550–8. doi: 10.1016/j.ejvs.2020.12.012

8. Georgiadis GS, van Herwaarden JA, Antoniou GA, Hazenberg CE, Giannoukas AD, Lazarides MK, et al. Systematic review of off-the-shelf or physician-modified fenestrated and branched endografts. *J Endovasc Ther.* (2016) 23:98–109. doi: 10.1177/1526602815611887

9. de Niet A. *Endovascular Approaches To Complex Aortic Aneurysms.* Netherlands: University of Groningen (2020).

10. Farber MA, Vallabhaneni R, Marston WA. "Off-the-shelf" devices for complex aortic aneurysm repair. *J Vasc Surg.* (2014) 60:579–84. doi: 10.1016/j.jvs.2014.03.258

11. Ou J, Cheng SW, Chan YC. The compatibility of p-branch "off-the-shelf" fenestrated endovascular graft in Asian patients with juxtarenal aortic aneurysm. *J Vasc Surg.* (2015) 61:1417–23. doi: 10.1016/j.jvs.2014.12.061

12. Oderich GS, Greenberg RK, Farber M, Lyden S, Sanchez L, Fairman R, et al. Results of the United States multicenter prospective study evaluating the Zenith fenestrated endovascular graft for treatment of juxtarenal abdominal aortic aneurysms. *J Vasc Surg.* (2014) 60:.1420–8.e1–5. doi: 10.1016/j.jvs.2014.08.061

frontiers | Frontiers in Cardiovascular Medicine

TYPE Study Protocol
PUBLISHED 10 January 2023
DOI 10.3389/fcvm.2022.1089968

OPEN ACCESS

EDITED BY
Guido Iaccarino,
University of Naples Federico II, Italy

REVIEWED BY
Susana Pedras,
Centro Hospitalar Universitário do Porto, Portugal
Vincenzo De Luca,
Università degli Studi di Napoli Federico II, Italy

*CORRESPONDENCE
Dunja Bruch
dunja.bruch@mhb-fontane.de

SPECIALTY SECTION
This article was submitted to Hypertension, a section of the journal Frontiers in Cardiovascular Medicine

RECEIVED 04 November 2022
ACCEPTED 22 December 2022
PUBLISHED 10 January 2023

CITATION
Bruch D, Muehlensiepen F, May S, Wengemuth E, Johannsen O, Reber KC, Blankenstein E-L, Fleige G, Middeke M, Albes J, Heinze M, Lehnen M and Spethmann S (2023) Digital preventive measures for arterial hypertension (DiPaH) – a mixed-methods study protocol for health services research. *Front. Cardiovasc. Med.* 9:1089968. doi: 10.3389/fcvm.2022.1089968

Digital preventive measures for arterial hypertension (DiPaH) – a mixed-methods study protocol for health services research

Dunja Bruch [1,2]*, Felix Muehlensiepen [2,3], Susann May [1,3], Eileen Wengemuth [1], Olen Johannsen[4], Katrin Christiane Reber[5], Eva-Lotta Blankenstein[6], Gerrit Fleige[6,7], Martin Middeke [8], Johannes Albes [1,2], Martin Heinze [3], Marc Lehnen[6] and Sebastian Spethmann [7,9]

[1]Department of Cardiovascular Surgery, Heart Center Brandenburg, Immanuel Klinikum Bernau, University Hospital Brandenburg Medical School (Theodor Fontane), Bernau bei Berlin, Germany, [2]Faculty of Health Sciences, Brandenburg Medical School Theodor Fontane, Neuruppin, Germany, [3]Center for Health Services Research, Brandenburg Medical School Theodor Fontane, Rüdersdorf bei Berlin, Germany, [4]Hypertension Care UG, Ingolstadt, Germany, [5]AOK Nordost – Die Gesundheitskasse, Strategische Versorgungsanalysen/GeWINO, Berlin, Germany, [6]revFLect GmbH, Hanover, Germany, [7]Brandenburg Medical School Theodor Fontane, Neuruppin, Germany, [8]Hypertension Center Munich, Munich, Germany, [9]Medical Department, Division of Cardiology and Angiology, Charité – Universitätsmedizin Berlin, Corporate Member of Freie Universität Berlin and Humboldt-Universität zu Berlin, Berlin, Germany

Introduction: Digital health measures promise to further improve the quality of cardiovascular care but have not yet been widely implemented in routine care. The research project Digital preventive measures for arterial hypertension (DiPaH) will systematically identify structural and individual factors in different stakeholders that influence the use of digital preventive measures in patients with arterial hypertension in Germany. Special focus is given to remote and sparsely populated areas, the age-specific impact, as well as influence of digital health literacy.

Methods and analysis: The DiPaH project is an exploratory cross-sectional study with a mixed-methods design, in which written surveys and interviews with patients and physicians will be conducted. In addition, secondary data from a health insurance company will be analyzed. In module 1, individuals from the database of the health insurance company with confirmed arterial hypertension will be interviewed (1,600 questionnaires, 30 interviews). Module 2 includes users of digital prevention offers and apps (400 questionnaires, 40 interviews) and in module 3, family physicians and cardiologists will be interviewed (400 questionnaires, 40 interviews). In a final module, the overall results will be analyzed and recommendations for interventions in clinical care will be derived.

Discussion: The DiPaH project will contribute to a patient-oriented and demand-based improvement of arterial hypertension prevention services in

health care. Challenges and barriers will be analyzed and the respective target groups identified based on their prevention needs and social characteristics to enable a patient-centered implementation of digital prevention of arterial hypertension and cardiovascular services in general, and finally to improve cardiovascular outcomes.

Clinical trial registration: https://drks.de/search/de/trial/DRKS00029761, identifier DRKS00029761.

KEYWORDS

hypertension, digital prevention measures, mixed-methods design, digital health literacy, rural regions

Introduction

Despite effective guideline-based prevention and treatment options, cardiovascular diseases remain the leading cause of death worldwide (1). Arterial hypertension is one of the most important risk factors for cardiovascular diseases (2), affecting over one billion people worldwide (3). In addition to a genetic predisposition, the development of hypertension is strongly influenced by individual factors such as lifestyle (4), but also by local access to and quality of health care (5). In Germany, the prevalence of such risk factors varies greatly depending on the region. For example, obesity is more prevalent in the rural federal states (6). But it is precisely there that accessibility to medical care is limited due to a low density of doctors (7). As a result, hypertension-related diseases such as ischemic heart disease are most frequent in these states (8). On an individual level, there is also an association between hypertension and lower socioeconomic status and lower educational attainment (9). In summary, there are significant regional differences in Germany, with a higher incidence of arterial hypertension in socioeconomically disadvantaged areas (10).

In order to overcome these geographical disparities in health care and to strengthen individual health behavior even in regions with poor access to health care and aging population, digital prevention measures are an innovative and promising approach (11). These are digital applications such as remote monitoring (i.e., telemonitoring), e-learning, or m-health apps. The characteristics of digital preventive measures for arterial hypertension are shown in **Figure 1**. With telemonitoring, patient data is transmitted to the attending physicians (12). E-learning provides patients with information, e.g., on lifestyle modification through interactive and web-based educational material (12), and m-health apps are stand-alone software on a smartphone or tablet (13). Despite existing technical possibilities, digital health applications have so far only been insufficiently implemented (11), so that there is an increasing risk of a "digital divide" (14), whereby vulnerable groups with low digital health literacy are progressively excluded from innovative health offers. Current data (15) from Germany show low mobile Internet use among older people (only 36% of the population born up to 1945) and among people with lower educational attainment. Importantly, usage is lower in the more rural eastern German states than in the western states. Since people with lower incomes have less access to digital devices (15), one cause could be the lower gross average income in eastern Germany (16). However, people who are more limited in their mobility and have a higher risk of illness could particularly benefit from digital measures. Importantly, data on hypertension-specific digital applications are lacking so far.

Due to the importance of digital health interventions, the ESC e-Cardiology Working Group has published a position paper in 2019 addressing the challenges of digital health adoption in cardiovascular medicine (11). In addition to technical issues, there are also patient- and physician-related barriers [e.g., lack of information about available and qualified m-health apps (17), lack of digital skills (15)] as well as reimbursement and legal considerations to the introduction of digital health in cardiovascular medicine that need to be carefully analyzed and addressed prior to their successful deployment.

To overcome such barriers, the healthcare research project digital preventive measures for arterial hypertension (DiPaH) will therefore systematically identify individual, structural and application-related factors that influence the use of digital preventive measures in patients with arterial hypertension in

Abbreviations: G-BA, Federal Joint Committee (Gemeinsamer Bundesausschuss); ESC, European Society of Cardiology; DiPaH, digital preventive measures for arterial hypertension.

Type of prevention	• Primary prevention: development of hypertension • Secondary prevention: control of hypertension
Aim	Patient supply
Purpose of digital applications	• Information and e-learning (i.e. websites, tutorials, digital information, videos) • Communication (i.e. video consultation, e-mails) • Electronic documentation, measurement and remote monitoring (i.e. telemonitoring) • Hands-on exercises (i.e. online courses, video exercises) • Tracking (i.e. wearables) • Combined functions (i.e. m-health apps)
Contents of non-medication prevention	Health behaviors: Physical exercise, weight control, nutrition, stress reduction, non-smoking, salt reduction, alcohol reduction.

FIGURE 1
Characteristics of digital preventive measures for arterial hypertension.

Germany. Due to the regional differences already described, a particular focus of the study is on remote and sparsely populated areas, the age-specific effects as well as the influence of digital health literacy.

The study identifies not only general barriers to the use of digital prevention services, but also barriers specific to patient groups (e.g., with regard to motivation and health literacy). In order to take into account the complexity of prevention in statutory health insurance, the DiPaH study relates the experiences of patients and users of digital applications to the perspective of physicians. In this way, potentials, but also barriers that only emerge in the overall context of the health care system, can be identified and corresponding concrete recommendations for implementation can be derived.

This study protocol presents the study design for each subgroup and describes the study population, the methodological approach (including data collection and data analysis), the relevant outcomes and the quality criteria of the study, and discusses the expected benefits and limitations. The aim is to give an overview of the different sub-studies (modules), to describe contexts and to present the methodological approach.

Methods and analysis

Design and setting of the study

The mixed-methods study will be conducted in multiple phases. Quantitative and qualitative methods will be performed in a parallel or in a sequential order (18). Standardized surveys are used to obtain a representative and comprehensive understanding of the different stakeholder groups and to make the answers comparable. The qualitative methods are suitable to contextualize and interpret the data appropriately (18). The methodological openness of qualitative methods also allows aspects to be included that arise from everyday conditions and are accordingly not yet theoretically accessible at the beginning of the study, for example organizational barriers in everyday practice (19). Methodological triangulation allows the results of quantitative and qualitative interviews to be validated against each other (20).

Figure 2 shows a summary of the study design, methods and the main focus of interest in each module. Since the focus is on the user perspective, we will include patients with arterial hypertension, users of digital health services and physicians. The timeline of recruitment is presented in **Table 1**.

The study will be conducted in Germany with a regional focus on the metropolitan area of Berlin and the rural, sparsely populated federal states of Brandenburg and Mecklenburg-Western Pomerania.

Selection of subjects

The sub-study specific inclusion criteria are summarized in **Table 2**. Exclusion criteria are age under 18, lack of consent and considerable limitations to speak and understand German fluently.

In module 1, insured persons of the statutory health insurance company AOK Nordost with arterial hypertension will be surveyed on preferences and barriers to the use of (digital) prevention measures (n = 1,600 questionnaires). Questionnaire data will be linked to routine data to analyze further health-related factors. Prior to the AOK Nordost survey, a preparatory qualitative interview study will be conducted with hypertension patients recruited through clinics and practices (n = 30).

In module 2a, users of (digital) prevention services offered by AOK Nordost will be surveyed on their motivation to participate in the interventions, the advantages and disadvantages of digital vs. analog measures, and possible barriers to the services (n = 200 questionnaires, n = 20 interviews).

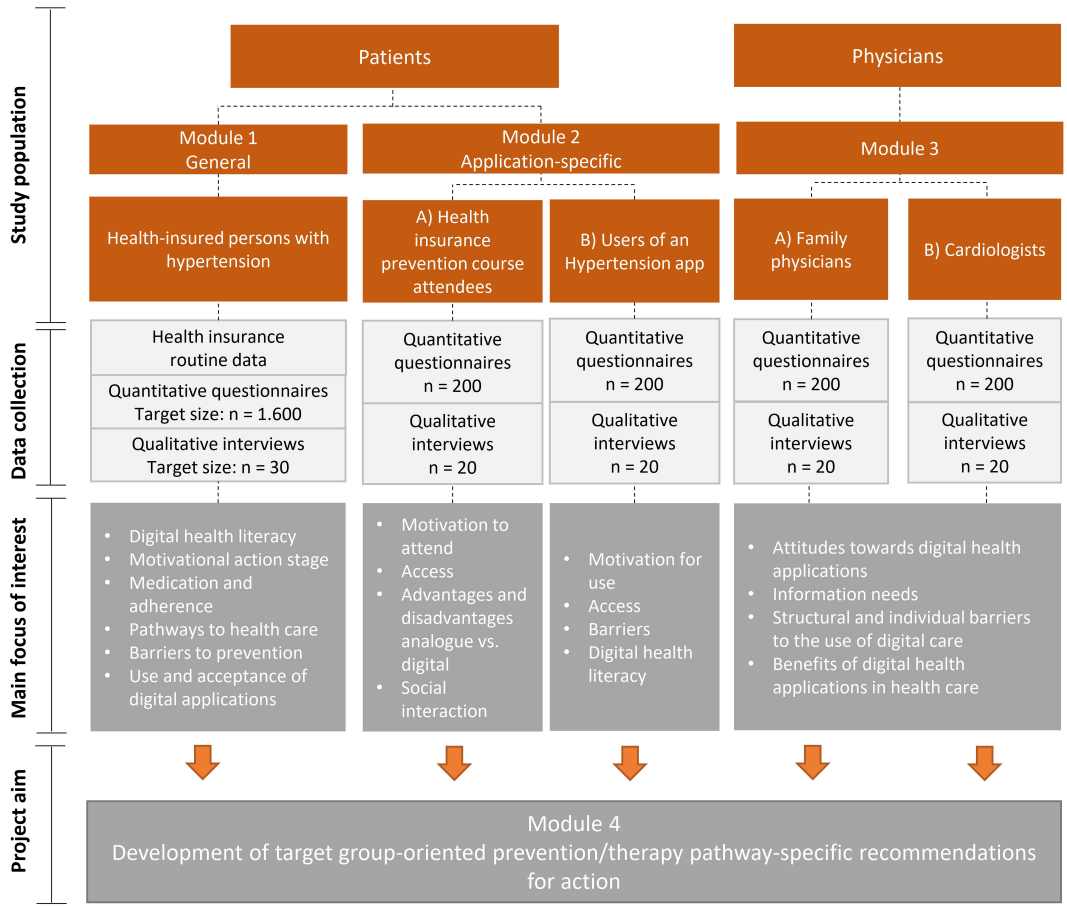

FIGURE 2
Study design.

In module 2b, users of the hypertension-specific app "Hypertonie.App" (21) will be interviewed about their motivation for using the app, about possible restraining factors when using a hypertension app and how they became aware of the app (n = 200 questionnaires, n = 20 interviews). The app includes features for documenting blood pressure, personalized health information, breathing exercises, and reminder functions.

In module 3, family physicians (3a) and cardiologists (3b) will be surveyed on their attitudes toward digital health applications, structural and individual barriers, and information needs in medical practice (n = 400 questionnaires, n = 40 interviews).

Sample size calculation

A sample number of n = 200 is required per subgroup. The sample number is calculated according to an *a priori* power analysis (G*Power) for the χ^2 test for dichotomous variables with the following assumptions: moderate effect (w = 0.2), α = 0.05, power (1-β) = 0.80, Df = 1 (required sample size n = 197).

In Module 1, eight subgroups will be identified by age, gender, and rural vs. urban residence (per subgroup n = 200, total n = 1,600).

Outcomes

The DiPaH study will collect data through questionnaires and interviews on a one-time basis. The relevant outcomes are digital health literacy [eHEALS (22, 23)], health literacy [HLS-EU-Q6 (24, 25)], motivation action stage [HAPA Assessment (26, 27)], self-concept related to information and communication technology (28), perception of usability [System Usability Scale (29, 30)], guideline-adherent medication (4), adherence [MMAS-8D (31, 32)]. The outcomes and measurement tools are presented in **Table 3**. In addition, the following outcomes will be explored in all modules: attitudes toward digital prevention, use of digital prevention, motivation to use digital prevention, barriers to digital prevention, perceived advantages and disadvantages of digital prevention, information needs, and – just for patients – pathways to health care. For these outcomes, module-specific items will be developed and piloted by the research team. In addition,

these themes will be explored in greater detail in the qualitative interviews.

Input variables in all modules will be sociodemographic characteristics of patients (age, gender, rural vs. urban residence, federal state, education, income) and physicians (age, gender, rural vs. urban location of medical practice, federal state, experience). In Modules 1 and 2b, health-related characteristics will be collected in more detail (current medication, disease status, comorbidities). In Module 2a, the interactivity of the course is additionally assessed as an input variable.

Statistical analyses

First, the data from the standardized questionnaires will be presented descriptively (absolute and relative frequency, median and standard deviation). In further steps, correlation analyses will be performed. The correlation between two binary variables is analyzed with the $\chi 2$-test. For continuous outcome variables and binary influence factors, *t*-tests will be performed and means and 95% confidence intervals will be reported. Regression analyses will be performed to analyze possible associations between patient characteristics (such as sociodemographic variables) and outcomes of interest (e.g., digital health literacy).

Qualitative analyses

For the qualitative part of the study, problem-centered interviews will be conducted. In this type of exploratory interview, the theoretical concepts are changeable in the research process. Thus, the method enables to integrate the subjective perspectives, experiences and contextual conditions of the participants. In addition to the interview guide, short questionnaires will be applied to collect sociodemographic and health-related characteristics.

The interviews will be recorded and transcribed. The qualitative data from the interviews and from the free text answers in the questionnaire will be analyzed with the qualitative content analysis according to Kuckartz (33). This allows a rule-driven reduction and systematization of the data. The aim is to develop a comprehensive category system. For validation of the category system, a member check will be performed (34).

Data capture and storage

In modules 1 and 2a, the insured persons receive the questionnaire from their health insurer AOK Nordost with a stamped return envelope. By giving written consent, participants in module 1 agree to the linking of questionnaire data with the billing data of the health insurance funds. The pseudonymization of the data will be carried out by a trust center on the basis of a coding list. The trust center is separated from the evaluating unit in terms of space, technology, and staff. In modules 2 and 3 online participation will also be possible. For this, participants will receive a link to the questionnaire on the online platform "unipark" (35).

To receive the incentive (money or gift card), participants need to consent that their contact details will be used for this purpose. Written consent is also required for the audio recording of the interviews. The interviews will be coded with a pseudonym before the analysis. Contact information and consent will be kept separate from research data.

Research data will not contain personal data that would allow the identification of individuals. The data will be stored securely on the server of the Brandenburg Medical School or on local computers.

Data quality

To ensure high data quality, several data validation checks will be performed: checking for correct data type, numeric value ranges, data format, missing data, and consistency of the chronology in the dates. The completeness of the data is checked per case. The quality of the interview data will be controlled by a member check (36).

TABLE 1 Dates of recruitment.

Substudy	Dates of recruitment
Module 1 interviews	Q3 2022 – Q1 2023 (6 months)
Module 1 questionnaires	Q4 2023 – Q1 2024 (4 months)
Module 2a interviews and questionnaires	Q4 2022 – Q3 2023 (11 months)
Module 2b interviews and questionnaires	Q4 2022 – Q3 2023 (11 months)
Module 3a interviews	Q4 2022 – Q2 2023 (5 months)
Module 3a questionnaires	Q4 2023 – Q1 2024 (4 months)
Module 3b interviews	Q4 2022 – Q2 2023 (5 months)
Module 3b questionnaires	Q4 2023 – Q1 2024 (4 months)

Q, quarter. Q1 = Jan–Mar, Q2 = Apr–Jun, Q3 = Jul–Sep, Q4 = Oct–Dec.

TABLE 2 Additional inclusion criteria.

Substudy	Inclusion criteria
Module 1 interviews	Diagnosis of arterial hypertension
Module 1 questionnaires	Diagnosis of arterial hypertension and health-insured by the AOK Nordost
Module 2a	Participation in a behavioral prevention course offered by AOK Nordost
Module 2b	Use of a hypertension app within the last 2 years
Module 3a	Current work as a family physician
Module 3b	Current work as a specialist in cardiology

Discussion

Global health systems today confront fundamental challenges in providing optimal care due to aging populations, shortages of health workers, financing, accessibility and affordability of cardiovascular disease medicines and services. Digital health technologies have the potential to overcome these challenges (37). Consequently, the establishment of e-health to improve widespread cardiovascular care is a central goal of the ESC. In terms of arterial hypertension, a digital hypertension program and m-health tools have already been shown to lead to significant improvement in blood pressure control rates and lifestyle change compared to standard care (38, 39). However, before successful and widespread implementation, there is still a great need for research on hindering and supportive elements in special patient populations (11). To our knowledge, DiPaH is the largest health services research study on the topic of digital cardiovascular prevention measures and will fill this important knowledge gap. Different patient cohorts will be characterized according to their prevention needs and possible barriers to the use of digital prevention measures. At the same time, physicians will be involved as a main contact for their patients in order to identify structural and individual obstacles as well as information needs in medical practice. Based on this, practical recommendations will eventually be developed at the levels of patients, physicians, service providers, and health insurers to increase the implementation, accessibility, use of, as well as the adherence to digital prevention measures. These will enable hypertensive patients to take a more active role in their own care and will have the potential to significantly improve current clinical care pathways (11). We are also convinced that these findings will help to implement digital health-based care models for cardiovascular disease in general, beyond the application field of arterial hypertension.

Strengths and limitations

The strengths of DiPaH include an integrative approach of a mixed-methods study protocol that comprehensively considers the perspectives of patients, physicians and participants of analog and digital prevention measures. Special attention is paid to rural and sparsely populated areas, age-specific effects and the influence of digital health literacy. This allows concrete recommendations to be derived for wider adoption and sustainable use of digital prevention interventions in cardiovascular medicine. A limitation of the study is that it is only conducted in Germany. But by using internationally validated questionnaires, relevant findings can also be obtained for other countries.

Even though we are only survey the users of a single hypertension app, the aim is not to evaluate this one app. Rather, in DiPaH we want to characterize the app users and find out why they use a digital hypertension app. Accordingly, a gain in knowledge is expected for other apps. In particular, it is assumed that barriers, motivations, attitudes, and pathways to health care are not app-specific.

TABLE 3 Outcomes and measurement tools.

Outcome	Measurement tools	References	Items	Reliability	Module				
					1	2a	2b	3a	3b
Digital health literacy	eHEALS	Norman and Skinner (22), German: Soellner et al. (23)	8	Cronbach's α = 0.828 to Cronbach's α = 0.877	x	x	x		
Health literacy	HLS-EU-Q6	Sørensen et al. (24), Short Version: Pelikan et al. (25)	6	Cronbach's α = 0,803	x	x			
Motivation action stage	HAPA Assessment: stage assessment	Lippke et al. (27)	1	Sensitivity = 70% to 80% Specificity = 80% to 87%	x		x		
Self-concept related to information and communication technology	General ICT-SC	Schauffel et al. (28)	5	Cronbach's α = 0.95	x	x			
Perception of usability	System Usability Scale	Brooke (30), Bangor et al. (29)	10	Cronbach's α = 0.911			x		
Adherence	MMAS-8	Morisky et al. (32), German: Arnet et al. (31)	8	Cronbach's α = 0.41	x				
Guideline-adherent medication	ESC guideline criteria	Williams et al. (4)			x				

However, the AOK Nordost is the largest statutory health insurance fund in north-eastern Germany with about 1.7 million insured and covers about 18% of the population in north-eastern Germany (approx. 7.82 million inhabitants, 2021 (40)). As there is no standardized electronic patient record in Germany so far, we will not use primary data from hospitals and health care facilities. Surveying participants *via* a health insurer has the advantage that there are no gatekeepers, e.g., physicians enrolling patients in the study and thereby selecting them (intentionally or unintentionally), and that the billing data is complete. The limitation of billing data (e.g., shows only picking up medications, not actually taking them) is compensated for by the use of questionnaires. The secondary data from the health insurance funds are available 9 months later. This time period was taken into account in the study design.

Conclusion

The roadmap for digital health adoption in cardiology is challenging but imperative to address future challenges in cardiovascular medicine. DiPaH will make an important contribution by identifying the specific barriers to the adoption of digital health technologies for arterial hypertension and providing recommendations for overcoming them.

Ethics statement

The study complies with good clinical practice in accordance with the Declaration of Helsinki and the laws and regulations applicable in Germany. The local Ethics Committee of the Brandenburg Medical School approved the study (Record number E-02-20220620). Due to the sequential approach of the mixed-methods design, the questionnaires in modules 1 and 3 will be modified based on the qualitative analysis. Therefore, an amendment will be requested from the Ethics Committee before the survey starts. If necessary, the relevant information in the German Clinical Trials Register will be updated.

Author contributions

DB, SS, ML, MH, FM, SM, E-LB, EW, GF, OJ, and MM contributed to the study conception and design. SS, DB, and ML contributed to the obtaining funding. DB, SS, SM, FM, EW, JA, E-LB, KR, and OJ contributed to the collection of data. DB, SM, FM, EW, and E-LB contributed to the analysis of data. SS, DB, ML, MH, JA, and MM contributed to the supervision. DB and SS drafted and revised the manuscript. All authors read and approved the final manuscript.

Funding

This project was supported by a grant of the Federal Joint Committee (Gemeinsamer Bundesausschuss, G-BA) in Germany from May 2022 to April 2025 (Innovation fund grant number 01VSF21042). The funder of the study had no influence in the study design.

Acknowledgments

We gratefully acknowledge Dr. Sebastian Liersch (at that time AOK Nordost) for his contributions to the study concept.

Conflict of interest

E-LB was employed by revFLect GmbH. GF and ML are the CEOs of revFLect GmbH. OJ is CEO of Hypertension Care UG, which offers the Hypertonie.App. OJ and MM are the founder of the Hypertonie.App.

The remaining authors declare that the research was conducted in the absence of any commercial or financial relationships that could be construed as a potential conflict of interest.

Publisher's note

References

1. Roth G, Mensah G, Johnson C, Addolorato G, Ammirati E, Baddour L, et al. Global burden of cardiovascular diseases and risk factors, 1990-2019: update from the GBD 2019 study. *J Am Coll Cardiol.* (2020) 76:2982–3021. doi: 10.1016/j.jacc.2020.11.010

2. Forouzanfar M, Liu P, Roth G, Ng M, Biryukov S, Marczak L, et al. Global burden of hypertension and systolic blood pressure of at least 110 to 115 mm Hg, 1990-2015. *JAMA.* (2017) 317:165–82. doi: 10.1001/jama.2016.19043

3. Parati G, Torlasco C, Omboni S, Pellegrini D. Smartphone applications for hypertension management: a potential game-changer that needs more control. *Curr Hypertens Rep.* (2017) 19:48. doi: 10.1007/s11906-017-0743-0

4. Williams B, Mancia G, Spiering W, Agabiti Rosei E, Azizi M, Burnier M, et al. 2018 ESC/ESH guidelines for the management of arterial hypertension: the task force for the management of arterial hypertension of the European Society of

Cardiology (ESC) and the European Society of Hypertension (ESH). *Eur Heart J.* (2018) 39:3021–104. doi: 10.1093/eurheartj/ehy339

5. Egan B, Li J, Sutherland S, Rakotz M, Wozniak G. Hypertension control in the United States 2009 to 2018: factors underlying falling control rates during 2015 to 2018 across age-and race-ethnicity groups. *Hypertension.* (2021) 78:578–87. doi: 10.1161/HYPERTENSIONAHA.120.16418

6. Steffen A, Holstiege J, Akmatov M, Bätzing J. *Trends in Prevalence of Obesity in the Outpatient Health Service Sector in Germany, 2009 to 2018*. Berlin: Central Research Institute of Ambulatory Health Care in Germany (2021).

7. Kassenärztlichen Vereinigung Brandenburg [KVBB], Association of Statutory Health Insurance Physicians Brandenburg. *Demand Planning in 2020 for the Area of the Association of Statutory Health Insurance Physicians Brandenburg*. Potsdam: Association of Statutory Health Insurance Physicians Brandenburg (2020).

8. Holstiege J, Akmatov M, Steffen A, Bätzing J. *Ischemic Heart Disease in German Ambulatory Care—Temporal Trends and Regional Variations*. Berlin: Versorgungsatlas-Bericht (2020).

9. Leng B, Jin Y, Li G, Chen L, Jin N. Socioeconomic status and hypertension: a meta-analysis. *J Hypertens.* (2015) 33:221–9. doi: 10.1097/HJH.0000000000000428

10. Holstiege J, Akmatov M, Steffen A, Bätzing J. *[Trends in Prevalence of Hypertension in the Outpatient Health Service Sector in Germany]*. Berlin: Versorgungsatlas-Bericht (2020).

11. Frederix I, Caiani E, Dendale P, Anker S, Bax J, Böhm A, et al. ESC e-Cardiology Working Group Position Paper: overcoming challenges in digital health implementation in cardiovascular medicine. *Eur J Prev Cardiol.* (2019) 26:1166–77. doi: 10.1177/2047487319832394

12. Frederix I, Vandenberk T, Janssen L, Geurden A, Vandervoort P, Dendale P. eEduHeart I: a multicenter, randomized, controlled trial investigating the effectiveness of a cardiac web-based elearning platform – rationale and study design. *Cardiology.* (2017) 136:157–63. doi: 10.1159/000448393

13. Neubeck L, Cartledge S, Dawkes S, Gallagher R. Is there an app for that? Mobile phones and secondary prevention of cardiovascular disease. *Curr Opin Cardiol.* (2017) 32:567–71. doi: 10.1097/HCO.0000000000000428

14. Cornejo Müller A, Wachtler B, Lampert T. [Digital divide-social inequalities in the utilisation of digital healthcare]. *Bundesgesundheitsblatt Gesundheitsforschung Gesundheitsschutz.* (2020) 63:185–91. doi: 10.1007/s00103-019-03081-y

15. Initiative D21. *D21-Digital-Index 2021/2022. Jährliches Lagebild zur digitalen Gesellschaft [Annual report on the digital society]*. Berlin: Vertiefungsthema (2022).

16. Federal Statistical Office. *Average Gross Wages per Employee in East and West Germany from 1996 to 2020*. Wiesbaden: Federal Statistical Office (2022).

17. Wangler J, Jansky M. *Gesundheits-Apps in der hausarztbasierten Versorgung–Empirische Befunde zur Perspektive von Allgemeinmedizinern und Patienten. mHealth-Anwendungen für chronisch Kranke*. Berlin: Springer (2020). doi: 10.1007/978-3-658-29133-4_10

18. Creswell J, Klassen A, Plano Clark V, Smith K. *Best Practices for Mixed Methods Research in the Health Sciences*. Bethesda, MD: National Institutes of Health (2011). doi: 10.1037/e566732013-001

19. Craig P, Dieppe P, Macintyre S, Michie S, Nazareth I, Petticrew M, et al. Developing and evaluating complex interventions: the new Medical Research Council guidance. *BMJ.* (2008) 337:a1655. doi: 10.1136/bmj.a1655

20. O'Cathain A, Murphy E, Nicholl J. Three techniques for integrating data in mixed methods studies. *BMJ.* (2010) 341:c4587. doi: 10.1136/bmj.c4587

21. Hypertension Care. *Hypertonie.App*. Ingolstadt: Hypertension Care (2022).

22. Norman C, Skinner H. eHEALS: the eHealth literacy scale. *J Med Internet Res.* (2006) 8:e27. doi: 10.2196/jmir.8.4.e27

23. Soellner R, Huber S, Reder M. The concept of eHealth literacy and its measurement: German translation of the eHEALS. *J Media Psychol.* (2014) 26:29. doi: 10.1027/1864-1105/a000104

24. Sørensen K, Van den Broucke S, Pelikan J, Fullam J, Doyle G, Slonska Z, et al. Measuring health literacy in populations: illuminating the design and development process of the European Health Literacy Survey Questionnaire (HLS-EU-Q). *BMC Public Health.* (2013) 13:948. doi: 10.1186/1471-2458-13-948

25. Pelikan J, Röthlin F, Ganahl K. Measuring comprehensive health literacy in general populations: validation of instrument, indices and scales of the HLS-EU study. *Proceedings of the 6th Annual Health Literacy Research Conference*. Bethesda, MD (2014).

26. Schwarzer R. Modeling health behavior change: How to predict and modify the adoption and maintenance of health behaviors. *Appl Psychol.* (2008) 57:1–29. doi: 10.1111/j.1464-0597.2007.00325.x

27. Lippke S, Ziegelmann J, Schwarzer R, Velicer W. Validity of stage assessment in the adoption and maintenance of physical activity and fruit and vegetable consumption. *Health Psychol.* (2009) 28:183. doi: 10.1037/a0012983

28. Schauffel N, Schmidt I, Peiffer H, Ellwart T. Self-concept related to information and communication technology: Scale development and validation. *Comput Hum Behav Rep.* (2021) 4:100149. doi: 10.1016/j.chbr.2021.100149

29. Bangor A, Kortum P, Miller J. An empirical evaluation of the system usability scale. *Int J Hum–Comput Interact.* (2008) 24:574–94. doi: 10.1080/10447310802205776

30. Brooke J. SUS-A quick and dirty usability scale. *Usabil Eval Ind.* (1996) 189:4–7.

31. Arnet I, Metaxas C, Walter P, Morisky D, Hersberger K. The 8-item Morisky Medication Adherence Scale translated in German and validated against objective and subjective polypharmacy adherence measures in cardiovascular patients. *J Eval Clin Pract.* (2015) 21:271–7. doi: 10.1111/jep.12303

32. Morisky D, Ang A, Krousel-Wood M, Ward H. Predictive validity of a medication adherence measure in an outpatient setting. *J Clin Hypertens.* (2008) 10:348–54. doi: 10.1111/j.1751-7176.2008.07572.x

33. Kuckartz U. *Qualitative Inhaltsanalyse*. 4 Edn. Weinheim: Beltz Juventa (2018).

34. Onwuegbuzie A, Leech N. Validity and qualitative research: An oxymoron? *Qual Q.* (2007) 41:233–49. doi: 10.1007/s11135-006-9000-3

35. Tivian XI GmbH. *Online Survey Software: Surveys Made Easy With Unipark*. Cologne: Tivian XI GmbH (2021).

36. Kuper A, Lingard L, Levinson W. Critically appraising qualitative research. *BMJ.* (2008) 337:a1035. doi: 10.1136/bmj.a1035

37. Tromp J, Jindal D, Redfern J, Bhatt A, Séverin T, Banerjee A, et al. World heart federation roadmap for digital health in cardiology. *Global Heart.* (2022) 17:61. doi: 10.5334/gh.1141

38. Milani R, Lavie C, Bober R, Milani A, Ventura H. Improving hypertension control and patient engagement using digital tools. *Am J Med.* (2017) 130:14–20. doi: 10.1016/j.amjmed.2016.07.029

39. Albini F, Xiaoqiu L, Torlasco C, Soranna D, Faini A, Ciminaghi R, et al. An ICT and mobile health integrated approach to optimize patients' education on hypertension and its management by physicians: the Patients Optimal Strategy of Treatment(POST) pilot study. *Annu Int Conf IEEE Eng Med Biol Soc.* (2016) 2016:517–20. doi: 10.1109/EMBC.2016.7590753

40. Federal Statistical Office. *Population – Number of Inhabitants in the Federal States in Germany on December 31, 2021*. Wiesbaden: Federal Statistical Office (2022).

frontiers | Frontiers in Cardiovascular Medicine

TYPE Study Protocol
PUBLISHED 16 February 2023
DOI 10.3389/fcvm.2023.1133014

OPEN ACCESS

EDITED BY
Giuseppe Andò,
University of Messina, Italy

REVIEWED BY
Giovanni Luigi De Maria,
University of Oxford, United Kingdom
Vincenzo Sucato,
University of Palermo, Italy

*CORRESPONDENCE
Tommaso Gori
✉ tommaso.gori@unimedizin-mainz.de

SPECIALTY SECTION
This article was submitted to Clinical and Translational Cardiovascular Medicine, a section of the journal Frontiers in Cardiovascular Medicine

RECEIVED 28 December 2022
ACCEPTED 30 January 2023
PUBLISHED 16 February 2023

CITATION
Ullrich H, Olschewski M, Münzel T and Gori T (2023) Randomized, crossover, controlled trial on the modulation of cardiac coronary sinus hemodynamics to develop a new treatment for microvascular disease: Protocol of the MACCUS trial.
Front. Cardiovasc. Med. 10:1133014.
doi: 10.3389/fcvm.2023.1133014

Randomized, crossover, controlled trial on the modulation of cardiac coronary sinus hemodynamics to develop a new treatment for microvascular disease: Protocol of the MACCUS trial

Helen Ullrich[1,2], Maximilian Olschewski[1,2], Thomas Münzel[1,2] and Tommaso Gori[1,2]*

[1]Department of Cardiology, Cardiology I, University Medical Center Mainz, Mainz, Germany, [2]German Centre for Cardiovascular Research, Standort RheinMain, Mainz, Germany

Background: Microvascular angina (MVA) is a frequent condition for which our understanding of the disease pathophysiology and therapeutic perspectives remain unsatisfactory. The current study is designed to test whether an improvement in microvascular resistances could be achieved by elevating backward pressure in the coronary venous system, based on the hypothesis that an increase in hydrostatic pressure could cause a dilatation of the myocardial arterioles, resulting in a reduction of vascular resistances. This approach might have potential clinical implications, as it might suggest that interventions aimed at increasing coronary sinus (CS) pressure might result in a decrease in angina in this subset of patients. The aim of our single-center, sham-controlled, crossover randomized trial is to investigate the effect of an acute increase in CS pressure on a number of parameters of coronary physiology, including parameters of coronary microvascular resistance and conductance.

Methods and analysis: A total of 20 consecutive patients with angina pectoris and coronary microvascular dysfunction (CMD) will be enrolled in the study. Hemodynamic parameters including aortic and distal coronary pressure, CS and right atrial pressure, and the coronary microvascular resistance index will be measured at rest and during hyperemia in a randomized crossover design during incomplete balloon occlusion ("balloon") and with the deflated balloon in the right atrium ("sham"). The primary end point of the study is the change in index of microvascular resistances (IMR) after acute modulation of CS pressure, while key secondary end points include changes in the other parameters.

Discussion: The aim of the study is to investigate whether occlusion of the CS is associated with a decrease in IMR. The results will provide mechanistic evidence for the development of a treatment for patients with MVA.

Clinical trial registration: https://clinicaltrials.gov/, identifier NCT05034224.

KEYWORDS

coronary microvascular dysfunction, microvascular angina, arterial microcirculation, coronary sinus, fractional flow reserve

Introduction

Microvascular angina pectoris (MVA) is a complex clinical condition in which functional and/or structural changes in the coronary microcirculation result in an increased vascular tone. MVA is diagnosed as symptoms of ischemia with objective evidence of impaired coronary microvascular function [e.g., an index of microvascular resistance (IMR) > 25] in the absence of obstructive epicardial disease (1, 2). While the clinical attention and academic interest in this field is growing, the mechanisms behind its pathophysiology and the therapeutic alternatives available remain incompletely investigated (3). Despite these uncertainties, there is a consensus that this condition is clinically relevant as it affects up to two-thirds of patients who suffer from stable angina and either have no epicardial coronary stenosis at angiography or have combined epicardial and microvascular disease (4).

Microvascular angina caused by a dysfunctional microvascular bed cannot be treated by standard revascularization therapies and the pharmacological strategies (e.g., nitrates, calcium channel blockers, ranolazine) available also provide limited benefit. As well, while pressure-controlled intermittent coronary sinus occlusion has been shown to improve microvascular resistances in the setting of acute myocardial infarction (5), there is little evidence that interventions may improve microvascular resistances in patients with chronic coronary syndromes.

As a possible alternative to pharmacological agents, the hypothesis of improving myocardial perfusion by diverting blood from the coronary venous system to an ischemic region ("venous retroperfusion") has again gained attention during recent years. This therapy is based on the concept that an elevation in backward pressure in the coronary venous system provokes dilatation of the subendocardial arterioles, resulting in a relative reduction of vascular resistance in this area and a redistribution of blood flow to the ischemic subendocardial layers (6–8). Numerous studies confirm the efficacy of this approach for the therapy of patients who have angina and are not candidates for "traditional" revascularization (6). The study presented here aims to investigate the effect of an increase in coronary sinus pressure on microvascular function, a potentially new therapeutic concept.

Abbreviations: CFR, coronary flow reserve; CS, coronary sinus; FFR, fractional flow reserve; IMR, index of microvascular resistances; LAD, left anterior descending; MVA, microvascular angina; Pa, pressure, aortic; Pd, pressure, distal; Tmn, mean transit time.

Materials and methods

Overview

We investigate whether an increase in coronary sinus pressure leads to a change in coronary microvascular resistances in patients with angina pectoris due to microvascular dysfunction.

Study design

The study is a sham-controlled, crossover, randomized trial to investigate the effect of changes in coronary venous pressure on microvascular resistances. The hypothesis of the study is that occlusion of the coronary sinus (CS) will be associated with a decrease in the index of microvascular resistances (IMR). The protocol complies with good clinical practice and the ethical principles described in the Declaration of Helsinki and has been approved by the local ethics committee. All patients will provide written informed consent before enrollment.

Study population

Patients must meet all of the following inclusion criteria: chronic coronary syndrome (including patients with anginal equivalents); reversible ischemia on non-invasive testing; absence of epicardial stenosis that are compatible with the symptoms and the evidence of ischemia; evidence of microvascular dysfunction as demonstrated by an IMR $\geq$ 25; willingness to participate and ability to understand, read, and sign the informed consent; age > 18 years.

Patients will be excluded from eligibility for study enrollment if any of the following criteria applies: previous coronary artery bypass graft (CABG) with patent graft to the left anterior descending coronary (LAD) such that IMR cannot be measured; epicardial coronary disease (FFR < 0.80 with evidence of a focal stenosis) in the LAD territory; second and third degree atrioventricular block; severe valvular heart disease; any cardiomyopathy; pulmonary or renal disease; inability to provide informed consent; any disease reducing life expectancy. Patients unable to understand the scope of the study are classified as not able to give informed consent and are excluded for eligibility for study enrollment. Likewise, patients unable to consent, e.g., for a neurological damage, are treated as not able to give informed

consent and are excluded for eligibility for study enrollment (Table 1).

Procedures

Recruitment

Patients will be enrolled among those treated at the Department of Cardiology, Cardiology I of the University Medical Centre Mainz or, eventually, cooperating centers.

Randomization

Microvascular function measurements will be made (both at rest and during hyperemia) twice in each patient in a sham-controlled, randomized, crossover design. Randomization will be performed after informed consent and if all inclusion criteria and no exclusion criteria are met. Patients will be randomized 1:1 to one of the two study arms (sham/balloon or balloon/sham) (Figure 1). After the first set of rest/hyperemia measurements in the first condition (balloon or sham, Figure 1), and a 10 min waiting time, patients will cross-over to the other condition (sham or balloon) and the measurements (rest/hyperemia) will be repeated.

For the measurements during balloon inflation, incomplete CS occlusion will be achieved with a Swan-Ganz catheter advanced into the CS with access through the femoral or jugular vein. The position of the balloon will be chosen in order to cause a ∼80–90% CS lumen reduction while maintaining stability throughout the measurements. For the sham measurements, the balloon will be kept deflated in the right atrium. Randomization will be done by a computer-generated random sequence (MedCalc, Ostend, Belgium).

Hemodynamic measurements

Coronary angiography and microvascular function assessments will be performed in the left anterior descending coronary artery using the wire-based thermodilution method. Five to seven thousand international units of intravenous heparin and intracoronary nitrates will be administered before measurements when systolic blood pressure is above 100 mmHg systolic. A guiding catheter will be advanced to the ostium of the left coronary. A pressure wire (Pressure Wire X; Abbott Vascular, Santa Clara, CA, United States) equipped with pressure sensor and thermistor will be advanced placed approximately 8 cm into the LAD after ostial equalization. Maximal hyperemia will be induced through intravenous adenosine (140 $\mu g \cdot kg^{-1} \cdot min^{-1}$) or, in patients with asthma, intracoronary papaverine (10 mg). The distal sensor of the pressure wire will be kept in the same position and the same hyperemic agent will be used for the two sets of measurements (sham and balloon). For the assessment of the mean transit time (Tmn) and IMR, 3 boli of 3 ml room-temperature saline will be injected briskly into the guiding catheter as per instructions for use. The presence of drift will be checked at the end of the measurements. All assessments will be performed using the CoroFlow software (Coroventis, Uppsala, Sweden).

Trial endpoints

The primary analysis will be on the per-protocol principle (i.e., including all patients who are not protocol violators).

Primary endpoint: change in IMR during inflation of the CS balloon as compared to sham.

Key secondary endpoints: changes in the following physiological parameters

1. Aortic (Pa) and distal coronary pressure (Pd) at rest and during hyperemia (aortic and coronary pressure);
2. Pressure in the right atrium (Pra) and in the coronary sinus (Pcs);
3. RFR (resting flow ratio);
4. FFR calculated as Pd/Pa and as (Pd-Pcs)/(Pa-Pcs);
5. Tmn (transit mean time) at rest and during hyperemia, average of the three boli;
6. CFR: coronary flow reserve;
7. IMR calculated as $[(P_d - CS) \times T_{mn}]$ and using the standard formula (IMRst = $P_d \times T_{mn}$). CFR is the ratio of baseline T_{mn}/hyperaemic T_{mn}.

Safety

All measurements (including hemodynamic measurements) are applied as clinically indicated and according to CE certificate

TABLE 1 In- and exclusion criteria.

Inclusion criteria (ALL)	Exclusion criteria (ANY)
• Chronic coronary syndrome (including patients with anginal equivalents)	• Previous CABG with patent grafts such that IMR cannot be measured
• Reversible ischemia on non-invasive testing	• Epicardial coronary disease (FFR < 0.80 with evidence of a focal stenosis) in the LAD territory
• Evidence of microvascular disease with IMR = 25	• Second and third degree atrioventricular block
• Willingness to participate and ability to understand, read, and sign the informed consent	• Severe valvular heart disease
• Age > 18 years	• Any cardiomyopathy
	• Pulmonary or renal disease
	• Inability to provide informed consent
	• Any disease reducing life expectancy

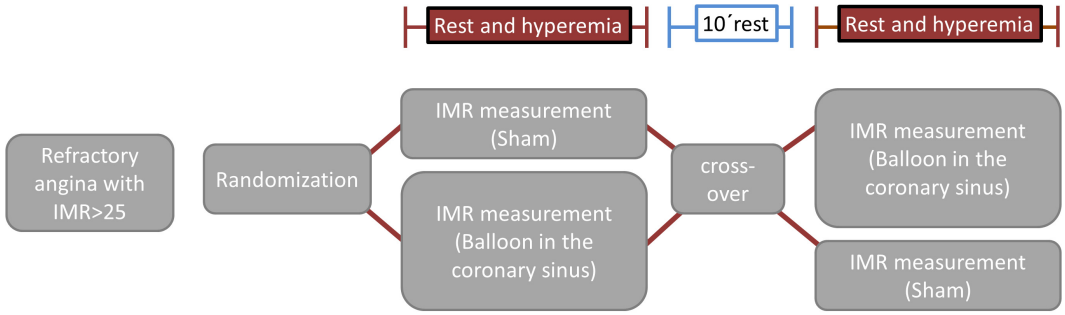

FIGURE 1
Randomization.

and the instruction for use. Vascular access is performed using the femoral or jugular vein; the expansion of the balloon is incomplete and performed using low pressure (2–4 ATM). The risk of trauma is thereby minimal. Thus, it is not to be expected that the participation in the study will lead to unneeded or harmful therapeutic interventions.

Statistics

Statistical analysis will be performed with MedCalc (Ostend, Belgium).

Power calculation

The study is powered for the primary efficacy endpoint IMR. In the OxAMI-PICSO study (5), PICSO reduced the IMR in patients with no reflow after ST-elevation myocardial infarction from 45 [22–51] to 25 [19–36]. In unselected coronary artery disease patients, Mangiacapra et al. (9) reported a decrease in IMR from 27 ± 11 to 19 ± 9 after intracoronary enalaprilat; Suda et al. (10) reported a decrease in IMR from ∼28[21–35] to ∼19[17–23] ($P < 0.0001$, median decrease ∼35%) in response to fasudil. Luo (11) reported baseline IMR of 33 units in patients with microvascular dysfunction (i.e., our expected population), with a baseline SD of 7.6 units. When assuming a baseline IMR of 33 and conservatively using the pooled baseline SD of IMR 13 units of both treatment groups from Mangiacapra, and assuming a similar effect as that observed in the papers by Mangiacapra and Suda, this will result in an effect size of ∼0.69 (∼9/13). With this effect size and a power of 80%, 19 patients are needed. In case of missing data, this sample size could be increased to 25.

Statistical analysis

The primary analysis will be done for the IMR measurement. The primary hypothesis is H0: μExp = μSham, vs. H1: μExp ≠ μSham, where μExp and μSham are the expected values of the IMR with experimental intervention (balloon) and sham. The primary analysis will be performed as within-subject comparison of the primary parameter. Statistical tests and effect estimates will be calculated using the Wilcoxon test. The effect of randomization and baseline measurements as covariates will be investigated. No treatment by time interaction is expected because the balloon from the experimental intervention will produce a transient increase in CS pressure which will normalize upon deflation. The primary comparison will be performed at a two-sided significance level of $\alpha = 0.05$. Treatment differences will be displayed by adjusted estimates and 95% confidence intervals. Bias is minimized by randomized sequence allocation. The randomization ratio of the treatment sequences will be 1:1 without any stratification factors. Randomization with permuted blocks will be applied.

Data management

Patient data will be pseudonymized and collected by the study team. Pseudonymized patient data will be stored digitally on an external hard-drive not connected to the clinical intranet and only accessible to the members of the study team. After 10 years of storage, data will be destroyed. It is not intended to give study participants' data to a third party. All data will be analyzed after the last patient is discharged from index hospitalization. No interim analysis is intended. However, a Data Safety Monitoring Board consisting of two physicians not affiliated with the study will monitor the safety of the subjects throughout the study. In case a study participant withdraws consent after having his data collected from him, the patient's data will be anonymized.

Ethics and publication policy

The protocol has been approved by the local state medical association's ethics committee. In accordance with the WMA Declaration of Helsinki–Ethical Principles for Medical Research Involving Human Subjects, researchers, authors, sponsors, editors, and publishers all have ethical obligations with regard to the publication and dissemination of the results of research. Researchers have a duty to make publicly available the results of their research on human subjects and are accountable for the completeness and accuracy of their reports. All parties should adhere to accepted guidelines for ethical reporting. Negative and inconclusive as well as positive results must be published or otherwise made publicly available. Sources of funding, institutional affiliations and conflicts of interest must be declared in the publication. Reports of research not in accordance with the principles of this Declaration should not be

accepted for publication. The PI of this study, recognizing the seminal importance of this investigation, is committed to the unrestricted and widespread dissemination of all primary and secondary endpoint results and tertiary analyses. At the conclusion of the study, an abstract reporting the primary results will be prepared by the Principal Investigators and presented at an annual scientific meeting. A publication will similarly be prepared for publication in a reputable scientific journal. Following analysis and presentation of the primary endpoint results, active participation of all study group members will be solicited for data analysis and abstract and manuscript preparation and therefore included as co-authors. Submission of all abstracts and publications regarding the primary endpoint and secondary endpoints from the study requires approval by the Principal Investigators after review by all members of the study group.

Insurance

Since all procedures (except for randomization) are clinically indicated and acknowledged in the current literature, a study insurance is not planned.

Trial status

Data collection is ongoing.

Financing

The study will be financed by own means of the Department of Cardiology of the University Medical Center Mainz (=Sponsor) and means of the W3-Professorship of Translational myocardial and cardiovascular function. Additionally, the research project will be supported by the Clinician Scientist program of Helen Ullrich, which was granted by the German Centre for Cardiovascular Research (DZHK).

Discussion

To assess coronary circulatory function, three different physiological indexes were measured in the present study. FFR is defined as the ratio of maximal coronary blood flow in a diseased artery to maximal coronary blood flow in the same artery without stenosis. FFR is a surrogate marker of inducible myocardial ischemia caused by epicardial coronary stenosis (12). CFR is the ratio of hyperemic to baseline flow and is a marker of the integrity of both epicardial and microvascular domains of coronary circulation. Therefore, CFR represents the microvascular status when there is no significant epicardial disease. IMR is the minimum achievable coronary microcirculatory resistance and a more specific marker of the coronary microcirculation than CFR. It is calculated as the ratio of distal coronary pressure to coronary flow at hyperemia and presented in unit.

Approximately half of patients undergoing diagnostic coronary angiography for typical angina symptoms do not have significant obstructive coronary stenoses (10). This large number of patients rarely receive a definitive diagnosis, are often inappropriately labeled, and by and large remain symptomatic (13). Half of these patients suffer from CMD. The disease is associated with higher rates of serious cardiovascular events, making identification of CMD a therapeutic target with unmet needs (13). In this context, MVA still represents an underestimated clinical challenge, which, however, is increasingly proving to be an important factor in cardiac prognosis (14). In their prospective study, Suda et al. (10) showed that coronary functional abnormalities, including epicardial coronary spasm, decreased microvascular vasodilation, and increased microvascular resistance, frequently coexist in patients with angina and non-obstructive coronary artery disease. Here, the IMR correlated with the occurrence of severe cardiovascular events, and an IMR of 18.0 turned out to be the best cut-off value. Our randomized and sham-controlled trial investigates the acute effect of increasing coronary sinus pressure on microvascular resistance in patients with MVA. Our hypothesis states that occlusion of the CS is associated with a decrease in IMR. This retrograde treatment approach to myocardial ischemia through the coronary venous system has been studied in the past in the context of acute coronary syndrome, coronary revascularization, and cardiothoracic surgery (15). Several small studies support the approach that occlusion of the CS may preserve ischemic myocardium and improve microvascular perfusion and function (5, 12, 15, 16). In this context, the results of our work may provide evidence for a possible new therapeutic strategy.

Initial evidence from animal studies and a series of patients appears to support the hypothesis that coronary sinus occlusion (CSO) improves microvascular function: Ido et al. (15) demonstrated that CSO lead to dilatation of the subendocardial arterioles, resulting in a significant reduction of vascular resistance in this area and a redistribution of blood flow to these ischemic subendocardial layers. In a small case series by Giannini et al. (16), patients with microvascular angina showed a clinical improvement after CSO, an effect similar to that shown in the randomized, sham-controlled trial COSIRA (12) (improvement of 2 Canadian cardiovascular society angina classes in 35% of the patients). In the paper by de Maria et al. (5), percutaneous-intermittent CSO (PICSO) improved microvascular perfusion and resistances in patients with no reflow after ST-elevation myocardial infarction. Finally, we recently provided mechanistic evidence that CSO might improve microvascular function in a patient with evidence of severe CMD: in a recent publication (Gori T, Eurointervention online), we described a case of a patient with MVA that benefited from the implantation of the coronary sinus reducer device. This 61-year old patient with a history of insulin-dependent diabetes, hypertension, and multiple PCIs underwent implantation of the coronary sinus reducer for chronic angina refractory to maximal therapy. His symptoms included a CCS III angina leading to 4 hospitalizations in the 6 months before the sinus reducer implantation. In order to better understand the pathophysiology of his symptoms, a full hemodynamic assessment was performed. The fractional flow reserve (FFR) in the left anterior descending (LAD) was 0.87, witnessing the absence of epicardial disease. In contrast, the index of microvascular resistances (IMR) was 63, documenting increased microvascular resistances as a mechanism of his symptoms. Based

on this evidence, and on compassionate grounds, a coronary sinus reducer was implanted. After implantation, the "trans-sinus" gradient was 3mmHg. FFR and resting full-cycle ratio (RFR) were unchanged (0.93 and 0.85), but IMR dropped to 37. Since implantation (currently 12 months follow-up at the time of this writing), the patient has never been admitted again to hospital and is symptom-free.

Although this is just preliminary data, they suggest that the redistribution of blood from the subepicardial to the subendocardial space might be associated with a drop in total microvascular resistances and therefore relief of symptoms.

Our study has several limitations. First, the present study is a mechanistic study conducted exclusively at one center. In addition, only a relatively small number of patients will be enrolled in each of the two study groups. Furthermore, we only studied the effect of a single occlusion of the CS on microvascular function. Repeated CSO as well as a permanent CSO could alter the effects of a single CSO (15). Larger studies with follow-up periods are needed to build on the results and to investigate the role of potential new therapeutic strategies.

Author contributions

HU and TG wrote the first draft. All authors provided critical appraisal and corrections and approved the submitted version.

Funding

TG was principal investigator of the DZHK, funded by the Ministry of Research, Germany. HU was supported by a grant from the DZHK.

Conflict of interest

TG received speaker fees and grant support from Abbott Vascular, Neovasc, Boston Scientific, Bayer, Astra Zeneca, SMT (not in relationship with this research).

The remaining authors declare that the research was conducted in the absence of any commercial or financial relationships that could be construed as a potential conflict of interest.

Publisher's note

References

1. Knuuti J, Wijns W, Saraste A, Capodanno D, Barbato E, Funck-Brentano C, et al. 2019 ESC Guidelines for the diagnosis and management of chronic coronary syndromes. *Eur Heart J.* (2020) 41:407–77.

2. Beltrame J, Crea F, Kaski J, Ogawa H, Ong P, Sechtem U, et al. International standardization of diagnostic criteria for vasospastic angina. *Eur Heart J.* (2017) 38:2565–8.

3. Suzuki H. Different definition of microvascular angina. *Eur J Clin Invest.* (2015) 45:1360–6. doi: 10.1111/eci.12552

4. Villano A, Lanza G, Crea F. Microvascular angina: prevalence, pathophysiology and therapy. *J Cardiovasc Med.* (2018) 19(Suppl. 1):e36–9. doi: 10.2459/JCM.0000000000000638

5. De Maria G, Alkhalil M, Borlotti A, Wolfrum M, Gaughran L, Dall'Armellina E, et al. Index of microcirculatory resistance-guided therapy with pressure-controlled intermittent coronary sinus occlusion improves coronary microvascular function and reduces infarct size in patients with ST-elevation myocardial infarction: the oxford acute myocardial infarction - pressure-controlled intermittent coronary sinus occlusion study (OxAMI-PICSO study). *EuroIntervention.* (2018) 14:e352–9. doi: 10.4244/EIJ-D-18-00378

6. Konigstein M, Giannini F, Banai S. The reducer device in patients with angina pectoris: mechanisms, indications, and perspectives. *Eur Heart J.* (2018) 39:925–33. doi: 10.1093/eurheartj/ehx486

7. Sandler G, Slesser B, Lawson C. The beck operation in the treatment of angina pectoris. *Thorax.* (1967) 22:34–7. doi: 10.1136/thx.22.1.34

8. Beck C, Leighninger D. Scientific basis for the surgical treatment of coronary artery disease. *J Am Med Assoc.* (1955) 159:1264–71. doi: 10.1001/jama.1955.02960300008003

9. Mangiacapra F, Peace A, Di Serafino L, Pyxaras S, Bartunek J, Wyffels E, et al. Intracoronary EnalaPrilat to reduce MICROvascular damage during percutaneous coronary intervention (ProMicro) study. *J Am Coll Cardiol.* (2013) 61:615–21. doi: 10.1016/j.jacc.2012.11.025

10. Suda A, Takahashi J, Hao K, Kikuchi Y, Shindo T, Ikeda S, et al. Coronary functional abnormalities in patients with angina and nonobstructive coronary artery disease. *J Am Coll Cardiol.* (2019) 74:2350–60. doi: 10.1016/j.jacc.2019.08.1056

11. Luo C, Long M, Hu X, Huang Z, Hu C, Gao X, et al. Thermodilution-derived coronary microvascular resistance and flow reserve in patients with cardiac syndrome X. *Circ Cardiovasc Interv.* (2014) 7:43–8. doi: 10.1161/CIRCINTERVENTIONS.113.000953

12. Verheye S, Jolicśur E, Behan M, Pettersson T, Sainsbury P, Hill J, et al. Efficacy of a device to narrow the coronary sinus in refractory angina. *N Engl J Med.* (2015) 372:519–27. doi: 10.1056/NEJMoa1402556

13. Rahman H, Corcoran D, Aetesam-Ur-Rahman M, Hoole S, Berry C, Perera D. Diagnosis of patients with angina and non-obstructive coronary disease in the catheter laboratory. *Heart.* (2019) 105:1536–42. doi: 10.1136/heartjnl-2019-315042

14. Sara J, Widmer R, Matsuzawa Y, Lennon R, Lerman L, Lerman A. Prevalence of coronary microvascular dysfunction among patients with chest pain and nonobstructive coronary artery disease. *JACC Cardiovasc Interv.* (2015) 8:1445–53. doi: 10.1016/j.jcin.2015.06.017

15. Ido A, Hasebe N, Matsuhashi H, Kikuchi K. Coronary sinus occlusion enhances coronary collateral flow and reduces subendocardial ischemia. *Am J Physiol Heart Circ Physiol.* (2001) 280:H1361–7. doi: 10.1152/ajpheart.2001.280.3.H1361

16. Giannini F, Baldetti L, Ielasi A, Ruparelia N, Ponticelli F, Latib A, et al. First experience with the coronary sinus reducer system for the management of refractory angina in patients without obstructive coronary artery disease. *JACC Cardiovasc Interv.* (2017) 10:1901–3. doi: 10.1016/j.jcin.2017.06.062

frontiers | Frontiers in Cardiovascular Medicine

TYPE Study Protocol
PUBLISHED 23 February 2023
DOI 10.3389/fcvm.2023.1003546

OPEN ACCESS

EDITED BY
Tommaso Gori,
Johannes Gutenberg University Mainz,
Germany

REVIEWED BY
Peiren Shan,
First Affiliated Hospital of Wenzhou Medical University,
China
Ankush Gupta,
Army Institute of Cardiothoracic Sciences (AICTS), India

*CORRESPONDENCE
Yao-Jun Zhang
13770668667@139.com

†These authors have contributed equally to this work

SPECIALTY SECTION
This article was submitted to Coronary Artery Disease, a section of the journal Frontiers in Cardiovascular Medicine

RECEIVED 26 July 2022
ACCEPTED 06 February 2023
PUBLISHED 23 February 2023

CITATION
Zhu Y-X, Liang L, Parasa R, Li Z, Li Q, Chang S, Ma W-R, Feng S-L, Wang Y, Xu B, Bourantas CV and Zhang Y-J (2023) Early vascular healing after neXt-generation drug-eluting stent implantation in Patients with non-ST Elevation acute Coronary syndrome based on optical coherence Tomography guidance and evaluation (EXPECT): study protocol for a randomized controlled trial. *Front. Cardiovasc. Med.* 10:1003546. doi: 10.3389/fcvm.2023.1003546

Early vascular healing after neXt-generation drug-eluting stent implantation in Patients with non-ST Elevation acute Coronary syndrome based on optical coherence Tomography guidance and evaluation (EXPECT): study protocol for a randomized controlled trial

Yong-Xiang Zhu[1†], Li Liang[1†], Ramya Parasa[2,3†], Zheng Li[1], Qian Li[1], Shang Chang[1], Wen-Rui Ma[1], Si-Li Feng[1], Yang Wang[4], Bo Xu[4], Christos V. Bourantas[2,3] and Yao-Jun Zhang[1*]

[1]Department of Cardiology, Xuzhou Third People's Hospital, Xuzhou Medical University, Xuzhou, China, [2]Department of Cardiology, Barts Heart Center, Barts Health NHS Trust, London, United Kingdom, [3]Cardiovascular Devices Hub, Centre for Cardiovascular Medicine and Devices, William Harvey Research Institute, Queen Mary University of London, London, United Kingdom, [4]Fuwai Hospital, National Center for Cardiovascular Diseases, Chinese Academy of Medical Sciences and Peking Union Medical College, Beijing, China

Background: There is limited evidence about vessel wall healing response following implantation of next-generation drug-eluting stents (DES) in patients admitted with a non-ST elevation acute coronary syndrome (NSTE-ACS). Cumulative data indicate that optical coherence tomography (OCT) imaging can optimize percutaneous coronary intervention results and expedite stent endothelialization in the general population but there is lack of data in NSTE-ACS patients.

Methods: The EXPECT study is an investigator-initiated, prospective, randomized trial to assess early vascular healing response following next-generation DES implantation in patients admitted with NSTE-ACS based on OCT guidance and evaluation. Sixty patients are randomized at 1:1:1 ratio to OCT-guided percutaneous coronary intervention (PCI) with 3-month follow-up OCT imaging (O3 group, n=20), to angiography-guided PCI with 3-month follow-up OCT imaging (A3 group, n=20) and to angiography-guided PCI with 6-month follow-up OCT imaging (A6 group, n=20). The primary endpoint of the study is stent strut coverage rate at 3- or 6- month follow-up in the studied groups. The secondary endpoints of the study include OCT imaging endpoints, clinical endpoints, and molecular biology endpoints at the different time points. The clinical endpoints comprised of major cardiovascular adverse events and individual components. The molecular biology endpoints comprised of lipid levels and the levels of inflammatory indicators.

Discussion: The findings of the EXPECT study are anticipated to provide novel insights into vessel wall healing in NSTE-ACS population following implantation of next-generation DES, underscore the value of OCT imaging in expediting strut

coverage in this setting, and explore the potential of an early discontinuation of dual antiplatelet therapy (DAPT) in this population.

Clinical Trial Registration: ClinicalTrials.gov, NCT04375319.

KEYWORDS

non-ST elevation acute coronary syndrome, optical coherence tomography, percutaneous coronary intervention, early vascular healing, stent struts coverage

Introduction

Over the past few decades, percutaneous coronary intervention (PCI) has significantly improved clinical outcomes in acute coronary syndrome (ACS) patients. The improved prognosis in this high-risk population has been at least partially attributed to enhanced medical therapy, the broad use of PCI as well as to the introduction of the second-generation drug-eluting stents (DES) that have increased efficacy and high safety profile (1). Current guidelines recommend treatment with dual antiplatelet therapy (DAPT) for 1 year after PCI regardless of stent types (2, 3). However, long-term DAPT may increase the risk of bleeding in the elderly, frail patients and those prone to bleeding with hematological, gastro intestinal, and liver pathologies. DAPT is also associated with a risk of serious bleeding in vulnerable patients with history of falls, previous hemorrhagic cerebrovascular events and can be a limiting factor in patients awaiting elective surgery. In the era of next-generation DES, large-scale randomized studies and meta-analyses have demonstrated that the duration of DAPT can be shortened to 6 months or even to 3 months with no clinical consequences while recent studies currently examine the safety and efficacy of aspirin single antiplatelet therapy post stent implantation (4–7).

In patients admitted with non-ST elevation acute coronary syndrome (NSTE-ACS) that have complex and highly thrombotic lesions, shorter-term DAPT can be considered only in cases of early strut coverage which constitutes a marker of early endothelialization (8). Indeed, cumulative data have underscored the prognostic implications of incomplete strut coverage indicating that this is associated with a high incidence of stent thrombosis (ST) (9) and future major adverse cardiovascular events (MACE) (10–12).

The introduction of optical coherence tomography (OCT) enabled *in vivo* assessment of strut coverage and allow us to calculate vascular repair index (13) and to identify predictors associated with a delayed vessel wall healing. In particular, stent design (i.e., stent polymer, stent strut thickness, and drug elution), strut embedment and apposition, the composition of the underlying plaque, and the time interval between stent implantation and follow-up imaging seem to determine strut coverage (14). Moreover, several studies have shown that in patients with NSTE-ACS the incidence of incomplete strut apposition is greater than in patients with a chronic coronary syndrome while the recently published study (8) has shown that the use of OCT during next-generation stent implantation is associated with a higher incidence of stent embedment and faster endothelialization comparing to angiography-guided PCI. However, most of the recruited patients in this study were suffering from a stable angina. The present investigator-initiated, prospective, randomized trial was designed to investigate the vessel wall healing response following implantation of a next-generation DES with low dose sirolimus elution in NSTE-ACS population and to explore the value of OCT imaging in expediting strut endothelialization.

Methods and analysis

Study design

The EXPECT study is an investigator-initiated, prospective, multicenter, randomized clinical trial (www.clinicaltrials.gov, NCT04375319). The objective of this study is to evaluate vessel wall healing response over time in NSTE-ACS patients receiving a next-generation DES implantation, and to examine the value of OCT-guided PCI in expediting stent strut coverage, aiming to underscore the potential of a lower duration DAPT in high bleeding risk population.

Patient enrollment and randomization

Sixty patients with NSTE-ACS (includes unstable angina pectoris and non-ST segment elevation myocardial infarction) from three centers in Huaihai economic zone (Supplementary Table S1) will be enrolled in this trial. The main inclusion and exclusion criteria are listed in Tables 1, 2, respectively.

The recruited patients will be randomized at 1:1:1 ratio to three groups using a computer-generated random sequence table. Patients

TABLE 1 Inclusion criteria.

1. Male or non-pregnant female aged 18–80 years.
2. Clinical diagnosis of acute non-ST segment elevation myocardial infarction.
3. *De novo* coronary artery lesions. Multiple target lesions should be located in different epicardial vessels.
4. Each target lesion should have a length ≤ 40 mm, and diameter between 2.5–4.5 mm by visual assessment.
5. Target lesion with ≥70% diameter stenosis or ≥ 50% diameter stenosis with myocardial ischemia evident by functional assessment.
6. Each patient is allowed to undergo a maximum of three stent implantations, if necessary (except for bailout stent implantation), each target lesion is allowed to be stented with a maximum of two stents.
7. The coronary anatomy is amenable to PCI.
8. Ability to understand the trial purpose, sign informed consent, and have good compliance with medications.

PCI, percutaneous coronary intervention.

enrolled in the first group will have OCT-guided revascularization and 3-month follow-up OCT imaging (O3 group, $n = 20$), those in the second group angiography-guided PCI and 3-month follow-up OCT imaging (A3 group, $n = 20$) while the patients recruited in the third group angiography-guided PCI and 6-month follow-up OCT imaging (A6 group, $n = 20$).

Treatment device

All the recruited patients will be implanted with Excrossal (JW Medical Systems, Shandong, China) stent, a novel next-generation sirolimus-eluting stent with a cobalt-chromium alloy and a biodegradable polymer. The dose of sirolimus in this device is reduced to 1/3 of the former product used while the polymer consists of biodegradable polylactic acid. Following stent implantation, the polymer coating degrades into lactic acid, which expedites vascular healing process while the low dose sirolimus elution provides the advantage of accelerating endothelialization without affecting the rate of restenosis (15, 16).

Treatment and follow-up procedures

In the OCT-guided group, OCT imaging will be performed before PCI to appropriately size stent implantation and following stenting to assess the final results and guide further optimization if needed. A final run will be performed at the end of the procedure to confirm optimal results and exclude common causes of stent failure reported in the literature (17). Patients will be given DAPT (oral aspirin 100 mg once daily, clopidogrel 75 mg once daily, or ticagrelor 90 mg twice daily) and will be put on secondary prevention medications according to the recommended ESC guidelines.

Post discharges all patients will have a follow-up appointment or will be contacted by phone at 1 month, 3 months, 6 months, and 1 year. Subjects assigned to O3/A3 arms will undergo coronary angiography and OCT imaging at 3 months, while those assigned to A6 arm will have invasive assessment and OCT imaging at 6 months after the index procedure (Figure 1). The schedule of enrolment, interventions, and assessments is outlined in Figure 2. The data of each center will be summarized and checked by an independent data monitoring committee.

TABLE 2 Exclusion criteria.

1. Acute ST segment elevation myocardial infarction within the past 1 month.
2. Chronic total occlusive lesion, severe left main stem stenosis, lesions with length > 40 mm, bifurcation lesion requiring double stenting, target vessel diameter > 4.5 mm, and vessels unsuitable for OCT imaging such as severely tortuous vessels and vessels with severe dissection, current infection or any active inflammatory diseases.
3. Non interpretable OCT images.
4. Severe calcific lesions that require treatment with debulking techniques.
5. In stent restenosis lesions.
6. Hemodynamic instability such as cardiogenic shock, or left ventricular ejection fraction <40% (by echocardiography or left ventriculography).
7. Renal impairment: eGFR < 60 ml/(min·1.73 m^2) or serum creatinine>2.5 mg/dL (178 μmol/L), or patients on hemodialysis.
8. Bleeding tendency, history of active peptic ulcer, history of cerebral hemorrhage or subretinal hemorrhage, history of stroke within the past half year, or contraindications for antiplatelet or anticoagulant treatment.
9. Allergy to antithrombotic medications, contrast agent, or Cobalt Chromium.
10. Life expectancy less than 12 months.
11. Participation in other clinical trial.
12. Poor compliance, unable to provide written informed consent.
13. Heart transplantation.
14. Undergoing chemotherapy or immunosuppressive therapy.
15. Elective surgery requiring stopping anti-platelet therapy within half a year post stent implantation.
16. Platelet count lower than 100×10^9/L, or more than700×10^9/L, and white blood cell lower than 3×10^9/L, liver diseases (such as hepatitis).

OCT, optical coherence tomography; eGFR, estimated glomerular filtration rate

Blood sample measurement

Blood samples (4–5 mL) will be collected from all subjects prior to the procedure and at 12–24 h after the procedure. Blood samples will be also collected at 3 and 6 months follow up. The samples will be centrifuged at 3,000 r/min for 10 min, and the serum obtained will be isolated and stored at −80°C. Serum levels of total cholesterol (TC), low-density lipoprotein (LDL-C), high-density lipoprotein (HDL-C), and triglyceride (TG) will be measured by automatic biochemical analyzer, the pentraxins 3 (PTX-3), vascular cell adhesion molecule 1 (VCAM-1), and matrix metalloproteinase 9 (MMP-9) by enzyme-linked immunosorbent assay, and the high-sensitivity C-reactive protein (hs-CRP) detected by the immune turbidity method.

QCA and OCT data acquisition and analysis

Intracoronary nitrate will be administered prior to diagnostic angiography in all the recruited patients unless contraindicated due to

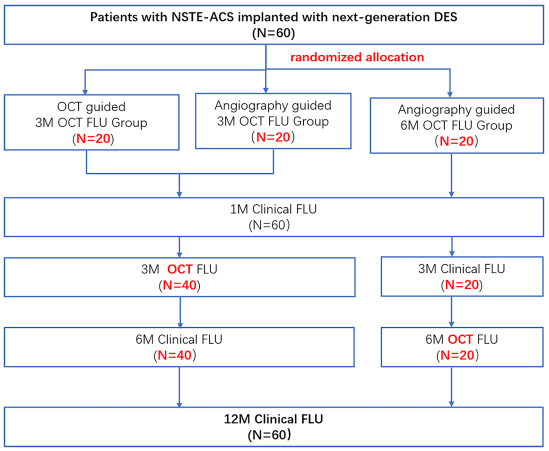

FIGURE 1
Study flow chart. NSET-ACS, non-ST elevation acute coronary syndrome; OCT, optical coherence tomography; FLU, follow up; 3 M, 3-month; 6 M, 6-month; and 12 M, 12-month.

project	Admission and treatment				follow-up			
Time point	Screen	During procedure	12-24 hours post-procedure	discharge	1-month	3-month	6-month	12-month
Window period					±7d	±7d	±14d	±30d
Informed consent	X							
Inclusion criteria	X							
Exit criteria		X	X	X	X	X	X	X
Patient's characteristics	X					X	X	
Pregnancy test	X							
Physical examination	X					X	X	
Vital signs		X		X		X	X	
Routine blood, urine and feces	X			X		X	X	
Blood biochemistry	X			X		X	X	X
Creatine Kinase/Creatine Kinase-MB	X		X			X	X	
Troponin	X		X			X	X	
Clinical evaluation		X						
ECG	X		X	X		X	X	X
Echocardiography	X					X	X	X
CCS classification	X			X	X	X	X	X
Anticoagulant / antiplatelet agents	X	X	X	X	X	X	X	X
Other drugs	X	X	X	X	X	X	X	X
OCT		X				X	X	
QCA		X				X	X	
Cardiovascular clinical event record				X	X	X	X	X
Adverse event record		X	X	X	X	X	X	X

FIGURE 2
Time schedule of enrolment, interventions, and assessments of the study. ECG, electrocardiogram; CCS, Canadian cardiovascular society; OCT, optical coherence tomography; and QCA: quantitative coronary angiography.

low blood pressure. Antithrombotic therapy will be administered according to the local protocol prior to insertion of a guidewire in the coronary arteries.

In the angiography-guided group, stent implantation will be performed and optimized with angiography guidance according to local standard practice based on operator's visual assessment (stent to artery ratio, 1:1). At the end of the procedure, an OCT examination will be performed for research purposes. The collected images will not be available to the operators and these images will be stored and transferred to a dedicated core-lab for image analysis.

In the OCT-guided groups, PCI will be performed under OCT guidance according ILUMIEN III: OPTIMIZE PCI algorithm. The overall procedural approach for OCT-guided stent implantation and post-implant optimization also follows this algorithm (18). In short, the stent size is chosen based on OCT measurement, and post-dilation performed under OCT guidance to achieve fully stent struts apposition and satisfactory stent area (19).

Optical coherence tomography images will be acquired in the culprit vessel and non-culprit vessels using a commercially available C7 or OPTIS imaging system (Abbott, Santa Clara, United States). The imaging catheter will be advanced at least 10 mm distally to the culprit lesion and will be pulled-back using an automated pull-back device under contrast media injection for blood clearance. A second pull-back will be performed in case of long lesions so as the catheter to cover the entire segment of interest.

Repeat coronary angiography and OCT imaging will be also performed at 3- or 6-month follow-up according to the study protocol. The angiographic and OCT imaging data collected at baseline and follow-up will be anonymized and transferred to an independent core laboratory for further analysis.

Study endpoints

The primary endpoint of the study is the incidence of stent strut coverage (%) at 3- or 6-month follow-up.

The secondary endpoints of the study include angiographic, OCT, and clinical and biomarker outcomes that are listed in Table 3.

Statistical considerations

The sample size of this study is based on the previously published literature and the corresponding research hypothesis. This study intends to demonstrate that the incidence of strut coverage in the OCT-guided group is higher than that of angiography-guided group at 3-month follow-up (hypothesis 1). The second hypothesis of this study is that the incidence of stent strut coverage in the OCT-guided group at 3 months is similar to the incidence of strut coverage in the angiography-guided group at 6 months (non-inferiority analysis). If the above hypothesis is confirmed then an additional analysis will be performed that aims to demonstrate that the incidence of covered struts is higher at 3 months in the OCT-guided group compared to the rate of strut coverage noted at 6 months in the angiography-guided PCI (hypothesis 3). In order to control for the type I error, the test significance levels of hypothesis 1 and 2 are set at one-sided 0.025. Since hypothesis 3 is a sequential test carried out on the basis of hypothesis 2, the test significance level is set at one-sided 0.05.

The sample size calculation is based on the assumption that each patient will receive on average 1 stents, and that each stent will have a length of 24 mm. OCT analysis will be performed at 0.4/0.6 mm interval and that 7.9 struts in each cross section will be detected. Based on these assumptions, it is estimated that 474 strut results will be obtained from each patient. We estimate that we will need 7,305 strut estimations in

each group to prove with 95% power the primary endpoint of the study. Based on the above assumptions, we estimate that 16 patients should be recruited in each group. Considering a 20% drop-off rate, we estimate that 20 patients should be included in each group (Table 4).

Continuous variables will be described as means and SDs if they are normally distributed or median and interquartile range in the case of asymmetric data distribution. Categorical variables will be presented as numbers and percentages. Comparisons of numerical variables are conducted with the Student's *t* test or Mann–Whitney' *U* test as appropriate, categorical variables and outcomes were compared by using the chi-squared test or Fisher exact test. A statistical package (SPSS 21.0) will be used for analysis. Two-tailed $p < 0.05$ will be considered statistically significant.

Discussion

Dual antiplatelet therapy is recommended following stent implantation, but the optimal duration remains controversial in ACS patients, the current ACC/AHA and ESC guidelines recommend DAPT for 12 months after PCI (2, 3). However, prolonged DAPT is associated with worse outcomes in high bleeding risk populations. A consensus from the Academic Research Consortium for High Bleeding Risk (ARC-HBR) defined 14 and six clinical criteria as major or minor criteria, respectively. If patients meet at least one major or two minor criteria, they are considered to be at high bleeding risk (20). According to the ARC-HBR criteria, 40% patients in real-world PCI registry are at high bleeding risk (21). These patients are often excluded from or underrepresented in clinical trials about stents and antiplatelet therapy. The development of advanced stent platforms and the optimal stent deployment—even with the use of intravascular imaging guidance—is expected to enable shorter duration of DAPT in high bleeding risk ACS patients undergoing PCI. Several studies have shown that shorter-term DAPT in ACS patients implanted with next-generation DES is non-inferior to the standard or longer duration of DAPT. More specifically the "all-comer" ITALIC randomized controlled trial demonstrated that after the implantation of next-generation DES, 6-month DAPT followed by aspirin monotherapy is non inferior to 24-month DAPT in terms of all-cause mortality, myocardial infraction (MI), target vessel revascularization (TVR), stroke, and major bleeding in a low risk profile for ischemic events population (22). Similarly, the randomized OPTIMA-C trial (NCT03056118) showed that the MACE rate at 12-month follow-up was not different in patients receiving 6-month DAPT and those treated for 12-month DAPT after implantation of next-generation DES (23). The multicenter REDUCE trial enrolled 1,496 patients admitted with an ACS treated with the next-generation COMBO stent who were randomized to 3-month ($n = 751$) or 12-month ($n = 745$) DAPT. The primary endpoint was a composite of all-cause mortality, MI, ST, stroke, TVR, and bleeding and its incidence was similar in the two groups (8.2 vs. 8.4%, p non-inferiority<0.001) at 1- or 2-year follow-up (11.6 vs. 12.1%, $p = 0.76$) (24).

There is compelling evidence that strut coverage is a predictor of ST (25). The next-generation DES with thinner struts, safer polymer profiles and improved drug kinetics appear to enable faster endothelialization and have known to reduce the incidence of ST compared to the first generation DES (25). The OCT sub-study of the OPTIMA-C trial revealed favorable strut coverage at 6 months after next-generation DES implantation (23), similarly the FUNCOMBO trial showed almost complete strut coverage of the next-generation DES in patients who presented with STEMI (26). Moreover, a small study reported that in the biodegradable polymer Synergy stent strut coverage was 94.5% at 3 months and 96.6% at 6 months (27) whereas the TARGET All Comers study showed a similar incidence of strut coverage in biodegradable polymer Firehawk and durable polymer XIENCE stent group (99.9 ± 0.3 vs. $100 \pm 0.1\%$, $p = 0.26$) (28). Conversely, the biodegradable polymer BuMA Supreme stent was found to be superior to the XIENCE stent

TABLE 3 Endpoints of the trial.

Primary endpoint
The degree of stent struts neointimal coverage (%) at 3 and 6 months
Secondary endpoint
OCT endpoint: Assessed at 3 and 6 months
1. Average and minimal stent diameter, area, and volume.
2. Average and minimal lumen diameter, area, and volume.
3. Average and minimal strut coverage thickness.
4. Strut malposition rate.
5. Vascular repair index.
Clinical endpoints: Assessed at 1, 3, 6, and 12 months
1. Major adverse cardiac events (MACE) composite of cardiac death, target vessel myocardial infarction (TV-MI), and clinical ischemia-driven revascularization.
2. Cardiac death.
3. Non-fatal MI.
4. All revascularization.
5. Target lesion revascularization.
6. Target vessel revascularization.
7. ARC-defined stent thrombosis (early, late, very-late, definite, probable, and possible stent thrombosis).
Molecular biology endpoints: Assessed at baseline, 3 and 6 months
1. Lipid levels (total cholesterol, low-density lipoprotein, high-density lipoprotein, ratio of low-density lipoprotein to high-density lipoprotein, and triglyceride).
2. Molecule indicators (hs-CRP, PTX-3, VCAM-1, and MMP-9).

ARC, academic research consortium; hs-CRP, high sensitive C-reactive protein; PTX-3, pentraxin-3; VCAM-1, vascular cell adhesion molecule-1; and MMP-9, matrix metalloprotein-9.

TABLE 4 Parametric assumptions for hypothesis.

	Experimental group coverage	Control group coverage	Non-inferiority margin	Sample size (stent struts)
Hypothesis 1	93.6%	92%	Not applicable	6,781
Hypothesis 2	95%	95%	1.3%	7,305
Hypothesis 3	96.5%	95%	Not applicable	3,912

in terms of strut coverage at both 1 month and 2 months in the PIONEER-II OCT trial (29). However, stent implantation in these studies was mostly performed under angiography guidance. The DETECT-OCT (NCT01752894) trial was the first that highlighted the value of OCT imaging in optimizing stent apposition and in this way accelerating strut coverage. In this trial, the percentage of uncovered struts at 3 months was lower in the OCT-guided group (7.5%) than in the angiography-guided group (9.9%; $p = 0.009$) (8). However, the DETECT-OCT trial mainly included patients suffering from stable angina and did not include the group of patients undergoing OCT at a longer follow-up period. This study was designed to provide additional insights as it aims to include NSTE-ACS patients, and include the group of patients that will undergo OCT imaging at 6 months to examine late strut coverage in patients undergoing angiography guided PCI.

Additionally, clinical studies have found that MACE after PCI not only comes from in-stent restenosis or ST in ACS patients but also due to progression of mild to moderately graded disease in the non-culprit vessels as it is a well-known factor that patients presenting with ACS often have multivessel disease (30, 31). A study involving nearly 13,000 ACS patients showed that over 80% of ischemic events occurring after 30 days were unrelated to the culprit lesion that was stented, but were rather spontaneous, or *de novo* events in a non-culprit vessel (32). Intravascular imaging research revealed that non-culprit lesions in ACS patients are often vulnerable plaques, with characteristics such as thin-cap fibroatheroma and those with heavy lipid load. The progress and rupture of these vulnerable plaques in non-culprit vessels can also result in adverse events like thrombosis after PCI (33, 34). Therefore, understanding the evolution of plaque in non-culprit vessels is of great significance to prevent future adverse cardiac events and may potentially influence decision making in the use of DAPT duration. Thus, our study innovatively performs OCT examination in both culprit and non-culprit vessels at baseline and follow-up, to explore vulnerable plaque progression in non-target vessels, measure the changes in the thickness of the fibrous cap over lipid-rich plaques, and examine changes in macrophages accumulations and in the lipid content and in the vulnerable plaques, and their transformation at various time points. Furthermore, plaque progression is usually accompanied with lipid infiltration and inflammatory response. The positive correlation of cholesterol levels, proinflammatory cytokines, and atherosclerotic evolution is well established (35). Stent implantation is associated with vessel wall injury and endothelium disruption while it is well known that strut polymer and drug elution can trigger a pro-inflammatory and hypersensitivity reaction leading to the formation of neoatherosclerotic lesions (34). There are however limited data about the association between vulnerable plaque progression in native segments and neointima proliferation and neoatherosclerotic lesion formation in segments treated with stents. The present study has been designed to provide additional insights and explore the implications of the lipid profile and systemic inflammation assessed by circulatory biomarkers on neointima characteristics and atherosclerotic disease progression in native segments.

This study has several limitations. Firstly, only three centers in Huaihai economic zone are participated in this study. Therefore, the findings of this analysis may not be relevant to other populations. Secondly, "different operators" experience may impact the procedure outcomes, which is the source of uncontrolled bias. Finally, several studies revealed that the early strut coverage of biodegradable polymer DES is not similar with other next-generation DES (36, 37), which implies the results of our study may not be simply generalized to other DES with different design concept.

Ethics and dissemination

The study protocol has been approved by the ethics committee of Xuzhou Third People's Hospital, Xuzhou Cancer Hospital (Xuzhou city, Jiangsu Province). The reference number is 2019-02-006-H02. A Chinese original document and an English translation of the ethical approval document are attached at Additional file 2. Written informed consent is provided by patients before enrollment.

The study results will be submitted for publication in peer-reviewed journals. Data will be disseminated and presented at scientific meetings.

Patient and public involvement

Patients or the public were not involved in the design, or conduct, or reporting, or dissemination plans of this trial.

Ethics statement

The studies involving human participants were reviewed and approved by Ethics committee of Xuzhou Third People's Hospital, Xuzhou Cancer Hospital (Xuzhou city, Jiangsu Province). The patients/participants provided their written informed consent to participate in this study.

Author contributions

Y-XZ, LL, and Y-JZ co-designed the study protocol. Y-XZ, LL, and RP co-drafted the manuscript. ZL, QL, SC, and S-LF were involved with study conduct and data acquisition. W-RM and YW provided the statistical analysis. CB, BX, and Y-JZ further aided in assessment and revision of the protocol and revised the manuscript. All authors contributed to the article and approved the submitted version.

Funding

This investigator-initiated study is supported by JW Medical Systems (Shandong, China, grant number: N/A), 333 High-level Talent Training Program of Jiangsu Province (grant number: BAR2018275), and full-time introduction of special medical talents in 2018 of Xuzhou city (grant number: 2019-TPRC-1). These funding bodies are only providing financial support. The authors are solely responsible for the design and conduct of this study, analysis of the study data, drafting and editing of the paper, and the final content of the paper.

Acknowledgments

The authors wish to thank all participating centers, hospitals, researchers, and patients of the EXPECT study.

Conflict of interest

The authors declare that the research was conducted in the absence of any commercial or financial relationships that could be construed as a potential conflict of interest.

The handling editor TG declared a past collaboration with the author CB.

Publisher's note

Supplementary material

The Supplementary material for this article can be found online at: https://www.frontiersin.org/articles/10.3389/fcvm.2023.1003546/full#supplementary-material

References

1. Gu, D, Qu, J, Zhang, H, and Zheng, Z. Revascularization for coronary artery disease: principle and challenges. *Adv Exp Med Biol*. (2020) 1177:75–100. doi: 10.1007/978-981-15-2517-9_3

2. Levine, GN, Bates, ER, Bittl, JA, Brindis, RG, Fihn, SD, Fleisher, LA, et al. 2016 ACC/AHA guideline focused update on duration of dual antiplatelet therapy in patients with coronary artery disease: a report of the American College of Cardiology/American Heart Association task force on clinical practice guidelines: an update of the 2011 ACCF/AHA/SCAI guideline for percutaneous coronary intervention, 2011 ACCF/AHA guideline for coronary artery bypass graft surgery, 2012 ACC/AHA/ACP/AATS/PCNA/SCAI/STS guideline for the diagnosis and Management of Patients with Stable Ischemic Heart Disease, 2013 ACCF/AHA guideline for the management of ST-elevation myocardial infarction, 2014 AHA/ACC guideline for the Management of Patients with non-ST-elevation acute coronary syndromes, and 2014 ACC/AHA guideline on perioperative cardiovascular evaluation and Management of Patients Undergoing Noncardiac Surgery. *Circulation*. (2016) 134:e123–55. doi: 10.1161/CIR.0000000000000404

3. Collet, JP, Thiele, H, Barbato, E, Barthélémy, O, Bauersachs, J, Bhatt, DL, et al. 2020 ESC guidelines for the management of acute coronary syndromes in patients presenting without persistent ST-segment elevation. *Eur Heart J*. (2021) 42:1289–367. doi: 10.1093/eurheartj/ehaa575

4. Nakamura, M, Iijima, R, Ako, J, Shinke, T, Okada, H, Ito, Y, et al. Dual antiplatelet therapy for 6 versus 18 months after biodegradable polymer drug-eluting stent implantation. *JACC Cardiovasc Interv*. (2017) 10:1189–98. doi: 10.1016/j.jcin.2017.04.019

5. Yin, SH, Xu, P, Wang, B, Lu, Y, Wu, QY, Zhou, ML, et al. Duration of dual antiplatelet therapy after percutaneous coronary intervention with drug-eluting stent: systematic review and network meta-analysis. *BMJ*. (2019) 365:l2222. doi: 10.1136/bmj.l2222

6. Khan, SU, Singh, M, Valavoor, S, Khan, MU, Lone, AN, Khan, MZ, et al. Dual antiplatelet therapy after percutaneous coronary intervention and drug-eluting stents: a systematic review and network meta-analysis. *Circulation*. (2020) 142:1425–36. doi: 10.1161/CIRCULATIONAHA.120.046308

7. Costa, F, Windecker, S, and Valgimigli, M. Dual antiplatelet therapy duration: reconciling the inconsistencies. *Drugs*. (2017) 77:1733–54. doi: 10.1007/s40265-017-0806-1

8. Lee, SY, Kim, JS, Yoon, HJ, Hur, SH, Lee, SG, Kim, JW, et al. Early strut coverage in patients receiving drug-eluting stents and its implications for dual antiplatelet therapy: a randomized trial. *JACC Cardiovasc Imaging*. (2018) 11:1810–9. doi: 10.1016/j.jcmg.2017.12.014

9. Cutlip, DE, Windecker, S, Mehran, R, Boam, A, Cohen, DJ, van Es, GA, et al. Clinical end points in coronary stent trials: a case for standardized definitions. *Circulation*. (2007) 115:2344–51. doi: 10.1161/CIRCULATIONAHA.106.685313

10. Finn, AV, Joner, M, Nakazawa, G, Kolodgie, F, Newell, J, John, MC, et al. Pathological correlates of late drug-eluting stent thrombosis: strut coverage as a marker of endothelialization. *Circulation*. (2007) 115:2435–41. doi: 10.1161/CIRCULATIONAHA.107.693739

11. Lee, R, Foin, N, Ng, J, Allen, J, Soh, N, Ang, I, et al. Early coverage of drug-eluting stents analysed by optical coherence tomography: evidence of the impact of stent apposition and strut characteristics on the neointimal healing process. *EuroIntervention*. (2016) 12:e605–14. doi: 10.4244/EIJV12I5A100

12. Gori, T, Polimeni, A, Indolfi, C, Räber, L, Adriaenssens, T, and Münzel, T. Predictors of stent thrombosis and their implications for clinical practice. *Nat Rev Cardiol*. (2019) 16:243–56. doi: 10.1038/s41569-018-0118-5

13. García-García, HM, Muramatsu, T, Nakatani, S, Lee, IS, Holm, NR, Thuesen, L, et al. Serial optical frequency domain imaging in STEMI patients: the follow-up report of TROFI study. *Eur Heart J Cardiovasc Imaging*. (2014) 15:987–95. doi: 10.1093/ehjci/jeu042

14. Kim, JS, Ha, J, Kim, BK, Shin, DH, Ko, YG, Choi, D, et al. The relationship between post-stent strut apposition and follow-up strut coverage assessed by a contour plot optical coherence tomography analysis. *JACC Cardiovasc Interv*. (2014) 7:641–51. doi: 10.1016/j.jcin.2013.12.205

15. Wang, G, Sun, Z, Jin, Q, Xu, K, Li, Y, Wang, X, et al. First-in-man study evaluating the safety and efficacy of a second generation biodegradable polymer sirolimus-eluting stent in the treatment of patients with de novo coronary lesions: clinical, angiographic, and OCT outcomes of CREDIT-1. *Catheter Cardiovasc Interv*. (2015) 85:744–51. doi: 10.1002/ccd.25862

16. Wang, G, Wang, H, Xu, B, Yang, Y, Yang, Z, Li, H, et al. Efficacy and safety of a biodegradable polymer cobalt-chromium sirolimus-eluting stent (EXCROSSAL) in treating de novo coronary artery disease: a pooled analysis of the CREDIT II and CREDIT III trials. *Catheter Cardiovasc Interv*. (2017) 89:512–9. doi: 10.1002/ccd.26887

17. Taniwaki, M, Windecker, S, Zaugg, S, Stefanini, GG, Baumgartner, S, Zanchin, T, et al. The association between in-stent neoatherosclerosis and native coronary artery disease progression: a long-term angiographic and optical coherence tomography cohort study. *Eur Heart J*. (2015) 36:2167–76. doi: 10.1093/eurheartj/ehv227

18. Ali, ZA, Maehara, A, Généreux, P, Shlofmitz, RA, Fabbiocchi, F, Nazif, TM, et al. Optical coherence tomography compared with intravascular ultrasound and with angiography to guide coronary stent implantation (ILUMIEN III: OPTIMIZE PCI): a randomised controlled trial. *Lancet*. (2016) 388:2618–28. doi: 10.1016/S0140-6736(16)31922-5

19. Gupta, A, Shrivastava, A, Vijayvergiya, R, Chhikara, S, Datta, R, Aziz, A, et al. Optical coherence tomography: an eye into the coronary artery. *Front Cardiovasc Med*. (2022) 9:854554. doi: 10.3389/fcvm.2022.854554

20. Urban, P, Mehran, R, Colleran, R, Angiolillo, DJ, Byrne, RA, Capodanno, D, et al. Defining high bleeding risk in patients undergoing percutaneous coronary intervention: a consensus document from the academic research consortium for high bleeding risk. *Eur Heart J*. (2019) 40:2632–53. doi: 10.1093/eurheartj/ehz372

21. Ueki, Y, Bär, S, Losdat, S, Otsuka, T, Zanchin, C, Zanchin, T, et al. Validation of the academic research consortium for high bleeding risk (ARC-HBR) criteria in patients undergoing percutaneous coronary intervention and comparison with contemporary bleeding risk scores. *EuroIntervention*. (2020) 16:371–9. doi: 10.4244/EIJ-D-20-00052

22. Didier, R, Morice, MC, Barragan, P, Noryani, AAL, Noor, HA, Majwal, T, et al. 6- versus 24-month dual antiplatelet therapy after implantation of drug-eluting stents in patients nonresistant to aspirin: final results of the ITALIC trial (is there a life for DES after discontinuation of Clopidogrel). *JACC Cardiovasc Interv*. (2017) 10:1202–10. doi: 10.1016/j.jcin.2017.03.049

23. Lee, BK, Kim, JS, Lee, OH, Min, PK, Yoon, YW, Hong, BK, et al. Safety of six-month dual antiplatelet therapy after second-generation drug-eluting stent implantation: OPTIMA-C randomised clinical trial and OCT substudy. *EuroIntervention*. (2018) 13:1923–30. doi: 10.4244/EIJ-D-17-00792

24. De Luca, G, Damen, SA, Camaro, C, Benit, E, Verdoia, M, Rasoul, S, et al. Final results of the randomised evaluation of short-term dual antiplatelet therapy in patients with acute coronary syndrome treated with a new-generation stent (REDUCE trial). *EuroIntervention*. (2019) 15:e990–8. doi: 10.4244/EIJ-D-19-00539

25. Torii, S, Jinnouchi, H, Sakamoto, A, Kutyna, M, Cornelissen, A, Kuntz, S, et al. Drug-eluting coronary stents: insights from preclinical and pathology studies. *Nat Rev Cardiol*. (2020) 17:37–51. doi: 10.1038/s41569-019-0234-x

26. Gómez-Lara, J, Oyarzabal, L, Brugaletta, S, Salvatella, N, Romaguera, R, Roura, G, et al. Coronary endothelial and microvascular function distal to polymer-free and endothelial cell-capturing drug-eluting stents. The randomized FUNCOMBO trial. *Rev Esp Cardiol*. (2021) 74:1013–22. doi: 10.1016/j.rec.2021.01.007

27. de la Torre Hernández, JM, Tejedor, P, Camarero, TG, Duran, JM, Lee, DH, Monedero, J, et al. Early healing assessment with optical coherence tomography of everolimus-eluting stents with bioabsorbable polymer (synergy™) at 3 and 6 months after implantation. *Catheter Cardiovasc Interv*. (2016) 88:E67–73. doi: 10.1002/ccd.26299

28. Baumbach, A, Lansky, AJ, Onuma, Y, Asano, T, Johnson, T, Anderson, R, et al. Optical coherence tomography substudy of a prospective multicentre randomised post-market trial to assess the safety and effectiveness of the Firehawk cobalt-chromium coronary stent (rapamycin target-eluting) system for the treatment of atherosclerotic lesions: TARGET all comers. *EuroIntervention*. (2018) 14:1121–8. doi: 10.4244/EIJ-D-18-00226

29. Asano, T, Jin, Q, Katagiri, Y, Kogame, N, Takahashi, K, Chang, CC, et al. A randomised comparison of healing response between the BuMA supreme stent and the XIENCE stent at one-month and two-month follow-up: PIONEER-II OCT randomised controlled trial. *EuroIntervention*. (2018) 14:e1306–15. doi: 10.4244/EIJ-D-18-00461

30. Taruya, A, Tanaka, A, Nishiguchi, T, Ozaki, Y, Kashiwagi, M, Yamano, T, et al. Lesion characteristics and prognosis of acute coronary syndrome without angiographically significant coronary artery stenosis. *Eur Heart J Cardiovasc Imaging*. (2020) 21:202–9. doi: 10.1093/ehjci/jez079

31. Montone, RA, Niccoli, G, Crea, F, and Jang, IK. Management of non-culprit coronary plaques in patients with acute coronary syndrome. *Eur Heart J*. (2020) 41:3579–86. doi: 10.1093/eurheartj/ehaa481

32. Scirica, BM, Bergmark, BA, Morrow, DA, Antman, EM, Bonaca, MP, Murphy, SA, et al. Nonculprit lesion myocardial infarction following percutaneous coronary intervention in patients with acute coronary syndrome. *J Am Coll Cardiol*. (2020) 75:1095–106. doi: 10.1016/j.jacc.2019.12.067

33. Russo, M, Kim, HO, Kurihara, O, Araki, M, Shinohara, H, Thondapu, V, et al. Characteristics of non-culprit plaques in acute coronary syndrome patients with layered culprit plaque. *Eur Heart J Cardiovasc Imaging*. (2020) 21:1421–30. doi: 10.1093/ehjci/jez308

34. Xing, L, Higuma, T, Wang, Z, Aguirre, AD, Mizuno, K, Takano, M, et al. Clinical significance of lipid-rich plaque detected by optical coherence tomography: a 4-year follow-up study. *J Am Coll Cardiol*. (2017) 69:2502–13. doi: 10.1016/j.jacc.2017.03.556

35. Zhu, Y, Xian, X, Wang, Z, Bi, Y, Chen, Q, Han, X, et al. Research Progress on the relationship between atherosclerosis and inflammation. *Biomol Ther*. (2018) 8:80. doi: 10.3390/biom8030080

36. Otaegui, I, Pérez de Prado, A, Massotti, M, López-Benito, M, Sabaté, M, Martí, G, et al. Intrapatient randomization to study strut coverage in polymer-free versus biodegradable-polymer Sirolimus-eluting stent implantations. *JACC Cardiovasc Interv*. (2020) 13:899–900. doi: 10.1016/j.jcin.2019.11.020

37. Suzuki, S, Sotomi, Y, Kobayashi, T, Hamanaka, Y, Nakatani, S, Shiojima, I, et al. Early vessel healing after implantation of biodegradable-polymer and durable-polymer drug-eluting stent: 3-month angioscopic evaluation of the RESTORE registry. *Int J Card Imaging*. (2019) 35:973–80. doi: 10.1007/s10554-019-01580-2

frontiers | Frontiers in Cardiovascular Medicine

TYPE Study Protocol
PUBLISHED 24 May 2023
DOI 10.3389/fcvm.2023.1130216

OPEN ACCESS

EDITED BY
Danilo Menichelli,
Sapienza University of Rome, Italy

REVIEWED BY
Roberto Franco Enrico Pedretti,
MultiMedica (IRCCS), Italy
Gianluca Gazzaniga,
University of Milan, Italy

*CORRESPONDENCE
Dong-Ju Choi
djchoi@snubh.org

RECEIVED 23 December 2022
ACCEPTED 05 May 2023
PUBLISHED 24 May 2023

CITATION
Yoon M, Park JJ, Hur T, Hua C-H, Shim CY, Yoo B-S, Cho H-J, Lee S, Kim HM, Kim J-H, Lee S and Choi Dong-Ju (2023) The ReInforcement of adherence via self-monitoring app orchestrating biosignals and medication of RivaroXaban in patients with atrial fibrillation and co-morbidities: a study protocol for a randomized controlled trial (RIVOX-AF).
Front. Cardiovasc. Med. 10:1130216.
doi: 10.3389/fcvm.2023.1130216

The ReInforcement of adherence via self-monitoring app orchestrating biosignals and medication of RivaroXaban in patients with atrial fibrillation and co-morbidities: a study protocol for a randomized controlled trial (RIVOX-AF)

Minjae Yoon[1], Jin Joo Park[1], Taeho Hur[1], Cam-Hao Hua[2], Chi Young Shim[3], Byung-Su Yoo[4], Hyun-Jai Cho[5], Seonhwa Lee[6], Hyue Mee Kim[7], Ji-Hyun Kim[8], Sungyoung Lee[2] and Dong-Ju Choi[1]* for the RIVOX-AF investigators

[1]Division of Cardiology, Department of Internal Medicine, Seoul National University Bundang Hospital, Seoul National University College of Medicine, Seongnam, Republic of Korea, [2]Department of Computer Science and Engineering, Kyung Hee University, Yongin, Republic of Korea, [3]Division of Cardiology, Department of Internal Medicine, Severance Hospital, Yonsei University College of Medicine, Seoul, Republic of Korea, [4]Department of Internal Medicine, Yonsei University Wonju College of Medicine, Wonju, Republic of Korea, [5]Department of Internal Medicine, Seoul National University Hospital, Seoul National University College of Medicine, Seoul, Republic of Korea, [6]Division of Cardiology, Department of Internal Medicine, Cardiovascular Center, Keimyung University Dongsan Hospital, Daegu, Republic of Korea, [7]Division of Cardiology, Department of Internal Medicine, Chung-Ang University Hospital, Seoul, Republic of Korea, [8]Cardiovascular Center, Dongguk University Ilsan Hospital, Goyang, Republic of Korea

Background: Because of the short half-life of non-vitamin K antagonist oral anticoagulants (NOACs), consistent drug adherence is crucial to maintain the effect of anticoagulants for stroke prevention in atrial fibrillation (AF). Considering the low adherence to NOACs in practice, we developed a mobile health platform that provides an alert for drug intake, visual confirmation of drug administration, and a list of medication intake history. This study aims to evaluate whether this smartphone app-based intervention will increase drug adherence compared with usual care in patients with AF requiring NOACs in a large population.

Methods: This prospective, randomized, open-label, multicenter trial (RIVOX-AF study) will include a total of 1,042 patients (521 patients in the intervention group and 521 patients in the control group) from 13 tertiary hospitals in South Korea. Patients with AF aged ≥19 years with one or more comorbidities, including heart failure, myocardial infarction, stable angina, hypertension, or diabetes mellitus, will be included in this study. Participants will be randomly assigned to either the intervention group (MEDI-app) or the conventional treatment group in a 1:1 ratio using a web-based randomization service. The intervention group will use a smartphone app that includes an alarm for drug intake, visual confirmation of drug administration through a camera check, and presentation of a list of medication intake history. The primary endpoint is adherence to rivaroxaban by pill count measurements at 12 and 24 weeks. The key secondary endpoints are clinical composite endpoints, including systemic embolic events, stroke, major bleeding requiring transfusion or hospitalization, or death during the 24 weeks of follow-up.

Discussion: This randomized controlled trial will investigate the feasibility and efficacy of smartphone apps and mobile health platforms in improving adherence to NOACs.
Trial registration: The study design has been registered in ClinicalTrial.gov (NCT05557123).

KEYWORDS
atrial fibrillation, NOAC, drug adherence, mobile application, mobile health

Introduction

For the management of patients with atrial fibrillation (AF), stroke prevention with oral anticoagulants is central to guideline-recommended management (1–3). Previous large randomized controlled trials for AF have demonstrated improved safety and comparable effectiveness of non-vitamin K antagonist oral anticoagulants (NOACs) compared with warfarin (4–8). Also, in contrast to warfarin, NOACs have minimal drug or food interactions and predictable effectiveness with fixed dosing without the need for laboratory monitoring. Because of these benefits, NOAC use is expanding globally (9, 10), and the current guidelines favor NOACs over warfarin for stroke prevention in AF (1, 2).

However, there are issues with the relatively short half-life of NOACs. When doses are missed, there is a higher risk of a prothrombotic state (11). Therefore, during NOAC therapy, constant medication compliance is crucial to sustain the anticoagulation's effect on stroke prevention (12, 13). Failed persistence or poor drug adherence to NOACs may increase the risk of stroke, which may result in rising overall health care costs (14–17).

Recently, Desteghe et al. showed that telemonitoring with or without feedback resulted in higher NOAC adherence (18). However, monitoring and feedback by health care providers have high costs and require more infrastructure and manpower and, thus, are challenging to incorporate in an actual clinical setting. Currently, smartphones are available to most of the general population at affordable costs. With the advent of mobile technology and advances in artificial intelligence (AI), mobile-based feedback algorithms may be promising strategies to improve medication adherence with easy distribution (19). Although there are some debates over their efficacy, smartphone applications (apps) are currently acknowledged as an effective method for improving drug adherence (20–28). Smartphone apps can transmit push alarms or notifications to remind the patient to take their medication, which may function to increase drug adherence (29). There are some previous studies regarding mobile apps for improving drug adherence of NOACs (30, 31). However, these studies had a small number of participants and limited application functions. Considering the low drug adherence of NOACs in patients with AF in the real world (13, 17, 32), we developed a mobile health platform to provide an alert for drug intake, visual confirmation of drug administration, and a list of medication intake history. This study aims to evaluate whether this smartphone app-based intervention will increase drug adherence compared with usual care in a large population of patients with AF requiring NOACs.

Methods and analysis

Study design

The ReInforcement of adherence Via self-monitoring app Orchestrating biosignals and medication of RivaroXaban in patients with Atrial Fibrillation and co-morbidities (RIVOX-AF) study is a prospective, randomized, open-label, nationwide, multicenter trial to evaluate the efficacy of smartphone apps (MEDI-app) in improving drug adherence to NOACs in patients with AF. Thirteen tertiary university hospitals in South Korea will participate in this study. Enrollment began in March 2022, is currently ongoing, and is expected to be completed in late 2023. The study design has been registered at ClinicalTrials.gov (NCT05557123).

Study population

We will enroll patients with AF aged 19 years or older with one or more comorbidities, including heart failure, myocardial infarction, stable angina, hypertension, or diabetes mellitus. Patients can be enrolled 3 months after myocardial infarction or percutaneous coronary intervention. Rivaroxaban (Rivoxaban, Samjin Pharm, Seoul, Korea) will be administered to the participants at an open-label dosage of 20 mg once daily. Patients using other NOACs can be enrolled after swiching to Rivoxaban. The dosage will be reduced to 15 mg or 10 mg once daily if creatinine clearance is 15–49 ml/min or at the physician's discretion. Since smartphone usage is essential in this study, participants should be proficient in the use of smartphones and be able to understand and follow Korean instructions for using the program. Patients with severe chronic kidney disease (creatinine clearance <15 ml/min), moderate or severe mitral valve stenosis, or a history of mitral valve replacement or repair will be excluded. The detailed inclusion and exclusion criteria are listed in **Table 1**.

At baseline, sex, age, and comorbidities will be evaluated in all participants. The CHA_2DS_2-VASc score for stroke risk prediction will be calculated by the summation of all assigned points: one point each for congestive heart failure (C), hypertension (H), age between 65 and 74 years (A), diabetes mellitus (D), vascular disease (V), and female sex (Sc) and 2 points each for a history

TABLE 1 Inclusion and exclusion criteria.

Inclusion criteria:
1. Patients with AF aged 19 years or older with one or more comorbidities including heart failure, myocardial infarction, stable angina, hypertension or diabetes mellitus (Patients can be enrolled 3 months after myocardial infarction or percutaneous coronary intervention).
2. Patients with AF who are taking or initiating newly-prescribed rivaroxaban
3. Patients who can use a smartphone and are fluent in Korean
4. Patients who voluntarily consent to participate in this clinical trial
Exclusion criteria:
1. Creatinine clearance less than 15 ml/min
2. Moderate or severe mitral stenosis
3. Previous history of mitral valve replacement or mitral valve repair
4. Previous history of alcohol or drug abuse
5. Patients who are judged as both legally and psychologically inadequate to participate in the clinical study by the investigator
6. Patients who have participated in clinical studies with other investigational drug products within 4 weeks prior to screening
7. Patients unwilling to participate in the clinical study

AF, atrial fibrillation.

of stroke/transient ischemic attack/thromboembolism (S_2) or age ≥75 years (A_2) (1, 33).

Patient recruitment and randomization

Any patient who comes to the clinic for AF management will be considered a potential participant. After a comprehensive interview, eligible participants will be asked to provide written consent for participation in the trial. A baseline survey covering demographics and cardiovascular comorbidities will be given to eligible participants (Table 2). These data will be collected by a research nurse, who will re-interview the patient and refer to the doctor's notes. Then, using a web-based central randomization service (http://matrixmdr.com), eligible participants will then be randomly assigned to either the intervention group (MEDI-app) or the conventional treatment group in a 1:1 ratio. It will not be possible to blind the participants to group allocation owing to the nature of the intervention.

Intervention (smartphone app-conditioned feedback) and follow-up

We developed a mobile application (MEDI-app) to improve NOAC adherence in patients with AF. Participants in the intervention group will install the study app provided by a research nurse on their smartphones (Figure 1). Because the app is not an open application available to the public, the control group cannot access the application. The workflow, operating system, and display of the smartphone application are shown in Figures 1, 2. The patient can use facial recognition to log in to the app (Supplementary Figure S1). The design, development, and utilization details of the physician-oriented web and patient-oriented smartphone app are described in the online Supplementary material.

The research coordinator will enter the information on rivaroxaban administered to the patient into the mobile application and will set the alarm initially. The participants will be able to change the time of the alarm for rivaroxaban. When the alarm sounds at a pre-specified time, the patient will be reminded to take rivaroxaban. The app also determines whether the patient takes the medication through medication and action recognition software (Supplementary Figure S2). To elaborate, the first step is medication recognition, which determines whether the patient is taking the correct pill. A deep learning model of medication recognition will be exported after the completion of the training phase to perform real-time inference on the server from a picture captured by the camera on the patient's smartphone to match the name, shape, and color of the pill. In the second step, the app will visually confirm if the patient has taken the pill through action recognition via the smartphone camera by watching the patient put the medicine into their mouth through the camera.

TABLE 2 Standard protocol items: Recommendation for interventional trials (SPIRIT) check list.

	STUDY PERIOD			
	Enrolment	Allocation	Post-allocation	Close-out
TIMEPOINT	Day -28 to 0	Visit 1 (day 0)	Visit 2 (12 weeks)	Visit 3 (24 weeks)
ENROLMENT:				
Eligibility screen	X			
Informed consent	X			
Allocation		X		
INTERVENTIONS:				
Intervention (MEDI-app)		◆————	————	————◆
Control (Conventional Treatment)		◆————	————	————◆
ASSESSMENTS:				
Baseline characteristics	X			
Drug adherence		X	X	X
Secondary endpoints			X	X

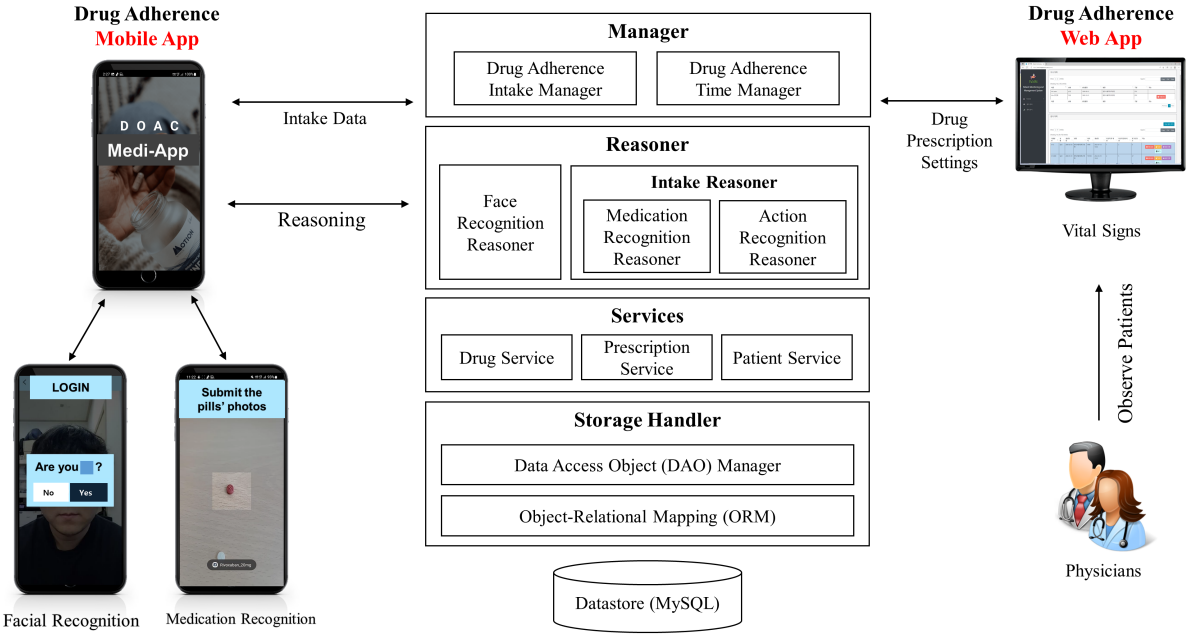

FIGURE 1
System architecture and structural workflow.

If the patients do not confirm taking the medication at the scheduled time, the app will send an alert message to ensure that the patients take the medicine until 2 h after the set drug intake time. If the patient does not comply with the pill intake procedure within these 2 h, it is assumed that the patient did not take the pill, and the app will send non-intake data to the server accordingly. As an alternative, patients can also confirm that they have taken the medicine by pressing the intake button within a day, rather than using action recognition via the camera. This information can be updated on the server. Data regarding the time of rivaroxaban intake will be stored daily, and patients can check the list of drug adherence per week or month on a calendar through the app. The dashboard system is designed to show the physicians the history and number of days that the participants confirmed taking their medication (**Supplementary Figure S3**). In this study, the app will be initially configured only for the rivaroxaban dose, frequency, and pill supply.

The control group will receive only standard care which is recommended in the guidelines, including education on the disease and the importance of medication compliance by physicians at each scheduled visit. No other specific interventions will be performed. Follow-up visits will be scheduled at 12 (visit two) and 24 (visit three) weeks after randomization (**Figure 3**).

Study outcomes

The primary endpoint of the study is adherence to rivaroxaban at 12 and 24 weeks. Drug adherence will be evaluated with the "pill count" measurements. The patients brought the remaining tablets to each scheduled visit, and trained and certified research nurses counted the number of returned drugs and calculated drug adherence as follows:

$$\text{Drug adherence} = \frac{\text{number of pills dispensed} - \text{number of pills returned}}{\text{number of days between dispensing date and follow} - \text{up date}}$$

In addition, we will evaluate the concordance of drug adherence by pill count measurements and app-calculated indices.

The key secondary endpoints are clinical composite endpoints, including systemic embolic events, stroke, major bleeding requiring transfusion or hospitalization, or death during the 24 weeks of follow-up. Other secondary endpoints include (1) major adverse cardiac and cerebrovascular events and hospitalization, (2) thromboembolism (stroke, transient ischemic attack, pulmonary embolism), (3) major bleeding requiring hospitalization or transfusion, or (4) minor bleeding. To evaluate the feasibility of the smartphone app, additional analysis will be conducted regarding the frequency of smartphone app use.

Sample size and statistical analysis

To date, no large studies have evaluated the use of a smartphone app to improve adherence to NOACs using pill count measurements. Thus, precise sample size calculation is not possible. We assumed that drug adherence would be 91% in the control group and 95% in the intervention group with a standard deviation of 17%, considering previous studies (30, 34, 35). With a two-tailed alpha of 0.05, power of 0.95, and a dropout rate of 10%, 1,042 patients (521 patients in

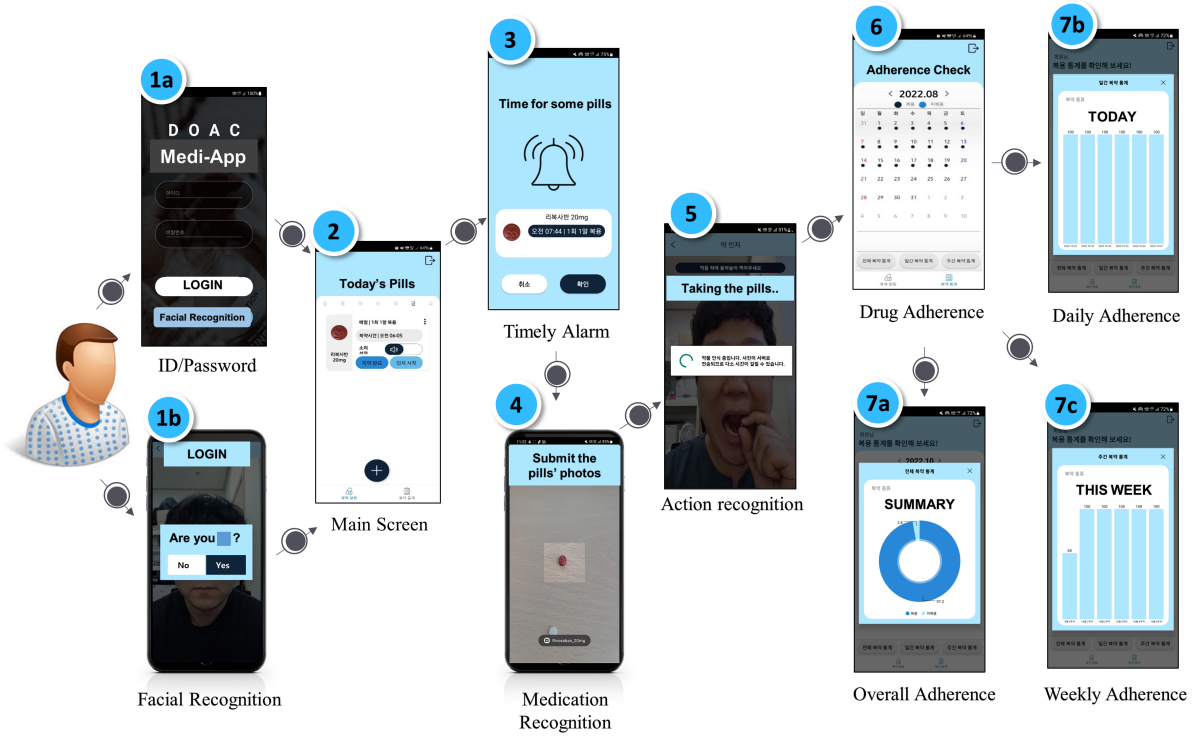

FIGURE 2
Operating system and sample display of the smartphone app. Workflow of facial login, medication recognition, action recognition, and drug adherence are shown.

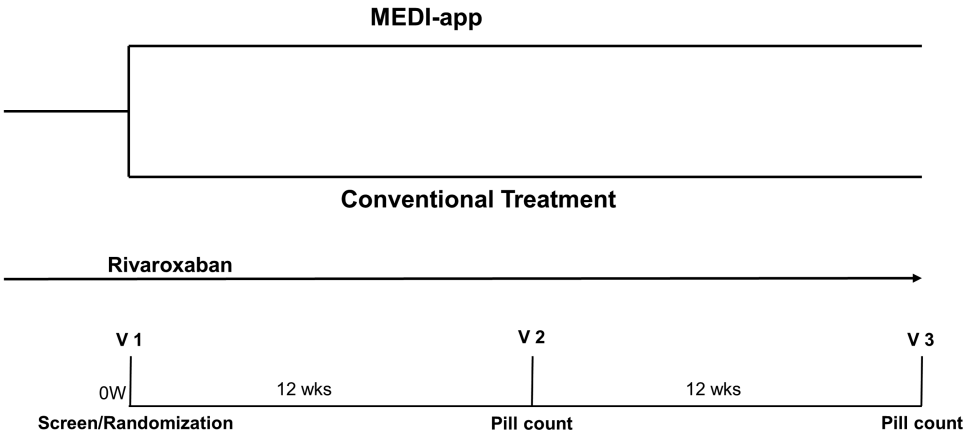

FIGURE 3
Study design of RIVOX-AF. Patients taking rivaroxaban will be randomized to either an application-conditioned feedback group or a conventional treatment group. Follow-up visits will be scheduled at 12 (visit two) and 24 (visit three) weeks after randomization.

the intervention and 521 patients in the control groups) are required.

Categorical variables will be reported as frequencies (percentages), and continuous variables will be expressed as means ± standard deviations or medians with interquartile ranges. Categorical variables will be compared using Pearson's chi-square test or Fisher's exact test, and continuous variables will be compared using Student's *t*-test or the Mann–Whitney *U* test.

Intention-to-treat analyses will include all randomized patients. Efficacy endpoints will be mainly analyzed using the full analysis set, which includes all randomly assigned participants who underwent at least one assessment of the primary endpoint. We will also perform a per-protocol sensitivity analysis, including all

patients who completed the study protocol. In the subgroup analyses, we will evaluate the differential effects of the intervention on the primary outcomes with respect to sex, age and other comorbidities.

All tests will be two-tailed, and a *P*-value <0.05 will be considered statistically significant. Statistical analyses will be performed using R version 4.2.0 (The R Foundation for Statistical Computing, Vienna, Austria).

Discussion

This randomized controlled trial will investigate the feasibility and efficacy of smartphone apps and mobile health platforms in improving adherence to NOACs. Additionally, current study will also evaluate the benefits of app-based interventions in the reduction adverse clinical events related to AF. We believe that this prospective, randomized, large, multicenter trial will be helpful in developing public health strategies to improve NOAC adherence through smartphone use.

Poor drug adherence to NOACs may increase the risk of stroke, which may result in rising overall health care costs (14–17). Therefore, consistent drug adherence is important to maintain the effect of anticoagulation during NOAC therapy. Recently, Thakkar et al. demonstrated that mobile phone text messaging improves medication adherence in chronic disease (36). Also, Desteghe et al. showed that telemonitoring with or without feedback resulted in higher NOAC adherence (18). However, text messaging, telemonitoring, and feedback by health care providers require time, financial expenditure, and personnel and, thus, are challenging to incorporate in a real clinical setting. Today, smartphones are available to most of the general population at affordable costs. With the advent of mobile technology and advances in AI, mobile-based feedback algorithms may be promising strategies to assist in the self-management and improvement of drug adherence in chronic diseases, including AF, using cost-effective and accessible methods. We believe that our approach of using a smartphone app would be an efficient way to improve drug adherence at a minimum cost.

There have been some previous studies on mobile apps for improving drug adherence to NOACs (30, 31). However, these studies had a limitation. The studies by Labovitz et al. (30) and Turakhia et al. (31) enrolled only small numbers of patients, 28 and 139 patients, respectively. In addition, their smartphone app functions were different from ours; our mobile app and mobile health platform functions include an alarm for drug intake, visual confirmation of drug administration through a camera check, and presentation of a list of medication intake history using AI and action recognition. The study by Turakhia et al. (31) failed to determine the primary and secondary drug adherence outcomes. We believe that these heterogeneous and diverse functions of mobile interventions could affect the benefits and outcomes of mobile apps, especially for improving medication adherence.

This study's objective differs from that of the ongoing trial at our institution. In the Adhere-App study (35), patients received an alarm to take their medication and measure heart rate (HR) and blood pressure (BP) according to a pre-specified schedule on the smartphone app. The automatic BP machine is connected to the smartphone via Bluetooth, and the measured BP and HR are automatically updated on the smartphone app. The Adhere-App study is designed for the context of active participation in vital sign measurement; using a smartphone app-based feedback system could help patients become more aware of their underlying condition. In turn, this may affect their self-care habits and increase drug adherence. In the current RIVOX-AF study, we aim that smartphone app-based intervention including an alert for drug intake, visual confirmation of drug administration, and a list of medication intake history would increase drug adherence

Limitations and strengths

This study has several limitations. First, the results of our trial may not be applicable to patients who are not capable of using smartphones, such as the elderly, because we will only enroll participants who have smartphones and are able to use them. As a large proportion of patients with AF are elderly and have difficulties using smartphones, excluding them from participation may lead to bias and study limitations. Second, the participants who consent to participate in the study may be more concerned with their own health. As a result, their medication adherence may be greater than that of the general AF population. Third, our sample size calculation may not be accurate because no prior large-scale trial has evaluated the use of smartphone apps to improve NOAC adherence. It is also possible that our estimates of drug adherence may overestimate the actual adherence, considering the findings of a previous study (17). In addition, the sample size has been calculated to determine differences in drug adherence; it is not powered to reveal any differences in adverse clinical events. Fourth, the follow-up period of this study was limited to 24 weeks. Although longer follow-up periods may provide a more reliable data on adherence, the follow-up period in our study was decided on the basis of manpower and cost.

Despite these limitations, this study is a nationwide, multicenter randomized control trial with a relatively large number of participants compared with previous studies (30, 31). Additionally, in our study, drug adherence will be evaluated by the "pill count" method, in which the number of returned drugs will be counted. Drug adherence by pill count may be more accurate than the drug score (37, 38), and this is a strength of our study compared with previous studies. In addition, we will evaluate the concordance of drug adherence by pill count measurements or app-calculated indices.

Ethics statement

The studies involving human participants were reviewed and approved by the Institutional Review Board of Seoul National University Bundang Hospital (B-2021-661-301). The patients/

participants provided their written informed consent to participate in this study.

Author contributions

DJC, MY, and JJP contributed to the conception of the study. DJC, MY, and JJP participated in the design of the study. MY and DJC drafted and finalized the manuscript. JJP, TH, CHH, CYS, BSY, HJC, SL, HMK, JHK, and SL revised the manuscript critically for important intellectual content. All authors contributed to the article and approved the submitted version.

Funding

This research was supported by a grant from Samjin Pharmaceuticals via the SNUBH (Seoul National University Bundang Hospital) 06-2021-0092 and an Institute of Information & communications Technology Planning & Evaluation (IITP) grant funded by the Korea government (2022-0-00078, Explainable Logical Reasoning for Medical Knowledge Generation) and the MSIT (Ministry of Science and ICT), Korea, under the Grand Information Technology Research Center support program (IITP-2022-2020-0-01489) supervised by the IITP.

Conflict of interest

The authors declare that the research was conducted in the absence of any commercial or financial relationships that could be construed as a potential conflict of interest.

Publisher's note

All claims expressed in this article are solely those of the authors and do not necessarily represent those of their affiliated organizations, or those of the publisher, the editors and the reviewers. Any product that may be evaluated in this article, or claim that may be made by its manufacturer, is not guaranteed or endorsed by the publisher.

Supplementary material

The Supplementary Material for this article can be found online at: https://www.frontiersin.org/articles/10.3389/fcvm.2023.1130216/full#supplementary-material.

References

1. Hindricks G, Potpara T, Dagres N, Arbelo E, Bax JJ, Blomstrom-Lundqvist C, et al. 2020 ESC guidelines for the diagnosis and management of atrial fibrillation developed in collaboration with the European association of cardio-thoracic surgery (EACTS). *Eur Heart J*. (2021) 42(5):373–498. doi: 10.1093/eurheartj/ehaa612

2. January CT, Wann LS, Calkins H, Chen LY, Cigarroa JE, Cleveland JC Jr, et al. 2019 AHA/ACC/HRS focused update of the 2014 AHA/ACC/HRS guideline for the management of patients with atrial fibrillation: a report of the American college of cardiology/American heart association task force on clinical practice guidelines and the heart rhythm society in collaboration with the society of thoracic surgeons. *Circulation*. (2019) 140(2):e125–51. doi: 10.1161/CIR.0000000000000665

3. Joung B, Lee JM, Lee KH, Kim T-H, Choi E-K, Lim W-H, et al. 2018 Korean guideline of atrial fibrillation management. *Korean Circ J*. (2018) 48(12):1033–80. doi: 10.4070/kcj.2018.0339

4. Ruff CT, Giugliano RP, Braunwald E, Hoffman EB, Deenadayalu N, Ezekowitz MD, et al. Comparison of the efficacy and safety of new oral anticoagulants with warfarin in patients with atrial fibrillation: a meta-analysis of randomised trials. *Lancet*. (2014) 383(9921):955–62. doi: 10.1016/S0140-6736(13)62343-0

5. Connolly SJ, Ezekowitz MD, Yusuf S, Eikelboom J, Oldgren J, Parekh A, et al. Dabigatran versus warfarin in patients with atrial fibrillation. *N Engl J Med*. (2009) 361(12):1139–51. doi: 10.1056/NEJMoa0905561

6. Patel MR, Mahaffey KW, Garg J, Pan G, Singer DE, Hacke W, et al. Rivaroxaban versus warfarin in nonvalvular atrial fibrillation. *N Engl J Med*. (2011) 365(10):883–91. doi: 10.1056/NEJMoa1009638

7. Granger CB, Alexander JH, McMurray JJ, Lopes RD, Hylek EM, Hanna M, et al. Apixaban versus warfarin in patients with atrial fibrillation. *N Engl J Med*. (2011) 365 (11):981–92. doi: 10.1056/NEJMoa1107039

8. Giugliano RP, Ruff CT, Braunwald E, Murphy SA, Wiviott SD, Halperin JL, et al. Edoxaban versus warfarin in patients with atrial fibrillation. *N Engl J Med*. (2013) 369 (22):2093–104. doi: 10.1056/NEJMoa1310907

9. Lee SR, Choi EK, Han KD, Cha MJ, Oh S, Lip GYH. Temporal trends of antithrombotic therapy for stroke prevention in Korean patients with non-valvular atrial fibrillation in the era of non-vitamin K antagonist oral anticoagulants: a nationwide population-based study. *PLoS One*. (2017) 12(12):e0189495. doi: 10.1371/journal.pone.0189495

10. Huisman MV, Rothman KJ, Paquette M, Teutsch C, Diener HC, Dubner SJ, et al. The changing landscape for stroke prevention in AF: findings from the GLORIA-AF registry phase 2. *J Am Coll Cardiol*. (2017) 69(7):777–85. doi: 10.1016/j.jacc.2016.11.061

11. How CH. Novel oral anticoagulants for atrial fibrillation. *Singapore Med J*. (2015) 56(12):657–8; quiz 9. doi: 10.11622/smedj.2015184

12. Yao X, Abraham NS, Alexander GC, Crown W, Montori VM, Sangaralingham LR, et al. Effect of adherence to oral anticoagulants on risk of stroke and major bleeding among patients with atrial fibrillation. *J Am Heart Assoc*. (2016) 5(2):e003074. doi: 10.1161/JAHA.115.003074

13. Kim D, Yang P-S, Jang E, Yu HT, Kim T-H, Uhm J-S, et al. The optimal drug adherence to maximize the efficacy and safety of non-vitamin K antagonist oral anticoagulant in real-world atrial fibrillation patients. *EP Europace*. (2020) 22 (4):547–57. doi: 10.1093/europace/euz273

14. Raparelli V, Proietti M, Cangemi R, Lip GY, Lane DA, Basili S. Adherence to oral anticoagulant therapy in patients with atrial fibrillation. *Thromb Haemostasis*. (2017) 117(02):209–18. doi: 10.1160/TH16-10-0757

15. Deshpande CG, Kogut S, Willey C. Real-world health care costs based on medication adherence and risk of stroke and bleeding in patients treated with novel anticoagulant therapy. *J Manag Care Spec Pharm*. (2018) 24(5):430–9. doi: 10.18553/jmcp.2018.24.5.430

16. Borne RT, O'Donnell C, Turakhia MP, Varosy PD, Jackevicius CA, Marzec LN, et al. Adherence and outcomes to direct oral anticoagulants among patients with atrial fibrillation: findings from the veterans health administration. *BMC Cardiovasc Disord*. (2017) 17(1):1–7. doi: 10.1186/s12872-017-0671-6

17. An J, Bider Z, Luong TQ, Cheetham TC, Lang DT, Fischer H, et al. Long-term medication adherence trajectories to direct oral anticoagulants and clinical outcomes in patients with atrial fibrillation. *J Am Heart Assoc*. (2021) 10(21):e021601. doi: 10.1161/JAHA.121.021601

18. Desteghe L, Vijgen J, Koopman P, Dilling-Boer D, Schurmans J, Dendale P, et al. Telemonitoring-based feedback improves adherence to non-vitamin K antagonist oral anticoagulants intake in patients with atrial fibrillation. *Eur Heart J*. (2018) 39 (16):1394–403. doi: 10.1093/eurheartj/ehx762

19. Armitage LC, Kassavou A, Sutton S. Do mobile device apps designed to support medication adherence demonstrate efficacy? A systematic review of randomised

controlled trials, with meta-analysis. *BMJ Open*. (2020) 10(1):e032045. doi: 10.1136/bmjopen-2019-032045

20. Weisman O, Schonherz Y, Harel T, Efron M, Elazar M, Gothelf D. Testing the efficacy of a smartphone application in improving medication adherence, among children with ADHD. *Isr J Psychiatry Relat Sci*. (2018) 55(2):59–63.

21. Morawski K, Ghazinouri R, Krumme A, Lauffenburger JC, Lu Z, Durfee E, et al. Association of a smartphone application with medication adherence and blood pressure control: the MedISAFE-BP randomized clinical trial. *JAMA Intern Med*. (2018) 178(6):802–9. doi: 10.1001/jamainternmed.2018.0447

22. Huang Z, Tan E, Lum E, Sloot P, Boehm BO, Car J. A smartphone app to improve medication adherence in patients with type 2 diabetes in Asia: feasibility randomized controlled trial. *JMIR Mhealth Uhealth*. (2019) 7(9):e14914. doi: 10.2196/14914

23. Sarzynski E, Decker B, Thul A, Weismantel D, Melaragni R, Cholakis E, et al. Beta testing a novel smartphone application to improve medication adherence. *Telemed J E Health*. (2017) 23(4):339–48. doi: 10.1089/tmj.2016.0100

24. Yoon CH, Ritchie SR, Duffy EJ, Thomas MG, McBride S, Read K, et al. Impact of a smartphone app on prescriber adherence to antibiotic guidelines in adult patients with community acquired pneumonia or urinary tract infections. *PLoS One*. (2019) 14(1):e0211157. doi: 10.1371/journal.pone.0211157

25. Wu YP, Linder LA, Kanokvimankul P, Fowler B, Parsons BG, Macpherson CF, et al. Use of a smartphone application for prompting oral medication adherence among adolescents and young adults with cancer. *Oncol Nurs Forum*. (2018) 45 (1):69–76. doi: 10.1188/18.ONF.69-76

26. Yu C, Liu C, Du J, Liu H, Zhang H, Zhao Y, et al. Smartphone-based application to improve medication adherence in patients after surgical coronary revascularization. *Am Heart J*. (2020) 228:17–26. doi: 10.1016/j.ahj.2020.06.019

27. Talmor G, Nguyen B, Keibel A, Temelkovska T, Saxon L. Use of software applications to improve medication adherence and achieve more integrated disease management in heart failure. *Trends Cardiovasc Med*. (2018) 28(7):483–8. doi: 10.1016/j.tcm.2018.04.001

28. Johnston N, Bodegard J, Jerstrom S, Akesson J, Brorsson H, Alfredsson J, et al. Effects of interactive patient smartphone support app on drug adherence and lifestyle changes in myocardial infarction patients: a randomized study. *Am Heart J*. (2016) 178:85–94. doi: 10.1016/j.ahj.2016.05.005

29. Kelders SM, Kok RN, Ossebaard HC, Van Gemert-Pijnen JE. Persuasive system design does matter: a systematic review of adherence to web-based interventions. *J Med Internet Res*. (2012) 14(6):e152. doi: 10.2196/jmir.2104

30. Labovitz DL, Shafner L, Reyes Gil M, Virmani D, Hanina A. Using artificial intelligence to reduce the risk of nonadherence in patients on anticoagulation therapy. *Stroke*. (2017) 48(5):1416–9. doi: 10.1161/STROKEAHA.116.016281

31. Turakhia M, Sundaram V, Smith SN, Ding V, Ho PM, Kowey PR, et al. Efficacy of a centralized, blended electronic, and human intervention to improve direct oral anticoagulant adherence: smartphones to improve rivaroxaban ADHEREnce in atrial fibrillation (SmartADHERE) a randomized clinical trial. *Am Heart J*. (2021) 237:68–78. doi: 10.1016/j.ahj.2021.02.023

32. Manzoor BS, Lee TA, Sharp LK, Walton SM, Galanter WL, Nutescu EA. Real-world adherence and persistence with direct oral anticoagulants in adults with atrial fibrillation. *Pharmacotherapy*. (2017) 37(10):1221–30. doi: 10.1002/phar.1989

33. Lip GY, Nieuwlaat R, Pisters R, Lane DA, Crijns HJ. Refining clinical risk stratification for predicting stroke and thromboembolism in atrial fibrillation using a novel risk factor-based approach: the euro heart survey on atrial fibrillation. *Chest*. (2010) 137(2):263–72. doi: 10.1378/chest.09-1584

34. Hwang J, Han S, Bae HJ, Jun SW, Choi SW, Lee CH, et al. NOAC Adherence of patients with atrial fibrillation in the real world: dosing frequency matters? *Thromb Haemost*. (2020) 120(2):306–13. doi: 10.1055/s-0039-1697954

35. Kim I-C, Lee JH, Choi D-J, Park S-J, Lee J-H, Park SM, et al. Rationale design and efficacy of a smartphone application for improving self-awareness of adherence to edoxaban treatment: study protocol for a randomised controlled trial (adhere app). *BMJ Open*. (2022) 12(4):e048777. doi: 10.1136/bmjopen-2021-048777

36. Thakkar J, Kurup R, Laba T-L, Santo K, Thiagalingam A, Rodgers A, et al. Mobile telephone text messaging for medication adherence in chronic disease: a meta-analysis. *JAMA Intern Med*. (2016) 176(3):340–9. doi: 10.1001/jamainternmed.2015.7667

37. Farmer KC. Methods for measuring and monitoring medication regimen adherence in clinical trials and clinical practice. *Clin Ther*. (1999) 21(6):1074–90. doi: 10.1016/S0149-2918(99)80026-5

38. Erdine S, Arslan E. Monitoring treatment adherence in hypertension. *Curr Hypertens Rep*. (2013) 15(4):269–72. doi: 10.1007/s11906-013-0369-9

frontiers | Frontiers in Cardiovascular Medicine

TYPE Original Research
PUBLISHED 13 July 2023
DOI 10.3389/fcvm.2023.1131962

OPEN ACCESS

EDITED BY
Serafino Fazio,
Federico II University Hospital, Italy

REVIEWED BY
Leonidas Poulimenos,
General Hospital Asklepieio Voulas, Greece
Branko Celler,
University of New South Wales, Australia

*CORRESPONDENCE
Fuyou Liang
✉ fuyouliang@sjtu.edu.cn
Jianping Lu
✉ 18930177452@163.com

RECEIVED 26 December 2022
ACCEPTED 23 June 2023
PUBLISHED 13 July 2023

CITATION
Zhang X, Jiang Y, Liang F and Lu J (2023) Threshold values of brachial cuff-measured arterial stiffness indices determined by comparisons with the brachial–ankle pulse wave velocity: a cross-sectional study in the Chinese population.
Front. Cardiovasc. Med. 10:1131962.
doi: 10.3389/fcvm.2023.1131962

Threshold values of brachial cuff-measured arterial stiffness indices determined by comparisons with the brachial–ankle pulse wave velocity: a cross-sectional study in the Chinese population

Xujie Zhang[1], Yumin Jiang[2], Fuyou Liang[1,3]* and Jianping Lu[2]*

[1]Department of Engineering Mechanics, School of Naval Architecture, Ocean & Civil Engineering, Shanghai Jiao Tong University, Shanghai, China, [2]Physical Examination Center, Shanghai Sixth People's Hospital, Shanghai Jiao Tong University School of Medicine, Shanghai, China, [3]World-Class Research Center "Digital biodesign and personalized healthcare", Sechenov First Moscow State Medical University, Moscow, Russia

Background: Arterial Velocity-pulse Index (AVI) and Arterial Pressure-volume Index (API), measured by a brachial cuff, have been demonstrated to be indicative of arterial stiffness and correlated with the risk of cardiovascular events. However, the threshold values of AVI and API for screening increased arterial stiffness in the general population are yet to be established.

Methods: The study involved 860 subjects who underwent general physical examinations (M/F = 422/438, age 53.4 ± 12.7 years) and were considered to represent the general population in China. In addition to the measurements of AVI, API and brachial-ankle pulse wave velocity (baPWV), demographic information, arterial blood pressures, and data from blood and urine tests were collected. The threshold values of AVI and API were determined by receiver operating characteristic (ROC) analyses and covariate-adjusted ROC (AROC) analyses against baPWV, whose threshold for diagnosing high arterial stiffness was set at 18 m/s. Additional statistical analyses were performed to examine the correlations among AVI, API and baPWV and their correlations with other bio-indices.

Results: The area under the curve (AUC) values in ROC analysis for the diagnosis with AVI/API were 0.745/0.819, 0.788/0.837, and 0.772/0.825 (95% CI) in males, females, and all subjects, respectively. Setting the threshold values of AVI and API to 21 and 27 resulted in optimal diagnosis performance in the total cohort, whereas the threshold values should be increased to 24 and 29, respectively, in order to improve the accuracy of diagnosis in the female group. The AROC analyses revealed that the threshold values of AVI and API increased markedly with age and pulse pressure (PP), respectively.

Conclusions: With appropriate threshold values, AVI and API can be used to perform preliminary screening for individuals with increased arterial stiffness in the general population. On the other hand, the results of the AROC analyses imply that using threshold values adjusted for confounding factors may facilitate the refinement of diagnosis. Given the fact that the study is a cross-sectional one carried out in a single center, future multi-center or follow-up studies are required to further confirm the findings or examine the value of the threshold values for predicting cardiovascular events.

KEYWORDS

arterial stiffness index, brachial cuff, arterial velocity-pulse index, arterial pressure-volume index, threshold value, brachial-ankle pulse wave velocity

1. Introduction

Arterial stiffness is a measure of the mechanical properties of the arterial wall, which determines the systolic and pulse pressures, thereby affecting the dynamic tension of arteries and the systolic load of the left ventricle (1). The stiffness of large elastic arteries increases progressively during aging as a consequence of wall thickening, changes in wall composition, and elastin degeneration (2). Many risk factors such as diabetes mellitus, hypertension, obesity, smoking, and kidney disease can accelerate arterial stiffening (3, 4). The value of arterial stiffness in predicting the risk of cardiovascular events has been extensively proven in both clinical and community-based cohorts (5–8). Moreover, the benefits of using arterial stiffness indices to guide the treatment of hypertension have also been demonstrated (9).

Over the past few decades, various non-invasive techniques for measuring arterial stiffness have been proposed. Among them, pulse wave velocity (PWV) measurement is widely accepted as the "standard" method due to its clear biophysical meaning (10–12). Two commonly used global PWV metrics are carotid-femoral PWV (cfPWV) and brachial-ankle PWV (baPWV) (10, 13). In eastern Asia, baPWV has been more widely used than cfPWV, enabling the accumulation of a large amount of data on the clinical implications of baPWV. Moreover, there are other arterial stiffness indices, such as carotid intima-media thickness (Carotid IMT), augmentation index (AIx), and cardio-ankle vascular index (CAVI), that have been proved to have potential clinical value (14–19). However, their applications in routine clinical practice remain challenging due to technical or economic reasons. **Table 1** summarizes the strengths and limitations of various existing arterial stiffness indices. In this context, economically feasible and easier-to-use devices are desired. Such devices may facilitate routine screening for increased arterial stiffness in larger populations, thereby guiding the implementation of preventive interventions for individuals at an increased risk of cardiovascular disease (35, 36).

PASESA AVE-2000 (DAIWA Healthcare, Shenzhen, China) offers a fully automatic and rapid measurement of arterial stiffness, which can be easily implemented by clinicians or even by patients themselves. The compact and economical design of the device, which uses a single oscillatory brachial cuff to noninvasively measure physiological signals, makes it ideal for routine clinical use. The device provides two arterial stiffness indices, Arterial Velocity-pulse Index (AVI) and Arterial Pressure-volume Index (API), which respectively reflect the stiffness of the central arteries and brachial artery. The potential clinical value of AVI and API has been confirmed by many clinical studies. For example, AVI and/or API have been found to be significantly correlated with major adverse cardiac events during follow-up of outpatients (37), associated with the Framingham cardiovascular disease risk score in both outpatients

TABLE 1 Strengths and limitations of various arterial stiffness indices.

Indices	Strengths	Limitations
baPWV	• baPWV indicates the average stiffness of central and peripheral arteries in the upper and lower limbs (13) and is well-validated, providing good reproducibility (20). • baPWV has been demonstrated to be independently correlated with adverse cardiovascular events (20, 21) or the prognosis of chronic diseases like metabolic syndrome, type 2 diabetes, and kidney dysfunction (22–24).	• Some patients may feel uncomfortable due to long measurement time and postural requirement. • The equipment is pricey and necessitates skilled handling by professionals.
cfPWV	• cfPWV is considered the gold standard for arterial stiffness (10) and mainly reflects the stiffness of central arteries (13). • cfPWV has been shown to be a strong predictor of cardiovascular events and all-cause mortality (25) and has been extensively validated in various populations, including the elderly, diabetic patients, and patients with chronic kidney disease (26–28).	• Some patients might feel uneasy or embarrassed about exposing the inguinal area during the measurement of femoral pressure waveforms (13). • The measurement of cfPWV is technically challenging, and requires expertise and complex equipment.
Carotid IMT	• Carotid IMT is an intermediate phenotype for early atherosclerosis and can act as a surrogate marker for atherosclerosis (14). • Carotid IMT is associated with various cardiovascular risk factors and prevalent cardiovascular disease (CVD) (29), and is an independent predictor of cardiovascular events such as stroke and myocardial infarction (15).	• Carotid IMT assessment is a time-consuming and operator-dependent procedure (30), requiring training, experience, and standardized techniques. • Carotid IMT assessment can only be used to evaluate the carotid arteries, and cannot provide information on other areas of the vascular system.
AIx	• AIx is a measure of systemic arterial stiffness that is derived from the ascending aortic pressure waveform (16). • AIx can predict clinical events independently of peripheral pressures and has been shown to hold significant predictive value for cardiovascular events and all-cause mortality in various populations (17, 31).	• There is no standardized methodology for measuring AIx. • Arterial tonometry devices required to measure AIx are expensive and not widely available.
CAVI	• CAVI measures the stiffness of the arterial tree from the aorta to the ankle (32) and is independent of blood pressure changes during the measurements (33). • CAVI has been widely applied to assess high-risk populations, such as those at risk of developing or who have already developed coronary artery disease, cerebrovascular disease, diabetes mellitus, and chronic kidney disease (18, 19).	• CAVI cannot be accurately measured in patients with aortic stenosis, peripheral artery disease, or atrial fibrillation (34). • CAVI measurements should only be performed by trained medical professionals while the patient is in the supine position.

and the general population (38, 39), and predicative of early coronary artery atherosclerosis in patients with suspected coronary disease (40) and cardiovascular risk in hypertensive patients (41). These studies demonstrated the clinical implications of AVI and API, but did not provide threshold values for identifying subjects with abnormally high arterial stiffness in the general population. Therefore, the main purpose of this study was to fill this gap. For this purpose, we collected data from adult participants who underwent a general health check at the physical examination center. The study cohort was comprised of individuals aged in a large range, including both healthy subjects and patients with cardiovascular diseases, and was therefore considered to be representative of the general population in China. The threshold values of AVI and API for diagnosing high arterial stiffness were determined by using baPWV as the reference. The results demonstrated that given proper threshold values, AVI and API could be utilized to identify individuals with increased arterial stiffness. On the other hand, the threshold values were gender-dependent and considerably affected by certain confounding factors.

2. Methods

2.1. Study population

A total of 860 subjects, who were aged between 20 and 91 years and visited the physical examination center of Shanghai Sixth People's Hospital for a general health check, were recruited. The study was approved by the ethics committee of the hospital. Each participant provided written informed consent after receiving detailed information about the study's goals and procedures. Before data collection, each participant completed a written questionnaire about their medical history, including hypertension, major cardiovascular diseases, type 2 diabetes mellitus, any other cardiovascular-related abnormalities, and medications. Notably, participants without any reported diseases on the questionnaire were categorized into a disease group if their health check results indicated the presence of cardiovascular-related diseases. In this study, healthy subjects were those who did not suffer from hypertension, type 2 diabetes mellitus, dyslipidemia, obesity, or other cardiovascular diseases based on the questionnaire and health check report.

2.2. Measurements of AVI, API and baPWV

The measurements of AVI, API and baPWV were conducted in a separate room with a controlled environmental temperature of approximate 25°C. Each participant was asked to rest for at least 10 min before the measurements were taken. Firstly, AVI and API were measured together with brachial systolic pressure, diastolic pressure, and heart rate, in a sitting position using a commercial medical device (PASESA AVE-2000, DAIWA Healthcare, Shenzhen, China). Subsequently, the participant was asked to rest in a supine position for at least 5 min, and then baPWV was measured using BP-203RPEIII (Omron, Dalian, China). The reliability and validity of the baPWV device have been confirmed by a previous study (20). In this study, a baPWV of >18 m/s, as recommended in the guidelines for non-invasive vascular function tests (42), was adopted as the threshold for diagnosing high arterial stiffness. Hereafter, we briefly introduce the measuring principles of AVI and API.

AVI is calculated by analyzing the oscillation waves measured by a brachial cuff operating under high-pressure conditions (higher than the brachial systolic pressure). **Figure 1** illustrates the cuff oscillation waves and their first-order differentials measured in a middle-aged subject and an old subject, respectively. It can be observed that the second valley of the differentiated cuff oscillation wave in the old subject is lower than that in the middle-aged subject, whereas the peak is comparable between the two subjects. AVI is defined as the ratio

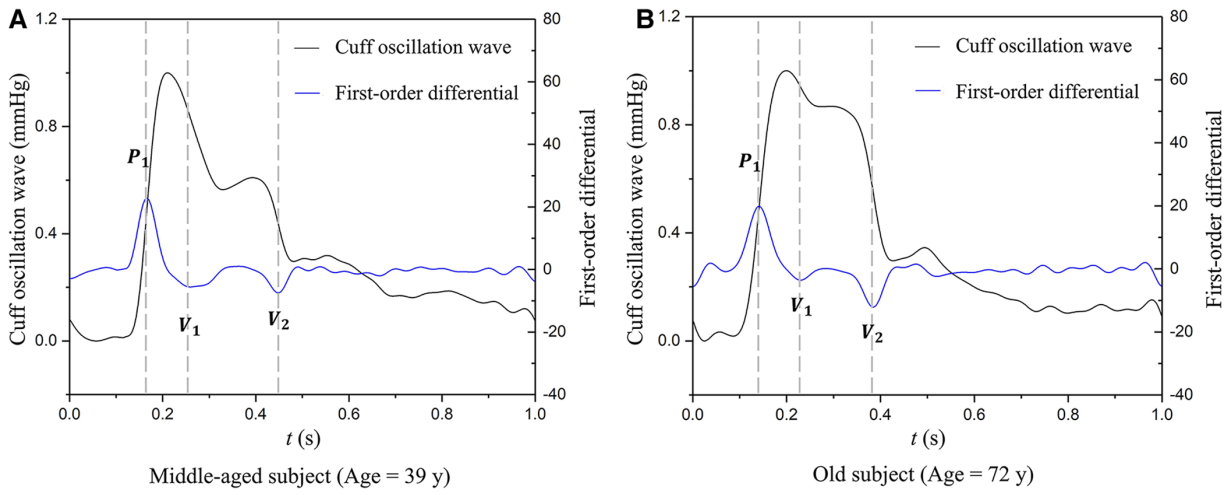

FIGURE 1
Examples of cuff oscillation waves (measured when the cuff operating pressure is higher than the brachial systolic pressure) and their first-order differentials used to calculate AVI: (A) data of a middle-aged subject, (B) data of an old subject. P_1, the first peak; V_1, the first valley; V_2, the second valley.

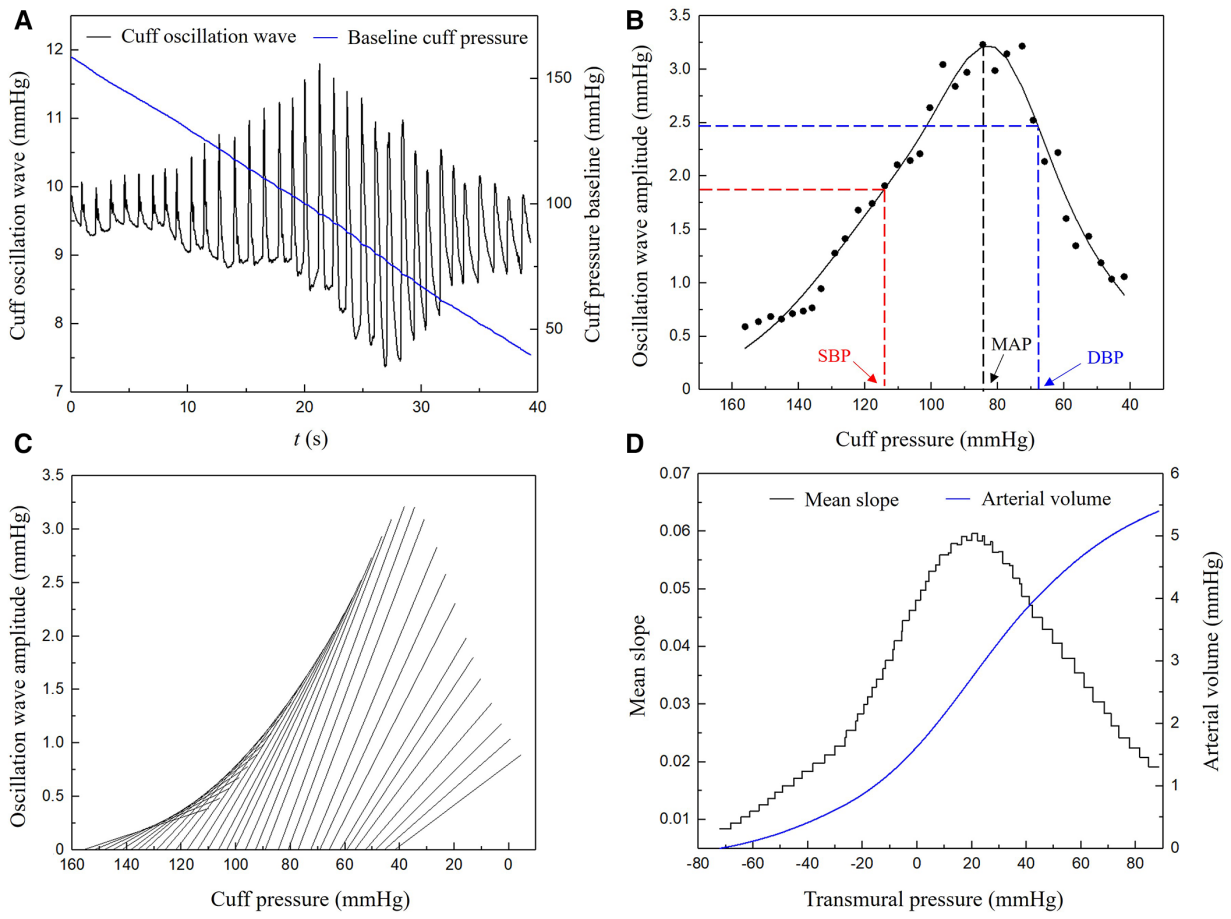

FIGURE 2
Procedure of deriving a pressure-vascular volume characteristic curve from measured time series cuff pressure: (A) baseline cuff pressure and cuff oscillation wave, (B) envelope curve and the estimation of brachial blood pressures, (C) local slopes of the cuff pressure-arterial volume characteristic curve, (D) arterial transmural pressure-volume characteristic curve. SBP, systolic blood pressure; DBP, diastolic blood pressure; MAP, mean blood pressure.

of the magnitude of the second valley ($|V_2|$) to that of the peak ($|P|$) multiplied by a constant (A).

$$\mathrm{AVI} = A \times |V_2|/|P| \tag{1}$$

API is calculated by analyzing the time series cuff oscillation waves monitored during the decrease of cuff pressure from a supra-systolic pressure level to a value lower than the diastolic pressure (43). The measuring principle is based on the biomechanical mechanism that the shape of the transmural pressure-area (or volume) curve of an artery is mainly determined by the stiffness of arterial wall when the transmural pressure is varied over a wide range. To construct this curve using noninvasively measured cuff signals, the following procedure was implemented: (1) digitally filter the original cuff pressure data to extract the time series baseline cuff pressure and oscillation component (i.e., oscillation waves) (**Figure 2A**); (2) construct the envelope curve based on the amplitudes of oscillation waves and estimate brachial blood pressures (**Figure 2B**); (3) calculate the local slopes of the cuff pressure—arterial volume characteristic curve (**Figure 2C**); and (4) reconstruct the arterial transmural pressure—volume characteristic curve by numerically integrating the slopes obtained in step 3) (**Figure 2D**). Finally, an arctangent function was used to fit the curve.

$$f(x) = a \arctan(bx + c) + d \tag{2}$$

where the reciprocal of b was taken as an indirect measure of the vascular wall stiffness under low transmural pressure conditions. API is defined as

$$\mathrm{API} = X \times 1/b \tag{3}$$

where X is a constant used to scale up the magnitude of API.

For a more detailed introduction of the measuring principles of AVI and API, please refer to the **Supplementary Material**.

2.3. Other measurements

All participants had their height and weight measured, and their body mass indices (BMIs) were calculated to evaluate

obesity. Blood samples were collected for laboratory examinations of indices considered to be related to diabetes mellitus or cardiovascular diseases, including fasting plasma glucose (FPG), glycated hemoglobin (HbA1c), total cholesterol (TC), triglycerides (TG), high-density lipoprotein cholesterol (HDL-C) and low-density lipoprotein cholesterol (LDL-C). The lipoprotein ratios (TC/HDL-C, LDL-C/HDL-C) were also calculated. In addition, urine samples were analyzed for microalbumin (UMAlb).

2.4. Statistical analysis

Baseline characteristics were presented separately for the male, female and pooled groups in form of either median and interquartile range or percentage. Statistical analyses were implemented in SPSS 24. Comparison of percentage values was performed using the Chi-square test. When comparing the quantitative data between the male and female groups, the student's *t*-test was employed if the data conform to a normal distribution, otherwise, the Mann–Whitney *U*-test was performed. Pearson or Spearman rank correlation analysis was applied to evaluate the correlations among AVI, API, baPWV and their correlations with other variables based on the results of normality test. The stepwise multiple linear regression analyses were carried out to evaluate the independent associations of AVI, API, baPWV with other bio-indices. Moreover, receiver-operating characteristic (ROC) curve analyses and covariate-adjusted ROC (AROC) analyses (44) were carried out to seek for the threshold values of AVI and API, where the sum of sensitivity and specificity was used as the criterion for evaluating diagnosis performance. Statistical significance was defined as $p < 0.05$.

3. Results

3.1. Characteristics of participants

Table 2 shows the diagnostic criteria for diseases and the disease-specific distributions of participants. The proportions of hypertension and type 2 diabetes in the study cohort were comparable to the prevalence of these diseases in Chinese adults as reported in the "2019 Report on Cardiovascular Health and Diseases in China and a national cross-sectional study on diabetes" (45) (hypertension: 30.8% vs. 33.5%; type 2 diabetes: 11.5% vs. 12.8%). Hence, the subjects involved in our study are roughly representative of the general Chinese population. The 860 participants constituted a pooled group, which was further divided into the male and female groups. The characteristics of participants in the three groups are presented in Table 3. There were no significant differences in demographic data between the male and female groups, except for BMI, DBP, MAP and HR. Serum lipid indices differed significantly between the male and female groups, with females having higher TC and HDL-C, and lower TG and lipoprotein ratios (TC/HDL-C, LDL-C/HDL-C). Overall, the proportion of females with dyslipidemia was much smaller than that of males. In addition, males had a significantly higher prevalence of hypertension and type 2 diabetes mellitus compared to females. If the subjects with hypertension were divided into the treated and untreated subgroups, SBP [139.96 ± 19.20 vs. 146.78 ± 17.69 (mmHg), $p = 0.002$], MAP [100.04 ± 16.49 vs. 104.41 ± 12.89 (mmHg), $p = 0.031$] and the three arterial stiffness indices [baPWV: 16.63 ± 3.23 vs. 17.74 ± 3.69 (m/s), $p = 0.005$; AVI: 21.81 ± 7.95 vs. 26.46 ± 8.64, $p < 0.0001$; API: 29.79 ± 8.06 vs. 32.69 ± 7.44, $p < 0.0001$] were all slightly lower in the treated subgroup, indicating the role of antihypertensive treatment in reducing arterial stiffness.

TABLE 2 Distributions of diseases in the studied population.

Diseases	*n* (%)	Diagnostic criteria
Hypertension	265 (30.8%)	Systolic blood pressure (SBP) > 140 mmHg, diastolic blood pressure (DBP) > 90 mmHg, or history of drug treatment for hypertension
Type 2 diabetes mellitus	99 (11.5%)	Fasting plasma glucose (FPG) ≥ 7.0 mmol/L, oral glucose tolerance test: two-hour plasma glucose ≥11.1 mmol/L, glycated haemoglobin (HbA1c) ≥ 6.5%, or history of treatment with insulin or an oral hypoglycemic agent
Major cardiovascular diseases	25 (2.9%)	History of diagnosed or treated cardiovascular diseases including but not limited to stroke, coronary heart disease, heart failure, or peripheral arterial disease

3.2. Differences of AVI, API and baPWV between male and female groups

The Mann–Whitney *U*-test was performed to compare AVI, API and baPWV between the male and female groups in different age brackets. The mean values and standard deviations (SDs) of the arterial stiffness indices grouped by sex and age brackets are presented in Figure 3. AVI, API and baPWV all increased with age. In the age bracket of <40 years, the mean values of AVI and API in the female group were significantly lower than those in the male group (AVI: $p < 0.0001$, API: $p = 0.03$), and the mean values of baPWV in the female group remained lower than those in the male group until the age increased over 50 years (<40 years: $p < 0.0001$, 40–49 years: $p < 0.0001$). In the age brackets of >50 years, all the arterial stiffness indices increased more rapidly with age in the female group, leading to obviously higher AVI, API and baPWV in older females.

3.3. Results of correlation analysis and regression analysis

In this study, since all datasets did not exhibit a strict normal distribution, the Spearman correlation analysis was performed in conjunction with Bonferroni correction for *p*-value thresholds to examine the pairwise correlations among AVI, API and baPWV, and their correlations with other bio-indices in the male, female and pooled groups, respectively. Figure 4 presents the results in the form of a heat map where gradually changing colors denote the strength of correlation while the white color indicates the

TABLE 3 Characteristics of the studied subjects.

	Male ($n = 422$)	Female ($n = 438$)	Pooled ($n = 860$)	p Value
Demographic data				
Age (years)	53.00 (45.00–62.00)	53.00 (46.00–62.00)	53.00 (45.00–62.00)	0.461
Gender (m/f %)	100.00/0.00	0.00/100.00	49.07/50.93	0.440
BMI (kg/m²)	24.39 (22.56–26.61)	22.99 (21.08–25.15)	23.66 (21.77–25.97)	<0.001***
SBP (mmHg)	127.00 (115.00–138.00)	124.00 (110.00–138.00)	125.00 (113.00–138.00)	0.079
DBP (mmHg)	78.00 (71.00–85.00)	73.00 (65.00–82.00)	76.00 (68.00–84.00)	<0.001***
MAP (mmHg)	94.33 (86.00–102.33)	90.00 (80.67–100.67)	92.67 (83.33–102.00)	<0.001***
HR (bpm)	78.00 (71.00–85.00)	72.00 (67.00–81.00)	72.00 (66.00–80.00)	0.029*
Laboratory data				
FPG (mmol/L)	5.11 (4.82–5.62)	5.11 (4.80–5.48)	5.11 (4.80–5.52)	0.195
HbA1c (%)	5.50 (5.40–5.80)	5.60 (5.40–5.80)	5.50 (5.40–5.80)	0.571
TC (mmol/L)	4.84 (4.23–5.44)	4.93 (4.36–5.60)	4.89 (4.31–5.52)	0.020*
TG (mmol/L)	1.74 (1.21–2.46)	1.31 (0.93–1.86)	1.49 (1.04–2.18)	<0.001***
LDL-C (mmol/L)	3.07 (2.58–3.67)	3.13 (2.56–3.71)	3.10 (2.57–3.68)	0.549
HDL-C (mmol/L)	1.15 (0.94–1.37)	1.41 (1.19–1.68)	1.28 (1.05–1.55)	<0.001***
TC/HDL-C	4.18 (3.45–4.97)	3.50 (2.91–4.28)	3.83 (3.10–4.65)	<0.001***
LDL-C/HDL-C	2.68 (2.06–3.29)	2.23 (1.71–2.84)	2.44 (1.86–3.11)	<0.001***
UMAlb (+/− %)	11.14/88.86	9.36/90.64	10.23/89.77	0.390
Clinical diagnosis				
Hypertension (treatment) (%)	34.83 (62.59)	26.94 (55.08)	30.81 (59.25)	0.012* (0.002**)
Type 2 diabetes mellitus (%)	14.69	8.45	11.51	0.004**
Cardiovascular disease (%)	3.79	2.97	3.37	0.504
Dyslipidemia (%)	52.61	34.02	43.14	<0.001***
Obesity (%)	12.09	8.90	10.47	0.128

BMI, body mass index; SBP, systolic blood pressure; DBP, diastolic blood pressure; MAP, mean blood pressure; HR, heart rate; FPG, fasting plasma glucose; HbA1c, glycated haemoglobin; TC, total cholesterol; TG, triglycerides; LDL-C, low-density lipoprotein cholesterol; HDL-C, high-density lipoprotein cholesterol; UMAlb, urine microalbumin. Data are presented in form of median (IQR) or percentage.
*$p < 0.05$.
**$p < 0.01$.
***$p < 0.001$ vs. male group.

lack of a statistically significant correlation between two indices. Herein, the statistical significance was defined as $p < 0.00263$ ($0.05/n$, where n denotes the number of selected variables in Bonferroni correction).

AVI and API were both positively correlated with baPWV, and the correlations were especially strong in the female group. AVI, API and baPWV were most strongly correlated with age, PP, and age & SBP, respectively ($r > 0.6$) in the pooled population, and

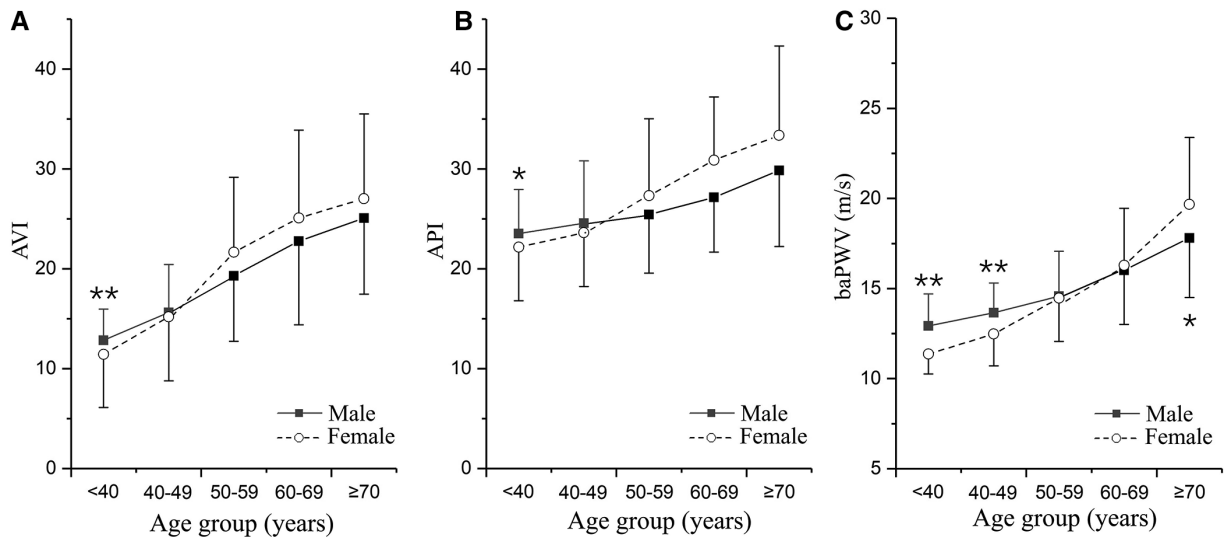

FIGURE 3
Changes in arterial stiffness indices with age differentiated by sex: (A) AVI, (B) API, and (C) baPWV. The plotted data are the means and standard deviations of arterial stiffness indices in different age groups. The numbers of males and females in the five age groups are as follows: <40 years, $n = 56/49$; 40–49 years, $n = 116/116$; 50–59 years, $n = 113/130$; 60–69 years, $n = 96/100$; and ≥70 years, $n = 41/43$. *$p < 0.05$, **$p < 0.01$ vs. male group.

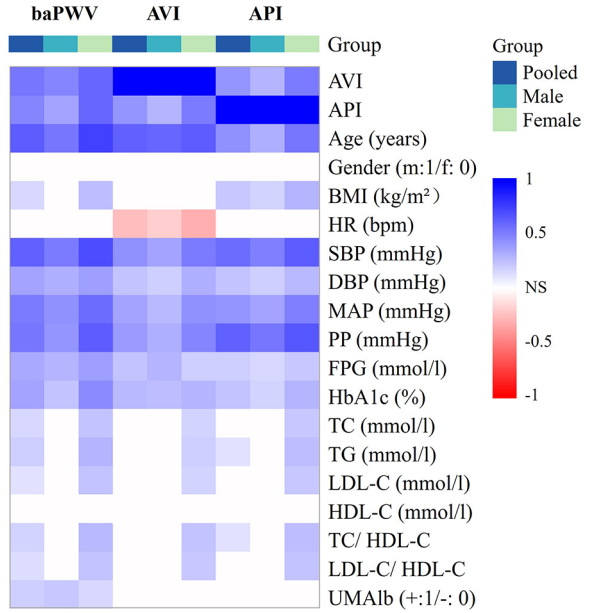

FIGURE 4
Heat map of the correlations among arterial stiffness indices and their correlations with other bio-indices.

the strong correlations were more evident in the female group. The stepwise multiple regression analysis was carried out to further identify the associated factors of AVI, API and baPWV for the male, female and pooled groups, respectively. The results showed that SBP, age, HR and FPG were positively associated with baPWV in all groups, gender and TG were positively associated with baPWV in the pooled group, whereas UMA1b was associated with baPWV only in the male group. Age, MAP and HR were the main relevant factors of AVI, and FPG was associated with AVI only in the male group. PP, BMI and age were significantly associated with API in the male group, whereas PP, age, SBP and HDL-C were significantly associated with API in the female group (**Table 4**).

3.4. Results of ROC analysis and AROC analysis

In order to determine the optimal threshold values of AVI and API for diagnosing high arterial stiffness, we took the results of diagnosis with baPWV as the reference to perform ROC analysis. In consideration of potential sex differences, the threshold values of AVI and API were determined separately for the male, female and pooled groups. **Figure 5** plots the results of ROC analyses with optimized threshold values of AVI and API, and the quantitative data are summarized in **Table 5**. The values of AUC (95% CI) for diagnosis with AVI/API were 0.745/0.819, 0.788/0.837, and 0.772/0.825 in males, females, and all subjects, respectively. In all groups, the larger AUC values of API indicate its better diagnosis performance than AVI, which can also be judged from the ROC curves plotted in **Figure 5**. In addition, the threshold values of AVI and API were both larger in females than in males, which led to mildly improved diagnosis performance for the female group. Furthermore, we carried out covariate-adjusted ROC (AROC) analysis (44) to investigate the influences of confounding factors (those identified by the multiple regression analysis for AVI or API). We set two confounding factors associated most closely with AVI or API as covariates and analyzed the data of the pooled group only. **Figure 6** shows that the threshold values of AVI and API changed markedly with the variations in covariate values. Specifically, the threshold value of AVI increased markedly with age and moderately with MAP, whereas the threshold value of API increased evidently with PP and mildly with BMI.

4. Discussion

Increased arterial stiffness, an important risk factor for cardiovascular diseases, remains under-diagnosed in the general population. Despite the existence of well-validated devices for measuring arterial stiffness indices such as baPWV or cfPWV, these devices are usually costly, require professional operations, and take over 10 min to complete measurement, which significantly hampers their wide use in routine medical practice. The present study attempted to determine the threshold values of arterial stiffness indices (i.e., AVI and API) measured by a cuff-based device (PASESA AVE-2000) in the general Chinese population by referring to the diagnosis results with baPWV. The threshold values of AVI and API giving rise to optimal diagnosis performance (evaluated by AUC values in ROC analysis) in the entire cohort were found to be 21 and 27, respectively, with corresponding AUC values of 0.767 and 0.825. If evaluated separately for the female and male groups, the diagnosis performances could be slightly improved in the female group if the threshold values of AVI and API were increased to 24 and 29, respectively. These results imply that AVI and API measured by the cuff-based device have the potential to be used as substitutes for baPWV in the assessment of arterial stiffness. In particular, since the device is portable and easy to use like a general blood pressure device, it may be employed to perform large-scale screening for individuals with high arterial stiffness in daily medical activities. Given the well-established value of arterial stiffness in predicting cardiovascular events, early diagnosis of high arterial stiffness would help initiate early preventative interventions (e.g., changes in lifestyle or medical treatment) that have been widely recognized as cost-effective strategies for reducing the risk of cardiovascular diseases (46, 47). AVI and API may also be used as complementary bio-indices for ambulatory PWV and ambulatory blood pressure (ABP), which can be measured outside the hospital and have been proved to have specific value in evaluating antihypertensive treatment or identifying individuals with an increased cardiovascular risk (48, 49), to strengthen the reliability of diagnosis.

Previous clinical studies have demonstrated the potential of threshold values of AVI and API for stratifying the cardiovascular risk of patients. For instance, setting the threshold

TABLE 4 Results of stepwise multiple regression analysis for arterial stiffness indices with respect to bio-indices.

baPWV									
	Pooled			Male			Female		
Adjusted R-squared value	0.623			0.518			0.699		
Variables	*β*	SE	*p*	*β*	SE	*p*	*β*	SE	*p*
SBP (mmHg)	0.065	0.004	<0.001	0.049	0.006	<0.001	0.069	0.005	<0.001
Age (years)	0.116	0.007	<0.001	0.107	0.009	<0.001	0.121	0.010	<0.001
HR (bpm)	0.051	0.006	<0.001	0.056	0.009	<0.001	0.049	0.009	<0.001
FPG (mmol/L)	0.241	0.054	<0.001	0.196	0.072	0.006	0.339	0.083	<0.001
Gender (m:1/f: 0)	0.387	0.143	0.007	NS	NS	NS	NS	NS	NS
TG (mmol/L)	0.127	.056	0.024	NS	NS	NS	NS	NS	NS
UMA1b (+:1/−: 0)	NS	NS	NS	0.739	0.331	0.026	NS	NS	NS
AVI									
	Pooled			Male			Female		
Adjusted R-squared value	0.370			0.307			0.438		
Variables	*β*	SE	*p*	*β*	SE	*p*	*β*	SE	*p*
Age (years)	0.285	0.022	<0.001	0.245	0.027	<0.001	0.299	0.034	<0.001
MAP (mmHg)	0.178	0.020	<0.001	0.110	0.028	<0.001	0.213	0.028	<0.001
HR (bpm)	−0.141	0.021	<0.001	−0.105	0.028	<0.001	−0.206	0.031	<0.001
FPG (mmol/L)	NS	NS	NS	0.432	0.216	0.046	NS	NS	NS
API									
	Pooled			Male			Female		
Adjusted R-squared value	0.431			0.310			0.498		
Variables	*β*	SE	*p*	*β*	SE	*p*	*β*	SE	*p*
PP (mmHg)	0.177	0.027	<0.001	0.232	0.025	<0.001	0.142	0.037	<0.001
BMI (kg/m^2)	0.382	0.068	<0.001	0.446	0.091	<0.001	NS	NS	NS
Age (years)	0.078	0.020	<0.001	0.081	0.025	0.001	0.117	0.031	<0.001
Gender (m:1/f: 0)	−1.675	0.426	<0.001	NS	NS	NS	NS	NS	NS
SBP (mmHg)	0.074	0.020	<0.001	NS	NS	NS	0.117	0.026	<0.001
HR (bpm)	−.043	0.018	0.017	NS	NS	NS	NS	NS	NS
HDL-C (mmol/L)	NS	NS	NS	NS	NS	NS	−2.666	0.816	0.001

β, regression coefficient; SE, standard error.

value of AVI to 27 was found capable of predicting major adverse cardiac events (MACEs) in outpatients in Japan (37). In Japanese patients suffering from heart failure with preserved ejection fraction (HFpEF), AVI > 30 was predictive of high E/e' ratio and high levels of high-sensitivity cardiac troponin T (hs-cTnT) (50). With respect to API, patients with API > 32 were found to suffer from a significantly increased risk of MACEs during a mean follow-up period of 769 ± 275 days (37). Similarly, a study on Chinese hypertensive patients with HFpEF (41) demonstrated that an increase in AVI over 27 or API over 31 was associated

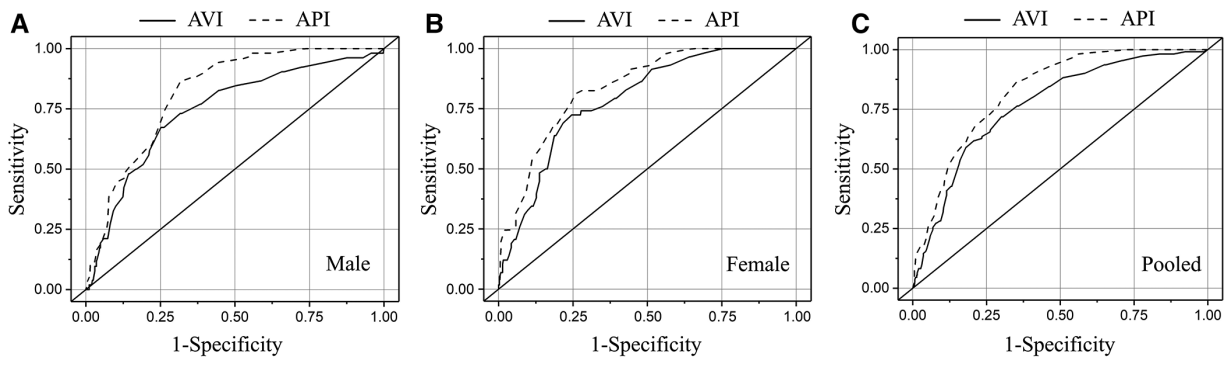

FIGURE 5
Results of ROC analyses on the diagnosis performances of AVI and API in different groups: (A) male, (B) female, and (C) pooled.

TABLE 5 Threshold values of AVI and API and the corresponding results of ROC analysis on the diagnosis performance.

	AUC (95% CI)	SE	Threshold	Sensitivity	Specificity	PPV	NPV	Accuracy	*p*
Male									
AVI	0.745 (0.672, 0.817)	0.037	21	0.673	0.749	0.273	0.942	0.739	<0.0001
API	0.819 (0.747, 0.891)	0.037	27	0.865	0.683	0.278	0.973	0.705	<0.0001
Female									
AVI	0.788 (0.729, 0.857)	0.035	24	0.724	0.755	0.311	0.947	0.751	<0.0001
API	0.837 (0.766, 0.898)	0.031	29	0.807	0.750	0.326	0.963	0.757	<0.0001
Pooled									
AVI	0.767 (0.717, 0.817)	0.026	21	0.718	0.700	0.260	0.944	0.702	<0.0001
API	0.825 (0.779, 0.872)	0.024	27	0.862	0.649	0.264	0.970	0.676	<0.0001

SE, standard error; AUC, area under curve; PPV, positive predictive value; NPV, negative predictive value.

with an increased risk of total cardiovascular events during follow-up. In our study, the relatively low threshold values of AVI and API may be explained by the following reasons: (1) we used baPWV > 18 m/s as the criterion for judging high arterial stiffness, which is associated with but not equivalent to the risk of cardiovascular events, and (2) our study was focused on the general population whose heath conditions are overall better than those of the outpatients investigated by previous studies. Nevertheless, adopting relatively conservative threshold values for AVI and API may facilitate the identification of individuals with potential cardiovascular risk from the general population for whom early preventive interventions would be especially necessary and beneficial.

Our study demonstrated that AVI and API differed evidently between females and males, especially with respect to their changes with age and the threshold values. While the threshold values of AVI and API in the male group were the same with those determined for the entire cohort, they were 3 and 2 units higher respectively in the female group. Accordingly, the diagnosis performance in the female group was slightly improved if higher threshold values of AVI and API were used (see Table 5), which implies that adopting gender-specific threshold values for AVI and API may facilitate more accurate identification of females with abnormally high arterial stiffness. The results may be explained by the different sensitivities of AVI, API and baPWV to age between females and males. As shown in Figure 3, AVI and API increase more rapidly with age in females than in males, especially when ages are higher than 50 years. Such gender differences are also observed for baPWV, but are relatively small. Mechanisms underlying the observations are complex and may involve multiple factors. Hormones, especially estrogen, play an important role in modulating arterial stiffness. Estrogen has been found to stimulate the release of nitric oxide, thereby contributing to improving the elasticity of blood vessels and reducing arterial stiffness (51, 52). However, the protective role of estrogen is markedly attenuated in postmenopausal women (aged over 45–55 years) (53) due to decreased estrogen secretion, causing arterial stiffness to increase rapidly with age (54, 55). It has been found that isolated systolic hypertension (ISH) preferentially affects old women (56), which may also contribute to the increase of arterial stiffness via its roles in promoting vascular thickening and fibrosis (57). In addition, aged women are more susceptible to the decrease in muscle mass and accumulation of visceral fat, both of which have been proved

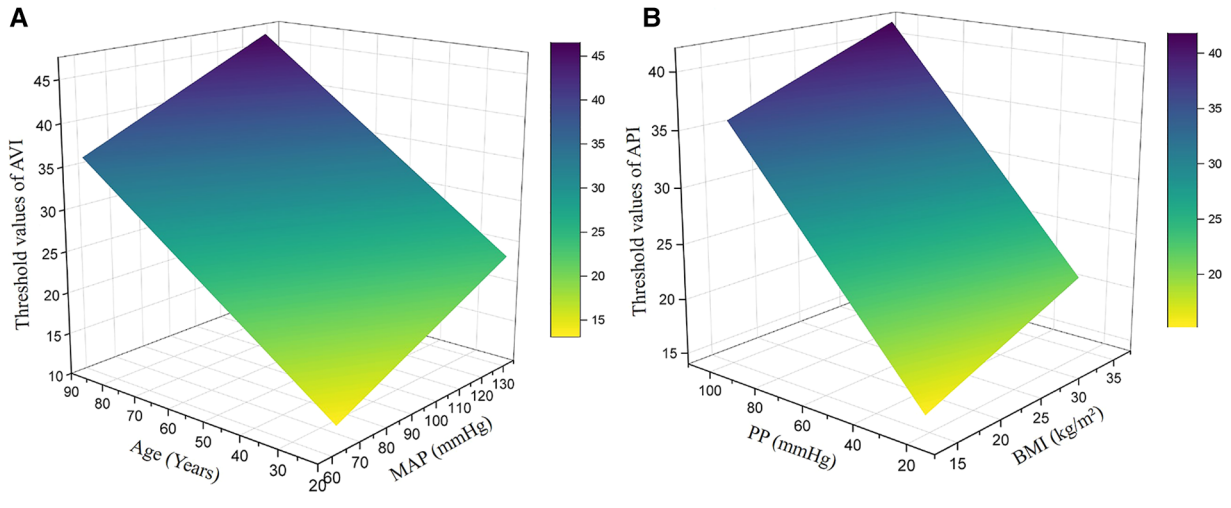

FIGURE 6
Threshold values of AVI and API in the pooled group after adjustment for major covariates: (**A**) AVI, (**B**) API. The major covariates were age and MAP for AVI, and PP and BMI for API.

to be associated with increased arterial stiffness in postmenopausal women (58, 59). These factors underline the need to take gender-related characteristics into account when diagnosing and managing arterial stiffness.

Many bio-indices were found to be correlated with AVI and API, which could be confounding factors compromising the validity of the threshold values of AVI and API determined by the general ROC analysis. To address the issue, we performed covariate-adjusted ROC (AROC) analyses on the pooled group, with major confounding factors identified by the multiple regression analysis being set as the covariates. The results revealed that age and PP were the two confounding factors that most evidently affect the threshold values of AVI and API, respectively. Specifically, the higher the age and PP were, the higher the adjusted threshold values of AVI and API became. The influence of age on the threshold value of AVI can be explained by the high sensitivity of AVI to age as indicated by the data presented in **Figure 3A**. As for PP, it significantly affects the threshold value of API because PP is a variable directly involved in the calculation of API (43). Therefore, adopting confounding factor-adjusted threshold values for AVI and API may be beneficial to the refinement of diagnosis. For instance, using higher threshold values for aged individuals with naturally high arterial stiffness and individuals with high brachial PP due to physiological rather than pathological factors can reduce the risk of misdiagnosis that might lead to unnecessary interventions or treatments. Despite the potential benefits, using threshold values adjusted for various confounding factors to perform diagnosis for large populations in routine medical practice could be challenging, as it significantly increases the complexity and time required for data collection and classification. In fact, current clinical guidelines or expert consensuses often recommend the use of a single threshold value for each physiological index, such as blood pressure or arterial stiffness.

The study has some potential limitations. Firstly, it was conducted in a single center and involved a relatively small population. In particular, the diagnostic accuracy of AVI and API using the threshold values was not validated in an independent sample, and hence the generalizability of our findings to other populations remains unclear. Secondly, the study, as a cross-sectional one, could not address the usefulness of the threshold values in predicting future cardiovascular events. To address the limitations, future multi-center or follow-up studies on larger populations would be required. Thirdly, in comparison with baPWV, cfPWV and carotid intima-media thickness (IMT) can provide a more specific assessment of central arterial stiffness, and hence may be better comparators of AVI. However, their measurements were not available in the physical examination center where we collected the data, and this limitation might be addressed in our future studies by introducing cfPWV devices and collaborating with clinicians in the ultrasound department. Fourthly, we fixed the threshold value of baPWV at 18 m/s for diagnosing high arterial stiffness. However, different threshold values of baPWV have been proposed in the literature (60–63). Therefore, it remains debatable whether choosing a different threshold value for baPWV might yield a more reasonable determinant for the threshold values of AVI and API.

5. Conclusions

The threshold values of AVI and API measured by a cuff-based device for diagnosing high arterial stiffness in the general Chinese population have been established through comparisons with baPWV. The performances of diagnosis (evaluated by AUC) were basically acceptable (AUC > 0.76 with AVI, and AUC > 0.82 with API) in the pooled group, which could be further improved if gender-specific threshold values were applied to the female group. In the meantime, the study revealed that age and PP had significant influences on the threshold values of AVI and API, respectively, indicating the potential of using confounding factor-adjusted threshold values to refine diagnosis. On the other hand, the findings of the study are limited by the relatively small sample and absence of follow-up data, which would be addressed by future multi-center or follow-up studies on larger populations.

Data availability statement

The original contributions presented in the study are included in the article/**Supplementary Material**, further inquiries can be directed to the corresponding authors.

Ethics statement

The studies involving human participants were reviewed and approved by the Ethics Committee of Shanghai Sixth People's Hospital. The patients/participants provided their written informed consent to participate in this study.

Author contributions

XZ, FL, and JL contributed to conception and design of the study. FL and JL provided administrative support. FL and JL provided study materials and samples. XZ and YJ contributed to collection and assembly of data. XZ and YJ performed the data analysis and interpretation. All authors contributed to the article and approved the submitted version.

Funding

This study was partly supported by a grant from the National Natural Science Foundation of China (12061131015) and the Interdisciplinary Program of Shanghai Jiao Tong University (grant No. YG2019ZDA03). FL was supported in part by the Ministry of Science and Higher Education of the Russian Federation within the framework of state support for the creation and development of World-Class Research Centers' "Digital biodesign and personalized healthcare" No. 075-15-2022-304.

Conflict of interest

The authors declare that the research was conducted in the absence of any commercial or financial relationships that could be construed as a potential conflict of interest.

Publisher's note

All claims expressed in this article are solely those of the authors and do not necessarily represent those of their affiliated organizations, or those of the publisher, the editors and the reviewers. Any product that may be evaluated in this article, or claim that may be made by its manufacturer, is not guaranteed or endorsed by the publisher.

Supplementary material

The Supplementary Material for this article can be found online at: https://www.frontiersin.org/articles/10.3389/fcvm.2023.1131962/full#supplementary-material

References

1. Liang F, Takagi S, Himeno R, Liu H. Biomechanical characterization of ventricular–arterial coupling during aging: a multi-scale model study. *J Biomech*. (2009) 42(6):692–704. doi: 10.1016/j.jbiomech.2009.01.010

2. Lee HY, Oh BH. Aging and arterial stiffness. *Circ J*. (2010) 74(11):2257–62. doi: 10.1253/circj.CJ-10-0910

3. Laurent S, Boutouyrie P, Asmar R, Gautier I, Laloux B, Guize L, et al. Aortic stiffness is an independent predictor of all-cause and cardiovascular mortality in hypertensive patients. *Hypertension*. (2001) 37(5):1236–41. doi: 10.1161/01.HYP.37.5.1236

4. Chirinos JA. Arterial stiffness: basic concepts and measurement techniques. *J Cardiovasc Transl Res*. (2012) 5(3):243–55. doi: 10.1007/s12265-012-9359-6

5. Mattace-Raso FU, van der Cammen TJ, Hofman A, van Popele NM, Bos ML, Schalekamp MA, et al. Arterial stiffness and risk of coronary heart disease and stroke: the rotterdam study. *Circulation*. (2006) 113(5):657–63. doi: 10.1161/CIRCULATIONAHA.105.555235

6. Tomiyama H, Koji Y, Yambe M, Shiina K, Motobe K, Yamada J, et al. Brachial-ankle pulse wave velocity is a simple and independent predictor of prognosis in patients with acute coronary syndrome. *Circ J*. (2005) 69(7):815–22. doi: 10.1253/circj.69.815

7. Boutouyrie P, Chowienczyk P, Humphrey JD, Mitchell GF. Arterial stiffness and cardiovascular risk in hypertension. *Circ Res*. (2021) 128(7):864–86. doi: 10.1161/CIRCRESAHA.121.318061

8. Zhou Z, Xing AJ, Zhang JN, Xia WH, Su C, Xu SY, et al. Hypertension, arterial stiffness, and clinical outcomes: a cohort study of Chinese community-based population. *Hypertension*. (2021) 78(2):333–41. doi: 10.1161/HYPERTENSIONAHA.121.17131

9. Laurent S, Chatellier G, Azizi M, Calvet D, Choukroun G, Danchin N, et al. Sparte study: normalization of arterial stiffness and cardiovascular events in patients with hypertension at medium to very high risk. *Hypertension*. (2021) 78(4):983–95. doi: 10.1161/HYPERTENSIONAHA.121.17579

10. Laurent S, Cockcroft J, Van Bortel L, Boutouyrie P, Giannattasio C, Hayoz D, et al. Expert consensus document on arterial stiffness: methodological issues and clinical applications. *Eur Heart J*. (2006) 27(21):2588–605. doi: 10.1093/eurheartj/ehl254

11. Liang F, Takagi S, Himeno R, Liu H. Multi-scale modeling of the human cardiovascular system with applications to aortic valvular and arterial stenoses. *Med Biol Eng Comput*. (2009) 47(7):743–55. doi: 10.1007/s11517-009-0449-9

12. Tang CJ, Lee PY, Chuang YH, Huang CC. Measurement of local pulse wave velocity for carotid artery by using an ultrasound-based method. *Ultrasonics*. (2020) 102:106064. doi: 10.1016/j.ultras.2020.106064

13. Tanaka H, Munakata M, Kawano Y, Ohishi M, Shoji T, Sugawara J, et al. Comparison between carotid-femoral and brachial-ankle pulse wave velocity as measures of arterial stiffness. *J Hypertens*. (2009) 27(10):2022–7. doi: 10.1097/HJH.0b013e32832e94e7

14. Lorenz MW, Markus HS, Bots ML, Rosvall M, Sitzer M. Prediction of clinical cardiovascular events with carotid intima-media thickness: a systematic review and meta-analysis. *Circulation*. (2007) 115(4):459–67. doi: 10.1161/CIRCULATIONAHA.106.628875

15. Cobble M, Bale B. Carotid intima-media thickness: knowledge and application to everyday practice. *Postgrad Med*. (2010) 122(1):10–8. doi: 10.3810/pgm.2010.01.2091

16. Wilkinson IB, MacCallum H, Flint L, Cockcroft JR, Newby DE, Webb DJ. The influence of heart rate on augmentation index and central arterial pressure in humans. *J Physiol (Lond)*. (2000) 525(Pt 1):263. doi: 10.1111/j.1469-7793.2000.t01-1-00263.x

17. Vlachopoulos C, Aznaouridis K, O'Rourke MF, Safar ME, Baou K, Stefanadis C. Prediction of cardiovascular events and all-cause mortality with central haemodynamics: a systematic review and meta-analysis. *Eur Heart J*. (2010) 31(15):1865–71. doi: 10.1093/eurheartj/ehq024

18. Saiki A, Sato Y, Watanabe R, Watanabe Y, Imamura H, Yamaguchi T, et al. The role of a novel arterial stiffness parameter, cardio-ankle vascular index (CAVI), as a surrogate marker for cardiovascular diseases. *J Atheroscler Thromb*. (2016) 23(2):155–68. doi: 10.5551/jat.32797

19. Shirai K, Hiruta N, Song M, Kurosu T, Suzuki J, Tomaru T, et al. Cardio-ankle vascular index (CAVI) as a novel indicator of arterial stiffness: theory, evidence and perspectives. *J Atheroscler Thromb*. (2011) 18(11):924–38. doi: 10.5551/jat.7716

20. Munakata M. Brachial-ankle pulse wave velocity in the measurement of arterial stiffness: recent evidence and clinical applications. *Curr Hypertens Rev*. (2014) 10(1):49–57. doi: 10.2174/1573402110011411111160957

21. Sugawara J, Hayashi K, Yokoi T, Cortez-Cooper MY, DeVan A, Anton M, et al. Brachial–ankle pulse wave velocity: an index of central arterial stiffness? *J Hum Hypertens*. (2005) 19(5):401–6. doi: 10.1038/sj.jhh.1001838

22. Nakanishi N, Shiraishi T, Wada M. Brachial-ankle pulse wave velocity and metabolic syndrome in a Japanese population: the minoh study. *Hypertens Res*. (2005) 28(2):125–31. doi: 10.1291/hypres.28.125

23. Wang R, Zhang J, Li Y, Liu T, Yu K. Neutrophil–lymphocyte ratio is associated with arterial stiffness in diabetic retinopathy in type 2 diabetes. *J Diabetes Complicat*. (2015) 29(2):245–9. doi: 10.1016/j.jdiacomp.2014.11.006

24. Chen SC, Chang JM, Liu WC, Tsai YC, Tsai JC, Hsu PC, et al. Brachial-ankle pulse wave velocity and rate of renal function decline and mortality in chronic kidney disease. *Clin J Am Soc Nephrol*. (2011) 6(4):724–32. doi: 10.2215/CJN.07700910

25. Sequi-Dominguez I, Cavero-Redondo I, Alvarez-Bueno C, Pozuelo-Carrascosa DP, de Arenas-Arroyo SN, Martinez-Vizcaino V. Accuracy of pulse wave velocity predicting cardiovascular and all-cause mortality. A systematic review and meta-analysis. *J Clin Med*. (2020) 9(7):2080. doi: 10.3390/jcm9072080

26. Zhang Y, Agnoletti D, Xu Y, Wang JG, Blacher J, Safar ME. Carotid–femoral pulse wave velocity in the elderly. *J Hypertens*. (2014) 32(8):1572–6. doi: 10.1097/HJH.0000000000000187

27. Tougaard NH, Theilade S, Winther SA, Tofte N, Ahluwalia TS, Hansen TW, et al. Carotid-femoral pulse wave velocity as a risk marker for development of complications in type 1 diabetes Mellitus. *J Am Heart Assoc*. (2020) 9(19):e017165. doi: 10.1161/JAHA.120.017165

28. Kong X, Ma X, Tang L, Wang Z, Li W, Cui M, et al. Arterial stiffness evaluated by carotid-femoral pulse wave velocity increases the risk of chronic kidney disease in a Chinese population-based cohort. *Nephrology*. (2017) 22(3):205–12. doi: 10.1111/nep.12750

29. Polak JF, Pencina MJ, Meisner A, Pencina KM, Brown LS, Wolf PA, et al. Associations of carotid artery intima-media thickness (IMT) with risk factors and prevalent cardiovascular disease: comparison of mean common carotid artery IMT with maximum internal carotid artery IMT. *J Ultrasound Med*. (2010) 29(12):1759–68. doi: 10.7863/jum.2010.29.12.1759

30. Faita F, Gemignani V, Bianchini E, Giannarelli C, Ghiadoni L, Demi M. Real-time measurement system for evaluation of the carotid intima-media thickness with a robust edge operator. *J Ultrasound Med*. (2008) 27(9):1353–61. doi: 10.7863/jum.2008.27.9.1353

31. Chirinos JA, Zambrano JP, Chakko S, Veerani A, Schob A, Willens HJ, et al. Aortic pressure augmentation predicts adverse cardiovascular events in patients with established coronary artery disease. *Hypertension*. (2005) 45(5):980–5. doi: 10.1161/01.HYP.0000165025.16381.44

32. Shirai K, Utino J, Otsuka K, Takata M. A novel blood pressure-independent arterial wall stiffness parameter; cardio-ankle vascular index (CAVI). *J Atheroscler Thromb*. (2006) 13(2):101–7. doi: 10.5551/jat.13.101

33. Shirai K, Song M, Suzuki J, Kurosu T, Oyama T, Nagayama D, et al. Contradictory effects of β1-and α1-aderenergic receptor blockers on cardio-ankle vascular stiffness index (CAVI)—CAVI is independent of blood pressure. *J Atheroscler Thromb*. (2011) 18(1):49–55. doi: 10.5551/jat.3582

34. Birudaraju D, Cherukuri L, Kinninger A, Chaganti BT, Haroun P, Pidikiti S, et al. Relationship between cardio-ankle vascular index and obstructive coronary artery disease. *Coron Artery Dis*. (2020) 31(6):550–5. doi: 10.1097/MCA.0000000000000872

35. Niiranen TJ, Kalesan B, Hamburg NM, Benjamin EJ, Mitchell GF, Vasan RS. Relative contributions of arterial stiffness and hypertension to cardiovascular disease: the framingham heart study. *J Am Heart Assoc*. (2016) 5(11):e004271. doi: 10.1161/JAHA.116.004271

36. Xia S, Du X, Guo L, Du J, Arnott C, Lam CS, et al. Sex differences in primary and secondary prevention of cardiovascular disease in China. *Circulation*. (2020) 141 (7):530–9. doi: 10.1161/CIRCULATIONAHA.119.043731

37. Sasaki-Nakashima R, Ishigami T, Kino T, Teranaka-Saigo S, Chen L, Doi H, et al. Successful prediction of clinical outcomes using arterial velocity pulse index, a new non-invasive vascular index, in Japan. *Vascular Failure*. (2020) 3(2):43–50. doi: 10.30548/vascfail.3.2_43

38. Sasaki-Nakashima R, Kino T, Chen L, Doi H, Minegishi S, Abe K, et al. Successful prediction of cardiovascular risk by new non-invasive vascular indexes using suprasystolic cuff oscillometric waveform analysis. *J Cardiol*. (2017) 69 (1):30–7. doi: 10.1016/j.jjcc.2016.06.004

39. Jin L, Tong L, Shen C, Du L, Mao J, Liu L, et al. Association of arterial stiffness indices with framingham cardiovascular disease risk score. *Rev Cardiovasc Med*. (2022) 23(8):287. doi: 10.31083/j.rcm2308287

40. Zhang Y, Yin P, Xu Z, Xie Y, Wang C, Fan Y, et al. Non-invasive assessment of early atherosclerosis based on new arterial stiffness indices measured with an upper-arm oscillometric device. *Tohoku J Exp Med*. (2017) 241(4):263–70. doi: 10.1620/tjem.241.263

41. Wan J, Liu S, Yang Y, Wang D, Ran F, Xia S, et al. Roles of arterial pressure volume index and arterial velocity pulse index trajectories in risk prediction in hypertensive patients with heart failure with preserved ejection fraction. *Clin Exp Hypertens*. (2020) 42(5):469–78. doi: 10.1080/10641963.2019.1705319

42. Tomiyama H, Matsumoto C, Shiina K, Yamashina A. Brachial-ankle pwv: current status and future directions as a useful marker in the management of cardiovascular disease and/or cardiovascular risk factors. *J Atheroscler Thromb*. (2016) 23(2):128–46. doi: 10.5551/jat.32979

43. Komine H, Asai Y, Yokoi T, Yoshizawa M. Non-invasive assessment of arterial stiffness using oscillometric blood pressure measurement. *Biomed Eng Online*. (2012) 11(1):1–12. doi: 10.1186/1475-925X-11-6

44. Janes H, Pepe M S. Adjusting for covariate effects on classification accuracy using the covariate-adjusted receiver operating characteristic curve. *Biometrika*. (2009) 96(2):371–82. doi: 10.1093/biomet/asp002

45. Li Y, Teng D, Shi X, Qin G, Qin Y, Quan H, et al. Prevalence of diabetes recorded in mainland China using 2018 diagnostic criteria from the American diabetes association: national cross sectional study. *Br Med J*. (2020) 369. doi: 10.1136/bmj.m997

46. Townsend RR, Wilkinson IB, Schiffrin EL, Avolio AP, Chirinos JA, Cockcroft JR, et al. Recommendations for improving and standardizing vascular research on arterial stiffness: a scientific statement from the American heart association. *Hypertension*. (2015) 66(3):698–722. doi: 10.1161/HYP.0000000000000033

47. Kerr AJ, Broad J, Wells S, Riddell T, Jackson R. Should the first priority in cardiovascular risk management be those with prior cardiovascular disease? *Heart*. (2009) 95:125–9. doi: 10.1136/hrt.2007.140905

48. Hermida RC, Smolensky MH, Ayala DE, Portaluppi F. Ambulatory blood pressure monitoring (ABPM) as the reference standard for diagnosis of hypertension and assessment of vascular risk in adults. *Chronobiol Int*. (2015) 32 (10):1329–42. doi: 10.3109/07420528.2015.1113804

49. Omboni S, Posokhov IN, Kotovskaya YV, Protogerou AD, Blacher J. Twenty-four-hour ambulatory pulse wave analysis in hypertension management: current evidence and perspectives. *Curr Hypertens Rep*. (2016) 18:1–18. doi: 10.1007/s11906-016-0681-2

50. Hitsumoto T. Clinical significance of arterial velocity pulse index in patients with stage B heart failure with preserved ejection fraction. *Cardiol Res*. (2019) 10(3):142. doi: 10.14740/cr864

51. Taddei S, Virdis A, Ghiadoni L, Mattei P, Sudano I, Bernini G, et al. Menopause is associated with endothelial dysfunction in women. *Hypertension*. (1996) 28 (4):576–82. doi: 10.1161/01.HYP.28.4.576

52. Mendelsohn ME, Karas RH. Molecular and cellular basis of cardiovascular gender differences. *Science*. (2005) 308(5728):1583–7. doi: 10.1126/science.1112062

53. Gold EB. The timing of the age at which natural menopause occurs. *Obstet Gynecol Clin*. (2011) 38(3):425–40. doi: 10.1136/bmj.m997

54. Mendelsohn ME. Protective effects of estrogen on the cardiovascular system. *Am J Cardiol*. (2002) 89(12):12–7. doi: 10.1016/S0002-9149(02)02405-0

55. Murphy E. Estrogen signaling and cardiovascular disease. *Circ Res*. (2011) 109 (6):687–96. doi: 10.1161/CIRCRESAHA.110.236687

56. Martins D, Nelson K, Pan D, Tareen N, Norris K. The effect of gender on age-related blood pressure changes and the prevalence of isolated systolic hypertension among older adults: data from NHANES III. *J Gend Spec Med*. (2001) 4(3):10–3. 20.

57. DuPont JJ, Kenney RM, Patel AR, Jaffe IZ. Sex differences in mechanisms of arterial stiffness. *Br J Pharmacol*. (2019) 176(21):4208–25. doi: 10.1111/bph.14624

58. Manojlović M, Protić-Gava B, Maksimović N, Šćepanović T, Poček S, Roklicer R, et al. Effects of combined resistance and aerobic training on arterial stiffness in postmenopausal women: a systematic review. *Int J Environ Res Public Health*. (2021) 18(18):9450. doi: 10.3390/ijerph18189450

59. Tanaka K, Kanazawa I, Sugimoto T. Reduced muscle mass and accumulation of visceral fat are independently associated with increased arterial stiffness in postmenopausal women with type 2 diabetes Mellitus. *Diabetes Res Clin Pract*. (2016) 122:141–7. doi: 10.1016/j.diabres.2016.10.014

60. Kim J, Song T-J, Song D, Lee KJ, Kim EH, Lee HS, et al. Brachial-ankle pulse wave velocity is a strong predictor for mortality in patients with acute stroke. *Hypertension*. (2014) 64(2):240–6. doi: 10.1161/HYPERTENSIONAHA.114.03304

61. Seo H-J, Ki Y-J, Han MA, Choi D-H, Ryu S-W. Brachial-ankle pulse wave velocity and mean platelet volume as predictive values after percutaneous coronary intervention for long-term clinical outcomes in Korea: a comparable and additive study. *Platelets*. (2015) 26(7):665–71. doi: 10.3109/09537104.2014.978274

62. Hwang I-C, Jin KN, Kim H-L, Kim Y-N, Im M-S, Lim W-H, et al. Additional prognostic value of brachial-ankle pulse wave velocity to coronary computed tomography angiography in patients with suspected coronary artery disease. *Atherosclerosis*. (2018) 268:127–37. doi: 10.1016/j.atherosclerosis.2017.11.026

63. Park H-W, Kim H-R, Kang MG, Kim K, Koh J-S, Park JR, et al. Predictive value of the combination of brachial-ankle pulse wave velocity and ankle-brachial index for cardiovascular outcomes in patients with acute myocardial infarction. *Coron Artery Dis*. (2020) 31(2):157–65. doi: 10.1097/MCA.0000000000000777

frontiers | Frontiers in Cardiovascular Medicine

TYPE Review
PUBLISHED 07 August 2023
DOI 10.3389/fcvm.2023.1228789

OPEN ACCESS

EDITED BY
Serafino Fazio,
Federico II University Hospital, Italy

REVIEWED BY
Fabrizio Salvucci,
Ticinello Cardiovascular and Metabolic Centre, Italy
Diederik Wouter Dimitri Kuster,
Amsterdam University Medical Center, Netherlands

*CORRESPONDENCE
Gianluigi Pironti
gianluigi.pironti@ki.se

RECEIVED 25 May 2023
ACCEPTED 10 July 2023
PUBLISHED 07 August 2023

CITATION
Pironti G (2023) State-of-the-art methodologies used in preclinical studies to assess left ventricular diastolic and systolic function in mice, pitfalls and troubleshooting. Front. Cardiovasc. Med. 10:1228789. doi: 10.3389/fcvm.2023.1228789

State-of-the-art methodologies used in preclinical studies to assess left ventricular diastolic and systolic function in mice, pitfalls and troubleshooting

Gianluigi Pironti[1,2]*

[1]Cardiology Research Unit, Department of Medicine, Karolinska Institutet, Stockholm, Sweden, [2]Department of Physiology and Pharmacology, Karolinska Institutet, Stockholm, Sweden

Cardiovascular diseases (CVD) are still the leading cause of death worldwide. The improved survival of patients with comorbidities such as type 2 diabetes, hypertension, obesity together with the extension of life expectancy contributes to raise the prevalence of CVD in the increasingly aged society. Therefore, a translational research platform that enables precise evaluation of cardiovascular function in healthy and disease condition and assess the efficacy of novel pharmacological treatments, could implement basic science and contribute to reduce CVD burden. Heart failure is a deadly syndrome characterized by the inability of the heart to meet the oxygen demands of the body (unless there is a compensatory increased of filling pressure) and can manifest either with reduced ejection fraction (HFrEF) or preserved ejection fraction (HFpEF). The development and progression of HFrEF is mostly attributable to impaired contractile performance (systole), while in HFpEF the main problem resides in decreased ability of left ventricle to relax and allow the blood filling (diastole). Murine preclinical models have been broadly used in research to understand pathophysiologic mechanisms of heart failure and test the efficacy of novel therapies. Several methods have been employed to characterise cardiac systolic and diastolic function including Pressure Volume (PV) loop hemodynamic analysis, echocardiography and Magnetic Resonance Imaging (MRI). The choice of one methodology or another depends on many aspects including budget available, skills of the operator and design of the study. The aim of this review is to discuss the importance of several methodologies that are commonly used to characterise the cardiovascular phenotype of preclinical models of heart failure highlighting advantages and limitation of each procedure. Although it requires highly skilled operators for execution, PV loop analysis represents the "gold standard" methodology that enables the assessment of left ventricular performance also independently of vascular loading conditions and heart rate, which conferee a really high physiologic importance to this procedure.

KEYWORDS

cardiovascular diseases, heart failure, systolic function, diastolic function, echocardiography, MRI, PV loop analysis

Introduction

The ability of the left ventricle (LV) to contract and propel blood to the rest of the organs is defined as systolic function. The percent of blood ejected from the left ventricle during cardiac cycle (ejection fraction, EF) is commonly measured to assess contractility performance of the heart. Diastolic function encompasses for relaxation and filling of

cardiac chambers to enable an adequate blood volume and maintain normal cardiac output. Myocardial relaxation significantly influences early ventricular filling, as well as passive end-diastolic ventricular stiffness, which impacts on late ventricular filling.

Heart failure with impaired systolic function (HFrEF) is frequently accompanied by left ventricular diastolic dysfunction, whereas heart failure with impaired diastolic function (HFpEF) also occurs in the absence of (or eventually precedes) severe systolic dysfunction. In the presence of either preserved or minimally depressed ejection fraction, diastolic dysfunction is the main determinant in patients with HFpEF. Conditions found to be associated with isolated HFpEF include hypertensive cardiac hypertrophy, atrial fibrillation, diabetes mellitus, obesity, metabolic syndrome and aging (1, 2).

Abnormal relaxation and/or increased myocardial stiffness of LV could cause diastolic dysfunction and eventually lead to elevated left ventricle filling pressures and manifestation of HF symptoms. Assessment of diastolic dysfunction is needed to characterize the phenotype of HFpEF, which currently accounts for nearly half of the HF patients, and its prevalence continues to rise due to the increasingly aged society and survival of patients with comorbidities such as type 2 diabetes, hypertension, and obesity (3). Although the prevalence of HFpEF keeps rising, the therapeutic and prevention options are limited or not effective, due to a lack of clear mechanism or pathophysiological understanding, patient heterogeneity, and underdiagnosis (4–7).

Preclinical animal research is the cornerstone of the development of preventive and treatment strategies for cardiovascular disease. A broad variety of preclinical HF models have been extensively employed in basic cardiovascular research to investigate novel pathophysiologic mechanism or test the effect of novel therapies (8, 9). Myocardial infarction (MI) or transverse aortic constriction (TAC), induced by permanent ligation of coronary artery or banding of ascending aorta to induce pressure overload respectively, represent established models of HFrEF (10–15). In absence of a direct myocardial injury, the impaired contractile performance of the heart has also been described in models of rheumatoid arthritis where chronic inflammation was associated with systolic dysfunction (16) while the acute phase of rheumatoid arthritis is characterized by impaired myofibrils cross-bridges formation in response to elevated intracellular Ca^{2+} (17). Several transgenic models have been used to identify important causes of heart failure or its progression and to identify putative targets for therapy (8, 9). Epigenetic factors play also a key role in cardiac remodelling and left ventricle dysfunction is observed in female offspring of obese mothers exposed to high androgen levels (18). Several cardiometabolic disease have been used as HFpEF models presenting impaired ventricle blood filling function rather than decreased contractility (19, 20). It is important to consider that all conditions that are frequently associated with HFpEF (e.g., hypertension, diabetes mellitus, obesity, kidney failure and aging) can be easily recreated in animal models (21) and cardiometabolic dysfunction might remain hidden and can only be revealed through a proper cardiovascular phenotype characterization. Therefore, in preclinical studies it is important to assess both systolic and diastolic cardiac function in all these models in order to have a comprehensive view of novel pathophysiological mechanism responsible of heart failure. Moreover, understanding the utility of different methodological approach and correct interpretation of cardiovascular outcomes will be necessary to establish a standardized translational research platform that allow precise evaluation of cardiovascular function in different pathophysiological stage of disease and evaluate efficacy of pharmacological treatment.

The scope of this review is to provide a detailed overview of state-of-the-art methodologies used in preclinical research for cardiovascular phenotype characterization aimed to implement the insights in this field and reduce cardiovascular disease burden.

Echocardiography, magnetic resonance imaging and Pressure Volume (PV) loop analysis are all valid tools to proper characterize the cardiovascular phenotype of preclinical models. However, the choice of one method or another depends on resources, skills of the operator, time available and study design (**Table 1**, comparison of different procedures). In this article we will discuss the advantage and disadvantages of different procedures, with focus on PV loop analysis, which represents the "gold-standard" method for the assessment of ventricular systolic and diastolic performance independently of ventricle load condition.

Echocardiography screening

Cardiovascular function is routinely assessed by echocardiographic ultrasound imaging in patients, while murine myocardial characterization requires high spatial and temporal resolution in order to maintain a physiological state. Small animal size (mouse, ~20 g), orientation of the heart, and high heart rates (HRs, 400–600 beats/min) are some of the challenges that have been overcome lately via high-frequency transducers (up to 70 MHz), improved signal processing, and superior imaging frame rates (700 frames/s), providing superior resolution (~30 μm) and image uniformity throughout the field with novel post-acquisition analysis, although considerable training in hands-on imaging is required.

Echocardiography screening allows non-invasive assessment of systolic function and cardiac morphology, however diastolic function evaluation through echocardiography becomes challenging due to the high heart rate (400–600 bpm) and the difficulty to orient the echo probe in mice using four chambers view of the heart. Detailed protocol for accurate echocardiography screening in murine models has been described in recently published guidelines by Zacchigna et al. (22).

The ultrasound imaging of the heart is a non-invasive method to screen for cardiac disfunction, that can be executed in relatively less time compared to other methodologies. However, it requires an advanced and costly echocardiography machine that include Pulse Wave and Tissue Doppler modules in order to trace the movement of targets (blood cells in Pulse Wave Doppler or myocardium in Tissue Doppler) for characterization of diastolic functions. This

TABLE 1 Comparison between different methodologies used to assess cardiac performance.

	PV loop	Echocardiography	MRI
Cost (euros)	30–40 thousand	300–400 thousand	1–3 million
Size	Portable, small size (it requires a laptop for the software)	Portable and easy to move as it stands on wheels	Not portable, requires a dedicated room due to big size of the equipment
Time of execution per mouse (minutes)	30–120	20–40	90–120
Advantages/Pros	Provides information of pressure and volume changes in real time. Allows assessment of load-independent systolic and diastolic function, i.e., end systolic and end diastolic pressure volume relationship. Allows measurements of several hemodynamic parameters pre and post drug administration within the same mouse.	Allows simultaneous measurements of physiologic parameters. Allows measurements of heart dimensions: chambers, pericardium, valves, strain. Non-invasive procedure. It can be used for serial measurements.	Allows measurements of cardiac fibrosis and tissue perfusion *in vivo*. Allows measurements of physiologic parameters and heart dimensions (chambers, pericardium, valves, strain). High spatial resolution and high accuracy and reproducibility. Non-invasive procedure. It can be used for serial measurements
Disadvantages/Cons	Invasive, terminal procedure, it does not allow serial measurements. Requires good surgical skills of the operator. Cannot give direct information about heart dimension. Possible artifacts due to outflow track obstruction or catheter entrapment in papillary muscles. Heart rate should be between 400 and 600 bpm and mean blood pressure should be more than 90 mmHg to ensure physiological relevance.	Technical variability due to type of anaesthesia used and skills of the operator. Acclimation is needed for serial measurements of the same mouse. Variability due to operator skills and type of anaesthesia used Pulse wave doppler artifacts due to high HR or lower transducer frequency (i.e., fusion of E/A waves). Load dependent data. Heart rate should be between 400 and 600 bpm to ensure physiological relevance.	Time consuming procedure. Not commonly used to assess diastolic function. Cardiac gating necessary. Signal to noise ratio limitation, risk of motion artifacts. Uses contrast agents. Load dependent data. Heart rate should be between 400 and 600 bpm to ensure physiological relevance.

latter requires an accurate four chambers projection during the echo imaging, which is definitely not easy to obtain due to the small size of the animals. Most of the echocardiography imaging is performed using a 2-D view of the heart (B-Mode) or single axis scanning (M-mode) displayed over time for assessment of cardiac dimension, visualization of anatomic structures or evaluation of systolic functional parameters (e.g., LV fractional shortening). The limitation of LV volumes and EF calculation using M-mode is linked to the assumption of a spherical or ellipsoid shape of the heart (referred as D3 formula or Teichholz formula, described below), which is not accurate and leads to greater errors in pathological models with aggravated heart remodelling (i.e., MI or TAC).

Alternatively, speckle-tracking echocardiography (strain imaging) is used to track the motions of the myocardium by analysing B-mode images of the "speckles" that deforms over time through a postprocessing computer algorithm (23). This technique is also referred as deformation imaging since it tracks the motion of the heart by calculating the amount of its deformation over time, which can be expressed as velocity (first derivation of the strain rate) and implement the functional information. In clinical studies strain imaging is commonly used due to the higher sensitivity for changes in myocardial contractility and regional wall motion (24). Technological implementation of modern ultrasound machines enabled the use of speckle tracking echocardiography also in preclinical studies (25, 26). An aspect that requires more investigation in preclinical studies is the assessment of the twisting and untwisting rates during systolic contraction and diastolic relaxation respectively. In fact, the base and the apex of the heart rotate in opposite directions due to the arrangement of myofiber sheets within the epicardium and endocardium wall resulting in the upward swing of the apex during systole which leads to accumulation of strain energy that is released during isovolumic relaxation. Hypertrophy, fibrosis and wall stiffening that mostly characterize hypertrophic cardiomyopathy causes myofibers disarray and impaired twisting properties and elastic recoil (27), therefore implementation of current methodologies with torsion analysis could simplify the detection of early diastolic dysfunction in murine preclinical models (28).

Systolic function

Bidimensional and line scan mono-dimensional (B and M mode, respectively) echocardiography screening allows assessment of LV chamber dimension and systolic function. Short axis projection is commonly used to measure LV dimension of interventricular septum (IVS) and posterior wall (PW), which will give information about LV hypertrophy, while LV diastolic dimension (LVD) and LV systolic dimension (LVS) will indicate changes in dimension of LV chambers (increased in dilatative cardiomyopathy).

Heart rate (HR) can be obtained from inputs coming from ECG and breathing heating pad integrated device that provide real time electrocardiogram information. Other parameters of LV are calculated using the following equation:

- FS% fractional shortening: (LVD-LVS)/LVD *100
- EDV end diastolic volume: LVD^3 (D^3 formula) or $7*LVD^3/(2.4+LVD)$ (Teichholz formula)
- ESV end systolic volume: LVS^3 (D^3 formula) or $7*LVS^3/(2.4+LVS)$ (Teichholz formula)
- EF% ejection fraction: (EDV-ESV)/EDV * 100

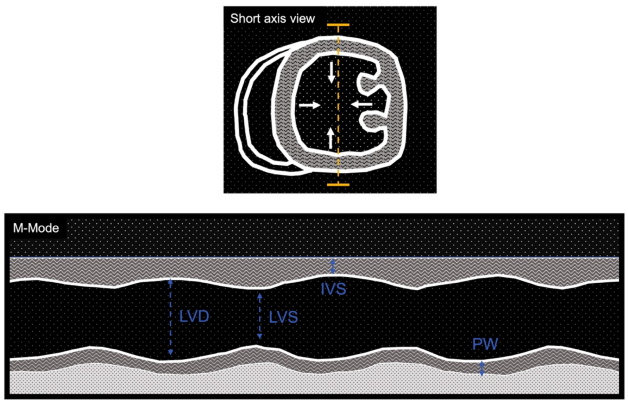

FIGURE 1
Cartoon depicting M-mode imaging of left ventricle short axis view. Top: short axis view of left ventricle (LV), which motions (arrows) are traced over time through a line scan (yellow dashed line). Bottom: mono-dimensional view of LV while is beating. Examples of measurements of left ventricle diastole (LVD), left ventricle systole (LVS), interventricular septum (IVS) and posterior wall (PW) dimensions.

TABLE 2 Echo cardio reference parameters in mice for systolic function and dimension of LV.

	Healthy	HFrEF	HFpEF	References
LVD (mm)	3.6–4.2	↑ ↑	←→/↓	(11, 16) (29)
LVS (mm)	1.5–1.9	↑ ↑ ↑ (MI) ↑ ↑ (TAC) ↑ (other DCM)	←→/↑	(16) (11)
FS%	40–55	↓ ↓ ↓ (MI) ↓ ↓ (TAC) ↓ (other DCM)	←→	(10, 11) (12–15, 30)
IVS (mm)	0.7–1.2	↑/←→ (MI) ↑ ↑ (TAC) ←→/↓ (other DCM)	↑	(18)
PW (mm)	0.6–1.2	↑	↑	(18)
HR (bpm)	450–600	←→	←→/↓	(10)

Increase (↑ up arrow), decrease (↓ down arrow), or no change (←→ horizontal arrows). LVD, left ventricle diastole; LVS, left ventricle systole; IVS, interventricular septum; PW, posterior wall; HR, heart rate. Reference values obtained from studies published that have used healthy mice and mice with HF.

- SV Stroke volume: EDV-ESV
- CO cardiac output: SV * HR heart rate

Example of measures obtained with M-mode in short axis view of LV is shown in **Figure 1**, while a list of reference parameters for systolic parameters in healthy and diseased animal models are listed in **Table 2**.

Diastolic function

Non-invasive evaluation of LV diastolic function is mostly assessed through ultrasound imaging. Different echocardiographic parameters provide information about different aspects of diastolic function, its consequences and/or determinants. As in humans, Pulsed-Wave (PW) Doppler can be used in rodents to measure transvalvular flow-velocity profiles, which are particularly useful in assessing LV filling velocity, determined by the ratio between early (E) and late (A) diastolic trans-mitral Doppler flow velocities (E/A) and mitral E wave deceleration time (DT) (**Figure 2**, PW doppler and **Table 3** reference values). PW-Doppler provides also information about the kinetics of LV systole, such as ejection time (ET) and isovolumic contraction time (IVCT), or LV diastole such as isovolumetric relaxation time (IVRT). The E/A ratio and the E-wave deceleration time (DT) are commonly used in human echocardiography to asses diastolic function of the heart. Prolongation of the isovolumic relaxation time (IVRT) or the mitral Doppler inflow E-wave deceleration time (DT) might reflect an impairment of left ventricle relaxation (32, 33). The fusion of the E- and A-wave is an indicator of diastolic dysfunction, however it is very challenging to measure these values consistently in mice since their high heart rates (>450 bpm) can cause artefactual fusion of E- and A-waves. Deeper anaesthesia slows down the heart rate in order to obtain a consistent measurement of E/A ratio in the mouse heart. However, this is undesirable due to the likelihood of associated cardiac depression. In fact, recent guidelines recommend to maintain the HR at physiological levels (>450 bpm) in order to avoid any cardio-depression effect and have reliable and reproducible data (22). Therefore, the assessment of these parameters through ultrasound imaging is unlikely to be useful in mouse echocardiography without a skilful and expert operator.

The ratio between early and late filling (E/A ratio) is usually referred to the ventricular filling pattern on trans-mitral Doppler. It is important to consider that E/A ratio is influenced not only by myocardial relaxation and ventricular stiffness but also by the left atrial pressure (34). Moreover, the left atrial pressure is itself affected by left ventricular properties as it rises when the ventricle becomes stiffer, therefore when left ventricle relaxation is impaired, the E/A ratio decreases. Another issue is the "pseudo-normalization" of the E/A ratio that rises again with the progression of diastolic dysfunction due to the increase of left atrial pressure, which makes even more complex the interpretation of the data. Therefore, additional Doppler pulmonary venous flow evaluation is required to validate LV diastolic dysfunction (35).

Further increase in LV passive stiffness leads to a predominantly early filling pattern with abrupt termination of filling, which is defined as a "restrictive" pattern. This causes a marked decrease in IVRT and DT along with an increase in E/A ratio. Therefore, multiple parameters need to be measured for an accurate interpretation of cardiac physiology. Left atrial pressure is a very important hallmark to assess diastolic function, therefore parameters that provide information about left atrial properties are very useful. B-mode four chambers view is commonly used to measure the area of left atrium (LA), which increases when the pressure in left atrium is high.

Tissue Doppler imaging is used to integrate data obtained from PW Doppler imaging and assess global and regional cardiac function. Tracing the motion velocity of the mitral annulus enables the measurement of e' (peak early diastolic mitral annular velocity), a' (peak velocity in atrial systole), and s' (peak

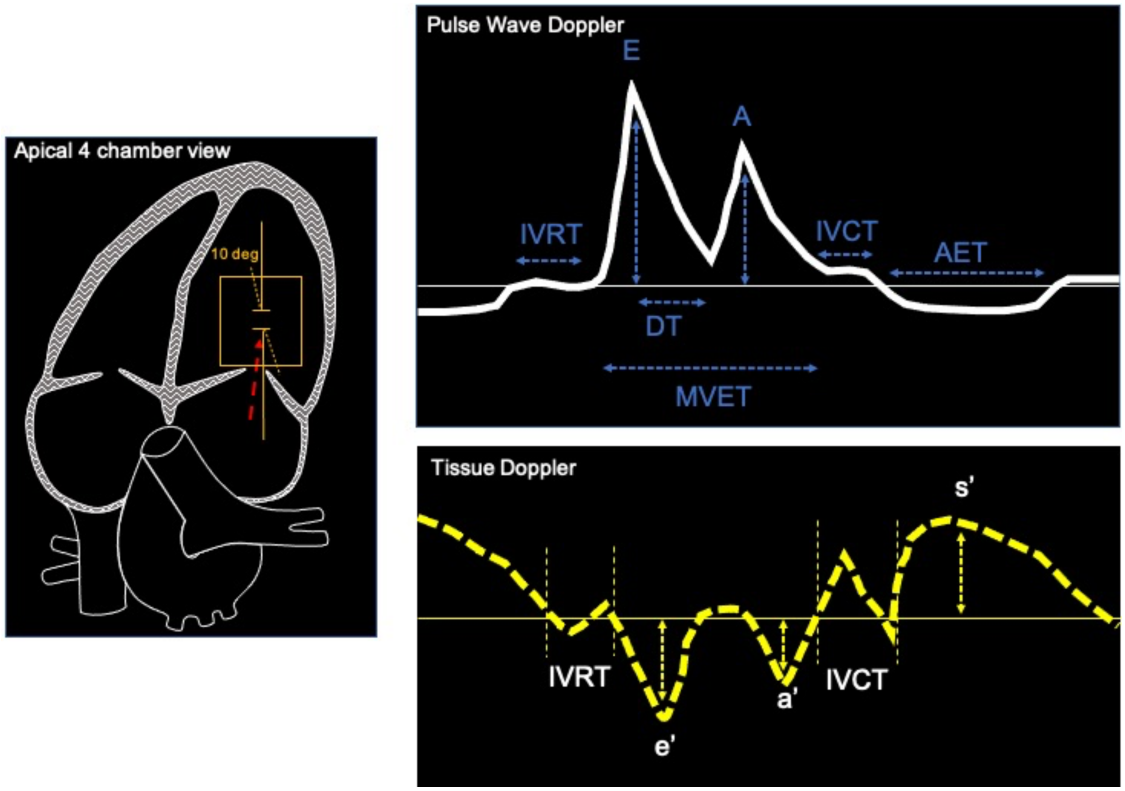

FIGURE 2
Example of apical 4 chamber view of the heart (left) used to record pulse wave Doppler (top) and tissue Doppler (bottom). Typical measurements of mitral blood flow with PW Doppler are: interventricular relaxation time, early and late mitral velocities (E and A waves), E wave deceleration time (DT), isovolumic contraction time (IVCT), aortic ejection time (AET). Tissue Doppler imaging are used to measure peak systolic velocities (s'), Peak early diastolic mitral annular velocities (e') during early filling at septal or lateral corner of mitral annulus, Peak velocity in atrial systole (a').

TABLE 3 Echo cardio reference parameters for diastolic function obtained through PW and TD Doppler.

	Healthy	HFrEF	HFpEF	References
E/A	1.1–1.5	↑	↑	(19, 20) (30, 31)
DT (ms)	16–31	↓	↓	(19, 20)
IVRT (ms)	16–19	↓	↓	(19, 20) (32, 33)
E/e'	19–38	↑	↑	(19, 20) (30, 32, 33)
LA area (mm^2)	0.4–2.5	↑	↑	(31–33)

Increase (↑ up arrow), decrease (↓ down arrow), or no change (←→ horizontal arrows). (E and A waves) Early and late mitral velocities, (DT) E wave deceleration time, (IVRT) Isovolumic relaxation time; (E/e') ratio, mitral inflow E wave/tissue Doppler mitral annulus velocity; (LA) left atrium. Reference values obtained from studies published that have used healthy mice and mice with HF.

systolic velocity) waves (**Figure 2**, Tissue Doppler trace). One drawback of the Tissue Doppler imaging method is that the analysis of radial function is limited to the anterior and posterior walls, while measurement of the circumferential function is limited to the septal and lateral walls, because Tissue Doppler can only measure velocities parallel to the ultrasound beam. Tissue Doppler imaging of mitral annulus provides another important parameter, the E/e' ratio (mitral inflow E wave/Tissue Doppler mitral annulus velocity), which correlates with left atrial pressure, while the size of left atrium provides a useful indication of chronically elevated left atrial pressure (36). PW and Tissue Doppler echocardiography are performed using a four chambers view, pointing the caliper (less than 20 degrees angle) at medial mitral annulus (**Figure 2**, four chamber view) to obtain the following parameters:

Parameters obtained with PW Doppler:

- Early and late mitral velocities (E and A waves)
- E wave deceleration time (DT)
- Isovolumic relaxation time (IVRT)
- Isovolumic contraction time (IVCT)

Parameters obtained with Tissue Doppler:

- Peak systolic velocities (s')
- Peak early diastolic mitral annular velocities (e') during early filling at septal or lateral corner of mitral annulus.
- Peak velocity in atrial systole (a')

Magnetic resonance imaging

Magnetic resonance Imaging (MRI) is another non-invasive though expensive procedure that has been employed to establish imaging parameters that can be adopted into clinical practice to predict cardiovascular outcomes also in animal models of

cardiomyopathy. This method provides high-quality resolution in static organs although, the quality of cardiac dynamic imaging might be challenged by the small size, the high heart rate and signal noise from respiration. Simultaneous ECG and respiration recording is commonly performed during MRI procedures for gating and synchronization of imaging with cardiac and respiratory cycles. Major limitations with the use of MRI include the high cost of the instrument and contrast agents, the massive size of the equipment, time and resource-intensive protocols, lower temporal resolution, signal-to-noise ratio limitations, which limit its more extensive use in preclinical studies. The major advantage of this technique is the accuracy in identifying tissue characteristics that correlate with histopathological findings, which makes this non-invasive procedure unique and very useful prognostic tool. In particular MRI allows detection of moderate to severe diffuse fibrosis, which makes MRI the only methodology available for *in vivo* assessment of cardiac fibrosis. This could enable studies that test new therapeutic strategies that can prevent, delay, or even reverse the effects of cardiac remodelling. Moreover, conventional two-dimensional cine images allow more accurate measurements of LV volumes and mass as the endocardium and epicardial areas calculations are performed in multi-planar short and long axis to cover the whole LV. The following parameters are commonly used to assess cardiac function and anatomy through MRI:

- LVEDV, left ventricle end diastolic volume: Σ (endocardial area over all slices at diastole) * thickness of the slice
- LVESV, left ventricle end systolic volume: Σ (endocardial area over all slices at systole) * thickness of the slice
- SV, stroke volume: LVEDV-LVESV
- EF (%), ejection fraction: SV/LVEDV * 100%
- CO, cardiac output: SV * HR
- RS, radial shortening: short axis (endocardial diameter at diastole − endocardial diameter at systole)/endocardial diameter at diastole * 100%
- LS, longitudinal shortening: long axis (endocardial diameter at diastole − endocardial diameter at systole)/endocardial diameter at diastole * 100%
- LVWV, left ventricle wall volume: Σ (epicardial area over all slices) * thickness of the slice − Σ (endocardial area over all slices) * thickness of the slice
- LVM, left ventricle mass: LVWV * 1.05 (myocardial density = 1.05 g/ml)

Quantitative evaluation of cardiovascular function with MRI imaging must consider the big gap in spatial resolution that exists between rodents (5- and 10-fold higher) and humans as the human heart size is 1,000-fold bigger with 5–10 times slower heart rate. The higher spatial resolution results in losing 100–1,000% of inherent signal/noise ratio (SNR). The signal-to-noise ratio and the image resolution is determined by the range of magnetic field strengths of the MRI scanners, which ranges between 4.7 and 9.4 T (for small animals) and from 1.5 to 3.0 T (for large animals). However, clinical 1.5 and 3.0 T scanners can be adapted for MRI imaging in small animals as described by Gilson and Kraitchamn (37), since high-field systems are not readily available at many institutions.

To ensure reproducibility and reliability of cardiovascular imaging studies, investigators should consistently report type and dose of anaesthesia, duration of the imaging procedure, and monitored heart rate and body temperature, which decrease while under anaesthesia during image acquisition. Temperature monitoring can be done using an MR-compatible rectal probe. Temperature maintenance can be accomplished by integrating a low-flow water-based heating blanket or pad into the cradle or by using heater fan over the animal.

It is possible to assess diastolic function using a temporal resolution of 1 msec using high-temporal-resolution cinematic magnetic resonance imaging (CINE MRI) (38), although this procedure is user-dependent and it is not commonly used in preclinical practice. Further methodological details of MRI procedures can be found in other excellent articles (39, 40).

PV loop analysis through invasive catheterization of left ventricle

History of PV loop analysis

Invasive left ventricle catheterization to measure pressure and volume has been introduced in dog's hearts in the 70′ using *ex vivo* settings (41) and later in the 90′ by Kass and colleagues in humans (42, 43). Microminiaturization of conductance catheters enabled the use of PV loop analysis for preclinical studies *in vivo* (44). This technique is the most rigorous and comprehensive way able to provide extensive information of systolic and diastolic function either dependent or independent by LV load and it is still considered the "gold standard" method to study cardiac pathophysiology in preclinical settings. Despite its invasiveness, this sophisticated methodology can be used to characterize cardiovascular function in transgenic mice, to test the hemodynamic effects of pharmacotherapies and studying cardiovascular pathophysiological conditions using small animals for genetic and pharmacological investigations (45). The main and unique advantage of this method compared to other non-invasive procedures (e.g., echocardiography, MRI) is that PV loop analysis can provide measures of LV performance independently of vascular loading conditions and heart rate.

Detailed protocols of PV loop analysis procedures have been reviewed in other excellent articles (45–48). The aim of this article is to overview the methodology for assessing systolic and diastolic dysfunction in mice including calibration of the equipment, surgical procedures and data interpretation.

PV loop description

Plotting hemodynamic changes of LV pressure on Y axis and volume on X axis will give a rectangular shaped loop known as

PV loop. An easy way to understand the cardiac cycle, which is very helpful for educational purpose, is to draw a line from the top left corner to the bottom right corner of the loop in order to reveal two triangles where the one on the top right refers to the LV systole, while the triangle on the bottom left represent the LV diastole. To better interpret and understand the PV loop data we will describe how pressure and volume change during cardiac cycle starting from the end of LV diastole (**Figure 3**, PV loop description). The point on the bottom right corner (blue circle) represents the end diastolic point. The LV has completed the blood filling phase and starts to contract causing indirectly the closure of mitral valve which leads to an increase of pressure without changes in volume (Isovolumetric contraction). When the pressure in the ventricle exceeds the pressure in the aorta, the aortic valve opens (top right corner) and the ejection phase begins. This allows the LV to reach its peak in pressure during systole. The relaxation phase starts at the end systolic point (top left corner, red circle) when the aortic valve closes as the LV pressure is now lower than aortic pressure. As the ventricle begins to relax with all valves closed there is a reduction of pressure without altering the volume (Isovolumetric relaxation). The LV will start the blood filling phase when the pressure in the LV is lower than the pressure in the atrium, which causes the mitral valve to open. In human beating hearts it has been demonstrated that the very rapid initial filling phase depends on the elastic properties of the heart. Indeed, in healthy condition the compression of the elastic element of the ventricle together with three-dimensional twisting deformation of the myocardium during systole, generate restoring forces resulting in a rapid negative diastolic pressure upon relaxation, while diseased and stiffed hearts manifest blunted protodiastolic suction (49, 50). The cardiac cycle concludes at the end of the filling phase (end diastolic point), when the mitral valve closes.

The peak of maximal pressure and minimal pressure are transposed for each cardiac cycle on *Y* axis to obtain values of end systolic and end diastolic pressure (ESP, EDP respectively). The difference between end diastolic volume and end systolic volume (transposed on *X* axis) defines the stroke volume of LV, which will be used to calculate cardiac ejection fraction.

End systolic point and end diastolic point are important to measure load independent cardiac function, e.g., the end systolic and end diastolic pressure volume relationship (ESPVR, EDPVR) obtained upon reduction in ventricle preload (described below in preload reduction paragraph).

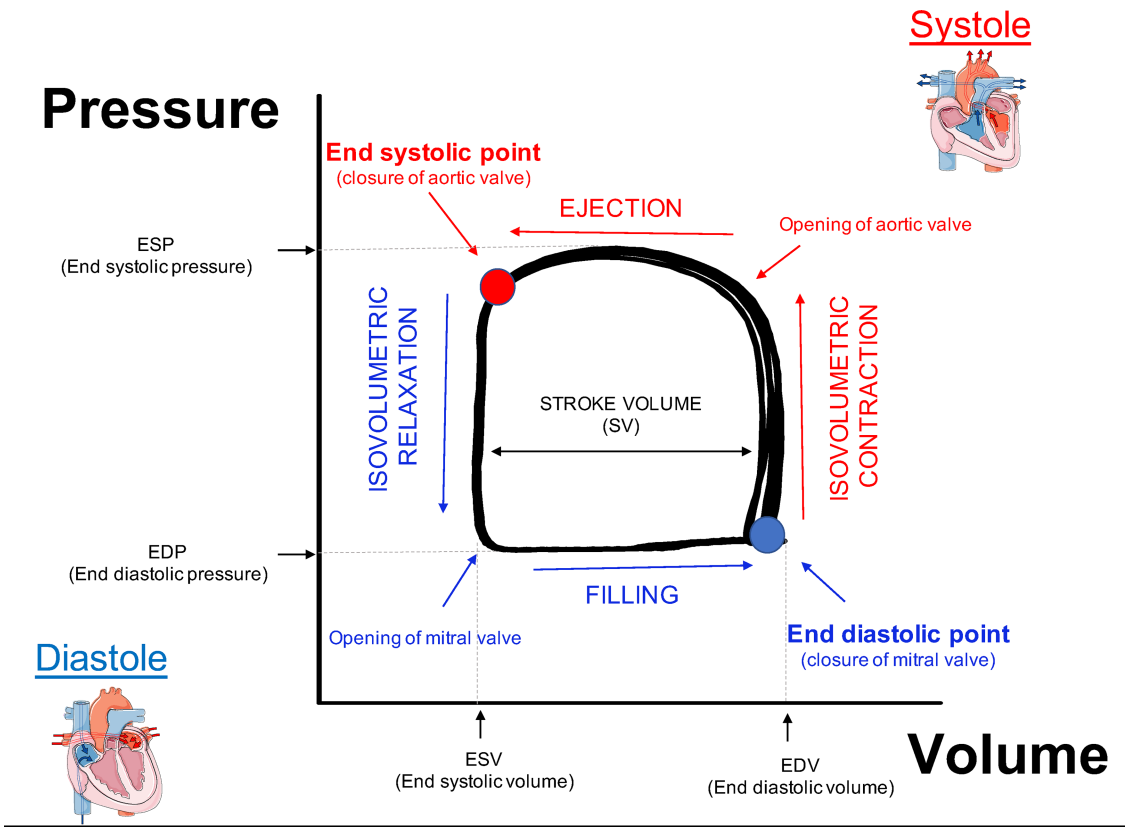

FIGURE 3
Description of PV loop. End diastolic point (blue circle): the LV has completed the blood filling phase and the mitral valve is closed. Isovolumetric contraction: aortic and mitral valves are closed while the ventricle starts to contract causing an increase of pressure without changes in volume. Ejection phase begins when the aortic valve opens. The end systolic point (red circle): when the aortic valve closes and the relaxation phase begins to relax. Isovolumetric relaxation: all the valves are closed during ventricle relaxation, which leads to reduction of pressure without altering the volume. Filling phase: the LV is filled with blood following opening of the mitral valve.

Surgical procedures for LV catheterization

Understanding the principle of this method involves two parts: (a) master the surgical procedure for placement the catheter in LV for pressure and volume measurements, (b) analyse the data obtained. For surgical procedures, isoflurane (1%–2%) has become the most popular anaesthetic for PV loop and other for non-invasive cardiac physiology analysis in mice (51), while the mixture of Ketamine and Xylazine has been shown to be unsuitable for physiological measurement mostly for the cardio depressant effect of Xylazine, which reduce HR and LV function compared to isoflurane. The use of different types of anaesthesia used in PV loop analysis contributes to the large interlaboratory variability of data for hemodynamic parameters (**Table 4**, hemodynamic parameters reference values in healthy mice) (46, 48).

TABLE 4 Selected hemodynamic parameters in healthy anaesthetised mice and their change in pathologic conditions.

	Healthy	HFrEF	HFpEF	References
HR (bpm)	470–640	←→	←→	(46, 48) (32, 33)
ESP (mm Hg)	92–118	↑ ↑ (in TAC) ←→/↓ (in MI and other DCM)	↑	(46) (19, 20)
EDP (mm Hg)	1–6	↑	↑↑	(46) (19, 20)
ESV (µl)	7–21	↑ (in TAC) ↑↑ (in MI and other DCM)	↑/←→/↓	(46) (52)
EDV (µl)	25–53	↑ (in TAC) ↑↑ (in MI and other DCM)	↑/←→/↓	(46) (52)
SV (µl)	17–30	↓ ↓	←→/↓	(46)
CO (ml/min)	8–16	↓ ↓	←→/↓	(46) (45, 51, 53)
EF %	55–72	↓	←→	(52) (32, 33)
Ea (mmHg/µl)	3–7	↑	↑	(52) (19, 20)
dP/dt_{max} (mmHg/s)	8,200–14,200	↓	←→/↓	(46, 48)
ESPVR slope, E_{es} or E_{max} (mmHg/µl)	7–14	↓ ↓	←→	(54)
PRSW (mmHg)	58–99	↓ ↓	←→/↓	(46, 48)
dP/dt_{max}/EDV (mmHg/s/µl)	580–799	↓ ↓	←→/↓	(46, 48)
$-dP/dt_{min}$ (mmHg/s)	(−)6,700–10,500	↓	↓	(46, 48) (32, 33)
Tau (ms)	7–12	↑ ↑	↑ ↑	(54) (32, 33)
EDPVR slope, β (mmHg/µl)	0.04–0.12	↑ ↑	↑↑	(19, 29, 55, 56)

HR, heart rate; ESP, end systolic pressure; EDP, end diastolic pressure; ESV, end systolic volume; EDV, end diastolic volume; SV, stroke volume; CO, cardiac output; Ea, arterial elastance (index of ventricular afterload); EF, ejection fraction; dP/dt_{max}, peak rate of pressure rise; E_{es} (E_{max}), end systolic elastance (slope of end-systolic relationship); PRSW, preload-recruitable stroke work (slope of stroke work-EDV relationship); (dP/dtmax)/EDV, slope of relationship between dP/dtmax and EDV; $-dP/dt_{min}$, Peak rate of pressure decline; Tau, relaxation time constant; EDPVR, β, slope of end diastolic pressure volume relationship (more steep, increased stiffness). Reference values obtained from studies published that have used healthy mice and mice with HF.

Anaesthesia with isoflurane

The mouse is sedated in the induction chamber saturated with 2%–3% isoflurane. Once the mouse is asleep the sedation is maintained through a mask connected to a respirator providing anaesthesia mixture (1.5%–2% isoflurane). The hair from the neck and the chest are removed using depilatory cream while the skin is cleaned with water and prepared for surgery with 0.5% chlorhexidine. Then a mid-sternal incision of the skin from the neck to the sternum will expose the salivary glands. These will be then separated in order to expose the trachea and confirm the correct placement of the endotracheal cannula. The endotracheal cannula can be custom made using an 18 G blunted needle. Before inserting the cannula, the mask is removed and the tongue is gently pulled to avoid obstruction during cannula insertion. Finally, the cannula is connected to a respirator providing gas anaesthesia mixture. For mice surgery, the respirator should be set at a stroke rate of 120–140 breaths per minute and a stroke volume (tidal volume) of 0.2–0.4 mm.

Cannulation of left jugular vein for saline infusion

The left jugular vein is the most common access point used to infuse fluids during PV loop analysis. The catheter can be custom made by using a PE-20 tube connected to a 29 G needle. Note that the needle will be inserted into the vein with bevel of the needle facing up, while the PE-20 tube will serve as connection to the adapter switch connected to other syringes containing different solutions. Before placing the catheter in the jugular vein, it is recommended to flush the catheter with the first solution that needs to be infused to check any possible obstruction of the catheter of the cannula. After exposing the jugular vein by moving proximally the salivary gland, the left jugular vein can be cannulated. In order to infuse different solutions in the same animal the cannulation tube is connected to a switch adapter so that more syringes (e.g., containing saline, hypertonic solution or drug that needs to be tested) can be connected to the same cannula and inject different solutions. Upon jugular vein cannulation, 12.5% albumin in normal saline is infused at 5 µl/min, after an initial 50-µl bolus to counteract the peripheral vasodilatation and hypotension induced by anaesthesia. PV loop analysis can be employed to assess any acute effects on cardiac physiology that a wide variety of drugs may induce upon infusion.

LV catheterization

The catheter most commonly used for PV loop analysis in mice is the Millar SPR 839 (size 1.4 French), which contains 4 electrodes with pressure sensor centred between E2 and E3 (45). Before starting any experiment, the catheter needs to be calibrated for volume and pressure according to manufacturer's instruction.

Before catheterization, the catheter tip needs to be pre-soaked in warm saline (37°C) for 30 min (at least) before use. This can be done by inserting the tip through a 1-ml syringe containing physiological saline solution placed on a heating pad.

There are two ways of inserting the catheter in left ventricle of mice: the closed chest approach from the right carotid, or the open chest approach directly from LV apex.

Closed chest approach

The closed approach consists in inserting the catheter through the right carotid, which will retrogradely reach the LV chamber. The critical part of this approach is to overcome the loop of aortic arch before reaching the LV, which is quite challenging due to the small size of the vessels and the limitation to adjust the catheter orientation within the ventricle. A potential problem with retrograde insertion of the catheter is the risk of outflow tract obstruction crossing the aorta, which becomes a significant issue in smaller hearts. The diameter of the mouse aorta varies from 0.8 to 1.2 mm while commercially available PV catheters have a diameter about 1/3 of mouse aorta diameter (ranging from 0.33 to 0.47 mm, 1.0 to 1.4 French respectively) (48). The closed-chest approach is more suitable for more prolonged experiments, because normal intrathoracic pressures are maintained, there is less risk of bleeding and the animals are more stable for a longer period of time. In a chronic heart failure model induced by ligation of the left anterior coronary artery characterized by the scar formation in the apex area the carotid approach should also be used. However, catheter entrapment is a common artifact of measurement that can be generated by direct compression of the transducer by a papillary muscle or other dynamic structure within the ventricle. This artifact can be detected by the typical spike in pressure at the end of systole, which often results in very small changes in LV volume during cardiac cycle (see representative image **Figure 4**). This can impact the analysis of PV loop data, because most methods for determining systolic function use the maximum pressure derivative. Therefore, data sets need to be examined closely for catheter entrapment to ensure meaningful data.

Open chest approach

This protocol is commonly used for drug testing and it consists in inserting the catheter in the LV via the apex, therefore it is easier to confirm the proper placement of the catheter in the LV, and the PV loop recording is more consistent while the whole procedure can be executed in less time. The open chest approach is also indicated if the carotid artery is severely atherosclerotic (e.g. in ApoE mice fed with a high-fat diet), or when the aortic valve is calcified (e.g., in advanced aging models) or in transverse aortic constriction (TAC)-induced hypertrophy and heart failure models. However, this procedure requires to cut the diaphragm in order to expose the apex of LV, which leads to loss of thoracic pressure impacting the venous return. Therefore, it is important to use consistently one surgical approach in order to obtain reliable PV loop data.

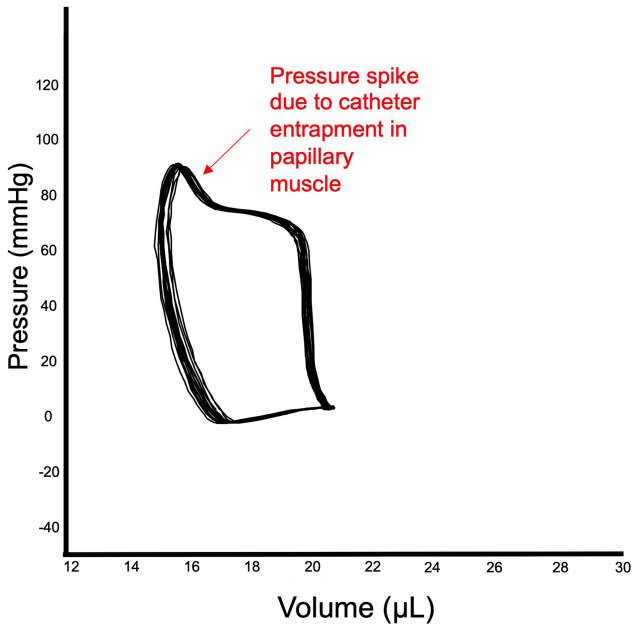

FIGURE 4
Catheter entrapment. Example of entrapment of catheter in papillary muscle of LV. The end of the systole reveals a spike in LV pressure, while stroke volume is relatively small.

Total peripheral resistance (TPR)

This parameter is very important for new drug that may also affect peripheral resistance. Using the carotid approach to insert the catheter provides the advantage of easily recording arterial pressure from the carotid artery at the start or at the end of the experiment, therefore total peripheral resistance (TPR) can be calculated afterwards as follows: *TPR = (mean arterial pressure–mean venous pressure)/cardiac output*.

Alternatively with the open chest approach, one of the femoral arteries can be cannulated with a PE tube (P10) and connected to another pressure transducer recording on separate record channel. This allows to calculate the total peripheral resistance (TPR) changes throughout the experiment.

Protocol for open chest approach

This is a quick and reproducible approach to insert the catheter in LV. In anesthetized and intubated animals connected to a mechanical respirator, the xiphoid process is exposed separating the skin from the ribs cage using blunt forceps. To reduce the risk of bleeding the operator should avoid to cut the ribs (particularly if a heat cauterization unit is not available). It is recommended that the operator lifts up

the xiphoid process of the mouse and cut the abdominal muscles underneath the ribs to expose the diaphragm. This latter can then be easily cut along the junction of the ribs cage. This will prevent any major bleeding in order to access the apex of the heart.

In order to have a clear view of the heart orientation, the ribs can be lifted up using chest retractors. The pericardium is gently removed from the heart with forceps.

The apex of the heart is stabbed wound with a 25 G needle attached to a syringe to prevent any sudden drop in ventricle pressure following the stabbing.

The orientation of the needle represents a critical point in order to have a clear noise-free PV loop signal. In fact, the needle needs to enter into left ventricle through the apex no more than 2–4 mm deep maintaining the orientation of the needle toward the base of the heart. Then the catheter tip can be quickly inserted into the left ventricle using the access point created by the needle. The catheter is pushed until the proximal electrode on the catheter (E4) is just inside the ventricular wall, while the orientation is parallel to the long axis of the ventricle. The correct position of the catheter can then be adjusted in order to obtain rectangular-shaped PV loops. Baseline PV loops are recorded after stabilization of the signal at steady state or following inferior vena cava occlusions in order to vary the preloads. This latter is particularly used to obtain various load-independent indices of systolic and diastolic function (see inferior vena cava occlusion below).

At the conclusion of the experiment, the catheter is gently pulled back through the stab wound and the animal is euthanized. The blood is collected in tubes with heparin and used for volume calibration with cuvettes (see volume calibration below).

It is recommended to place immediately the tip of the catheter into a syringe filled with saline solution (NaCl 0.9%) to prevent clotting. Finally, the catheter should be cleaned with detergent (e.g., Alconox) according to manufacturer's instructions as proper care of the catheter will considerably prolong its useful life.

Preload reduction through inferior vena cava (IVC) occlusion

Inferior vena cava occlusions can be performed in open-chest respirated animals by lifting a suture placed around the vessel, or compressing the vessels with a blunted forceps. Load independent measures of contractility and relaxation are obtained by reducing LV preload through occlusion of IVC for few seconds. By reducing the preload, there will be a reduction of pressure and volume in the ventricle (**Figure 5**, on the left) and a decrease in the amount of stretch of the ventricle prior to a contraction. Occlusion of IVC will be displayed as a series of smaller PV loops shifting to the left generated over a range of decreasing ventricular preloads. Each of these loops have their own end systolic point and end diastolic point (red and blue points in loops in **Figure 5**) that will be used by the software to calculate end systolic and end diastolic pressure volume relationship (ESPVR, EDPVR) as load-independent parameters of ventricle contractility and relaxation, respectively.

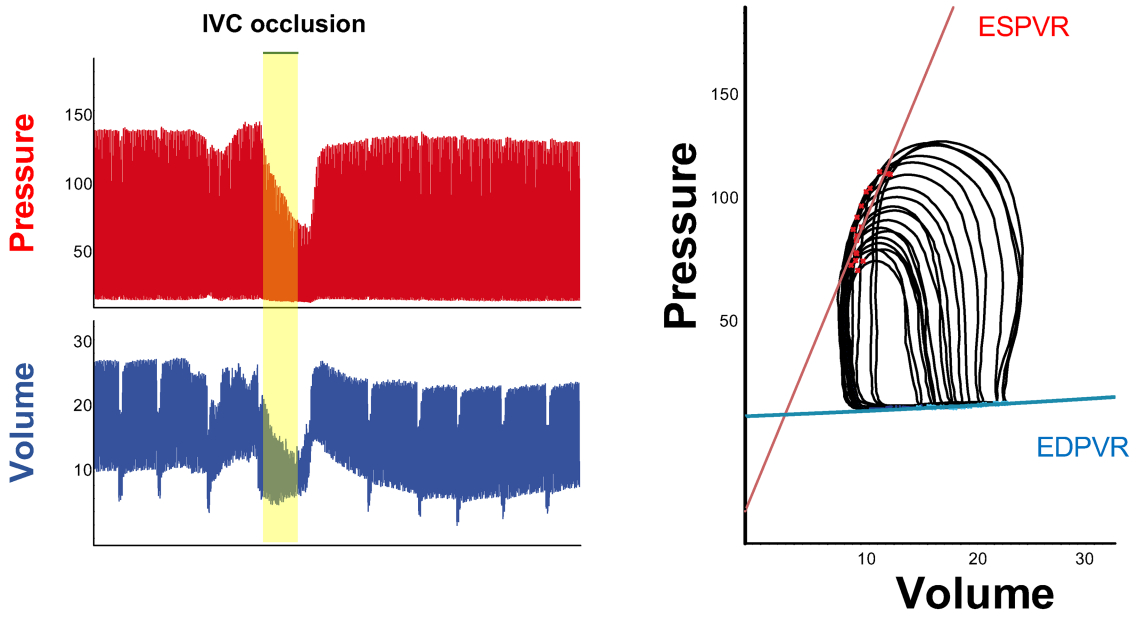

FIGURE 5
IVC occlusion. Example of change in pressure and volume following preload reduction through inferior vena cava occlusion (left). On the right, series of smaller PV loops shifting to the left generated over a range of decreasing ventricular preloads. Each of these loops has its own end systolic point and end diastolic point, which will be used to calculate load independent parameters such as ESPVR (red line) and EDPVR (blue line).

Load independent parameters

The interpretation of end systolic and diastolic pressure volume relationship (EDPVR and ESPVR) provides important information about the heart performance independently of load conditions. The maximal pressure that can be developed by the ventricle at any given LV volume is referred as end-systolic pressure volume relationship (ESPVR). This parameter is an improved index of systolic function over other hemodynamic parameters like ejection fraction, cardiac output, and stroke volume. The passive properties of the myocardium (passive filling curve for the ventricle) are described by the end-diastolic pressure volume relationship (EDPVR).

Volume calibration

The volume raw data are generally recorded as relative volume units (RVU), which can be converted in microliters (µl) in two steps: conversion of RVU to µl with blood cuvettes and correction for the parallel conductance volume with saline calibration. It is recommended to perform blood cuvette calibration and saline calibration for each animal at the end of each PV loop recording in order to have an accurate measurement of volumes. However, due to the limited amount of blood that can be collected from each mouse, it is also possible to pool together blood from different animals and perform one blood cuvette calibration at the end of each experimental day.

Step 1: convert the RVU in µl using blood cuvettes

Blood cuvettes are mock-up cylinders with known volumes that are filled with heparinized warm blood (body temperature) placed on the heating pad. The cuvettes are filled with blood using 22 G blunted needle long enough to reach the bottom of the cylinder (length 3.9 cm) avoiding formation of air bubbles. The catheter is inserted in each cuvette, submerging the 4 electrodes and keeping the position steady for 10–20 s, to record the changes in conductance values RVU. A calibration curve will be generated using 4–5 known cuvettes which will enable the conversion of the data from RVUs into units of true volume (µl) using PV loop analysis software. However, the conductivity of the heart muscle that surrounds the LV blood pool (parallel conductance) makes these estimated volume signals still larger than expected. Therefore, intravenous hypertonic saline calibration is performed (described below), to account and correct for parallel conductance.

Step 2: hypertonic saline calibration

Hypertonic saline calibration is performed because data generated from conductance catheters depend on the relationship between volume and conductance. Changes in conductance are measured by changes in current flowing from proximal to distal electrode, which is mostly given by movement of blood pool. However, the contribution of the ventricular wall, termed parallel conductance, must be subtracted to obtain absolute LV volume measurements (47). Indeed, the current applied to the excitation electrodes on the catheter does not go only through the blood, but some of the applied current flows also into the surrounding muscle, which is a conductor rather than an insulator, often causing an overestimation of the blood volume within the ventricle. Therefore, the heart muscle acts as a shunt to the applied current, referred as parallel conductance, or in volume calculations as parallel volume (Vp). To obtain a value for Vp, a bolus 15–20 µl of hypertonic saline (NaCl 30%) is injected through jugular vein into the animal at the conclusion of the experiment. This will cause a visible shift to the right in PV loops (increase volume conductance signal) without significant decrease in the pressure signal amplitude. The parallel volume (Vp) is calculated by solving a system of linear equations to locate the intersection of two lines. The first line is represented by the saline calibration data plotting end diastolic volume vs. end systolic volume (ESV) for each cardiac cycle during the phase where the volume signal appears to rise following the hypertonic saline bolus. The other line derives from the equation EDV = ESV, which represents equal end-systolic and end-diastolic volumes or in other words as the equivalent of a heart chamber devoid of blood. Then the PV loop software calculate the parallel volume (Vp) of muscle tissue that corresponds to the value at the intersection of the EDV = ESV line and the saline calibration line. Further details of the method and its underlying theory have been reported previously (45). It is recommended to perform at least 2–3 saline calibrations in each animal to minimize possible variability. The calculated Vp value from saline injection together with the parameters derived from blood cuvette calibrations will be used by the PV loop software (e.g., Lab Chart 8, Ad Instrument) to calculate the true volumes in microliters.

Alpha calibration (optional)

It is possible to use other non-invasive procedures (i.e., echocardiography or MRI) to measure of LV volumes in order to validate volume calibration performed with catheter (Alpha correction) (45). This represents an optional step where the alpha coefficient of Baan's equation is calculated by dividing the cardiac output (CO) or stroke volume (SV) recorded by PV loop module by the CO or SV calculated by other non-invasive methodologies. However, from a practical point of view the calibration can be performed independently of other non-invasive methodologies.

Duration of PV loop procedure

The whole procedure can last from 30 to 120 min depending on time necessary for anaesthesia, surgery and calibrations for one animal, however the experience and surgical skills of the investigator and study design play a critical role in the proper execution of this complex procedure. Starting with a few control animals on the day of the experiment will ensure that everything is optimized and working well before proceeding with

measurements in pathological states or following pharmacological treatment. Indeed, this could be useful to minimize potential errors in case the catheter needs to be replaced in the middle of the study by another one with slightly different properties.

Interpretation of hemodynamic parameters obtained from PV loop analysis

This sophisticated methodology enables simultaneous measurements of both pressure (on *Y* axis) and volume (on *X* axis) data in murine ventricle for each cardiac cycle both at steady state and during preload changes (IVC occlusion). Therefore, several hemodynamic parameters of systolic and diastolic function can be derived from the analysis of pressure and volume relationship. Generally, 10–12 cardiac cycles are selected and analysed with PV loop software to obtain the hemodynamic tables including systolic and diastolic parameters. We will describe the parameters that are most commonly used in cardiovascular preclinical studies and how they are calculated by the software.

The heart rate, expressed as beat per minutes (bpm), is calculated by the software by either automatically counting the cardiac cycles over time or by analysing the ECG signal recorded on a separate channel of the PV loop analysis software.

End systolic pressure (ESP), end diastolic pressure (EDP), expressed in mm of Hg, represent the maximal pressure and the minimal pressure respectively, that have been recorded during each cardiac cycle. End systolic volume (ESV) and end diastolic volume (EDV) are calculated following volume conversion in microliters (µl) (described above), indicate the volume of blood during ventricle contraction and relaxation respectively.

Systolic parameters

Stroke volume (SV) indicates how much blood is pumped by the ventricle following each contraction and it is obtained by subtracting the end diastolic volume to the end systolic volume (SV = EDV—ESV) and it is expressed in µl.

Ejection fraction (EF) represents the fraction of end diastolic blood volume that is propelled by the ventricle during each contraction. It is calculated dividing the stroke volume to end diastolic volume (EF = SV/EDV). This parameter is expressed in percent.

Cardiac output (CO) represents the amount of blood that is propelled by the ventricle each minute. CO it is calculated by multiplying the stroke volume to the heart rate (SV * heart rate). The unit of measurement is µl/min.

The maximal rate of rise of left ventricle pressure (dP/dt_{max}) is an index of contractility that relies on loading condition of the ventricle.

Arterial elastance (Ea) it is an index of arterial vascular load (LV afterload) and it is calculated by the ratio between end-systolic pressure and stroke volume (ESP/SV). The unit of measurement is mm Hg/µl.

Stroke work (SW) refers to the work done by the ventricle to eject a volume of blood. It refers to the area of the PV loop and is calculated by mean arterial pressure times cardiac output (MAP*CO).

Load independent systolic parameters (obtained following preload decrease with IVC occlusion)

The dP/dt_{max} –end-diastolic volume relation provides a load-independent contractility index, as preload dependence of dP/dt_{max} is effectively reduced by using this regression.

End-systolic pressure volume relationship (ESPVR) describes the maximal pressure developed by the ventricle at any given LV volume and is a measure of cardiac contractility.

Maximal elastance (Ees or Emax) is equal to the slope of the ESPVR curve. It is an index for chamber end systolic elasticity/stiffness and can be a useful measure of contractile function, particularly to assess acute changes.

Preload recruitable stroke work (PRSW) is another index of load independent contractility, which is obtained by plotting stroke work vs. end-diastolic volume for the set of load-altered loops.

Diastolic parameters

The minimum rate of pressure changes in ventricle (dP/dt_{min}) is the minimum derivative of change in diastolic pressure over time. Left ventricle traces first derivatives dP/dT_{max} and dP/dT_{min} give an indication of systolic and diastolic function where a decrease indicates an impaired function.

Isovolumic relaxation time constant (TAU, τ) represents the exponential decay of ventricular pressure during isovolumetric relaxation (pre-load-independent parameter).

Load independent diastolic parameters (obtained following preload decrease with IVC occlusion)

End diastolic pressure volume relationship (EDPVR) is a load-independent index of the passive filling properties of the ventricle and the passive properties of the myocardium. The slope of EDPVR is a measure of myocardial compliance (ventricle passive filling), which is the reverse of ventricular stiffness.

Hemodynamic changes during heart failure

In diseased animals, the shape of the PV loops may not be rectangular. In models of LV pressure overload (i.e., TAC), the LV walls become thicker and LV chamber size decreases or remains unchanged (52). The increased wall thickness can reduce compliance of LV, therefore the slope of EDPVR increases. During compensatory hypertrophy the systolic pressure is not suppressed and the end-systolic pressure (*Y*-axis) is not changed.

In models of HFrEF the EF is drastically reduced and there are clear signs of contractility disfunction (e.g., severe reduction of stroke volume and cardiac output), accompanied by diastolic disfunction (increased Tau and slope of EDPVR) (54). In models of HFpEF the EF is preserved or there might be mild signs of

contractility dysfunction, however diastolic disfunctions manifest as decrease in dp/dt_{min}, while Tau and slope of EDPVR increase (19, 29, 55, 56). In particular, an increased stiffness of the myocardium or a decreased compliance of LV will appear in PV loop analysis as an increased slope of EDPVR, which can be observed in both HFrEF or HFpEF models. Examples of PV loops in healthy and diseases models are depicted in **Figure 6**. In dilated cardiomyopathies (i.e., MI), ESV and EDV increase and LV pressure can remain unchanged, therefore the ESPVR and EDPVR are shifted to the right. Alternatively, when end-systolic pressure decreases and end-diastolic pressure increases the PV loop appears smaller (shorter) and rightward shifted (45, 51, 53). Upward shift in the EDPVR is observed in dilated cardiomyopathy associated with fibrosis and diastolic dysfunction. Chronic changes in Ees from heart disease can be a consequence of cardiac remodelling such as hypertrophy and fibrosis, and thus is not simply a reflection of impaired "contractility". In fact, Ea increases in HF models of pressure overload, i.e., TAC model (52). Ventricular hypertrophy and fibrosis are hallmarks of both HFrEF and HFpEF, where the ventricular compliance is decreased as the myocardium is stiffer, which results in higher ventricular end-diastolic pressures (EDP) at any given end-diastolic volume (EDV). A ventricle with a reduced compliance would have a smaller EDV due to impaired filling for a given EDP. Nevertheless, the EDV may be very high but the EDP may not be greatly elevated when ventricular compliance increases such as in MI or other dilated cardiomyopathy with massive ventricle dilation without appreciable thickening of the wall.

Discussion and troubleshooting

PV loop procedure can be summarized in three critical steps: (1) ensure appropriate ventilation through insertion of endotracheal tube (2) proper placement of the jugular vein catheter to infuse physiologic solution or testing drugs (3) ensure a proper placement of the PV catheter in the left ventricle.

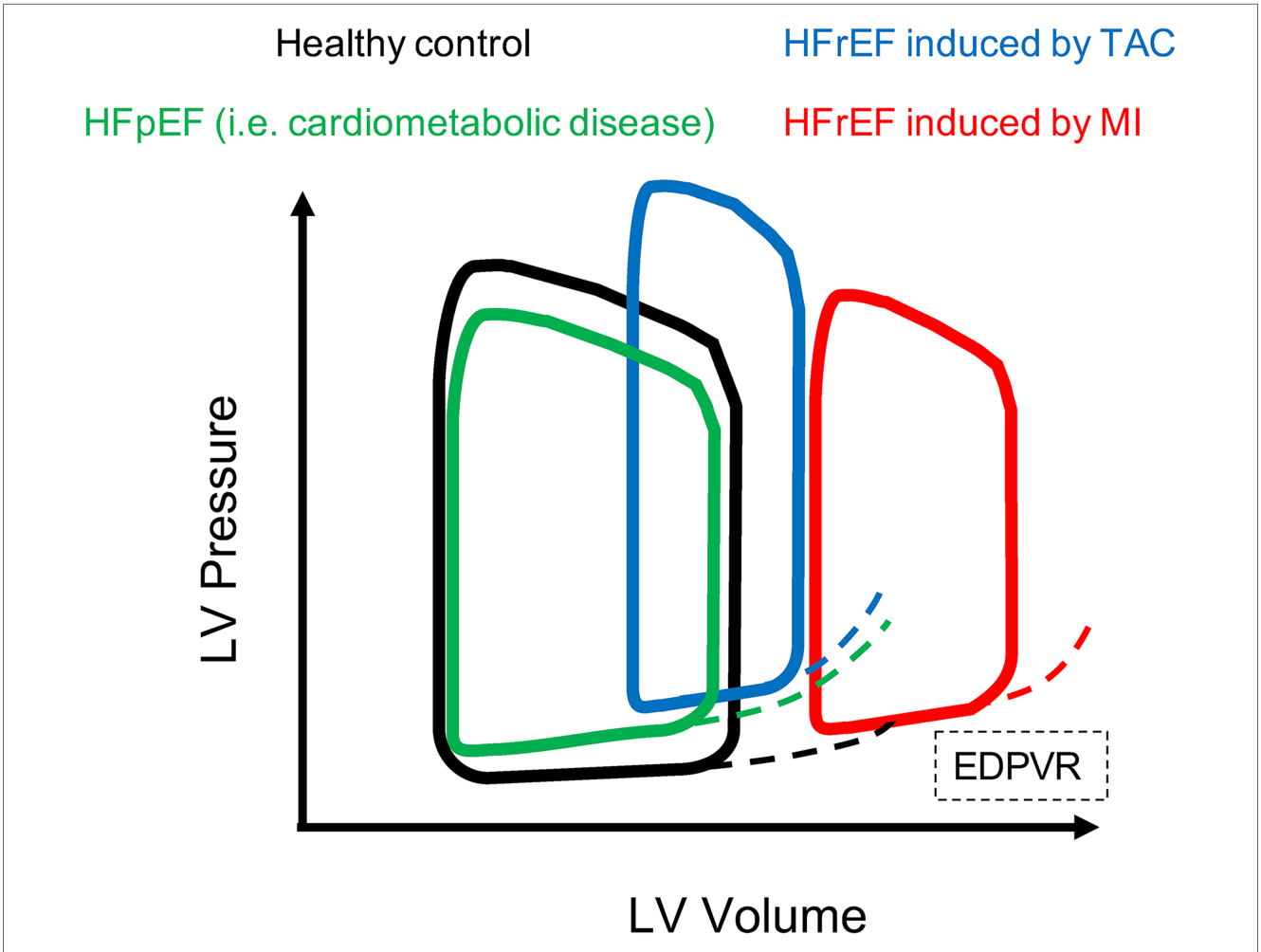

FIGURE 6
PV loops in healthy and HF models. Examples of PV loops. In black PV loop of healthy model, then models of HFrEF present PV loop shifted to the right. In particular HFrEF model induced by MI (red) presents enlargement of the LV chambers and impaired contractility, while HFrEF model induced by TAC (blue) presents increased ESP and EDP due to aggravated afterload, and increased EDPVR therefore the loop is shifted on the top right compared to healthy control. The model of HFpEF (green) is characterized by preserved contractile function, but impaired relaxation of hypertrophied and fibrotic LV therefore the PV loop is slightly shifted to the top and presents increased EDPVR compared to healthy control.

It is important to understand differences in respiratory rate between conscious and ventilated mice in order to provide adequate ventilatory support. In fact, conscious mice have rapid shallow breaths, while ventilated mice will have much larger tidal volumes, therefore a slower respiratory rate is required to ensure appropriate alveolar ventilation. Indeed, cardiac function might be altered by respiratory acidosis (caused by too little ventilation) or respiratory alkalosis (in case of too much ventilation). This problem is empirically solved by using the lowest respiratory rate that eliminates respiratory effort from the anesthetized mouse.

Another common issue occurs following blood loss or evaporation which results in decreased blood volume with hemodynamic parameters below the normal levels. This problem is minimised by administrating fluid to the animal. Hemodynamic function can be influenced by the core body temperature which is important to maintain constant during recording through a digital feedback system. Moreover, to improve cardiac performance the anaesthetic should be adjusted during the measurement period.

Despite the complexity, of the procedure due to the small size of the mouse, PV loop analysis provides the most unique and complete information of cardiac function that cannot be obtained through any other non-invasive methodology. Therefore, LV catheterization in murine models provides an important platform for the investigation of complex pathophysiologic mechanisms that characterize cardiac disease states such as heart failure and inherited cardiomyopathies. However, microsurgical skills are necessary to successfully perform these experiments as well as for all complicated procedures that require practice.

Concluding remarks

The greatest advantage of non-invasive methodologies for measuring cardiac function (echocardiography and MRI) is that they can be repeated in the same animal and provide direct quantification of absolute volumes and morphology. However, they are limited by their application to steady-state conditions and reliance on motion parameters that can be influenced by loading conditions and thus lack specificity to the ventricle itself. Contrarily the conductance catheter signal is proportional to volume but must be appropriately calibrated to provide accurate absolute volume measurements. Due to the high variability in the physiologic parameters reported in literature it is recommended to always use wild type control littermates to have a proper baseline as reference values. Implementation of morphological information of cardiac structure, histopathologic analysis of cardiac biopsies is always recommended to have more direct evidences for cardiac remodelling (i.e., hypertrophy, fibrosis, inflammatory cells infiltration), which represent a hallmark of heart failure.

Left ventricle catheterization requires good surgical skills of the operator, including proper endotracheal intubation for ventilator and vessels cannulation. The cost of the equipment for PV loop analysis is definitely cheaper than echocardiography machine or magnetic resonance apparatus, that still requires expert operators to run the imaging acquisition and data analysis. Moreover, PV loop analysis gives more accurate and complete information about systolic and diastolic parameters of the heart for each cardiac cycle. The major limitation of using an invasive LV catheterization procedure refers to its invasiveness, which makes this procedure not suitable for serial monitoring (contrary to echo and other non-invasive methodology). Therefore, the animal is usually sacrificed at the end of the experiment since the surgical procedure is terminal. However, PV loop analysis are suitable for evaluation of hemodynamic changes that occur in the same animal before and after drug administration.

Considering the large variability of physiological parameters observed in preclinical studies it is recommended to follow standardized guidelines regarding type of anaesthetic or detailed surgical procedure could potentially validate results across and between laboratories. This will enable the creation of a big data platform with cardiovascular physiological parameters. Clinical practice has greatly benefitted by the analysis of clinical registries (57, 58), however similar epidemiological studies in preclinical settings require more implementation and promotion. Preclinical registries for heart failure could contribute to understanding the phenotype of different models used in cardiovascular studies, or identifying new models that can be used for future cardiovascular studies. In addition, data from preclinical registry could be used to identify potential new treatments or testing the repurpose of known drugs for cardiovascular diseases. One step closer to this could be achieved by having highly specialized professional figures employed by the research institution serving as directors of preclinical cardiovascular units, responsible of coordinating collaborative studies that investigate novel mechanisms in cardiovascular pathophysiology. Another important aspect is the shortage of economic resources required to cover the cost for purchase and maintenance of equipment necessary to characterize the cardiovascular phenotype of small animals used in preclinical studies. Resources should be prioritized for groups that have established expertise in cardiac pathophysiology field, which could promote interdisciplinary collaborations with other research groups specialized in different disciplines (e.g., metabolism, diabetes, oncology, renal dysfunction, aging).

Author contributions

The author confirms being the sole contributor of this work and has approved it for publication.

Funding

GP was supported by grants from The Swedish Heart-Lung Foundation (20210498–20210607).

Conflict of interest

The authors declare that the research was conducted in the absence of any commercial or financial relationships that could be construed as a potential conflict of interest.

Publisher's note

References

1. Zile MR, Baicu CF, Gaasch WH. Diastolic heart failure–abnormalities in active relaxation and passive stiffness of the left ventricle. *N Engl J Med*. (2004) 350:1953–9. doi: 10.1056/NEJMoa032566

2. Rigolli M, Whalley GA. Heart failure with preserved ejection fraction. *J Geriatr Cardiol*. (2013) 10:369–76. doi: 10.3969/j.issn.1671-5411.2013.04.011

3. Pfeffer MA, Shah AM, Borlaug BA. Heart failure with preserved ejection fraction in perspective. *Circ Res*. (2019) 124:1598–617. doi: 10.1161/CIRCRESAHA.119.313572

4. Senni M, Paulus WJ, Gavazzi A, Fraser AG, Diez J, Solomon SD, et al. New strategies for heart failure with preserved ejection fraction: the importance of targeted therapies for heart failure phenotypes. *Eur Heart J*. (2014) 35:2797–815. doi: 10.1093/eurheartj/ehu204

5. Ponikowski P, Voors AA, Anker SD, Bueno H, Cleland JGF, Coats AJS, et al. 2016 ESC guidelines for the diagnosis and treatment of acute and chronic heart failure: the task force for the diagnosis and treatment of acute and chronic heart failure of the European society of cardiology (ESC) developed with the special contribution of the heart failure association (HFA) of the ESC. *Eur Heart J*. (2016) 37:2129–200. doi: 10.1093/eurheartj/ehw128

6. Bhatt DL, Szarek M, Steg PG, Cannon CP, Leiter LA, Mcguire DK, et al. Sotagliflozin in patients with diabetes and recent worsening heart failure. *N Engl J Med*. (2021) 384:117–28. doi: 10.1056/NEJMoa2030183

7. Savarese G, Stolfo D, Sinagra G, Lund LH. Heart failure with mid-range or mildly reduced ejection fraction. *Nat Rev Cardiol*. (2022) 19:100–16. doi: 10.1038/s41569-021-00605-5

8. Wang QD, Bohlooly YM, Sjoquist PO. Murine models for the study of congestive heart failure: implications for understanding molecular mechanisms and for drug discovery. *J Pharmacol Toxicol Methods*. (2004) 50:163–74. doi: 10.1016/j.vascn.2004.05.005

9. Houser SR, Margulies KB, Murphy AM, Spinale FG, Francis GS, Prabhu SD, et al. Animal models of heart failure: a scientific statement from the American heart association. *Circ Res*. (2012) 111:131–50. doi: 10.1161/RES.0b013e3182582523

10. Esposito G, Schiattarella GG, Perrino C, Cattaneo F, Pironti G, Franzone A, et al. Dermcidin: a skeletal muscle myokine modulating cardiomyocyte survival and infarct size after coronary artery ligation. *Cardiovasc Res*. (2015) 107:431–41. doi: 10.1093/cvr/cvv173

11. Lund LH, Hage C, Pironti G, Thorvaldsen T, Ljung-Faxen U, Zabarovskaja S, et al. Acyl ghrelin improves cardiac function in heart failure and increases fractional shortening in cardiomyocytes without calcium mobilization. *Eur Heart J*. (2023) 44(22):2009–25. doi: 10.1093/eurheartj/ehad100

12. Esposito G, Perrino C, Cannavo A, Schiattarella GG, Borgia F, Sannino A, et al. EGFR trans-activation by urotensin II receptor is mediated by beta-arrestin recruitment and confers cardioprotection in pressure overload-induced cardiac hypertrophy. *Basic Res Cardiol*. (2011) 106:577–89. doi: 10.1007/s00395-011-0163-2

13. Perrino C, Schiattarella GG, Sannino A, Pironti G, Petretta MP, Cannavo A, et al. Genetic deletion of uncoupling protein 3 exaggerates apoptotic cell death in the ischemic heart leading to heart failure. *J Am Heart Assoc*. (2013) 2:e000086. doi: 10.1161/JAHA.113.000086

14. Pironti G, Strachan RT, Abraham D, Mon-Wei Yu S, Chen M, Chen W, et al. Circulating exosomes induced by cardiac pressure overload contain functional angiotensin II type 1 receptors. *Circulation*. (2015) 131:2120–30. doi: 10.1161/CIRCULATIONAHA.115.015687

15. Schiattarella GG, Cattaneo F, Pironti G, Magliulo F, Carotenuto G, Pirozzi M, et al. Correction: akap1 deficiency promotes mitochondrial aberrations and exacerbates cardiac injury following permanent coronary ligation via enhanced mitophagy and apoptosis. *PLoS One*. (2016) 11:e0158934. doi: 10.1371/journal.pone.0158934

16. Pironti G, Bersellini-Farinotti A, Agalave NM, Sandor K, Fernandez-Zafra T, Jurczak A, et al. Cardiomyopathy, oxidative stress and impaired contractility in a rheumatoid arthritis mouse model. *Heart*. (2018) 104:2026–34. doi: 10.1136/heartjnl-2018-312979

17. Pironti G, Gastaldello S, Rassier DE, Lanner JT, Carlstrom M, Lund LH, et al. Citrullination is linked to reduced Ca(2+) sensitivity in hearts of a murine model of rheumatoid arthritis. *Acta Physiol*. (2022) 236:e13869. doi: 10.1111/apha.13869

18. Manti M, Fornes R, Pironti G, Mccann Haworth S, Zhengbing Z, Benrick A, et al. Maternal androgen excess induces cardiac hypertrophy and left ventricular dysfunction in female mice offspring. *Cardiovasc Res*. (2020) 116:619–32. doi: 10.1093/cvr/cvz180

19. Schiattarella GG, Altamirano F, Tong D, French KM, Villalobos E, Kim SY, et al. Nitrosative stress drives heart failure with preserved ejection fraction. *Nature*. (2019) 568:351–6. doi: 10.1038/s41586-019-1100-z

20. Mishra S, Kass DA. Cellular and molecular pathobiology of heart failure with preserved ejection fraction. *Nat Rev Cardiol*. (2021) 18:400–23. doi: 10.1038/s41569-020-00480-6

21. Valero-Munoz M, Backman W, Sam F. Murine models of heart failure with preserved ejection fraction: a "fishing expedition". *JACC Basic Transl Sci*. (2017) 2:770–89. doi: 10.1016/j.jacbts.2017.07.013

22. Zacchigna S, Paldino A, Falcao-Pires I, Daskalopoulos EP, Dal Ferro M, Vodret S, et al. Towards standardization of echocardiography for the evaluation of left ventricular function in adult rodents: a position paper of the ESC working group on myocardial function. *Cardiovasc Res*. (2021) 117:43–59. doi: 10.1093/cvr/cvaa110

23. Amzulescu MS, De Craene M, Langet H, Pasquet A, Vancraeynest D, Pouleur AC, et al. Myocardial strain imaging: review of general principles, validation, and sources of discrepancies. *Eur Heart J Cardiovasc Imaging*. (2019) 20:605–19. doi: 10.1093/ehjci/jez041

24. Smiseth OA, Torp H, Opdahl A, Haugaa KH, Urheim S. Myocardial strain imaging: how useful is it in clinical decision making? *Eur Heart J*. (2016) 37:1196–207. doi: 10.1093/eurheartj/ehv529

25. Bauer M, Cheng S, Jain M, Ngoy S, Theodoropoulos C, Trujillo A, et al. Echocardiographic speckle-tracking based strain imaging for rapid cardiovascular phenotyping in mice. *Circ Res*. (2011) 108:908–16. doi: 10.1161/CIRCRESAHA.110.239574

26. Bhan A, Sirker A, Zhang J, Protti A, Catibog N, Driver W, et al. High-frequency speckle tracking echocardiography in the assessment of left ventricular function and remodeling after murine myocardial infarction. *Am J Physiol Heart Circ Physiol*. (2014) 306:H1371–1383. doi: 10.1152/ajpheart.00553.2013

27. Pasipoularides A. LV twisting and untwisting in HCM: ejection begets filling. Diastolic functional aspects of HCM. *Am Heart J*. (2011) 162:798–810. doi: 10.1016/j.ahj.2011.08.019

28. Burns AT, La Gerche A, Prior DL, Macisaac AI. Left ventricular untwisting is an important determinant of early diastolic function. *JACC Cardiovasc Imaging*. (2009) 2:709–16. doi: 10.1016/j.jcmg.2009.01.015

29. Methawasin M, Strom J, Borkowski T, Hourani Z, Runyan R, Smith JE, et al. Phosphodiesterase 9a inhibition in mouse models of diastolic dysfunction. *Circ Heart Fail*. (2020) 13:e006609. doi: 10.1161/CIRCHEARTFAILURE.119.006609

30. Wu X, Liu H, Brooks A, Xu S, Luo J, Steiner R, et al. SIRT6 mitigates heart failure with preserved ejection fraction in diabetes. *Circ Res*. (2022) 131:926–43. doi: 10.1161/CIRCRESAHA.121.318988

31. Chen J, Norling LV, Mesa JG, Silva MP, Burton SE, Reutelingsperger C, et al. Annexin A1 attenuates cardiac diastolic dysfunction in mice with inflammatory arthritis. *Proc Natl Acad Sci U S A*. (2021) 118(38):e2020385118. doi: 10.1073/pnas.2020385118

32. Erkens R, Kramer CM, Luckstadt W, Panknin C, Krause L, Weidenbach M, et al. Left ventricular diastolic dysfunction in Nrf2 knock out mice is associated with cardiac hypertrophy, decreased expression of SERCA2a, and preserved endothelial function. *Free Radic Biol Med*. (2015) 89:906–17. doi: 10.1016/j.freeradbiomed.2015.10.409

33. Schnelle M, Catibog N, Zhang M, Nabeebaccus AA, Anderson G, Richards DA, et al. Echocardiographic evaluation of diastolic function in mouse models of heart disease. *J Mol Cell Cardiol*. (2018) 114:20–8. doi: 10.1016/j.yjmcc.2017.10.006

34. Nagueh SF, Smiseth OA, Appleton CP, Byrd BF 3rd, Dokainish H, Edvardsen T, et al. Recommendations for the evaluation of left ventricular diastolic function by echocardiography: an update from the American society of echocardiography and the European association of cardiovascular imaging. *J Am Soc Echocardiogr*. (2016) 29:277–314. doi: 10.1016/j.echo.2016.01.011

35. Yuan L, Wang T, Liu F, Cohen ED, Patel VV. An evaluation of transmitral and pulmonary venous Doppler indices for assessing murine left ventricular diastolic function. *J Am Soc Echocardiogr*. (2010) 23:887–97. doi: 10.1016/j.echo.2010.05.017

36. Ommen SR, Nishimura RA, Appleton CP, Miller FA, Oh JK, Redfield MM, et al. Clinical utility of Doppler echocardiography and tissue Doppler imaging in the estimation of left ventricular filling pressures: a comparative simultaneous Doppler-

catheterization study. *Circulation*. (2000) 102:1788–94. doi: 10.1161/01.CIR.102.15.1788

37. Gilson WD, Kraitchman DL. Cardiac magnetic resonance imaging in small rodents using clinical 1.5 T and 3.0 T scanners. *Methods*. (2007) 43:35–45. doi: 10.1016/j.ymeth.2007.03.012

38. Roberts TA, Price AN, Jackson LH, Taylor V, David AL, Lythgoe MF, et al. Direct comparison of high-temporal-resolution CINE MRI with Doppler ultrasound for assessment of diastolic dysfunction in mice. *NMR Biomed*. (2017) 30(10):e3763. doi: 10.1002/nbm.3763

39. Van De Weijer T, Van Ewijk PA, Zandbergen HR, Slenter JM, Kessels AG, Wildberger JE, et al. Geometrical models for cardiac MRI in rodents: comparison of quantification of left ventricular volumes and function by various geometrical models with a full-volume MRI data set in rodents. *Am J Physiol Heart Circ Physiol*. (2012) 302:H709–715. doi: 10.1152/ajpheart.00710.2011

40. Park CJ, Branch ME, Vasu S, Melendez GC. The role of cardiac MRI in animal models of cardiotoxicity: hopes and challenges. *J Cardiovasc Transl Res*. (2020) 13:367–76. doi: 10.1007/s12265-020-09981-8

41. Shapiro LR. Streamlining and implementing nutritional assessment: the dietary approach. *J Am Diet Assoc*. (1979) 75:230–7. doi: 10.1016/S0002-8223(21)05334-7

42. Kass DA, Chen CH, Curry C, Talbot M, Berger R, Fetics B, et al. Improved left ventricular mechanics from acute VDD pacing in patients with dilated cardiomyopathy and ventricular conduction delay. *Circulation*. (1999) 99:1567–73. doi: 10.1161/01.CIR.99.12.1567

43. Kass DA, Wolff MR, Ting CT, Liu CP, Chang MS, Lawrence W, et al. Diastolic compliance of hypertrophied ventricle is not acutely altered by pharmacologic agents influencing active processes. *Ann Intern Med*. (1993) 119:466–73. doi: 10.7326/0003-4819-119-6-199309150-00004

44. Georgakopoulos D, Mitzner WA, Chen CH, Byrne BJ, Millar HD, Hare JM, et al. In vivo murine left ventricular pressure-volume relations by miniaturized conductance micromanometry. *Am J Physiol*. (1998) 274:H1416–1422. doi: 10.1152/ajpheart.1998.274.4.H1416

45. Pacher P, Nagayama T, Mukhopadhyay P, Batkai S, Kass DA. Measurement of cardiac function using pressure-volume conductance catheter technique in mice and rats. *Nat Protoc*. (2008) 3:1422–34. doi: 10.1038/nprot.2008.138

46. Cingolani OH, Kass DA. Pressure-volume relation analysis of mouse ventricular function. *Am J Physiol Heart Circ Physiol*. (2011) 301:H2198–206. doi: 10.1152/ajpheart.00781.2011

47. Abraham D, Mao L. Cardiac pressure-volume loop analysis using conductance catheters in mice. *J Vis Exp*. (2015) 103:52942. doi: 10.3791/52942

48. Townsend D. Measuring pressure volume loops in the mouse. *J Vis Exp*. (2016). doi: 10.3791/53810

49. Nakatani S, Beppu S, Nagata S, Ishikura F, Tamai J, Yamagishi M, et al. Diastolic suction in the human ventricle: observation during balloon mitral valvuloplasty with a single balloon. *Am Heart J*. (1994) 127:143–7. doi: 10.1016/0002-8703(94)90519-3

50. Carrick-Ranson G, Hastings JL, Bhella PS, Shibata S, Fujimoto N, Palmer MD, et al. Effect of healthy aging on left ventricular relaxation and diastolic suction. *Am J Physiol Heart Circ Physiol*. (2012) 303:H315–322. doi: 10.1152/ajpheart.00142.2012

51. Lindsey ML, Kassiri Z, Virag JAI, De Castro Bras LE, Scherrer-Crosbie M. Guidelines for measuring cardiac physiology in mice. *Am J Physiol Heart Circ Physiol*. (2018) 314:H733–52. doi: 10.1152/ajpheart.00339.2017

52. Abraham DM, Lee TE, Watson LJ, Mao L, Chandok G, Wang HG, et al. The two-pore domain potassium channel TREK-1 mediates cardiac fibrosis and diastolic dysfunction. *J Clin Invest*. (2018) 128:4843–55. doi: 10.1172/JCI95945

53. Spinale FG. Assessment of cardiac function–basic principles and approaches. *Compr Physiol*. (2015) 5:1911–46. doi: 10.1002/cphy.c140054

54. Shioura KM, Geenen DL, Goldspink PH. Assessment of cardiac function with the pressure-volume conductance system following myocardial infarction in mice. *Am J Physiol Heart Circ Physiol*. (2007) 293:H2870–77. doi: 10.1152/ajpheart.00585.2007

55. Regan JA, Mauro AG, Carbone S, Marchetti C, Gill R, Mezzaroma E, et al. A mouse model of heart failure with preserved ejection fraction due to chronic infusion of a low subpressor dose of angiotensin II. *Am J Physiol Heart Circ Physiol*. (2015) 309:H771–8. doi: 10.1152/ajpheart.00282.2015

56. Bai B, Yang W, Fu Y, Foon HL, Tay WT, Yang K, et al. Seipin knockout mice develop heart failure with preserved ejection fraction. *JACC Basic Transl Sci*. (2019) 4:924–37. doi: 10.1016/j.jacbts.2019.07.008

57. Lund LH, Carrero JJ, Farahmand B, Henriksson KM, Jonsson A, Jernberg T, et al. Association between enrolment in a heart failure quality registry and subsequent mortality-a nationwide cohort study. *Eur J Heart Fail*. (2017) 19:1107–16. doi: 10.1002/ejhf.762

58. Savarese G, Carrero JJ, Pitt B, Anker SD, Rosano GMC, Dahlstrom U, et al. Factors associated with underuse of mineralocorticoid receptor antagonists in heart failure with reduced ejection fraction: an analysis of 11 215 patients from the Swedish heart failure registry. *Eur J Heart Fail*. (2018) 20:1326–34. doi: 10.1002/ejhf.1182

Frontiers in
Cardiovascular Medicine

Innovations and improvements in cardiovascular treatment and practice

Focuses on research that challenges the status quo of cardiovascular care, or facilitates the translation of advances into new therapies and diagnostic tools.

Discover the latest Research Topics

See more →

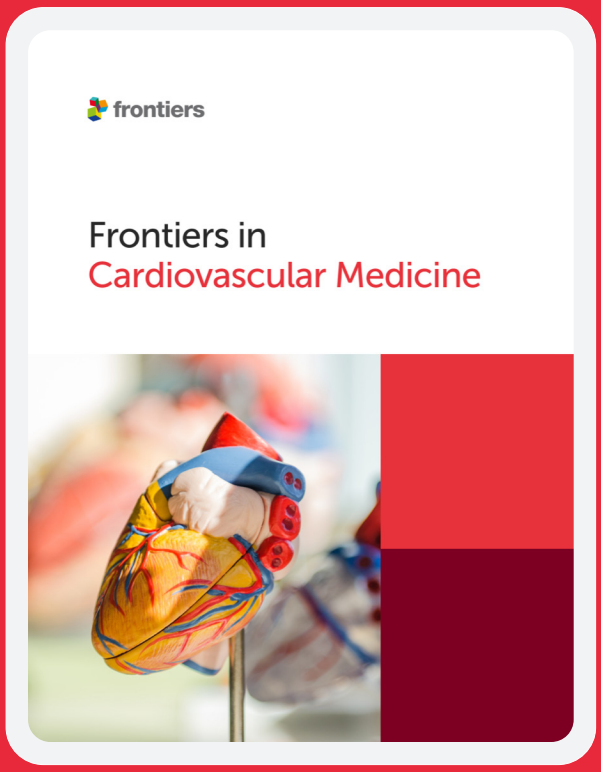

Frontiers

Avenue du Tribunal-Fédéral 34
1005 Lausanne, Switzerland
frontiersin.org

Contact us

+41 (0)21 510 17 00
frontiersin.org/about/contact